INTELLIGENT CONTROL
OF
AN AUTOMATED ADHESIVE DISPENSING CELL

By

Ali Razban

A thesis submitted for the degree of
Doctor of Philosophy of the University of London
and for the Diploma of Imperial Collage.

November 1993

Centre for Robotics
Mechanical Engineering Department
Imperial College of Science, Technology and Medicine,
University of London

To the memory of my father
Rostam Razban

ABSTRACT

Adhesives and sealants have been used in numerous manufacturing applications as well as for structural bonding. However to ensure the process integrity for reliable structural adhesive joints and to produce quality bonded joints for structural applications, such as in the automotive and aerospace industries, it is necessary to use robots and automated systems to achieve the required reliability and integrity of the joints.

An automated manufacturing cell has been developed for dispensing beads of adhesive and sealants using on-line control. A structured vision system was developed for on-line inspection of the adhesive and sealant dispensing process. The dispensed adhesive is controlled through a closed-loop control system by using a vision system as a feedback signal whilst the bead is being dispensed. In order to have a constant flow of information between the cell components, the cell has been fully integrated. The control process is achieved by continuous communication between the robot controller, dispensing controller and vision system.

The dispensing process has a long delay due to the transportation lag in the process and the time taken for image processing. It can be analysed as a lumped parameter dynamic model, with a pure time delay which is a function of the operating conditions. The modelling and control strategies for the adhesive dispensing process are covered. The simulation and implementation of different controllers and their performance are also discussed.

A rheological model of the adhesive has been obtained using a power-law expression. This model is also based on the experimental shear stress and rotational speed data obtained using a bob and cup viscometer. An analytical expression is then used to find the flow rate through the dispensing gun. These results are used for initial set-up of the process and as a basis for diagnosis when using knowledge-based expert system.

An overall supervisory-cell controller has been proposed using a rule-based method at different control levels. These levels are a flow controller, the adjustment of control gains based on the robot speed, node position learning, diagnosis and initial system set-up. Each control level has a different time scale, which can be anywhere in the range of msec to hours.

ACKNOWLEDGEMENTS

It is a great pleasure to express my gratitude to my supervisors, Mr. B.L. Davies of the Mechanical Engineering Department Robotics Section, and Prof. G.F. Bryant of the Electrical Engineering Department Control Section for their invaluable guidance, criticism, continuous support and encouragement through the course of this research and in the preparation of this thesis.

I would also like to thank Dr. R.H. Clarke of the Electrical Engineering Department for reviewing part of the thesis and his criticism and excellent suggestions.

Appreciation goes to Dr. J. Efstathiou, Dr. S. Sezgin and Dr. S. Harris for collaboration in some parts of this project.

I am also grateful to the Science and Engineering Research Council (ACME) for financial support of this work.

My thanks are also to my friends and colleagues especially Dr. A. F. Khorrami and Ms. J. Faridani for their support during this project.

I would like to thank my parents for their support and encouragement during the period of my higher education.

Last but not least, my wife deserves my special thanks for her love, care and support which made this work possible and worthwhile.

TABLE OF CONTENTS

LIST OF FIGURES

LIST OF TABLES

NOTATION

A	material constant
$a1$	denominator transfer function coefficient in Z-domain
$a2$	denominator transfer function coefficient in Z-domain
A_b	bob cross sectional area
B	rotational speed coefficient
$b1$	numerator transfer function coefficient in Z-domain
$b2$	numerator transfer function coefficient in Z-domain
C	modified power law coefficient
c	power law coefficient
C_1	integration constant
C_p	specific heat at constant pressure
C_v	specific heat at constant volume
D	process disturbance
$d(S)$	disturbance in S-domain
DAC	analogue to digital converter
D_b	bead dispensed diameter
D_g	diameter of the gun
D_N	diameter of the nozzle
DP	change in pressure delivery
dp	change in pressure
DP_g	gun pressure drop
$DP_{g/N}$	nozzle entrance pressure drop
DP_N	nozzle pressure drop
DP_T	total pressure drop
dr	differentiate in radial direction
Dt	change in time
dT	change in temperature
dV_z	change of velocity in z-direction
E	specific internal energy per unit mass
e_k, e_i	error between output & set-point
F	applied force

$F(t)$	function in time domain
$F(Z)$	function in Z-domain
g	gravity
$G(S)$	impulse response, transfer function
G_p	process transfer function
G_{pm}	process transfer function model
h	bob's height
K	on/off controller gain
K_a	process gain
K_i	integral gain
K_p	proportional gain
L	delay in open loop response
Lg	effective length of gun
L_N	length of nozzle
M	bob's torque
m'	time power index
$\dot{m}$	mass flow rate
$M(k)$	manual input
n	power law exponent
p	pressure
P_1	pressure transducer reading
P_2	interface pressure
P_A	atmospheric pressure
P_L	pressure at r = L
P_o	pressure at r = 0
Q	volume flow rate
q	heat flux vector
Q_g	gun flow rate
Q_n	nozzle flow rate
R	pipe radius
r	cylindrical coordinate
R_g	gun radius
R_N	nozzle radius
R_s	slop of open loop response
S	Laplace transform operator
$\dot{S}$	thermal energy source
T	temperature
t	time

$T.D.$	time delay
T_d	Transport delay
$T_d\,(A)$	adaptation time of flow rate
$T_d\,(p)$	transport lag due to the distance of the camera from nozzle tip
$T_d\,(V)$	vision computation time
T_{dm}	time delay model
T_R	reference temperature
T_s	sampling time
u	specific internal energy per unit mass
$U(S)$	transfer function input in S-domain
$U,\ U_k,\ U_{i+1}$	controller output
V	velocity vector
V_{in}	input voltage
V_θ	velocity in θ direction
V_R	robot speed
V_r	velocity in r direction
V_z	velocity in z direction
W	output width
W_{ref}	reference width
$y(S)$	process output in s-domain
$Y(t)$	process output in time domain
Y_m	model output
Z	Z-transform
z	cylindrical coordinate
$\dot{\gamma}$	shear rate
∇	gradient operator
α	material constant
$d\theta$	differentiate inθ direction
μ	Newtonian viscosity
θ	cylindrical coordinate
ρ	density
τ	shear stress
τ_R	wall shear stress
τ_{rz}	shear stress
τ_y	yield shear stress
Ω	rotational speed at r = R
ω	rotational speed

ω_n	natural frequency
ξ	Z-transform operator
ζ	damping ratio

CHAPTER I

INTRODUCTION

1.1 Aim of the Research

Over the past two decades the use of robots has vastly increased in all kinds of industrial application. This increase is basically due to several benefits such as improved quality, increased production speeds and lower costs of manufacturing. In recent years, the application of adhesive and sealant using robotics has also been given special attention in industry.

The need for having high integrity, structurally bonded adhesive and sealant joints throughout industry is increasing. To ensure process integrity, strict process control of the automated dispensing cell is essential. Many industries require the use of continuous beads of adhesive or sealant in applications where the integrity of the joint is critical e.g., structural bonding or gasket sealing. A continuous and uniform bead gives required strength for good performance of the joints. For these reasons a fully automated manufacturing cell needs to be developed which uses an in-process inspection system to check the size of the bead, whilst it is being laid down.

This thesis is concerned with the use of robots and automated systems to control dispensed adhesives and sealants. The aim of the research is the development of a fully automated cell for dispensing adhesives and sealants..

1.2 Manufacturing Automation

The major reason for the introduction of robots into manufacturing is their flexibility and reliability within the range of tasks in a manufacturing cell. Robots can be reprogrammed to cope with minor and major changes in the specification of the product. They are thus the key factor in flexible manufacturing systems. The word *automation* is used by industry to describe the introduction of machines into manufacturing and factories to perform the tasks

formerly done by humans. Automation is either fixed (hard) or flexible. Flexibility in automation is an important criterion, which makes the use of robots likely desirable. Hard automation is dedicated to a fixed number of tasks, whereas flexible automation can cope with a variety of products and enables the change from one task to another to be performed very easily. The real benefits of automation (particularly for small batch size and low volume production) become manifest in flexible automation. When flexible automation is considered, the application must be carefully planned and be cost effective.

The first applications of industrial robots in automated manufacturing were primarily for tasks such as *pick-and-place* and material handling. This process was quite simple as robot and workpiece were the only components of the automated cell. As the industrial applications of robots in automated manufacturing became more complex, the success of the automated cell depended primarily on its ability to communicate with its environment. Thus, the integration of the individual cell components (such as a robot with various sensory devices) became essential.

1.3 Automation Opportunities in The Dispensing of Adhesive & Sealant

Many industries have the desire to replace welded joints with bonded structures. This is for a variety of reasons, such as a lack of skilled welders or a desire to avoid *dressing* the weld and the consequent damage to the surface which can show through modern coating processes. The result is a need for a bonded joint which is not just a low strength gap filler for preventing vibration, but a structural joint with all the integrity that is implied. To achieve high structural integrity, two aspects need to be fulfilled. Firstly the adherent and adherend must have the necessary properties, not just in the short term, but after a number of years of use under often arduous conditions of environmental corrosion, changes in humidity and temperature [Davies 90a]. This long-term integrity is clearly primarily a materials problem. However a second aspect is also required; that the process be carried out in exactly the way that the material suppliers intended. This means that not only must the adhesive be placed in the right location, but it must also be of sufficient height to take up any gaps in the structure and sufficient width to provide the desired strength. There must not be any gaps or solid particles in the adhesives which may prevent closure; nor dust and grease on the materials which prevent the correct bonding of the surfaces. The use of manual processing under such circumstances is notoriously inadequate and prone to variability and cannot be tolerated in critical structural joints. Similar arguments can be made for the use of sealants in critical areas, such as in aircraft structures and automotive parts where, for example, gasket integrity is important or sealant quality is necessary [Huang 84]. It would therefore appear that the only way that these processes can have the

degree of integrity required for application in new, high-risk, areas is to use automated systems for both dispensing, to ensure that the process is correctly carried out, and for inspection, to ensure that everything is to specification.

The use of industrial robots has been increasing in many manufacturing industries, but their unpopularity in adhesive and sealant automation is due to difficulties in the application of adhesives and sealants, and the lack of knowledge regarding the process of adhesion. The most common reasons for the investigation of fully automated systems for adhesive and sealant dispensing are the maintenance of the quality of structural bonding and the potential cost saving from reduction in material usage. The use of robotics systems provides a significant reduction in costs as well as improvement in quality and production [Bowles 85, Turner 90]. Repeatability and accuracy are important factors, and robots need to have good accuracy and high repeatability so that the adhesives or sealants can be applied to the desired location with only small error in position. Robots can place adhesive or sealant beads accurately and in the proper orientation over the surface. This process can be repeated, and is an efficient method for material control.

The integration of the entire automated dispensing cell under the control of a supervisory computer, offers great potential for flexibility, quality control and a reduction in the long term costs. The great number of parameters influencing the dispensing process makes the integration of an automated adhesives and sealants dispensing cell rather difficult and complicated.

In recent years, the applications of adhesives and sealants for industrial assembly have grown very fast. Adhesives and sealants have been used in a number of structurally bonded joints and manufacturing applications. Structural adhesives have been used by major automotive manufacturers such as; PSA (Peugeot / Citroen) and Renault in France, Audi, Opel and Volkswagen in Germany, Fiat in Italy, Volvo in the Netherlands [Scheidle 90] and the Ford motor company in the U.K. [Industrial Robot 92]. Automotive industries usually use structural adhesives in combination with widely spaced spot welds, which result in a continuous, sealed joint with outstanding mechanical properties. In the aerospace industry, adhesives are used in metal bonding, honey-comb bonding and advanced composites [Industrial Robot 89b].

1.4 Relevant Research in Adhesives Dispensing

Among the manufacturers involved in the automation of adhesive and sealant dispensing is V & B of Turin, Italy. They have reported a considerable decrease in costs due to the

automated bonding of sub assemblies, including a sealant line for Renault and an adhesive line for Fiat [Anon 84a]. This reduction in costs, results from the speed and simplicity of the robot adhesive bonding system compared to equivalent welding units. General Motors also have an automated sealant line for the application of liquid sealant to the rear main crankshaft bearing gap in engines [Johnson 84, Schrieber 84]. Direct automobile glazing lines at Rover are another example of the use of an automated dispensing system in the automotive industry [Anon 84b]

In recent years great effort has been put into developing an automated dispensing adhesives and sealants cell. Hitchen et al [Hitchen 89] from Brunel University, U.K. have looked at the automation of two part adhesives, without using any sensory feedback. Their pre-mixed adhesives dispensers were mounted on a robot. Their work mostly emphasised the mixing and application of two parts adhesives, rather than quality control.

The application of robotic adhesive and sealant dispensing in the automotive industry and the discussion of different dispensing control strategies, were analysed by Turner [Turner 90] of Nordson in U.S.A., whereas Ludbrook [Ludbrook 85] of Evode Ltd. in the U.K. has discussed some of the advantages of using robots for dispensing adhesives in the automotive industry.

Whilst these systems have been available for some time, they are almost always of an *open loop* type in which there is no feedback for the quality dispensed material [Bowles 85, Pilarski 84, Preedy 85]. In such systems quality is achieved by a series of ad-hoc adjustments together with the manual inspection of the result. This manual inspection is as vulnerable to operator error as that of manual dispensing and cannot be relied upon if high joint integrity is to be guaranteed.

Preedy et al [Preedy 85] have examined the use of robots for dispensing adhesives. In their paper, the outline for the potential use of robotics in automated adhesives bonding is discussed. They have compared the dispensing process with the other continuous path applications (such as painting) and automated joining approaches (such as spot welding). They have also emphasised the need for intelligent sensors and the capture of physical information in real time.

Haung et al [Haung 84] of the Ford motor company, U.S.A. and Scafe [Scafe 88] of G.M. Fanuc Robotic Corporation, U.S.A., have also discussed the requirements for the use of robots in adhesive and sealant applications. They have discussed robot selection and sensor implementation. On the other hand, Bolhouse et al [Bolhouse 86] have examined the role of

the vision system in the automation of sealant application to vehicle bodies. They used a vision sensor for real time seam tracking.

Different aspects of on-line inspection have also been investigated by other researchers. The inspection and control of small droplets of adhesive in electronic manufacturing have been studied by Chandraker et al [Chandraker 90]. The adhesives are applied as small blobs, rather than continuous beads, to secure surface mounted electronic components in mixed technology printed circuits. They have implemented a rule based control system using vision feedback. Sawano et al [Sawano 84] have introduced a robot system with nine degrees of freedom. The robot hand is equipped with a camera for following the seam sealing trajectory. The vision system was used only for seam tracking, and it did not include any quality inspection. However, due to the change of adhesive viscosity with environmental variation and to ensure reliable structural adhesive joints, on-line inspection is essential in structural bonding. This requires the bead to be continuously inspected automatically by using on-line inspection techniques and a controller to keep the bead parameters within the desired tolerances. This is because no satisfactory method exists for NDT (Non Destructive Test) of closed cured metal joints [Teagle 85].

1.5 Achievements and Contributions

This dissertation contributes to the growing field of automated adhesives dispensing by proposing the design and implementation of a first intelligent automated adhesives dispensing cell. The concept of closed loop control for dispensing adhesives beads has been developed and implemented using visual feedback. The dispensed material is controlled through a closed loop system which is built around a six axis robot carrying a digitally controlled dispensing gun, a single axis linear table carrying the workpiece, and a vision system for on-line inspection and image processing as shown in Fig. (1.1).

This system uses a real time in-process inspection system to check the bead parameters (e.g. width and height) and adjust the bead size whilst it is being laid down. The control process is achieved by continuous communication between the robot controller, the dispensing controller and the microcomputer which hosts vision and control algorithms. The feedback signal, obtained from the vision system, is then fed to an on-line control facility to ensure that the bead parameters are maintained within a tolerance range of the reference value. The dispensing process has a long delay due to the transportation lag and the time taken for image processing. It can be analysed as a lumped parameter dynamic system with a pure time delay, which is a function of the operating condition. The use of different types of controller such as a conventional controller (e.g. PI controller) and the

Smith's predictive controller have been investigated using computer simulation. The implementation and performance of these controllers are also covered.

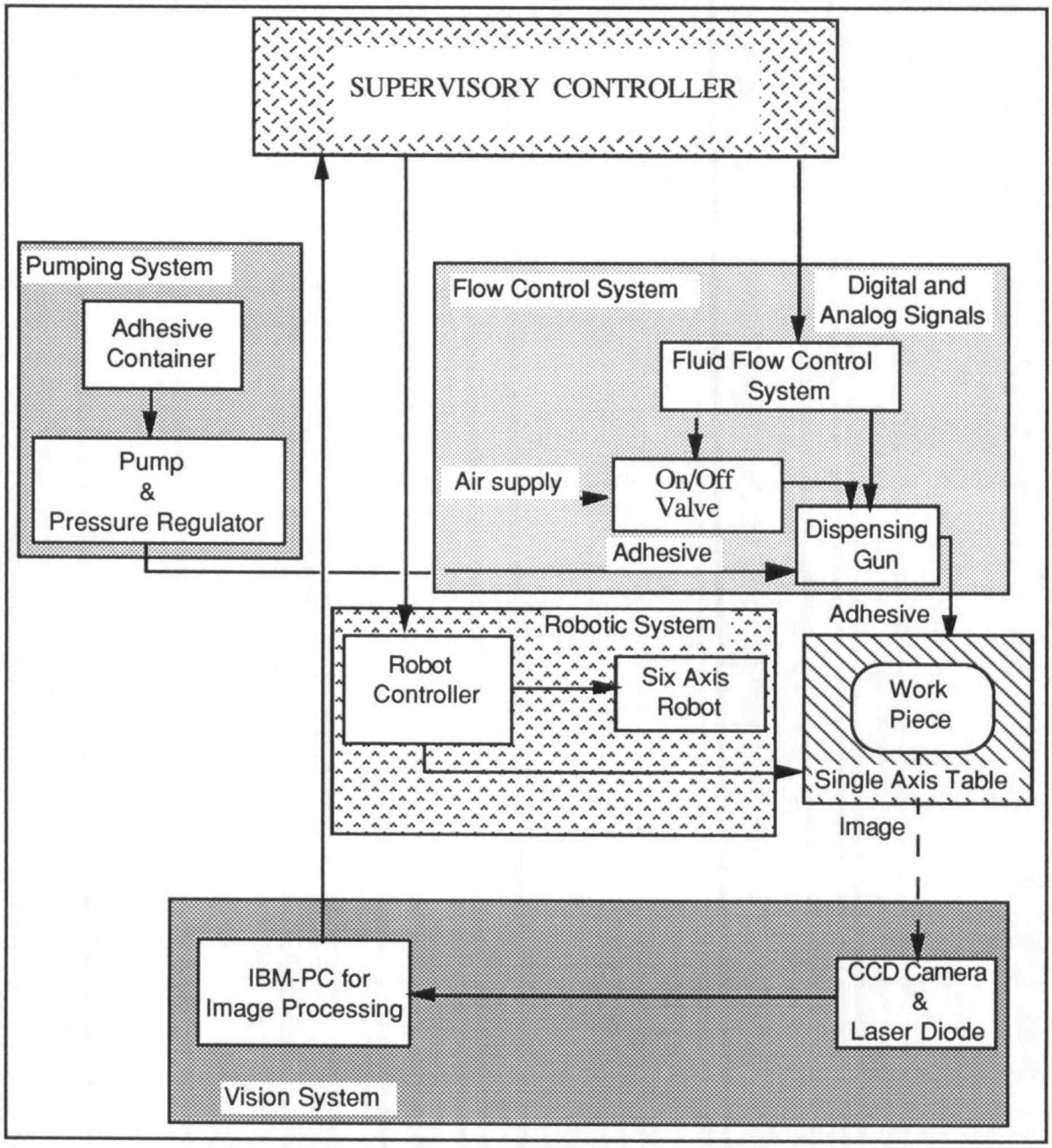

Figure 1.1: Schematic diagram of the automated cell.

A rheological model of the adhesive is obtained using a power law expression. This model is generic and is based on the experimental data. It can be used for different types of adhesive with similar rheological behaviour (where the elasticity effects are small), by using the experimental data of shear stress as a function of rotational speed at different temperatures. By having the power law expression, flow rate through the pipe and nozzle can be calculated by using a power law exponent and coefficient. An approximate nozzle flow rate therefore can be obtained theoretically by using the geometrical data, adhesive power law expression and the corrected gain factors. These results can be used for the initial set-up of the system and in the diagnosis using a knowledge-based expert system.

A cell supervisory controller has also been suggested which consists of four levels of controller. The supervisory controller includes a flow controller, the adjustment of control gains based on the robot speed, node position learning, diagnosis and initial process set-up.

1.6 Organisation of the Thesis

This thesis consists of nine chapters and four appendices. The second chapter provides an overview of (i) adhesives and their applications, advantages and disadvantages of using adhesives and (ii) different types of dispensing equipment and the benefits of using automation.

Chapter three covers the principles of machine vision. Some applications of vision systems in related industries and a range of vision techniques and image processing are also discussed. The requirements for on-line adhesives inspection, and hardware and software descriptions of commercial vision package and transputer-based vision are then covered.

The description and implementation of the automated cell is presented in chapter four. The robotics system, its controller and the communication structure for interfacing are also covered. Other cell equipment such as the single axis table, the dispensing system and implementation of vision system are also described. Interfacing within different elements of the cell and system integration are then discussed. At the end, the implementation results of different methods of the on/off controller used are discussed and compared. The need for an improved controller is then discussed.

The experimental modelling of adhesives beads is analysed in chapter five. The dispensing process variables and the assumptions made are discussed. The time responses and process modelling are covered, and a model for delays is then proposed. This is followed by a

calculation of controller gains. The simulation results using conventional controllers and a Smith's predictor controller are presented. The sensitivity analysis of the Smith's predictor and the implementation PI controller are then covered.

The analytical modelling of adhesives flow is considered in chapter six. The method of modelling is first presented, after which the use of the power law model is justified. The theoretical formulation of such a model is discussed. The analytical results are then compared with experimental data.

Chapter seven is devoted to the theoretical modelling of flow through a pipe. First the formulation of flow through a pipe is modified for adhesives. By using the results obtained from chapter six, the adhesive flow rate and the dispensed adhesive bead width are calculated. The results are compared with the analytical values. These results are used for the initial set-up of the automated adhesives cell. At the end, knowledge acquisition and the preliminary implementation of a knowledge-based system is covered.

The overall cell control is covered in chapter eight. Different levels of the muti-level controller for flow control, node position adjustment, diagnosis and initial system set-up are discussed. The knowledge elicitation of the intelligent cell is also covered.

The conclusions drawn from this work are presented in chapter nine. This is followed by suggestions and recommendations for possible future research.

CHAPTER II

ADHESIVES AND AUTOMATION

2.1 Introduction

Adhesives have been used in a sophisticated manner since ancient times. The Egyptians utilised glue, semiliquid balsams and resins from trees. The Romans caulked their ships with pine wood tar and beeswax. The ancient Chinese made bird lime, an adhesive from the juice of the mistetoe, with which they smeared twigs to catch small birds. The rubber and spyroxylin cements were introduced about one hundred years ago. In the last few decades, the natural adhesives have been improved and a number of synthetics adhesives have been developed [Skeist 90].

The utilisation of adhesives as a fastening technique has been restricted due to:

i) A lack of knowledge regarding the adhesion process and finding a suitable adhesives material
ii) Difficulties in the application of adhesives
iii) Little knowledge about bond design criteria.

The introduction of adhesives has led to a substantial reduction in the amount of conventional joining using methods such as welding, riveting and bolting, which have given way to bonding. They are finding increasing applications in manufacturing industry, primarily due to the much improved performance now offered by adhesive materials, which can be achieved on a variety of substrates. Vehicle steel doors manufactured using a combination of spot welds and epoxy adhesives along the hem are 400% structurally stronger than the ones produced by spot welding alone [Zaber 90].

This chapter aims to give a general review of adhesives and structural adhesives in particular. Advantages and disadvantages of using adhesives instead of conventional joining are then covered. This is followed by automation, to explore the principles of robotic systems and their application and benefits to the adhesive dispensing process. The

different methods of dispensing are then discussed. Finally, automated adhesives joining is compared with other continuous path applications such as painting and arc welding.

2.2 Adhesives Classification

Adhesives can be classified in two groups as organic and inorganic materials. Each group further may be divided into subgroups as shown in Fig. (2.1). Some of these products such as natural organic adhesives have been in use since ancient times. The most common engineering adhesives are based on *synthetic organic* materials.

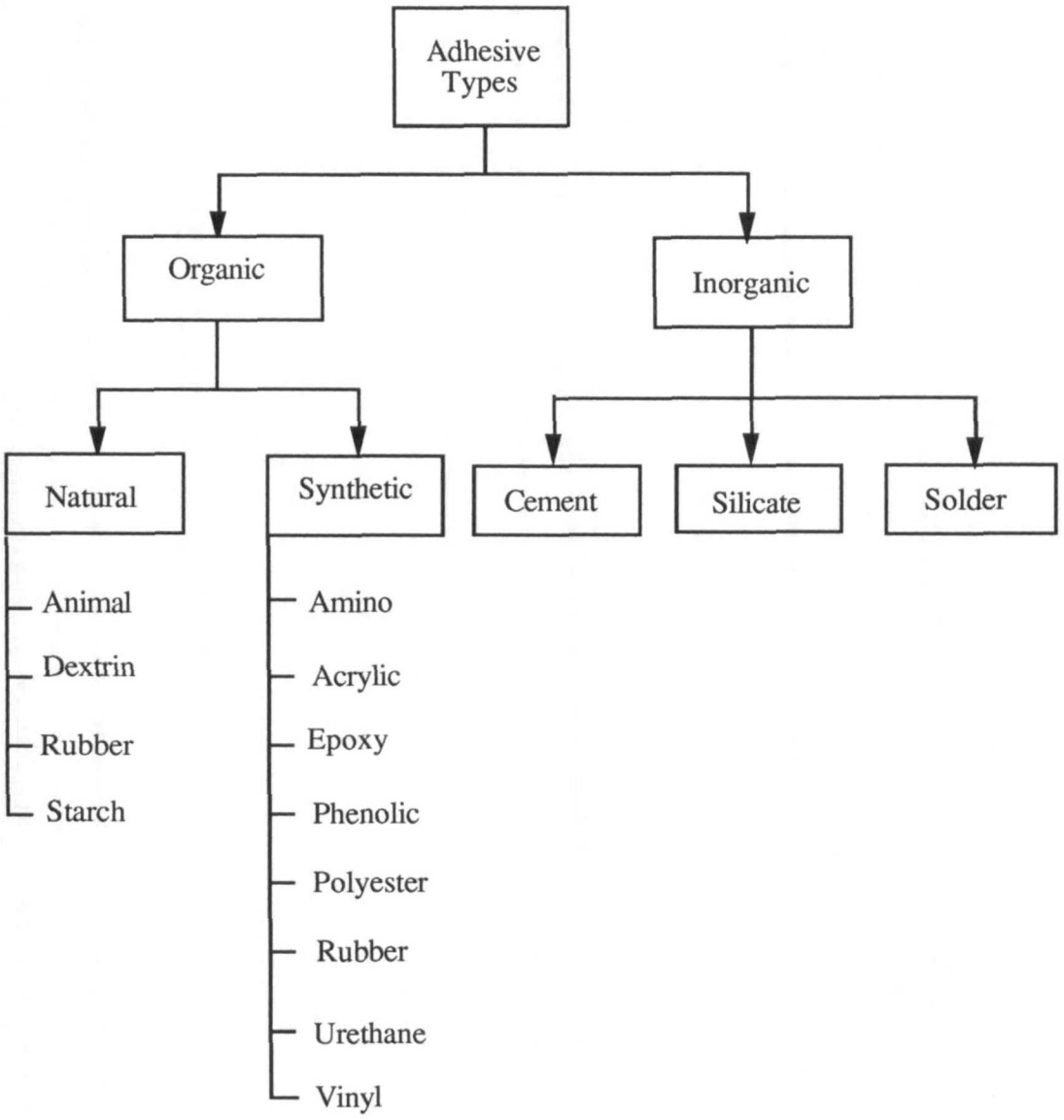

Figure 2.1 Principal of adhesive classification [Leeds 89].

Structural adhesives primarily can be classified in two group in terms of their application, stress bearing and non-stress bearing [Hayes 76]. The first group can withstand large applied stresses and cope with constant stress at elevated temperature. The shear strength is usually of the order of 15-25 N/mm^2. The latter group, however, has satisfactory performance under limited and occasional applied stress, and usually can not stand under applied stress for a long period of time, its shear strength is about 1-2 N/mm^2 [Lawley 87]. Adhesives can be used as single or multi-component materials. The multi-component adhesives are only used when the single component adhesives are not suitable for the application.

Two part adhesives are usually used where curing a single material is neither economical nor practical due to risk of distortion. They have the advantage of having a long shelf life over single component adhesives. However, their disadvantage are due to the difficulties encountered in developing pumping equipment, capable of delivering two components, thoroughly mixed and to be transferred in the right proportion to a dispensing nozzle [Lawley 87].

2.3 Adhesives Selection

Selection of an adhesive appropriate for a job depends on many factors such as substrates, environmental conditions and forces in the joints. However, some of the requirements which need to be considered are:

i) Strength: this is an important factor for structural bonding. The load bearing must be consistent with the required application.
ii) Adhesion: this needs to be maximised to substrate materials while maintaining a balance with toughness and impact resistance.
iii) Required Durability: the strength of the bond should be maintained under the design conditions.
iv) Heat Resistance: maximum surface temperature should be specified. Many bonds are not particularly heat resistant and most of the adhesives are not suitable for temperatures above 200 °C.
v) Joint Design: this is an important factor for having an effective joint which can be readily manufactured.
vi) Substrates: substrate cleaning and pre treatment is necessary for optimum performance of an adhesive.

2.4 Advantages of Adhesives and Sealants

Applying structural adhesives has the following advantages:

i) Enables joining of dissimilar materials, e.g. metals, plastics and wood.
ii) Allows the fabrication of complex shapes where other means of fastening are not practical.
iii) Reduces distortion of components by heat. Thus, it does not create any changes in metal characteristics that leave the metal prone to rust.
iv) Increases the corrosion protection by creating a moisture barrier in the inner cavity behind the hem flange preventing water, condensation and salt residue collection.
v) Reduces of the noise and vibration in the joints.
vi) Reduces weight.
vii) The bond is continuous, improving the strength. Stress tends to be uniformly distributed rather than concentrating on the stress points where spot welding and mechanical fasteners are located. This means that components can be constructed from thinner gauge metal, resulting in reduction of weight and metal costs [Politi 90].
viii) Increases design flexibility.
ix) Allows bonding of heat sensitive materials.
x) Allows thermal and electrical insulation.
xi) Sometimes cheaper and faster to use than mechanical fasteners.
xii) A sealed joint is normally achieved giving good environmental resistance.
xiii) There are no finishing costs.
xiiii) It is easy to combine with other fastening methods.

2.5 Disadvantages of Adhesives and Sealants

There are some disadvantages and limitations of using adhesives and sealants when compared to welding or mechanical fastening. These are as follows:

i) For optimum performance adhesives and sealants need to be carefully applied. Otherwise the operation can be very messy, and it can contaminate the component and subsequent processes.
ii) Good surface preparation is essential for proper adhesive performance.
iii) The engineering adhesives do not have a good resistance at high temperatures, i.e. 200-250 ^{o}C [Leeds 89], and increasing the service temperature usually decreases the bond strength.

iv) Accurate dispensing is usually required since it is not possible to paint over some adhesives or sealants. Otherwise, coating and finishing are recommended before painting.
v) The impact resistance at high speed is not good.
vi) The properties of the adhesive change with time, e.g. when subjected to changes in temperature, viscosity, humidity and chemical attack such as from salt corrosion.
vii) Visual inspection of the bead quality is generally a difficult task, and development of high quality inspection equipment such as vision is essential.
viii) The quality of bond adhesion for a cured joint, can not generally be obtained by NDT methods.

2.6 Adhesives and Sealant Bonding

Achieving the desired bonded assembly requires a range of disciplines including expertise in the following areas;

i) Adhesive or sealant formulation.
ii) Component design specification and use of engineering bonding manuals.
iii) Production engineering.
iv) Coating hardware.
v) Automation/robotics (in the case of using an automated system).
vi) On-line process control.
vii) Integration of quality control sensors.
viii) Quality inspection

2.6.1 Adhesives and Sealants Bonding Application

Structural adhesives were first used in the aerospace industry around 1920 for bonding structural components of aircraft, missiles and satellites [Politi 90]. Their usage then extended to the other industries especially into the automotive industry where they are used in highly stressed areas. Applications are in (metal to metal) hem flanges, roof rails, coach joints, radiator fins (plastic to plastic) body panels, roofs, deck lids [European Adhesive and Sealant 90]. Besides body structures, adhesive and sealant are used in:

i) Engine / transmission (bearing retention, joint sealing, nut locking).
ii) Engine / suspension mounting; metal to rubber bonding.
iii) Badge and trim fixing; pressure sensitive, hot melt and liquid forms.
iv) Air / oil filter manufacture.
v) Brake shoes and pads to linings.

vi) Electrical parts, e.g.. lamp reflectors to lenses, encapsulation of electronic parts [Lawely 87].

However, the potential application of adhesives has penetrated into other industries such as: defence industries, shoe manufacturing, packaging, electronics industries, construction, transportation, recreation, health and domestic appliances

2.6.2 Adhesives Bonding Quality

The major factors in the quality of adhesive bonding are viscosity, reaction (cure) rate, strength, durability and surface preparation. These will be discussed in more detail in the following paragraphs [Leeds 89].

i) Viscosity: the adhesive viscosity is one the most important factors affecting the bond characteristics. It is a function of temperature, age of adhesive, shear condition, batch variation and storage condition.

i-a) Shear condition and shear history: this factor can be ignored in most cases, since if the adhesive and pumping system have been designed to be suitable for one another, the conditions will be constant.

i-b) Temperature: if the temperature of the adhesive changes then so will its viscosity. This in turn affects the rate of application. Temperature changes may arise as normal fluctuations within the factory environment.

i-c) Batch variations: when a fresh drum of adhesive is brought into the factory from unheated storage area. Superimposed on the temperature effect is the batch to batch variations that constitute the normal manufacturing tolerances. Whilst manufacturers set their manufacturing tolerances as closely as practicable, some variation in viscosity is inevitable. The worst of the temperature effects can be minimised by placing a new drum 24 hours in advance to enable it to acclimatise.

i-d) Age of adhesive and conditions of storage. Adhesives have a finite shelf life, and the viscosity of adhesives tends to change in storage although the manufacturer usually sets a shelf life for the product such that it will be easy to pump.

ii) Reaction (cure) rate. The reaction rate is determined by temperature and gap between the components and catalytic activity of the surface.

iii) Strength: in addition to the materials used, the strength of the joint will be affected by bond line thickness, surface roughness, the components modules, the joint area and surface cleanliness.

iv) Durability: joint durability is a function of the environment, adhesive grade, component materials, surface condition and bond line thickness.

v) Surface Preparation: the quality of the surface is an important factor in the performance of adhesive bonds. Some of the adhesive can cope well with oily surfaces by dissolving mineral oils. However, slower cure, lower strength and poorer durability should be anticipated. Thus, substrate cleaning and pre treatment are necessary in order to get optimum performance of the adhesive.

One of the major benefits resulting for joints completely filled by adhesives, is that the ingress of air and moisture is suppressed and corrosion is thus prevented. This is beneficial where fasteners are used in an aggressive environment.

2.7 Automated Dispensing System

The need for a high quality adhesive bead with durability, requires the adhesives to be applied consistently and reliably, requiring strict adherence to processing procedures. This however, cannot be guaranteed when manual processes are used for the application of adhesives. Manual methods are notorious for their lack of consistency with many examples of incorrect preparation, the bead being dispensed in the wrong place or in the wrong quantity. Industry has many examples of workers not preparing the workpiece adequately, of dispensing the wrong quantity of adhesive, or putting it in the wrong place [Davies 90a].

This implies a need for automation in dispensing the adhesives. There are two principle methods associated with an automated dispensing system. These are:

i) Hard Automation: this generally consists of an X-Y table carrying a component. The adhesive may be applied just on one surface and the table is specifically designed for one workpiece. This method can not be used for a complicated bead pattern.

ii) Flexible Automation: uses a robot for carrying the dispensing applicator. The end effector can be moved along the desired path trajectory, and the robot can be programmed to be used for different parts with complex bead patterns. The use of robots to apply adhesives offers improvements with existing products and also favours their more

widespread use. The major advantage of robot and automated manufacture, in the context of adhesive use, is that a greater degree of control over the manufacturing process may be exercised to produce quality bonded joints. Also, the prepared surfaces are not contaminated during manual handling, prior to adhesive application.

2.7.1 Automated System Applications

The most common use of automated dispensing systems in body fabrication in the automotive industries are:

i) Interior seam sealing: this involves the sealing of body joints which prevents the entry of moisture and wind noise into the passenger compartment. The bond is generally 19.1-38.2 mm wide and 1.3-3.2 mm thick [Turner 90].

ii) Bonding of automotive doors: manual application of adhesives and sealants to hem-flanged assemblies is generally impractical because of the high accuracy required. An adhesive bead of 2.5 mm to 5.0 mm is dispensed on a panel with an extruded nozzle [Turner 90]. Accurate bond placement and uniform material deposition are critical in achieving structural bonding.

iii) Windshield bonding: structural adhesives are used to join the windshield to the car body. Windshield bonding often requires the dispensing of a rectangular bead with a 10.2 mm base and a 11.9 mm height [Turner 90].

iv) Sealing of body component joints: this is used in conjunction with welding. The sealant is usually applied with a diameter of 2.5 to 5.0 mm and the bead is compressed after welding to form a seal in the welded joints.

v) Threadlocking: the problem of loosening threaded fasteners is very common. This stems from the ability of the adhesive to completely fill the space between threaded components so as to prevent movement, whether axial, transverse, or rotational. In some situations the adhesive may be applied after a fastener is tightened. In this case, a very low viscosity liquid, capable of penetrating the joint, is required. In design the following factors need to be considered:

v-a) Whether the locked fastener has to be dismounted at the future date.
v-b) The strength of the fastener itself.
v-c) The severity of the service conditions.

2.7.2 Automated System Components

The majority of bonding operations are labour intensive with various manual dispensing units available for each case. Applying fine, precise beads of adhesive in such environments creates complications and difficulty which need to be overcome. The robot lends itself to automated adhesive dispensing because of its repeatability, flexibility, reliability and positional accuracy. The first applications of using robotics to apply adhesives were in the automotive industries.

In terms of equipment, the robotic dispensing system consists of:

i) A robot for carrying the dispensing gun to apply the adhesives.
ii) Dispensing and pumping equipment for supplying the adhesives to the gun.
iii) Quality inspection equipment.

2.8 Robotic Systems

The early concept of an industrial robot was first introduced by George C. Devel and Joseph F. Engelberger in the mid 1950's. They developed *Unimate* (for universal assistant) a servo-controlled manipulator for loading machines [Jabonowski 86]. In many industrial applications of robots, the objective is to replace human labourer with machine labourers that are more accurate, efficient and productive. Industrial robots are today used in a wide range of tasks in manufacturing industries such as; assembly lines, machine loading, injection moulding, spot welding, arc welding, painting and recently dispensing adhesives and sealants.

Before going into more detail about the applications of robots, it will be helpful to give a definition of the industrial robot. According to the British Robotic Association: "An industrial robot is a re programmable device designed to both manipulate and transport parts, tools, or specialised manufacturing implements through variable programmed motions for the performance of manufacturing tasks [BRA 83].

Industrial robots are usually powered by electric servo motors and controlled by a computer, to move parts, materials and tools through a pre-defined path trajectory. They are capable of laying down an adhesive bead over components in either 2-dimensional or 3-dimensional curved space at a variety of lay down speeds to suit straight and curved segments.

Some of the key factors for the robot selection are payload, speed, accuracy, repeatability, reach, articulation requirements, controller capability, programmability and proven performance in the field [Scafe 88]. In general, required robot performances for adhesives application are [Kelly 85]:

i) Smooth jerk-free motion.
ii) Good wrist articulation.
iii) Accurate output switching.
iv) Positional accuracy.
v) Repeatability.
vi) Continuous path capability.
vii) Control of end-effector altitude to panel interface with associated equipment.

Only servo-controlled robots offer acceptable performance in terms of these criteria. In addition the robot has to be programmed at different speeds for different parts of the path.

Many robot controllers allow for the control of external devices via analogue and digital signals. Thus, it is possible to control the adhesive flow rate through the robot controller. The analogue signals are usually available in the ranges of 0 - 10 volts or 0 - 12 volts or in terms of currents, in the ranges 0 - 20 mA, 4 - 20 mA or 0 - 50 mA. The digital signals are usually available for input and output interfacing.

2.8.1 Types of Robot Coordinates

The robots must be able to reach the workpiece and to perform the desired tasks. This requires the combined movements of arm, wrist and end-effector. Robots can move their arms in a variety of geometric configurations corresponding to their coordinate systems. These coordinates are Cartesian (rectangular), cylinder, polar and revolute coordinates [Engelberger 80]. For different applications a certain coordinate system may be more appropriate.

The robots using Cartesian coordinates are useful in providing an overhead carrier for working over a large floor area whereas cylindrical robots have restricted volume access. Polar (spherical) coordinate robots can cover a large volume from one central support. Robots with revolute (jointed) coordinate systems have the maximum flexibility and can reach any parts of the work volume. Industrial applications of different robot configuration are given in Tab. (2.1).

Robot Types	Application
Cartesian	pick-and-place, assembly operations, sealant, spot welding and arc welding.
Cylindrical	Assembly operations, handling of machine tools, spot welding, handling diecasting machines and arc welding.
Polar	handling of machine tools, spot welding, handling diecasting machines, fettling castings, gas welding and arc welding.
Revolute	Handling die casting machines, fettling castings, gas welding, arc welding and spray painting.

Table 2.1: The industrial application of different robot configurations [Hartley 83].

2.8.2 Types of Robot Control

Non-servo and servo control are the two major methods for controlling robots. Early generations of robots were of a non-servo type and used pneumatic cylinders, hydraulic cylinders or electric motors. The more advanced robots are servo control led robots and are powered by electric motors. They also use position sensors as a feedback to control the movement of the joints [Considine 86].

The robots are able to move point by point, continuous-path or controlled path. Point to point robots are the simplest form of robot and can move from one specified point to another, able to stop at any point only if previously designated. On the other hand, continuous-path robots are able to stop at any specified number of points along a path. But every point on the path must be stored in the memory of the robot. A more sophisticated type is controlled-path robots where the path trajectory is controlled by computer. The path generator of the robot can generate straight lines, circles and interpolated curves with high accuracy. Paths can be defined either geometrically or algebraically. All controlled-path robots are servo-controlled, thus their position is fed back in such a way that the controller can cause a particular path to be followed. But, the point to point and continuous path robots are usually non-servo robots. They often have end-point sensors (e.g. micro-switch).

2.8.3 Drive System

Drives are the source of power that drives robot articulated links to the desired location. They are usually applied at the joints either directly or indirectly for each robot articulation. The robot drives are usually hydraulic, pneumatic, electrical or some combination of these.

Hydraulic drives are either actuators using a linear piston controlled by solenoid-operated valves or rotary vane and motors using piston, gear, vane and ball configurations. They can generate greater power in a compact volume than electric drives. But their positioning accuracy is low and high precision hydraulic drives are more expensive and less reliable than low power electric drives [Critchlow 85].

Amongst the three, pneumatic drives are widely used in industry and are the simplest and cheapest drives. Both linear cylinders and rotary actuators are used to provide the motion required. Pneumatic drives have light weight when operating pressures are moderate but their efficiencies are low and to achieve high precision is quite difficult [Considine 86].

Electrical drives are in the forms DC (direct current), AC (alternating current), electric motors and electric stepping motors. DC motors run continuously and smoothly in one direction and do not have any inherent positioning control. Precise positioning control requires a closed loop system using position as a feedback. Whereas stepper motors are able to step precisely to a designated position under the control of electrical pulses and can be used either in open-loop or closed loop. On the other hand AC servo motors are more reliable than DC servo motors. Electrical drives are inherently clean and capable of high precision which makes them attractive for continuous-path operation. Electrically actuated robots can achieve smooth motion and high repeatability [Critchlow 85].

Robots used for adhesive dispensing applications must have the ability to carry an applicator consistently around a predefined path at a specified speed, eliminating the basic drawbacks of a manual system. They must also be able to move at different speeds at different segments of the bead path. Robots with 5 or 6 degree of freedoms usually are required for flexible automation of adhesives dispensing.

2.8.4 Robotic System Classification

The major components for the robotic systems are a robot, workpiece and a place to work. But the robotic system can be more complex with a few robots working together or to have

a greater flexibility and be integrated with its peripheral equipment. Basically, the robotic system can be classified as follow:

i) Simple systems: this type of system is like pick-and-place robots, where the gripper grasps the objects and moves them from one location to a specified location. The system arrangement is very simple and consists of a robot manipulator, a robot controller and a workpiece. There is no external communication in this type of system.

ii) Complex systems: in a complex system, there are more components than just a robot, such as sensory system, another robot or a conveyor. These components must work together and send and receive information during the course of operation. Usually, this procedure is required for computer communication and coordination between components, actions and control of the whole operation.

iii) Integrated systems: as a robotics system becomes more complex and more important in production lines and manufacturing, the robot's motion has to be coordinated with more than just a response from a single sensor. The system must be connected to the other production facilities such as CNC machines or intelligent sensors and be fully integrated into the whole cell (called an automated cell). The overall cell has a controller to coordinate and synchronise the operation of the individual components in the cell.

2.8.5 Advantages

The main advantages of the robot are the greater degree of control over the dispensing process and the non-contamination of the prepared surfaces prior to adhesive application through manual handling. Basically, a robotic system virtually eliminates human errors and increases production. In general, the advantages of using robots are:

i) Uniform application of the adhesive bead: to have higher quality bonded joints for structural applications such as in the automotive industry, a uniform adhesive bead is required. Robots can maintain, with high repeatability, a consistent bead of material while laying adhesives along accurate trajectories.

ii) Reduction in material cost: in manual cases the operator supplies too much material in the manual operation which also increases the amount of rejection during quality control inspection. Thus, the material cost saving both of workpiece and adhesive can be very significant over long periods of time by using robots.

iii) Better working environment: ability to operate in hazardous environments without workers having a direct contact with adhesive materials. This reduces the health hazards to workers from dispensed materials and potential long term problems.

iv) Process flexibility: the robot can easily be reprogrammed for any design changes, depending on the particular operation that is required.

v) Use of a wider range of adhesives: it is difficult to ensure that adhesives go into the right place when applied manually. Thus, the ability to remove the surplus is necessary which reduces the range of adhesives type which could be used manually.

vi) Use of cured adhesives: as it is difficult to ensure the location of an adhesive when manually applied, the ability to remove surplus adhesive easily has also become necessary. For this reason, almost all the adhesives and sealants used in the basic car have been either non-curing materials or heat curing products and are cured when the vehicle goes through the paint stoving ovens [Ludbrook 85]. Thus, due to high accuracy and repeatability cured adhesives can be easily applied using a robot.

2.8.6 Disadvantages

From the general description of the automated dispensing systems it is clear that they provide more control and flexibility over the dispensing cell than the human operated dispensing system. The use of robots eliminates many problems associated with the manual application of fluid adhesives. However, they have introduced a number of problems of their own.

i) Sight disability: although robots apply adhesives in a repeatable form, they are blind and unable to detect whether a gun is dispensing adhesive, or whether there is foreign matter or an obstacle along the path trajectory. It is hence important for the robot programmer to ensure that the robot follows the desired path and the path is free of obstacles. The robot has to move in a smooth continuous path motion along the desired trajectory without significant deviation from the path and jerkiness. Some means of detecting a break in adhesive flow such as post process inspection needs to be included in the system to detect any discontinuities in the adhesive bead.

ii) Slower cycle time: the robot based dispensing system is slower than multi-nozzle dispensers but compatible with single nozzles.

2.9 Dispensing Systems

A dispensing process is a very complex, and consists of a multitude of individual control loops, each of which requires measurement and control of at least one process variable. The simplest form of dispensing is the pump-gun combination used for manual applications which provides poor adhesive flow control.

McGinnis et al [McGinnis 91] from Boeing's manufacturing research and development department in Seattle, Washington have introduced a new hand gun dispensing system for two-part adhesives. The system has a dispenser, a duel-barrel cartridge and a plastic static mixer which work as an integrated unit. They claim the dispenser reduces waste and improves safety.

More sophisticated dispensing systems consist of pumping equipment and a flow control system.

2.9.1 Pumping Equipment

The pumping equipment usually consists of a high pressure pump, pressure regulator and flow meter. Pump selection depends on the properties of the material, the container size, and the dispensing rate.

2.9.2 Flow Control Systems

The systems which can be used to control material flow are:

i) Programmable pump: the flow rate at the applicator nozzle is controlled by changing the rate at which the transfer pump propels the adhesive along the delivery pipe, with a constant delivery orifice. The output is affected by the compressibility of the dispensed material. The disadvantage of this system is that the response time to fluctuating flows is slow and there is hysteresis in the system which reduces control over the output rate.

ii) Variable pressure regulator: the flow rate of the applicator is a function of adhesive line pressure, and can be set by the pressure regulator. Therefore, by changing the pressure setting in the adhesive line, the flow rate can be altered. The flow rate can be controlled through the robot controller. This is useful where only specific flow rate is required and a change of flow along the path is not essential. The response time for increasing the pressure is fast, but it is very slow when the pressure is lowered since it takes some time to

depressurise to the new level. It also might create a surge in the material line which will be difficult to control.

iii) Extrusion system: this method introduces less shear in the material than the other ones, thus it may have less effect on the rheology of the applied material. There are two possible methods;

iii-a) Extrusion at the point of application: this is achieved using a motorised ram that moves the piston of the extrusion cylinder at a specified rate and is designed for dispensing fluid silicone gasket type material. The system also has a simple on/off valve at the outlet point. The extrusion head should be mounted at the robot end effector which may create over load problems due to the limitation of robot payload. The size of the extrusion cylinder is a function of:
- adhesive bead size and path length, and
- material viscosity

iii-b) Extrusion from a point away from the head in the feed line: the adhesive may be extruded from a point away from the applicator by putting an extrusion cylinder piston on the robot arm. The cylinder has a hydraulic drive and uses an on/off valve for material discharge. There will be a transport lag in the system which can be minimised by mounting the cylinder as close as possible to the applicator.

iv) Programmable flow valves: the adhesive flow can be controlled by pumping adhesive to the applicator at a constant pressure and varying the orifice size. This is the most common method, and it has the widest range of applications. There are two different variable orifice systems:
- control at the applicator bead, and
- control ahead of the applicator bead.

iv-a) Control at the applicator bead: this variable orifice system works on a needle valve principle, the position of the needle valve being controlled by electric or pneumatic drive systems mounted on the applicator head. The material at the applicator head needs to be at a constant pressure in order for the process to be successful. The constant pressure can be achieved by;
- the use of a pressure regulator in the supply line or,
- the use of a single acting pump based device designed to have sufficient capacity in a single stroke to accommodate the maximum bead size.

This method is widely used in advanced dispensing systems such as the Nordson Pro-Flo dispensing system [Industrial Robot 89b, Nordson 90].

iv-b) Control ahead of the applicator bead: the variable orifice can be mounted on the robot arm ahead of the applicator which will reduce the load on the robot end effector. But this introduces some delay in response. However, the advantage of this method is that, it can be more robust. This method is used in the Graco Master-Flo dispensing system [Davies 90a].

There are a number of programmable flow valves in the market using a variable orifice. Intec from Germany has a product which is marketed by Mansign Engineering in the U.K., Kremlin in France, Nordson in the U.S.A. (Analogue and digital versions of Pro Flo system) and SCA in Germany [Industrial Robot 89a]. These systems are being used in major manufacturing plants world-wide.

2.11 Comparison of Continuous Path Application

For straight lines, adhesives can be laid at relatively high speeds with good accuracy. This is opposed to other continuous path processes such as arc welding which operates at much lower speed, and painting where positioning accuracy is not critical. In terms of seam geometry , adhesives can be applied to either 2-dimensional or 3-dimensional components while welding is just 2-dimensional and the dimension is flexible in painting. Both the bead size and bead location are important factors in adhesive dispensing as in welding: the seam position is the major concern. A summary of the comparison between adhesive application, arc welding and painting is given in Tab. (2.2).

2.12 Summary

This chapter was aimed at introducing the advantages and disadvantages of replacing adhesives with conventional methods of joining in industry. It is clear that the replacement of conventional methods of joining with structural adhesives has numerous advantages. The automation of the adhesive dispensing process and different methods of dispensing were also discussed. It was argued that for better joining quality, a consistent bead is essential. This necessitates the use of automated systems. The next chapter will cover the industrial vision system which has been used for automatic inspection in the automated cell.

	Adhesive/ Sealant	Painting	Arc welding
Accuracy (mm)	1	10	1
Speed (mm/sec)	100 - 1000	100 - 1000	10 - 100
Scan Height (mm)	1 - 2	-	5 - 10
Geometry	3 - D	Flexible	Planar
Work Space	Tight	Tight	Open
Medium	Viscoelastic	Liquid	Solid

Table 2.2: A comparison of requirements in continuous path applications [Haung 84].

CHAPTER III

COMPUTER VISION APPLICATIONS

3.1 Introduction

As industrial applications of robotic systems became more complex, it was obvious that the success of robotic applications was dependent on their ability to have some form of intelligent sensing for on-line quality inspection. Advances in the area of sensing technology enable designers to solve some of those problems with special purpose sensors. From the late 1960's many attempts have been made to emulate the human vision system in an industrial environment. A visual sensor is a non-contact sensor that detects and processes information in form of images. The requirement was to have a reliable, low cost and fast image processing technique. Thus, special vision system techniques were being used to handle specific industrial problems. The vision application can be classified in four groups; Recognition, predetermined guidance, continuing guidance and inspection [Braggins 86].

The image processing technique has been used in many areas such as medical diagnosis, manufacturing process inspection, assembly lines, guided vehicles, radar and satellite data analysis. Two major applications of vision systems in manufacturing are for the control of manipulators and for automated inspection [Kak 85]. Most of the vision systems use a static camera placed on the end-effector of the robot, or at a location above a workpiece. This has the advantage that while vision data are being acquired and processed, the robot can proceed with some other part of the industrial process. However, this has the disadvantage that the workpiece might be blocked or fall out of the domain of the vision system making the vision ineffective [Kak 85].

To increase the quality of bonded joints for structural application, the use of automated systems is essential. In order to achieve this goal, on-line quality control inspection of the automated dispensing of adhesives is inevitable. Thus, a computer vision system is used for calculation of bead parameters while an adhesive is being laid on the component. In this research, an active three dimensional vision system technique has been used. This is due to the fact that the adhesive bead is a three dimensional scene and there is a need for image

processing in real time. With this vision technique, 3-D information can be driven from 2-D images by using the interaction between a camera, a laser diode and the adhesive bead. Here, first, the use of vision systems in related industries, such as arc welding is covered. The principles of computer vision are then discussed. Then, the hardware and software descriptions of the Joyce Loebl and the transputer based vision system are covered. Finally the implementation of the customised vision systems in terms of both hardware and software is analysed.

3.2 Use of Vision Systems in Related Areas in Industry

The increasing demand for quality control in manufacturing industries makes the use of a computer vision sensory system essential for inspection and assembly lines. Some of the advantages of using a vision sensor in industry have been discussed by Schmitt et el [Schmitt 86]. Many applications based on using vision sensors for on-line inspection have also been developed and been implemented, but the most common use of vision systems in joining is in the welding industry.

Toda and Masaki [Toda 80] have developed a vision system called the Kawasaki vision system to be applied for path correction in arc welding. The system consists of a laser pattern recognition unit, an image detection unit and an image processing unit. The system operates by projection of an optical slit pattern from a laser pattern recognition unit. The pattern is transformed by the surface shape of the part to be welded and detected by the image detection unit. The pattern information is then transformed from the image detection to the image processing unit. Finally, the relative position of the welded point is calculated by using cross correlation values between template image and actual image. This method is quite time consuming and is more suitable for off-line applications or on-line applications where the speed is very low.

Another application of a vision system in welding has been developed by the National Research Council of Canada (NRCC) [Dufour 83]. This application combines the use of fast vision techniques with an image pre processor for real time control of the welding process. The pre-processor obtains a binary image using a video signal and a preselected threshold contained within a dynamically programmable rectangular window covering a small portion of the field of view. The area and the first moment of the white level figure contained within four independent rectangular windows in the field view of the camera are then calculated. Thus, visual sensing, image processing and welding are achieved simultaneously. This method is quite fast for arc welding applications and is used for robot

speeds up to 17 mm/sec. This robot speed is very low for adhesive dispensing process in which the robot speeds of up to 400 mm/sec are typical.

Clocksin et al [Clocksin 85] have implemented a model-based visual sensor for robotic arc welding. The system uses models for automatic visually guided control of a metal/inert-gas (MIG) welding robot. By using these models, the variations in sheet steel assemblies such as gap width, stand-off error and lateral error can be detected. Thus, the errors in the position of the welding torch are corrected to within ± 0.5 mm, which is a suitable tolerance for producing good welds in such assemblies. Furthermore, seam widths are detected to dynamically alter welding parameters.

Cincinnati Milacron [Webb 88] has used the Oldelft Seampilot Profile vision system in welding applications. Seampilot is comprised of a laser scanner/camera head, mounted on the end of the robot, a camera control unit and a signal processing computer. The developed system "Milascan", an integrated seam tracking system, is capable of compensation for part placement errors and provides a real time seam tracking function. The robot orientation and workpiece position are changed dynamically to achieve the desired process angle for real time seam tracking. The tracking accuracy is ± 1.3 mm and the tracking speed is 83 mm/sec.

An adaptive real time intelligent seam tracker using a robot held, laser based, vision system for automation of arc welding has been developed by N. Nayak at Pennsylvania State University [Nayak 89]. The automated cell has two levels of controller. A high level controller uses rule-based heuristics and model-based reasoning to achieve decision in real time. The low level controller tracks a three dimensional seam (using a vision system) with the correct torch orientation while keeping the specified welding speed. The design is based on the concept of a zero-pass technique where three dimensional information of the seam trajectory is collected and processed for real time guidance and control of the welding torch trailing behind the laser -based vision sensor. The zero-pass concept eliminates the need for pre-programming of the weld path and thus potentially enhances the welding cycle time for small batches. The system is designed to achieve a welding speed of about 25 mm/sec. Although the use of a knowledge-based system looks very useful, KBS is not considered for this part of the research.

In all of the above applications, the vision system is basically used for seam tracking and path correction where the time scale is in minutes. The major requirement is the correct position of the torch and the location of the weld spot whereas in the adhesive dispensing process, the main interest is in real time quality inspection of the adhesive bead. The application of arc welding is much slower than adhesive dispensing process (see § 2.11 for

further detail). This will be explored further in chapter 5 which covers the experimental modelling and control of the bead parameter using visual information.

3.3 Principles of Machine Vision

Machine vision (or computer vision) can be defined as a process of extracting, characterising and interpreting information from two or three dimensional images. It can be classified as two dimensional, three dimensional via two dimensional and active three dimensional. The first class is usually based on visible band luminance data and deals basically with sensing of patterns lying wholly on a surface. These patterns are reflectance variations already existing on the surface. They can be printed letters, geometrical marks or masks resulting from pads on an integrated circuit board [Corby 83].

The second class (three dimensional via two dimensional) uses various constraints to reduce the three dimensional problems to two dimensions and is widely used in robotic applications. The technique does not depend on a specific knowledge of interaction of illumination and surface. Rather it depends on identifying identical points or regions in multiple two dimensional images. The images can be produced from one or multiple sensors located at various points in space. The technique of obtaining multiple images is called stereo vision and is very complex and time consuming.

In the active three dimensional vision technique (the third category), specifically designed energy sources are used. Three dimensional information of the image is obtained by interaction between the energy source and the objects in the field of view. The two major techniques in active three dimensional vision are:

i) Structured light illumination, in which the image is obtained by the interaction of the structured light source and the object to produce two dimensional images and retrieve surface shape in three dimensions. The Structured light illumination technique is widely used in industry for inspection due to its flexibility and lower computing cost.

ii) Direct range images, in which the measurements can be made point by point and collected to form a three dimensional range image. This method is used in radars and sonars to measure the speed of propagation of phase related effects.

The computer vision process can be divided into four areas: sensing and image acquisition, reprocessing, segmentation and description, recognition and interpretation.

3.4 Sensing and Image Acquisition

Focusing on an optical image of the scene, the sensors (usually two dimensional transducers) convert the visual information to electrical signals. The most commonly used visual sensors are vidicon camera and solid state arrays [Gonzalez 82]. Special infrared cameras are also used for thermal imaging and ultra violet light is used in inspection techniques for track detection.

Vidicons are the vacuum tube cameras used as TV imaging devices and the input video signal after digitisation is transferred to an image in a computer. The image resolution is between 64x64 to 512x512 pixels. They are widely used due to their reasonable cost and availability. However, the image is not quite accurate and has signal drift, noise and distortion in the image.

Solid state arrays are available as linear and area arrays. Resolutions in linear array cameras range from 256 to 4096 pixels. Two dimensional (area) array cameras are similar but have a matrix format with resolution of 512 by 512 or 1024 by 1024 pixels. The exposure time (time between two successive scans) for a line scan array is typically less than 1 msec whereas area arrays operate at about 16 to 20 msec [Loughlin 89].

The most widely used solid state cameras are Charged Coupled Device (CCD) array sensors and consist of a row of silicon imaging elements called photosites. The amount of charge collected at each photosite is proportional to the illumination intensity.

Illumination of a scene is another important factor for minimising the complexity of the image resulting from an inspection. Arbitrary lighting of an environment may result in a low contrast image, specular reflections, shadows and extraneous details which make the resulting image unacceptable. Thus, lasers as a source of light have been used for their brightness, coherence, beam directionality and monochromaticity.

There are four different illumination techniques; diffuse lighting technique (for objects with a smooth and regular surface), backlighting (for applications where the silhouette of an object is sufficient for recognition and measurement), directional lighting (used for inspection of rough surfaces) and structured light technique.

The structured light technique uses a spatially modulated light source for object classification by projecting points, strips or grids onto an object. The shape of the object distorts the light pattern and the dimensional characteristics of the object are calculated by

measuring this distortion. This method of lighting is generally used to detect three dimensional properties of an object with only two dimensional images.

Ordinary light sources are not always the best choice in all of the above illumination techniques. In many inspection applications, lasers have proved to be more effective because of their brightness, coherence, beam directionality and monochromatically. Lasers used in inspection techniques usually emit from 1 mW up to a few Watts.

3.5 Image Reprocessing

Once images are captured and digitized, the digital images can then be reprocessed by digital processors to extract required features or be stored for later processing. The area of image processing is probably the most important part of a computer vision system. There has been a great deal of research using different reprocessing techniques for various applications. Batchelor [Batchelor 85] has given a detailed explanation of many image reprocessing and filtering techniques for edge detection and image enhancement.

There are two major methods for reprocessing: spatial domain methods and frequency domain methods. Spatial domain refers to the aggregate of pixels composing an image and they operate directly on these pixels. The neighbourhood of a pixel can be defined as any area around the centre pixel and can be either a square, a rectangle or a circle. This method is widely applied in machine vision and uses convolution masks or template filters. A mask can be a small 3x3 array used to detect isolated pixels in a predominantly constant intensity background as shown in Fig. (3.1). The sum of the pixels is zero if they all have the same

-1	-1	-1
-1	Positive Value	-1
-1	-1	-1

Figure 3.1: Array of 3x3 for detecting isolated pixels from a constant background.

value. However, if the central pixel of a mask is an isolated point, the sum is not zero. The centre isolated point is also stronger in magnitude than off centre points.

Frequency domain refers to an aggregate of complex pixels resulting from taking the Fourier transform of an image. This method requires extensive reprocessing time and is used for analysis of object description, object defect and object motion. Smyth [Smyth 87] has discussed the application of Fourier analysis in a computer vision system in more detail. However, the reprocessing time for the Fourier transformation is quite high which makes it unattractive for real time applications.

Smoothing is also used for noise reduction and elimination of spurious effects which may be present in an image as a result of sampling, quantization, transmission or disturbances during image acquisition. Smoothing techniques can also be used for binary images by labelling the dark points by 1 and light points by 0.

3.6 Segmentation

Segmentation is breaking up an image into its constituent parts with computation of the particular features for every part, such as size and shape. Segmentation algorithms are based on similarity (using thresholding and region drawing) or discontinuity (using edge detection).

i) Thresholding: thresholding (or binarization) of an image is assigning a binary value (0 or 1) for every pixel in the image based on brightness level. Thus, every pixel has a certain value for the thresholding, so every pixel, above this value is one and the rest of the values are zero, making the image just black and white. This procedure is quite fast and has widely been used in industry. Thresholdings are global (used where the objects markedly vary from their background), local (useful in gray scale images where the object and background are not clearly defined) or dynamic (using concepts such as proximity of points to separate objects from the background).

ii) Region Drawing: this technique is applicable to the cases where objects can not be differentiated from each other using thresholding techniques. This method is mostly used in scene analysis. This technique has not been widely used in industrial applications for real time inspection due to the required computational time.

iii) Edge Detection. This technique is based on the use of spatial convolution masks in order to reduce processing time. A mask is moved over the entire image and a measure proportional to the discontinuity of the image is computed.

Amongst these three techniques, The thresholding is the fastest one. Since the adhesive dispensing beads do not have a complicated scene and there is a time constraint for image processing, the thresholding technique is an attractive method for image segmentation.

iv) Boundary Tracking. By having the boundary outline of the scene, the next step is to discard isolated edge elements which are noise. After finding two adjacent edge elements using an edge tracking algorithm, a line can be drawn through these pixels to an adjacent pixel. If that pixel is an edge element, then the line continues in that direction. If no further edge pixel is found, the line terminates and a new pair of edge elements are found elsewhere. If there is an intersection between the lines in a scene, the edge tracking algorithm has multiple choices for continuation for drawing a line.

3.7 Feature Extraction

After analysing an input image, the next step is feature extraction of it which can be used for recognition tasks or inspection analysis. The characteristic of a binary image is its shape which is referred to as *blobs* . Holes in objects are also considered as a blob, but they are represented with a different colour than the one associated with the object. As the binary image is processed, the scalar feature of each blob such as area, perimeter and the centre of gravity can be calculated.

3.8 Implementation of a Custom Made Vision System

After analysing the basic principles of computer vision, the proper vision system needs to be chosen for the adhesive dispensing process. Every vision system consists of hardware (image sensors, light sources, computer for implementation of processing board) and software (image processing and parameter calculation).

To choose the best vision system for adhesive dispensing, the following requirements need to be taken into account:

i) Flexibility: The system has to be flexible enough to be mounted on the end-effector of a robot and to be used under industrial manufacturing conditions.

ii) Efficiency: To analyse only those data which are necessary for adhesive parameter calculation and to discard the unnecessary data in order to lower the processing time.

iii) Robustness: to be robust and reliable for use in manufacturing processes.

iv) Real time: The system should be able to operate in real time conditions and to take the image and analyse it while the robot dispenses adhesive. Thus, the speed of image processing is an important factor, particularly since the adhesive process is much faster than that of arc welding. Speeds of up to 400 mm/sec are frequently used.

Since the adhesive bead is three dimensional, an active three dimensional vision system is suitable for inspection. Thus, a structured light technique is used for extraction of 3-D information from 2-D images, by illuminating the scene with a geometrically known lighting configuration. The light source produces a plane of light which by its intersection with a surface will take the form of its contour, if it is at an angle with respect to the viewing device as shown in figure (3.2). When the object is not flat, the light line will be curved.

Based on the requirements described above, a complete vision system was developed. The overall vision system consists of;

i) A Hitachi CCD camera with a standard T.V. lens.
ii) A Newport (3mW) laser diode.
iii) A Joyce Loebl (IBM-PC based) vision board.

The complete vision system is shown in Fig. (3.2), and the details of the vision implementation are given in chapter 4.

3.8.1 CCD Camera

For image acquisition, a Hitachi CCD camera is used since the image is accessible to a normal camera system. The Hitachi CCD camera (with 12 VDC power supply) has the following features:

i) High sensitivity solid imaging device with 510 horizontal and 492 vertical pixel resolution, providing a sharp and clear image.
ii) Internal and external synchronisation modes.
iii) 20 mm lens.

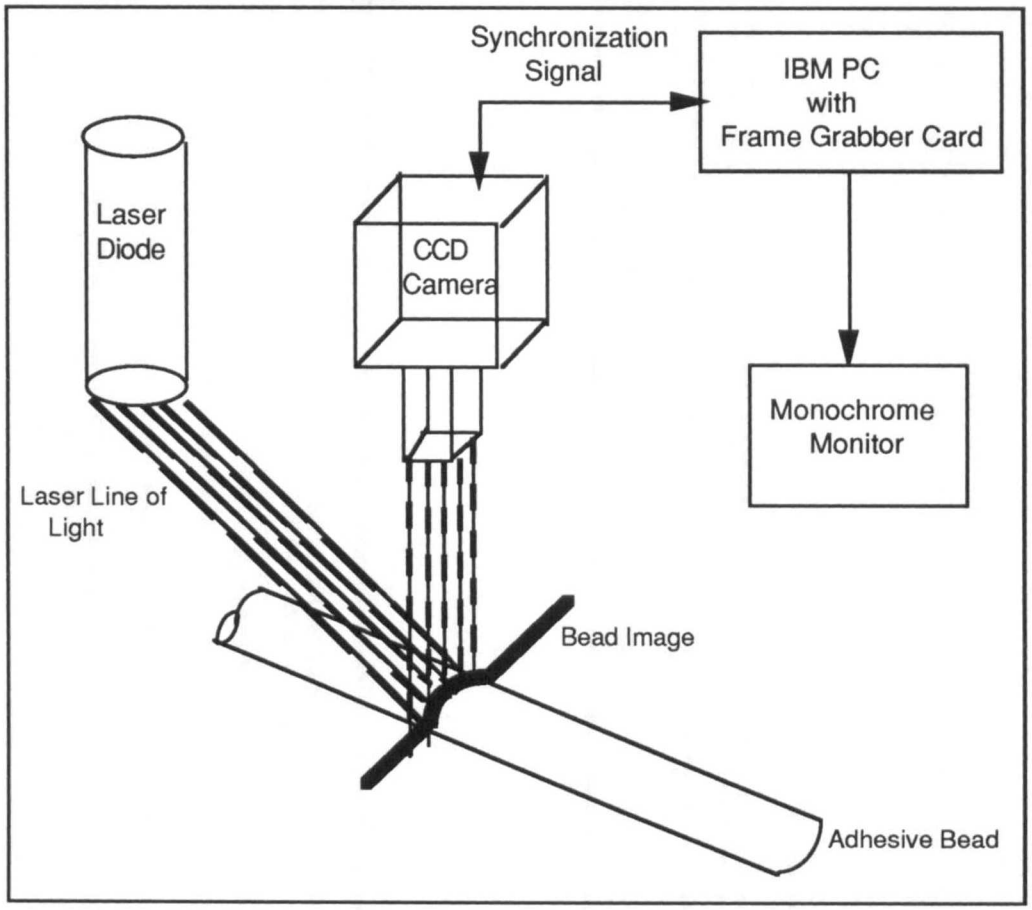

Figure 3.2: Schematic diagram of the vision layout.

iv) 6.25 mm extension tube for reducing the minimum focusing distance from 200 mm to 45 mm.

The power supply is mounted on the robot arm and the camera is placed at the end-effector of the robot. The video output of the camera is connected via a coaxial cable to the Joyce Loebl hardware board. The video signal is fed to an A/D converter, producing a 6 bit resolution word, in which a binary image is extracted using a thresholding technique. The signals provided by the vision system are also used to synchronise the camera.

3.8.2 Laser Diode

The laser diode is designed to project a precisely defined geometric distribution of optical radiation. The laser diode tube used, is a Newport *V-SLM-215* structured light system,

which projects a plane of light by its interaction with the target surface. This is viewed as a thin line of light that follows the contour of the object.

The laser diode tube consists of the following:

i) A laser diode tube with an adjustable stand-off from 10 cm to infinity
ii) A power supply.

The power supply is mounted on the robot arm and the tube is placed at the end-effector of the robot.

3.8.3 Joyce Loebl Vision Board

The vision board is *IV20* Joyce Loebl and is capable of capturing an image in grey level and in binary form simultaneously. The IV20 image processor is an IBM-PC XT/AT compatible board which uses Texas Instruments *TMS32020* (32 bit digital image processor) and shared memory techniques to provide a "256x252" pixel image processing system. The Texas Instruments TMS32020 digital image processor is the principal element of the main processor card. This controls most of the card functions and facilities. The system takes up a single slot in the IBM-PC and is made of three cards as follows:

i) Main PC, bus compatible, image processing card
ii) Analogue input card
iii) Edge enhancement function card.

IV-20 is equipped with a signal processing unit, able to process a large amount of data much faster than an ordinary PC based CPU like 80286. However, the image processing is performed in series in this board. Therefore, when a command is sent to the frame grabber, the PC waits until the command is completely performed, then goes to the next step of the programme. The main feature of this board is that programming is simple and the processing of images is not slowed down by the host computer.

The IV20 gets its fundamental commands from an 8K word block of program memory. This memory shares part of the IBM's address space. The IBM can then load programs for driving the IV20 directly into this space. The video frame store provides 252 line by 256 columns storage for the currently displayed frame, and it is the only area of memory from which data may be output to the monitor. The display device is a 23 cm black and white monitor connected with a 75 Ohms coaxial cable to the board.

The image memory consists of:

i) One 64 Kb block of video RAM (VRAM) which is the main RAM and used for image capture and display.

ii) Four 64 K word blocks of dynamic RAM (DRAM) which are used for image storage which need to be processed later. The DRAM's are not used for real time application due to the time constraint involvement.

Each of these RAM (video or dynamics) contains 8 planes called frames. Frames are numbered from zero to seven.

There are 8 auxiliary stores which are available to the user and can be read by the TMS32020. Data from these frame stores cannot be directly output to the monitor, and must first be transferred to the video frame store. Two overlay planes are available in bit positions six and seven of the video frame stores. Data can be written into these two frame stores while the image is being acquired. The incoming analogue video signal is fed to an analogue to digital converter. The converter produces a 6 bit digital equivalent of the analogue signal at its output with zero being black and 63 being white.

Programs are down loaded to the TMS 32020 program memory from the host computer by first putting the processor into hold condition and writing directly to the shared memory area. Program execution starts when the host releases the hold condition and resets the TMS 32020. There are 16 Kb program memory available by the host.

3.9 Software Development

After setting up the hardware, the next step is writing software for the image processor and obtaining desired characteristics from an acquired image. The Joyce Loebl has a library called *IVGENIAL* in Microsoft Pascal for IV20 board. There are two ways to develop a new program for IV20:

i) To run the standard package *GENIAS20*, and select the desired tasks from the interactive menu. In this way, the user has no control over the execution tasks and speed of an algorithm can not be optimised. Thus, it is not suitable for real time application.
ii) To create a program by using library IVGENIAL. This library contains several hundred subroutines which can be called in the main program. In this way, the user can create faster routines by having control over the software.

Pascal programs run on the IBM-AT computer which runs in parallel with the IV20, asking the latter to perform image operations when required.

The basic procedures to run a program are given in appendix I.

3.10 Transputer-based Vision System

To decrease image processing time, the Joyce Loebl vision board was replaced by a transputer-based vision system. The transputer system is hosted by i486DX at 33 MHz with VGA (Visual Graphic Arrays) graphics. The system has the following components:

i) 1x T800 CPU running at 25 MHz
ii) 4 Mbytes program memory
iii) 2x1 Mbyte frame buffers (one used for the input image and the second one for the image display.
iv) 1x512 Kbyte overlay buffer.
v) 1x input look-up table (8 bit to 8 bit), used for thresholding.
vi) 1x output look-up (8 bit to 24 bit), table use of to set grey scales on the output display and colour for annotation, text and graphs.
vii) Digitiser chip with programmable capture display timing and programmable input gain.
viii) Input from monochrome video camera CCIR standard.
ix) Output to multisync colour monitor.

The software is written in C and T800 assembly code. The program performs the following sequence of operations:

i) Initialise program arrays and set-up hardware for appropriate frequencies.
ii) Determine the threshold level.
iii) Synchronise vision with control software.
iv) Acquire input image (with hardware threshold).
v) Segment image by scanning for blobs and Freeman chain encoding round each blob once found. The chain encoding procedure determines a bounding rectangle for each blob along with the coordinate of the left-most part of the blob, the right-most part and the top-most part.
vi) Ignore blobs smaller than a threshold size. These blobs may be caused by noise in the image. Also join blobs very close together.
vii) Look through sequences of blobs for patterns of adhesive bead (see Fig. 4.9 for detail). If more than one such pattern appears, determine which is most likely to be the real

bead by predicting the probable position from previous measurements of the bead position and the speed at which its edges move.

viii) Measure the height of the bead, top of arc to baseline (see Fig. 4.9 for further detail). The width of the bead (space under arc), centre-deviation (the percentage by which the highest point of the arc deviates from the centre of the bead) and the baseline height (this gives a measure of nozzle flying height).

ix) Convert measurements in pixels to mm using calibration constants to take into account image scaling and changes in scaling with different heights.

x) Record all the measurements in an array.

xi) Repeat from step 4.

xii) Output all data off-line to cell controller over serial port.

xiii) Close file and end program.

3.11 Summary

A survey of the some of the work in the area of computer vision systems and their application in the manufacturing area has been presented in this chapter. The use of vision systems for automated inspection and image processing techniques has also been covered. The detailed description of the inspection hardware used for automated adhesive dispensing was given. The Joyce Loebl software package was briefly covered. The detailed software description, including some of the major procedures, are also discussed in appendix I. The hardware and software descriptions of the improved vision system using a transputer system was also covered. The next chapter discusses the implementation of the automated cell and the use of the vision system as part of the automated adhesive dispensing cell implementation.

CHAPTER IV

IMPLEMENTATION AND ON-LINE CONTROL OF AUTOMATED CELL

4.1 The Necessity for Integration

Having discussed the principles of the automated adhesives dispensing and vision system, the cell components need to be integrated. Here, the control and communication of the robotic system are considered first. This is followed by a description of the single axis table. After reviewing the Graco dispensing system, requirements and implementation of mounting the camera and the laser diode on the robot are covered. The system integration and interfacing the equipment within the cell are then discussed. This is followed by the implementation of a more advanced dispensing system, the Nordson Pro-Flo. The on-line control and processing times are then analysed. Finally, the experimental results are discussed and followed by the conclusion.

4.2 Automated Cell Components

The robotic cell is comprised of:

i) A six axis robot carrying an adhesive gun around the desired trajectory path.
ii) A single axis table carrying workpieces.
iii) A dispensing system unit. This includes the pumping system, a dispensing gun and a dispensing control device.
iv) A vision system unit, which includes CCD camera, 3 mW laser diode and an IBM-PC based image processing board for visual inspection.

Implementation of each unit and the integration within the cell are discussed in detail in the following sections.

4.3 Robotics System

The robot is the heart of the system and it is crucial to choose a robot which will be suitable for the adhesive application. Most dispensing systems require precise control of the end-effector's velocity and path trajectory. This is in contrast to assembly operations in which the velocity profile and path trajectory for picking parts are not critical. The dispensing rate also has to match with the velocity of the end-effector to control the size and shape of the adhesive bead. The geometry of the robot has to enable the hose and dispenser to move around the profile of the workpiece without motion restrictions. Also variables such as position and tool point speed have to be monitored.

There are basically three types of trajectory control in the robot (as discussed in Ch. 2): point to point, continuous path and continuous path with sensory feedback. Point to point trajectory control is used in spot welding. In painting, sealant and adhesive applications, continuous path control needs to be used. In this case, since the tasks are performed along a predefined path while the robot is moving and path tracking is crucial, a continuous path robot with capability of position sensory feedback is used.

The system which has been investigated is built around a 6-axes (GMFanuc, S-100) robot (as shown in Fig. 4.1) with a Pascal based *Karel* controller. The latter was chosen because

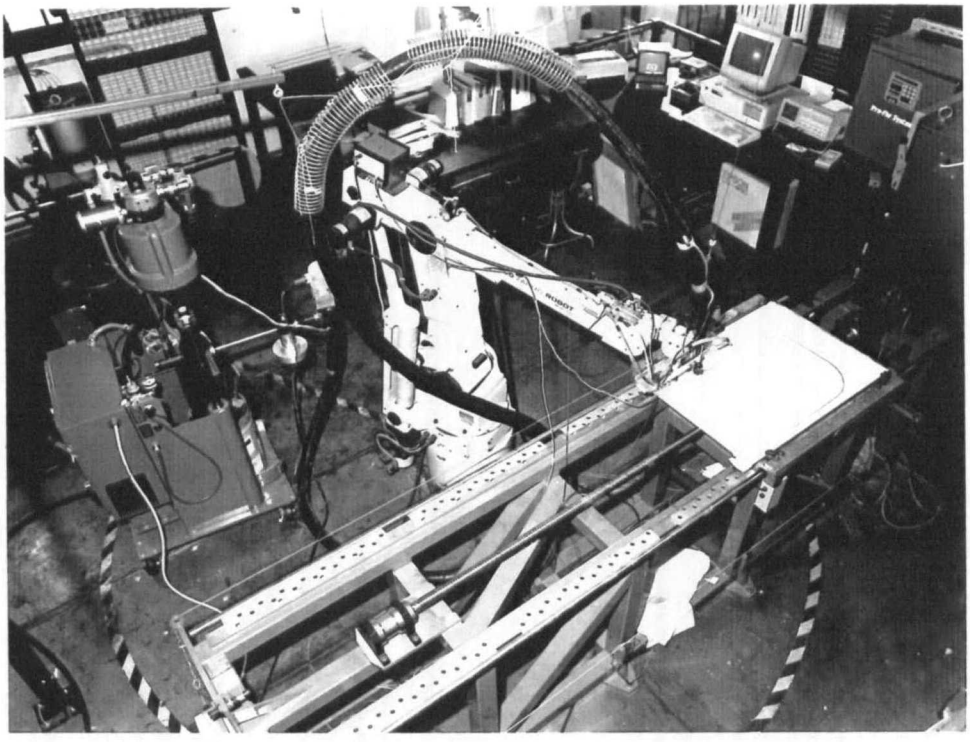

Figure 4.1: GMFanuc, S-100, six axis robot.

it offers an on-line control facility permitting the bead size or position to be adapted whilst the robot is running, in response to sensed variations. The Karel controller is part of a Karel system which includes mechanical and controller electronics (R-F Controller) [Karel 87a, Karel 87b]. Karel hardware interfaces, system software support programming, daily operation, maintenance and troubleshooting are included in the controller.

The robot is an articulated (jointed arm) type robot and has six axes (3 for position, and 3 for orientation). It has a 10 kg payload, electrical servo drives using AC servo motors and a repeatability of $\pm$ 0.2 mm [Fanuc 87]. This type of robot can be used for arc welding, spot welding and adhesives/ sealant dispensing. Karel is a high-level programming language (based on the Pascal programming language) specially developed to support Karel systems. The Karel system can include a variety of mechanical units and peripheral devices such as a robot, table and sensors.

4.3.1 Path Following Facility

To ensure a consistent bead size without modifying the dispensing gun characteristics, it is desirable to have a constant robot speed. However, this can be in conflict with the desire for the robot to follow an accurate path, particularly where the path moves around a corner. If the robot is to pass through a point which is on a sharp right-angled corner, then first the robot must slow down to a stop before again accelerating away from the corner. This clearly has problems for the dispensing system, since the flow-rate would have to slow down to zero when the robot comes to a stop. Because of the delays in the dispensing system, the flow-rate would need to be adjusted hundreds of millimetres before the robot starts to slow down. This is very difficult to achieve in practice and often leads to a great deal of ad hoc adjustment of the robot programme. It is therefore preferable to ensure that the robot does not slow down on a corner. This implies that wherever possible, the dispensed bead should be designed to have a large radius of curvature at each corner, thus minimising the need for changes in the robot velocity.

As with many sophisticated robots, the Fanuc controller can allow the acceleration compensation system to be progressively reduced to allow a continuous motion along the path trajectory. This means that with something like 50% acceleration control it is possible to traverse a corner without the robot slowing down appreciably. However, the result is that the robot path is not exactly the same as that for which it was programmed and may not be exactly repeated from one run to the next. This can be compensated for in part by programming points, off the desired path, so that during play-back the robot follows nearer to the desired trajectory. Once again, this ad hoc programming does not lend itself to automated procedures, and is best avoided either by designing corners with large radii, or

by the use of a very fast response dispensing system. Fig. 4.2 shows a series of traces with different percentage acceleration compensation compared for robot speed of 500 mm/sec.

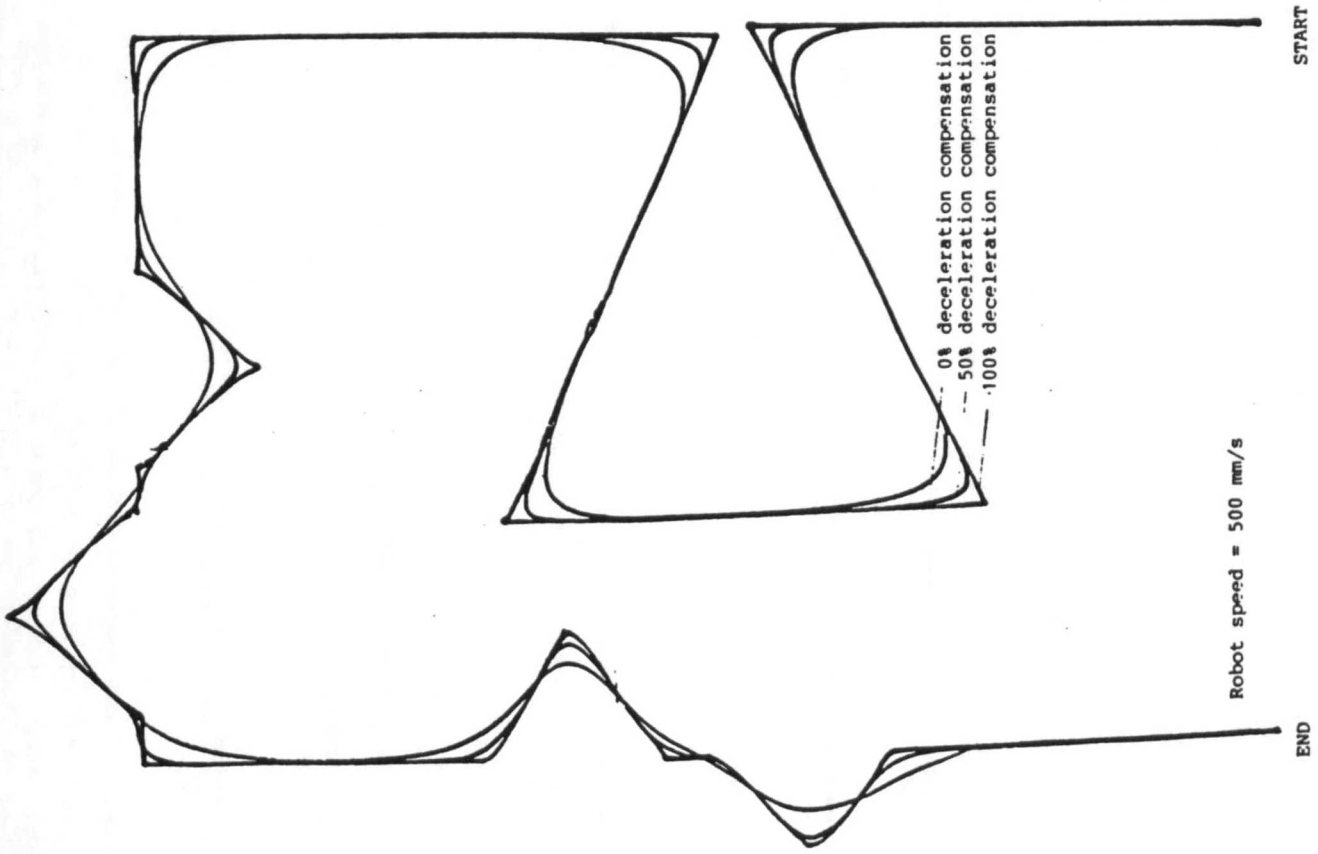

Figure 4.2: Path of robot for good positioning criterion (100% deceleration) compared to with constant speed criterion (0% deceleration).

4.3.2 Overview of Data Communication in The Karel Controller

Networking provides flexibility for coordinated control of cell equipment in an integrated manufacturing environment. This section describes the Karel language facilities to perform serial input/output operation. These operations include opening and closing data files and serial communication ports and reading from and writing to files, communication files, communication ports and user interface devices.

The Karel controller communicates through the RS-232-C serial communication ports. It can interface with connected equipment over a full duplex line. In this method of

communication, simultaneous communication can take place, as data flows in both directions and both communicating devices need to have full and independent transmitting and receiving capabilities. The input/output (I/O) system also provides a user interface with Karel through user-defined or system-defined I/O signals. The user-defined (I/O) signals are controlled in a Karel program and allow the user to communicate with peripheral devices.

DIN (Digital Input) & DOUT (Digital Output) signals provide access to data on a signal input or output line in a Karel program. The program treats the data as a Boolean data type. The value can be either ON (active) or OFF (inactive). Evaluation of DIN signals causes the system to perform read operations of the input port. Assignment to a DIN signal is an invalid operation. Evaluation of DOUT signals causes the system to return the currently output value from the specified output signal, and the assignment of a value to it causes the system to perform an output operation. These signals can be used for opening/closing of the dispensing gun.

GIN (Group Input) & GOUT (Group Output) signals provide access to DINs and DOUTs as a group of input or output signals in a Karel Program. A group can have a size of 1 to 16 bits, with each bit corresponding to an input or output signal.

AIN (Analogue Input) & AOUT (Analogue Output) signals provide access to analogue electrical signals in a Karel program. The program treats the input data as an integer data type. For output signals, an analogue voltage corresponding to a programmed integer value is outputted. The amount of opening of a gun can be assigned by using these signals [Karel 87a].

4.4 Single-Axis Table

The Karel controller has the ability to control three auxiliary axes. At the present, just one is being used for a single axis table. The single axis table was specially constructed using a Fanuc drive system. This enabled the table to be coupled to the robot as part of its control system so that the table acted as a true 7th-axis. The linear table is capable of carrying large components such as a car door over a distance of 2.5 meters at speeds up to 1.2 m/s. This is approximately the maximum speed of the manual dispenser. However, a considerably lower rate would be acceptable for a continuously operating robot. The use of the table allows the range and velocities required of the robot to be less demanding, and the robot does not have to reach quite as far or move as quickly as it does when the workpiece is

stationary. The robot and table allow continuous path control and also permit on-line adaptive control of their combined position and speed [Davies 90b, Razban 91a].

4.5 Graco Master-Flo Dispensing System

Although two different dispensers with two adhesives materials were used, Graco Master-Flo and Nordson Pro-Flo, the major part of the research was carried out using the Nordson Pro-Flo system. First, the Graco Master-Flo, its integration and on-line process control using this dispensing system is analysed. This is followed by implementation of the Nordson Pro-Flo.

The first adhesive dispensing system is the Graco Master-Flo pneumatic actuated controller. This is addressed directly from the robot controller to provide control of a slide dispensing valve mounted on the forearm of the robot structure. The valve was positioned to give a compromise between the load carrying capacity of the robot at high speeds and the desire to have the minimum pipe lengths (and hence delays) between the valve and the dispensed bead. An on/off valve with *snuff back* feature was mounted at the end of the robot. The pictures of the Graco pump used in the cell, Master-Flo controller and the dispensing valve are shown in figures in Fig. 4.3 through 4.5.

The Master-Flo dispensing system control valve was instrumented with a potentiometer which showed that for large changes of opening there was an initial dead time. To minimise this, a pair of pneumatic booster relays were adopted which put full system pressure across the valve at the initial opening. This had the effect of reducing the overall delay. The reduced time from fully closed to fully open was in the order of 200 msec. For a 50% change in opening, the transport lag for the flow-rate adaptation was reduced to 170 msec. The use of the snuff/back feature on the on/off valve helped to reduce blobs of adhesive at start and finish of dispensing, however these were still present. An alternative strategy evolved, in which the valve was opened gradually whilst dispensing adhesive onto scrap paper adjacent to where the bead was to be laid. The robot was then moved onto the workpiece whilst the adhesive was running. This is a commonly used tactic in industry.

It was felt necessary to minimise the length of hose between the dispensing valve and the on/off valve at the tip of the robot. The dispensing valve was therefore mounted on the robot forearm structure, as near to the robot tip as possible, without detracting from the ability of the robot to carry the on/off valve and hoses at the tip. However, the final hose cannot be made too short, as it is sometimes necessary for the robot to move to a calibration

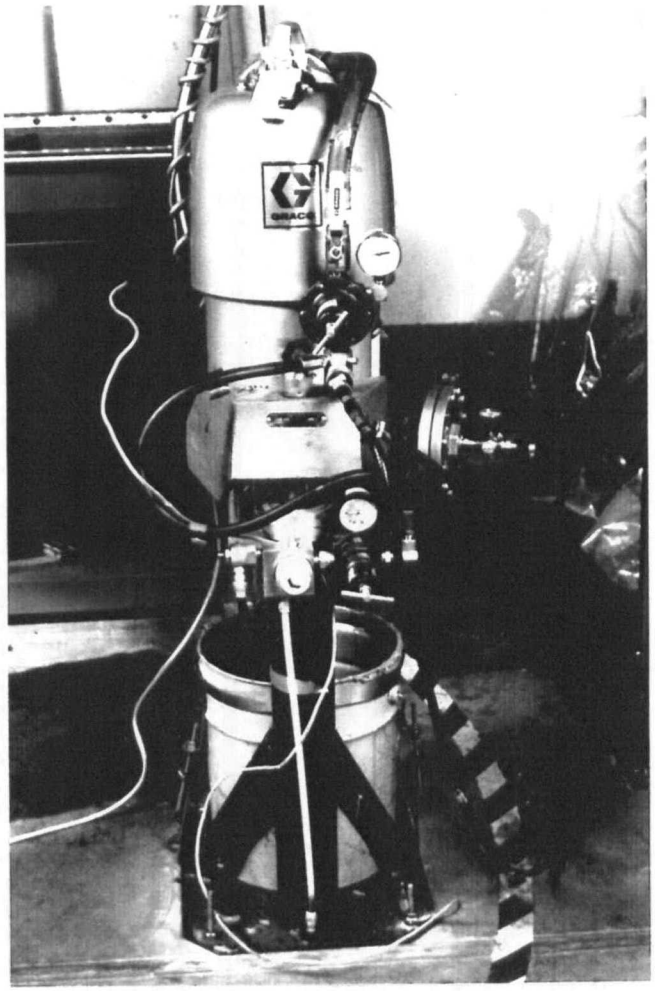

Figure 4.3: Graco pump used with Master-Flo controller.

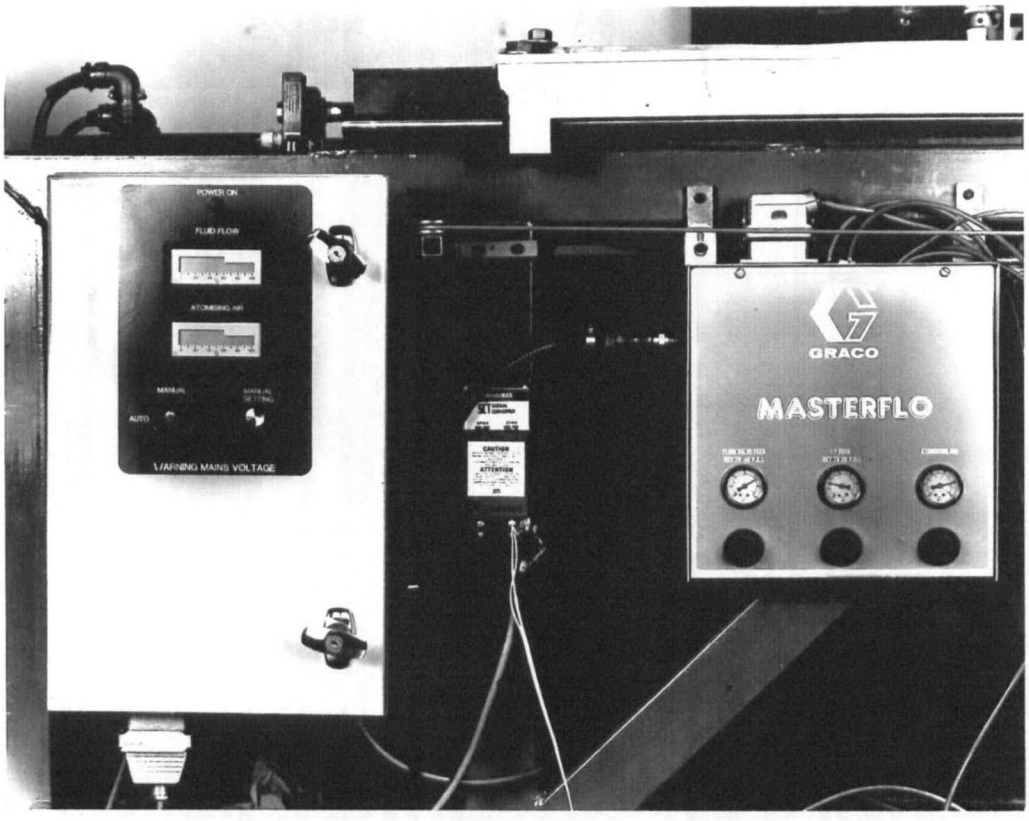

Figure 4.4: Master-Flo pneumatic actuated controller.

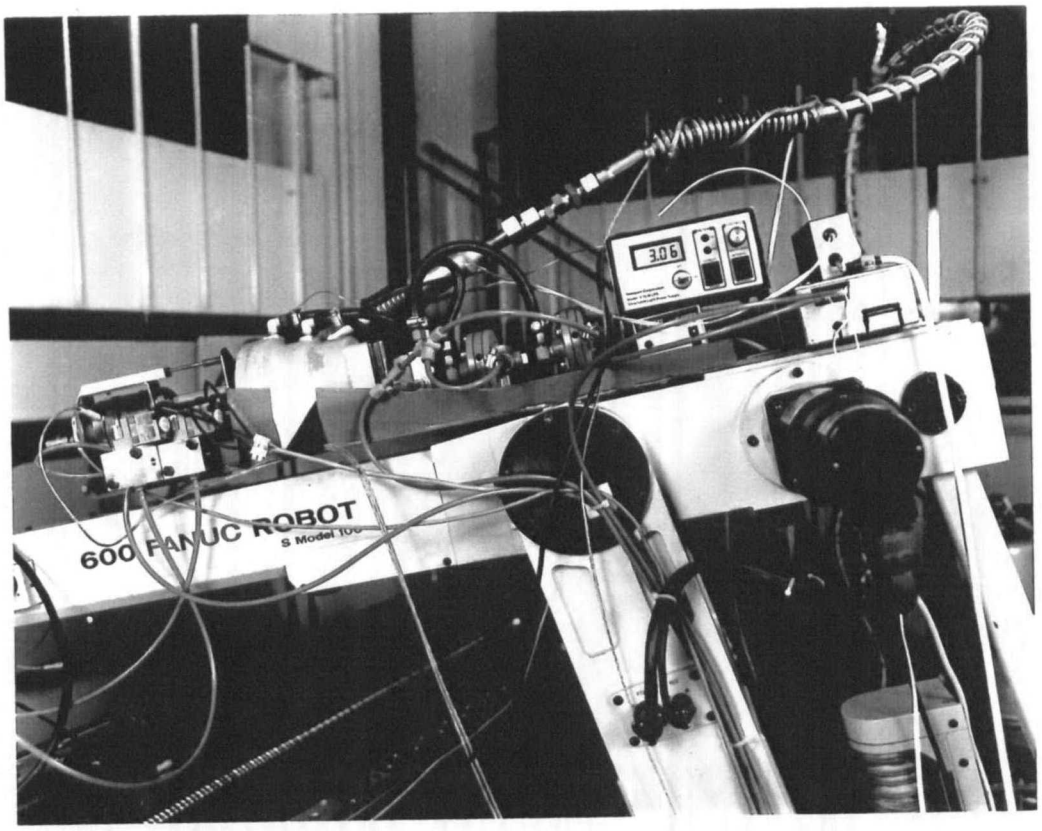

Figure 4.5: A slide dispensing valve on the forearm of the robot.

position, which can twist the hose considerably. If the hose were too short, it could rupture and also it would add excessive drag to the wrist rotations. Subsequent tests however, showed that the transmission delay from the dispensing valve to the on/off valve (from modifying the dispensing valve opening to changing the bead characteristics at the tip) was negligible. This is due to the almost incompressible nature of the particular adhesive used at these pressures. This transmission delay does not include the time to move the valve into an open position.

Variations in the dispensing valve opening were initially controlled from the Graco Master-Flo pneumatic controller, using signals sent from the robot to the controller. However, this was found to introduce unnecessary delays and it was found possible to control the dispensing valve directly from the robot Karel controller using only the Graco pneumatic transducer.

The adhesive was dispensed from a 5 litre drum using a high pressure pump operating around 90 bars (1300 lbf/in^2). The dispensing hose was heated to around 30 °C to ensure a consistent adhesive temperature (and hence viscosity) independent of the ambient temperature. This also had the effect of lowering the effective viscosity, making the

adhesive easier to pump at the very high shear rates required. The adhesive was initially a hot cure epoxy resin *EPRON 901*, specifically formulated by BP Chemicals PLC. EPRON 901 contains bisphenol A-epichlorhydrin epoxy resin, inorganic filters and curing agents [BP Chemical 87]. Its density is 1.3 g/cc at 30° C and its viscosity profile graph at 30 °C is given in Fig. 4.6. The formulation was a difficult compromise between the thixotropic requirements for pumping at high shear rates with reasonably low pressures, and the need to be sufficiently stiff when contacting the workpiece, so that the adhesive does not run down vertical surfaces. This, together with the need to have a high strength adhesive with consistent properties over a long product life, makes the adhesive a demanding product to formulate.

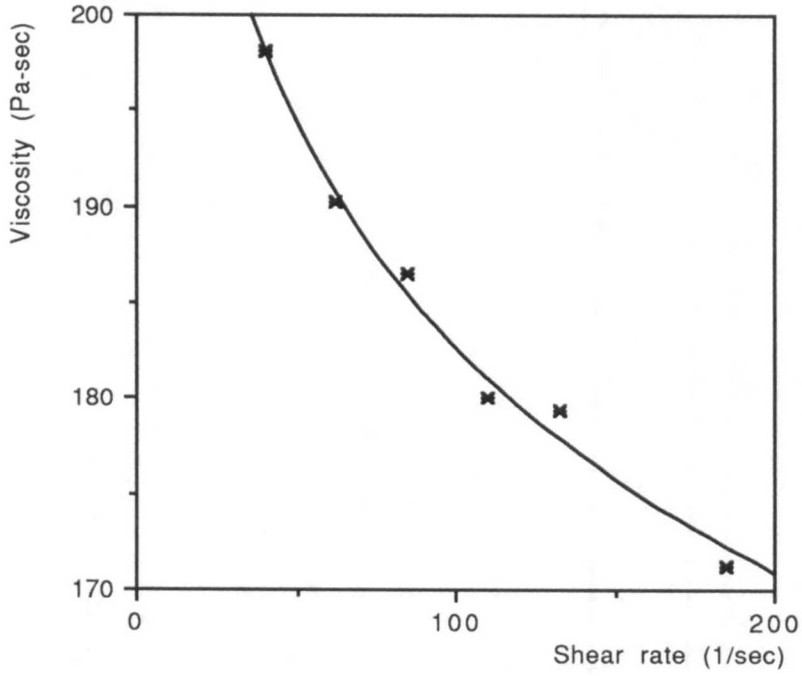

Figure 4.6: Viscosity profile for EPRON 901.

Because small quantities of adhesive were being formulated on an experimental basis, there were a number of problems due to lack of homogeneity of the mix of adhesive and due to the presence of air bubbles in the mixture. The latter required de-gassing of the adhesive pail prior to dispensing. These problems are quite common in the experimental phase of a project. However, provided good process control is adopted by the manufacturers together with large scale de-gassing of the adhesive, the above problems should not occur in large scale industrial practice. Adhesives which have the property of thinning at high shear rates (which allows them to be pumped at fast rates) also tend to have large viscosity variations

with temperature. This means that the temperature control system must be fairly precise. However, it was found that there is a temperature variation (about a few °C) across the diameter of the heated hose, thus when the adhesive passes through the hose, the outer section is hotter at a lower viscosity than the central. One way to avoid this is to heat the reservoir of the adhesive material. However, because a hot cure adhesive is being used, this can shorten the life of the product in the reservoir. An alternative procedure is to use a mixing chamber just prior to the nozzle dispensing tip.

4.6 Vision System

The advantages and disadvantages of using robotics system in adhesive dispensing applications were described in detail in (§ 2.8). However, in specific applications of the quality inspection of an adhesive dispensing bead for the system described in (§ 4.5), the robot is not able to detect if the adhesive is actually flowing from the dispensing nozzle. Although, the opening of the gun and the amount of the desired flow rate can be detected by electronic instruments, this does not measure the actual flow rate through the nozzle and the system is considered to be an open loop system. However, since there has been no sensing of the state of the adhesive, it is necessary to have manual inspection of the process prior to closing the joint. Manual inspection methods are usually subject to human error, due to fatigue and the qualitative nature of the inspection process. What is therefore required is some sort of automated sensing system which can check the quality of the adhesive bead, either in a post process inspection, or more preferably as an on-line inspection process (closed loop system).

Before giving a solution to the problem, some of the factors affecting the size of the adhesive bead or the existence of the adhesive on the component need to be mentioned. Those factors are: changes in viscosity, robot speed, delivery pressure, temperature, surface tension and the existence of the bubbles in the nozzle (see Ch. 5 for further details). Each of the above factors may effect the quality but not the existence of the deposited bead. Special purpose sensors have been used in industry to cope with some of the above problems. Jet sensors are used for break detection [Dueweke 83]. Another approach uses metallic particles in the adhesive which can be detected magnetically, or photoelectric sensors at the dispensing gun [Ludbrook 85].

All the sensors currently being used, are trying to deal with every single problem separately; not as a whole. This approach may lead to a point where either the problems are too many or they can not be solved separately. A better approach for detecting the existence of the adhesive and the quality of the bead is the use of vision systems. The vision system

can check the existence of the deposited bead and calculate the bead parameters while the adhesive is being laid by the robot.

On-line control can then be used, either for the robot parameters or for the dispensing gun, to ensure that the adhesive bead lies within a predefined tolerance band. In an attempt to eventually achieve adaptive control, a special purpose vision system was developed (as described in § 3.8), which checks the adhesive height and width on-line whilst the bead is being dispensed. This is because at this time there is no reliable NDT system for checking the quality of a cured adhesive bond in metal to metal bonding.

4.6.1 Vision Hardware Implementation

The principle of the vision system, the image processing software and the need for employing the vision system were discussed in the previous section and in Ch. 3. The next step is the taking and processing of images while the robot is dispensing adhesives onto the component. The vision sensory system thus has to be mounted on the end effector of the robot. The procedure for mounting a camera and laser diode on the robot end effector without affecting its performance is a quite complicated task. The mounting bracket should ensure that the camera and the laser diode can always follow the adhesives bead. The requirements for the mounting bracket can be divided into two categories: those associated with the robot and those for the vision system in terms of image acquisition.

In terms of the robot requirements, the bracket should not affect the robot performance. The robot's working envelope must be retained by ensuring that the bracket does not limit any of the movements. The bracket needs to be compact and light weight to reduce the loads applied to the end-effector. The final weight after mounting laser diode, camera and the dispensing nozzle should not exceed the robot load capacity 10 kg. Also, the moments about the central axis of the end effector have to be considered and all the loads must be distributed uniformly over the whole mounting bracket. The stiffness of the whole system also needs to take into account the high speeds and accelerations developed by the robot.

As for the vision system, the major requirement is that both camera and laser diode always follow the dispensed adhesive bead. The camera must also be at a certain angle with respect to the laser diode. The camera, the laser diode and the longitudinal axis of the adhesive bead should lie on the same plane in order to capture an acceptable image. The focusing distance of the camera has to be adjusted to the adhesive bead whilst the laser line of light must focus exactly on the adhesive bead and on the centre of the scene obtained by the camera. A degree of flexibility is necessary to adjust the final vision and diode position.

4.6.2 Design of the Mounting Bracket

Based on the above requirements, a mounting bracket is designed consisting of three parts, two auxiliary brackets and one main bracket. The two auxiliary brackets are a dispenser bracket for assembling the dispensing nozzle and a laser diode bracket for mounting the laser diode tube. The main body of the bracket is for assembling the camera and the two auxiliary brackets. The vision bracket design is represented in detail in appendix II. The complete bracket with a mounted CCD camera and the laser diode on the end effector of the robot as shown in (Fig. 4.7).

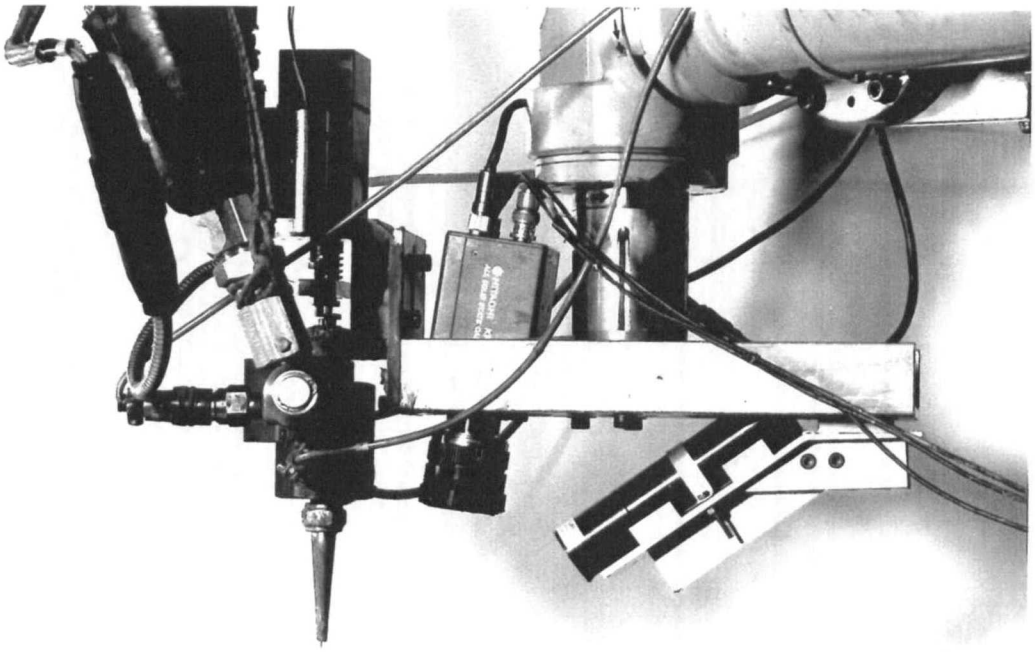

Figure 4.7: A mounted vision bracket on the end effector of the robot.

4.6.3 Vision Bracket Flexibility

To get a good image of the adhesives bead, the following parameters have to coincide :

i) the focusing distance of the camera
ii) the height of the dispenser gun
iii) the focusing distance of the laser diode, and
iv) the line of light projected by the camera.

To increase the flexibility, the bracket has 5 degrees of freedom (DOF) thus enabling several micro adjustments to be done simultaneously for the best image (as presented in Fig. 4.8).

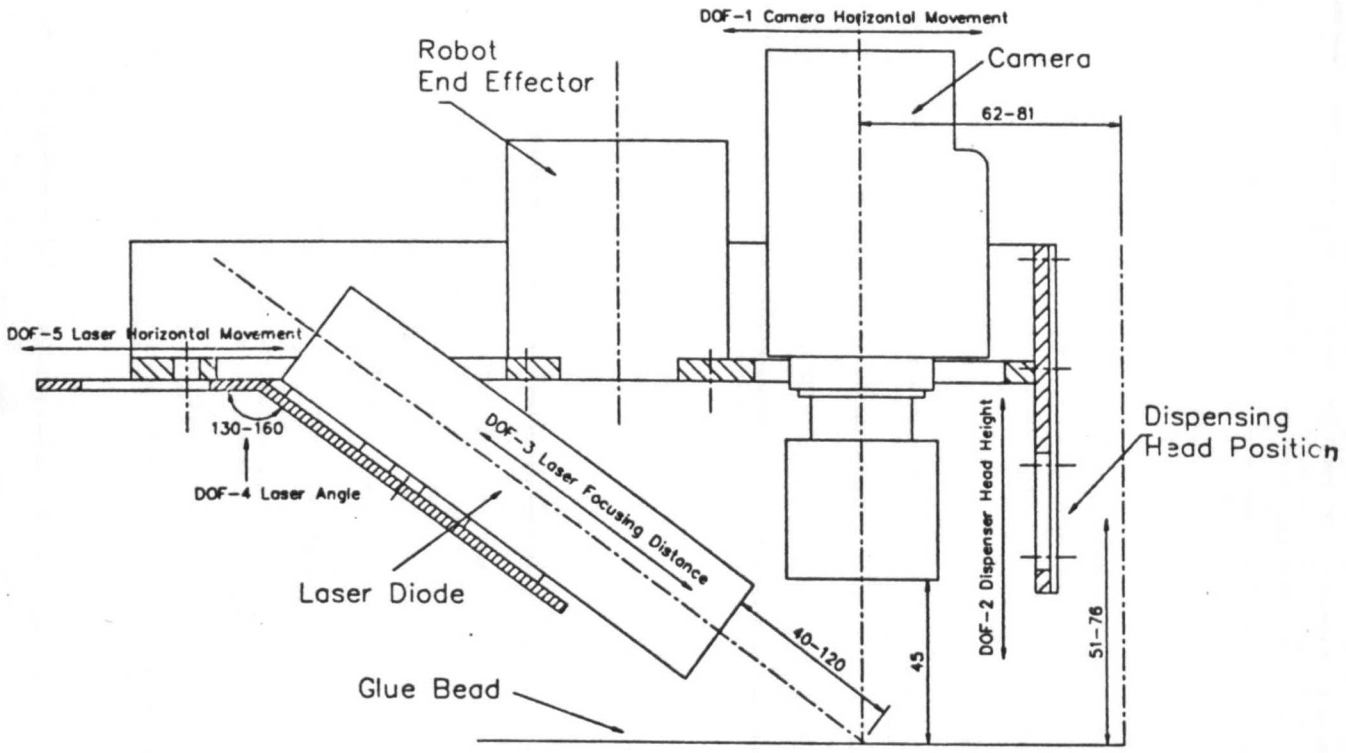

Figure 4.8: Detailed drawing of the main bracket with camera, laser diode and dispensing gun.

DOF-1 controls the horizontal movement of the camera. This affects the distance of the camera from the dispensing nozzle (62-81 mm). Since the camera is mounted at an angle, the actual distance of focusing point from the dispensing nozzle tip is 45 mm. This introduces a transport delay in the process control that represents the time lag between dispensing and actual image acquisition. However, this delay helps the adhesive to settle to the final form on the workpiece. If the distance of the camera from the nozzle is shortened,

the captured image may not be accurate at high speed and it may also affect the bracket momentum.

DOF-2 controls the distance between the tip of the dispensing gun and the component surface (51-76 mm). It also affects the shape of the dispensed bead and it is better to keep the distance constant. This delay allows the bead to be settled before image acquisition.

DOF-3 controls the movement of the laser diode tube along its mounting bracket which affects the focusing distance of the laser line of light. In the image acquisition, the width of the laser line of light is affected by changing the focusing distance.

DOF-4 controls the angle between the two parts of the laser diode bracket (130-160 degrees). This angle is used to direct the laser line of light towards the field of view of the camera and is equivalent to the angle of incidence of the laser light line, which affects the form of the image that is being captured.

DOF-5 controls the horizontal movement of the laser diode. The DOF-4 and DOF-5 are used together to find the optimum position for the laser diode in order to get a good quality image of the adhesive bead.

4.6.4 Vision Operation

A 3 mW laser diode is used to generate a line of light which can be shone at an angle across the bead. Where the line crosses the raised adhesive bead, the line of light is off-set by a value proportionate to the height of the bead. The width of the bead can also be measured. A CCD camera is used to look down on the scene and capture the image. The camera and laser diode are mounted on the robot tip just behind the adhesive dispenser. By this means, it is possible to obtain a measure of the size of the adhesive bead, in both width and height, whilst the bead is being dispensed. Typically, the width of the light line is approximately 10-12 pixels. This depends on the camera aperture (which controls the amount of light that passes through), the vertical cross section of the line and the area around it. The width of the line is a compromise between a large sized image, to give good accuracy, and a small image to allow a short process time with a robust algorithm that will allow the bead to be tracked around corners without losing the image from the field of view. The image may be continuous or segmented (Fig. 4.9) and may appear at any angle or position on a display. Hence, the time to process the image, to give a robust system that will work under all conditions, is quite long.

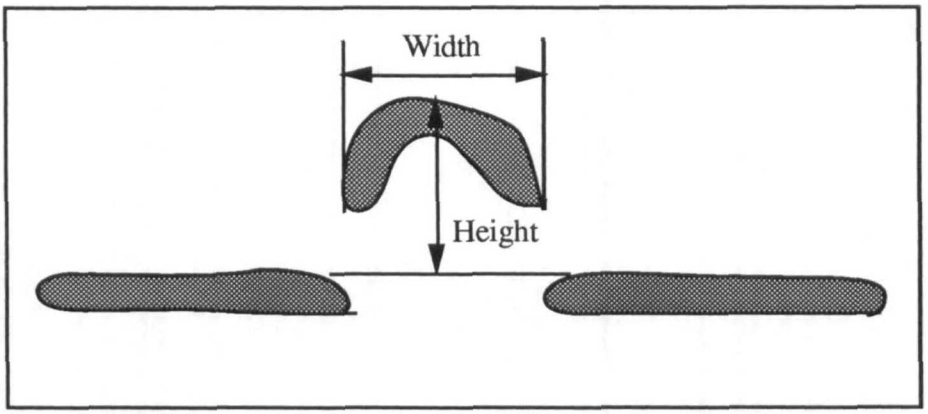

Figure 4.9: Typical bead image.

After image acquisition and bead parameters calculation, the bead parameters information can then be fed back to the robot controller, which can in turn modify the dispensing gun to change the rate of dispensing, or alternatively adjust the speed of the robot to ensure that the bead size stays within a permitted tolerance band width. The main difficulty is the need for high speed processing, both in the vision processing and in adjustment of the dispensing valve characteristics. When defining the vision algorithm, it is necessary to have a robust system which is capable of finding the bead of adhesive as it moves across the camera field of view.

The image may also be tilted when the adhesive is laid around a corner and the camera attempts to continue to track the bead. Thus the algorithm for finding the image must be fairly complex in order to deal with all possible conditions and return a size of bead which is accurate. These difficulties are further compounded by changes in the third dimension on real products such as car doors. The difficulty is that an algorithm will take a finite length of time to process and this can lead to a lengthy delay before a compensating signal can be sent to the adaptive controller. If the robot dispensing speed is relatively slow this does not matter appreciably, however where dispensing speeds of around 400 mm/sec are required, such delays will mean the up-date time is excessively long, e.g. if the vision system puts out a value every 1/20 sec, the next image will not be checked until the robot has moved a further 20 mm. This situation is aggravated by the length of time required for changing the bead size. As an illustrative example, if the robot instruction to the dispensing gun takes 100 msec and the gun takes a further 200 msec to change its parameters, the robot (moving at 400 mm/sec) would have travelled a total of 133 mm since the vision system first captured the image which indicated the need to change the dispensing characteristics. These examples show the necessity of having a fast vision system, the need for fast robot interruption rates and the need for a rapid adaptation of the dispensing bead

size. An alternative strategy is to have a slow robot traverse rate. This not only means that samples are taken at closer intervals of distance along the bead, but also that good path control will be easier to achieve, particularly on corners. The problem is that many tasks, such as in the car industry, have a fixed product cycle time. One solution used on car production lines, with product cycle times of less than one minute, is to use two robots to dispense adhesives onto a single car door or bonnet. This is an expensive solution however, and can cause many problems for the *choreography* of robots.

4.7 Integration of the cell

To have a closed loop system, the robot controller, flow controller and vision system have been linked together and an overall automated system has been developed with on-line process inspection. The schematic diagram of the cell with a description of the different signals is given in (Fig. 4.10). The opening of the gun, and its snuff back feature, are controlled from the robot controller through digital signals which are sent to the solenoid valve. The adhesive flow rate is also controlled from the robot controller through an analogue signal which controls the variation of the dispensing valve. This signal is sent to the control valve via a pneumatic transducer. In order to close this control loop, an IBM-PC (which includes a vision board) is interfaced with the robot controller. The connection between the robot and the IBM-PC is a three wire serial link, using signals associated with RS-232C standards. Therefore, the robot controller has a communication line with the vision algorithm through a RS-232C serial port and with the dispensing system through digital and analogue signals. The adhesives bead parameters can be transferred to the robot controller along the serial line for updating at a baud rate of 9600 [Razban 91a].

The acquisition of the bead height and width parameters, described above, is only the first activity in the adaptive chain. These dimensions are compared with a permitted size variation, held in a data base, and then the robot Karel controller is instructed to change the opening of the adhesive dispenser (time typically 100 msec). Different aspects of the processing time are given in Fig. (4.11). The Graco valve typically takes a further 200 msec to dispense the changed bead. This brings the Graco adaptation time to 200 msec, which was brought down to 170 msec by using pneumatic booster relays. Thus the total adaptation chain (including 200 msec for vision process) can take around 0.5 sec. This value does not include the delay associated with distance of the camera from dispensing nozzle tip. This is further discussed in detail in Ch. 5.

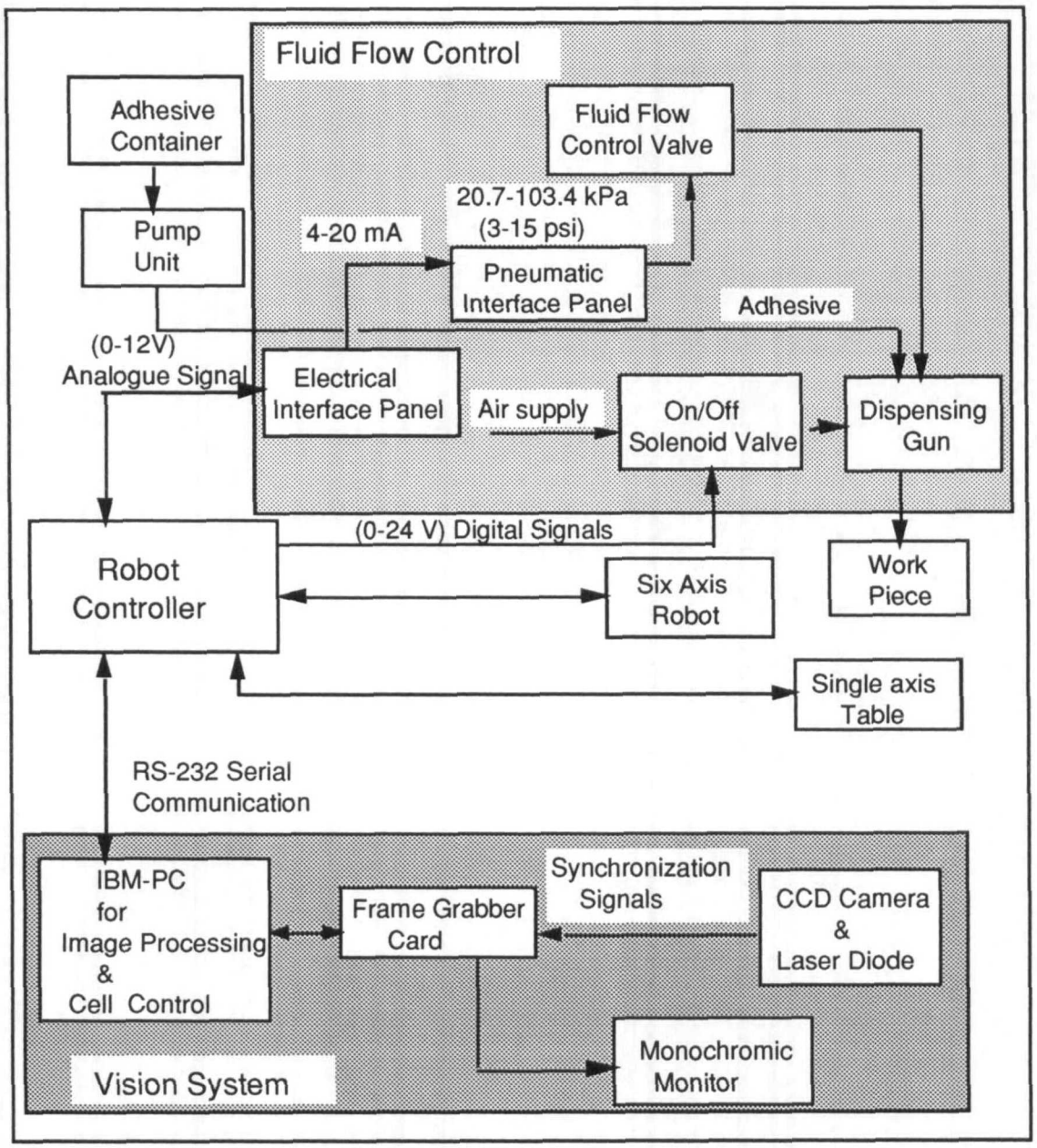

Figure 4.10: Schematic diagram of the cell using Graco Master-Flo dispensing unit.

In order to compete with manual dispensing speeds, it is desirable to dispense at around 400 mm/s on straight sections and 200 mm/s on corners. Thus, with a 0.5 sec delay, it is possible to move 200 mm from the point of acquiring the bead image before the characteristics can be changed. Clearly this is adequate only for correcting a gradual drift in the dispensed size and not for sudden discontinuities, such as air bubbles or blockages. These will need to be avoided by the provision of good process control techniques (e.g. evacuating air from the adhesive container and good filtration) as well as needing cameras for post process visual inspection to ensure a quality audit. However, the adaptive system

should prove adequate, since most variations in bead are gradual, e.g. due to changes in viscosity with temperature or non-homogeneity due to settling down of the product in the container.

In order to ensure that the adaptive system can operate as fast as possible, it is necessary to minimise the time taken for each of the phases. For this reason, a faster dispensing system was implemented (the Nordson *Pro-Flo* digital dispenser) and improved robot control software was developed. Further work is also being carried out on the vision system to ensure that it is fast whilst remaining robust.

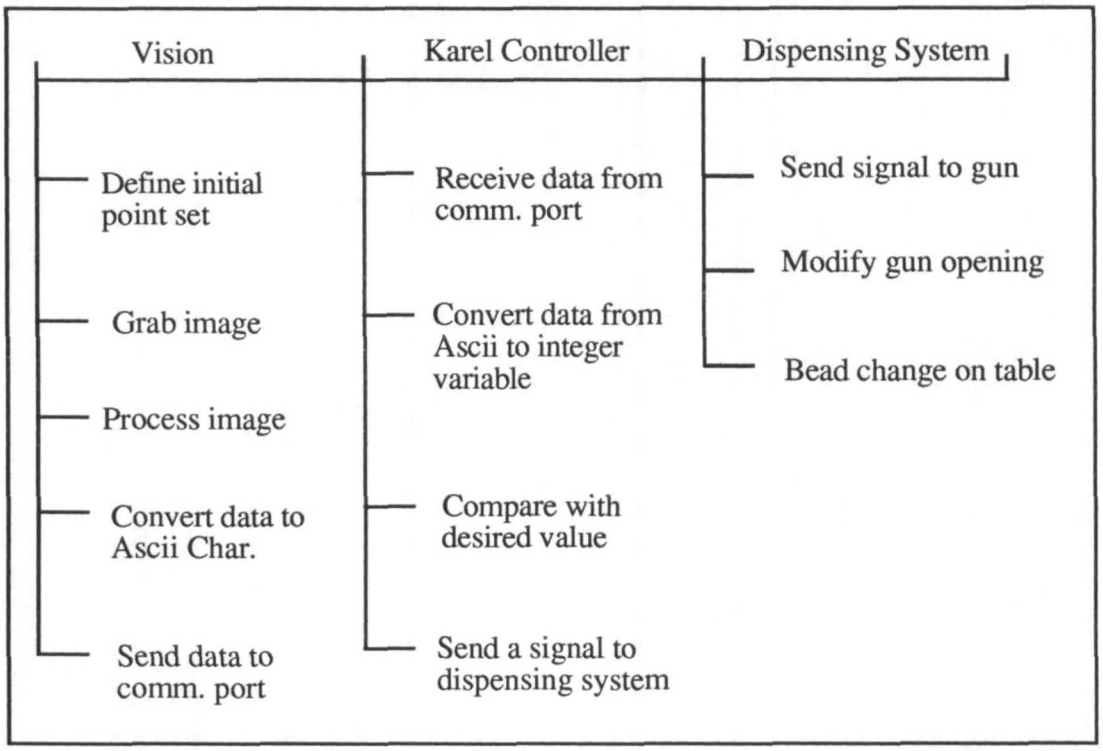

Figure 4.11: Different aspects of the processing time.

4.8 The Nordson digital Pro-Flo dispenser

To improve the dispensing response time and to have a better dispensing control system, the Graco Master-Flo was replaced with a more advanced dispensing system the "Nordson digital Pro-Flo". The Pro-Flo system with microprocessor controller, is designed for the robotic application of adhesive and sealant material. This system is addressed from the Karel controller through digital signal input/output, and an signal input. The revised version of the automated cell is presented in Fig.(4.12).

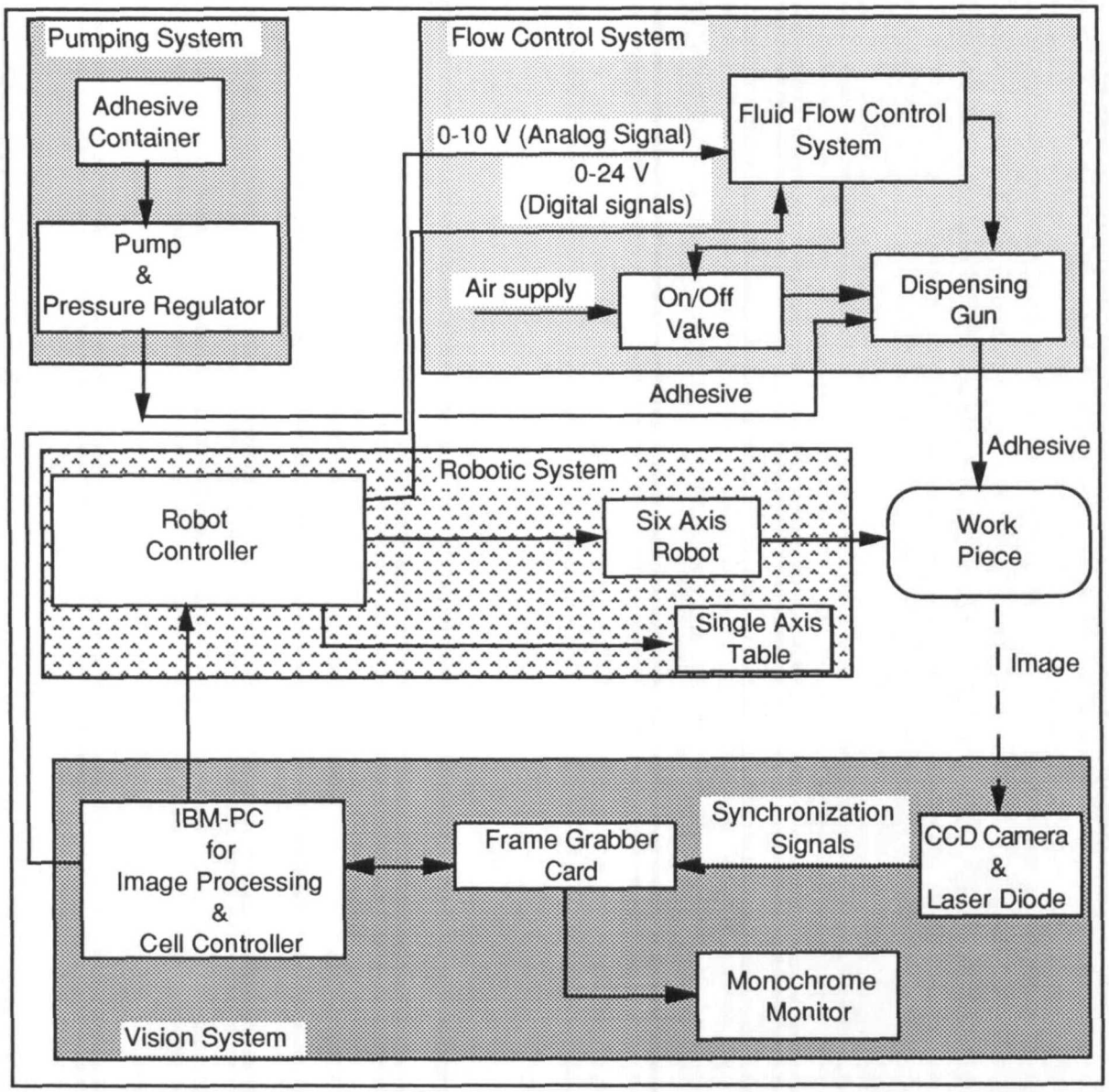

Figure 4.12: New version of the cell diagram using Nordson Pro-Flo dispensing system.

4.8.1 Pro-Flo Components

The Pro-Flo dispensing system consists of two systems: An *Applicator*, this is the "Nordson model 551" which is designed to dispense high viscosity, thermoplastic and thermal setting adhesives, sealants and other materials and a Pro-Flo microprocessor controller. This is addressed directly from the robot controller to provide control of a dispensing valve mounted at the wrist of the robot structure.

i) Applicator unit features. The Applicator is equipped with the following features as shown in (Fig. 4.13) [Nordson 90]:

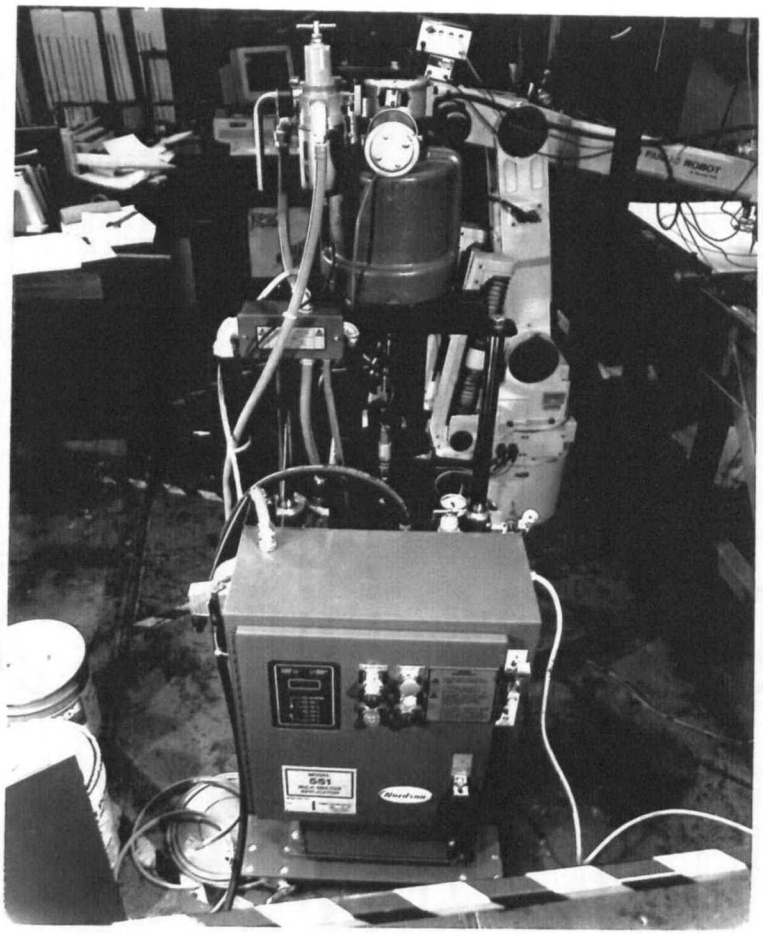

Figure 4.13: Nordson Pro-Flo pumping unit.

i-a) High pressure pump (42:1 air motor-to-pump ratio) with a filter and pressure regulator. The pump is a positive-displacement, dual-acting piston pump, and it transfers material from the pail to extrusion gun through an insulated hose. Pump pressure settings are manually adjustable.

i-b) Single heated hose.

i-c) Teflon-coated, aluminium platen with cast-in heater.

i-d) Automatic extrusion gun.

i-e) Heating unit for pump, platen, hose and gun.

i-f) User-selectable manual over temperature settings for pump, platen, hose and gun (temperature above 70 $^{\circ}$C).

i-g) Automatic shutdown if over_temperature condition occurs.

i-h) Low-level and empty drum indicator.

ii) Pro-Flo controller. The Pro-Flo system with microprocessor controller (as shown in Fig. 4.14), is designed for the robotic application of adhesive and sealant material. This system is addressed from the Karel controller through digital signals input/output, and an signal input as shown in Fig. (4.12) .

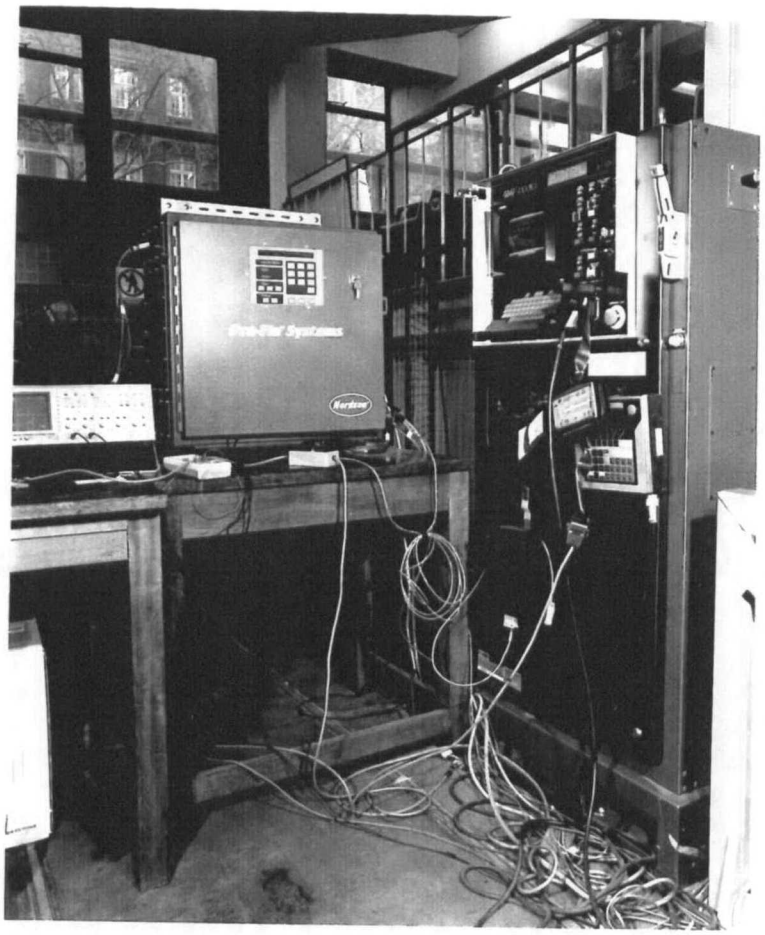

Figure 4.14: Nordson Pro-Flo microprocessor controller unit.

The Pro-Flo system includes the following components [Nordson 90]:

ii-a) Flow Meter, mounted after pressure regulator which counts the number of pulses of the flow rate and sends it to the Pro-Flo controller.

ii-b) Filter/Regulator, the combination of filter and regulator provides filtered air to the pneumatic actuator at the gun.

ii-c) Dispensing Nozzle, with a diameter of 3.8 mm. This is the largest nozzle available at Nordson at present, and can be changed (with a smaller orifice) for low viscosity materials.

ii-d) Pressure Transducer, mounted just before nozzle outlet, and is for sending a control signal to the controller by measuring the material pressure at the nozzle.

vii-e) Controller, has been interfaced to the robot controller.

The Pro-Flo controller adjusts gun output by maintaining a specific pressure in the nozzle, in relation to the input signal (0-10 volts) from the robot controller. The controller interprets this signal and then provides a gun control signal. This control signal adjusts the position of the needle in the gun, which determines material flow. The block diagram of the adhesive flow is presented in Fig. (4.15).

4.8.2 Interface Signals With the Robot Controller

The robot controller interfacing with Pro-Flo (microprocessor controller for dispensing adhesives) is as follows:

i) The signals sent by the Nordson controller are;
system ready, pressure, full open, full close, and over pressure.
(each one is 24 VDC)
ii) Signals received, are:
gun, purge, input (each one is 0 to 10 VDC)

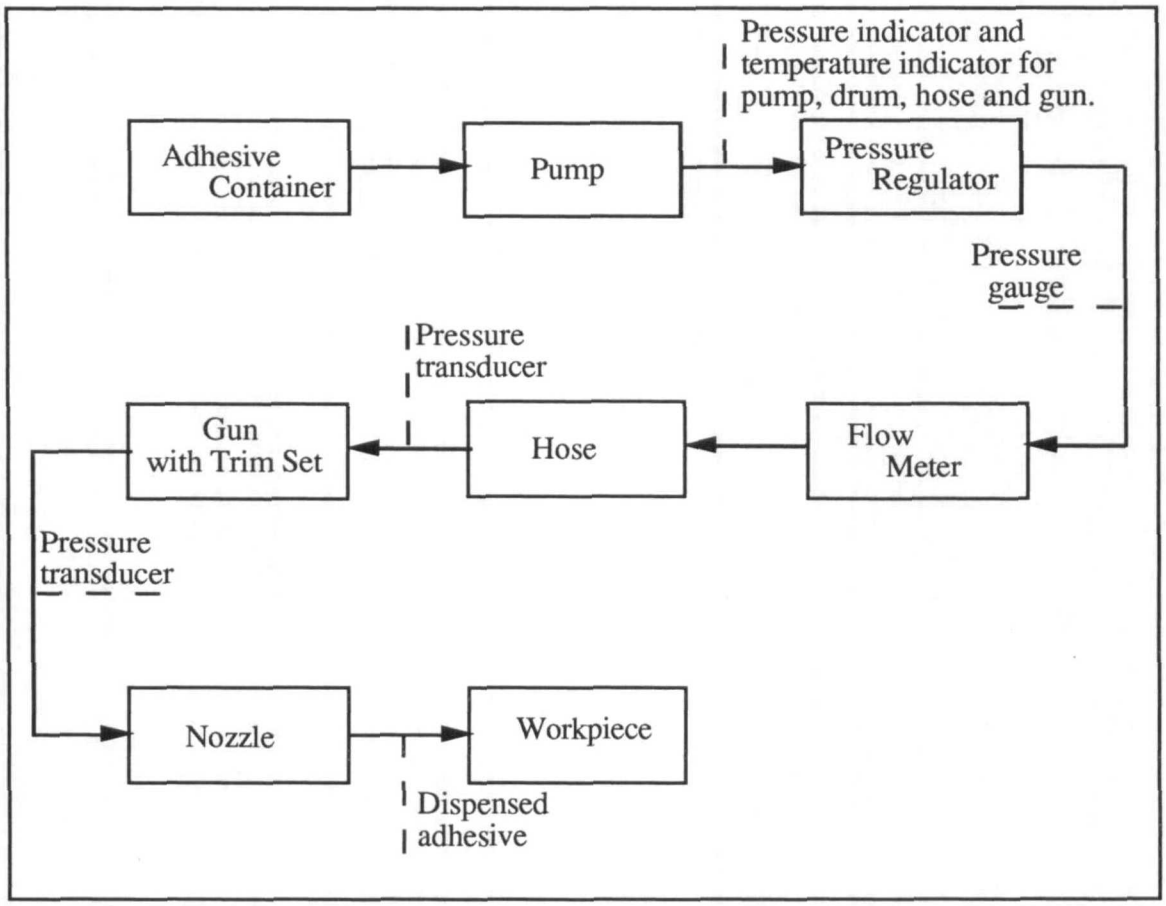

Figure 4.15: The adhesive flow diagram.

Nordson controller basically needs:
ii-a) 0 to 10 VDC
ii-b) Velocity proportioning
ii-c) Digital signals for opening and closing the gun.

4.8.3 Pro-Flo Operation

The Pro-Flo controller adjusts gun output by maintaining a specific pressure in the nozzle, in relation to the input signal (0-10 volts) from the robot controller. The controller interprets this signal and then provides a gun control signal. This control signal adjusts the position of the needle in the gun, which determines material flow.

A pressure transducer which is located upstream from the gun nozzle, sends a signal to the controller. This pressure indicates pressure in the nozzle, and is processed by the controller and converted to a gun control signal. These two signals then are added together in the control loop to adjust the material delivery pressure at the gun nozzle. In addition to this pressure feedback loop, the system measures the volume of material that is dispensed for each part and compares it to a pre-determined set point. This built-in volume compensation loop allows material viscosity to vary while not affecting the amount of material being dispensed on each part [Nordson 90].

The second adhesive used was an *Elastosol M23*, formulated by Evode Ltd. and typical of those used in the automotive industry. It is very thick, has thixotropic properties, is non-Newtonian in behaviour and is typical of those used in the automotive industry since the adhesive needs to be sufficiently stiff when contacting the workpiece, so that it does not run down vertical surfaces. The adhesive drum and the dispensing hose were heated to 35 ^{o}C to ensure a consistent temperature (and hence viscosity) independent of the ambient temperature. This also had the effect of lowering the effective viscosity, making the adhesive easier to pump at the very high shear rate. A detailed analysis of adhesive characteristics and material modelling are covered in Ch. 6.

4.9 On-line Control Using the Karel Controller

Having implemented the Nordson Pro-Flo dispensing system and integrated it within the automated cell, the next step is software development for on-line control of adhesive bead parameters. The bead parameters can be kept constant by having closed loop control for the flow rate adjustment. This control loop is based on the desired bead parameters (e.g., width and height) as a reference point, and can be accomplished by controlling the flow

rate. The change of the flow rate can then be achieved by opening and closing the dispensing gun.

On-line control software has two major parts: image processing software and robot movement along the desired path, which also includes the control algorithm. The first step in the vision algorithm is the initialisation of the variables for the image processing. The initial image will then be defined and the binary image captured. The next step will be a search for the arc, and if it is found, the bead width will be calculated. Otherwise, the initial pointset will be set as a current pointset and the binary image will be captured. The light line will then be obtained and the bead height calculated. The image processing flow chart is given in Fig. (4.16b) [Razban 91b].

After acquisition of the bead height and width, these parameters are compared to the reference values and, if necessary, the control algorithm is activated. Flow rate adjustment signals will then be sent to the robot controller via a RS232C serial communication port. The adjusted signal will then be sent to the dispensing unit from the robot controller. The flow chart for robot motion and control algorithm is given in Fig. (4.16a). The algorithm includes the motion trajectory, opening of the gun, and the control algorithm. The control algorithm controls the bead parameters by flow rate adjustment through the nozzle [Razban 91a].

The controller is an *on/off* controller which has two position modes. It is very simple and requires only an on/off actuator instead of a continuous one. If the error rises above a certain critical value, the controller output changes from 0% to 100%. If the error decreases, it must drop (or be equal to zero) before the output drops from 100% to 0%. Thus, there is always a deadband around zero error where there is no change in the controller output.

An on/off controller is realised by mounting a flag in the control algorithm. The flag interrupts the actuator input if the bead parameters are not between the tolerance range and modifies the input signal and sends the corrected input actuator to the process. The controller algorithm is;

$$U_k = K \quad \text{if } e_k > 0$$
$$U_k = 0 \quad \text{if } e_k \leq 0$$

The main advantage of this algorithm is that the accurate quantitative knowledge of the process dynamic is not required. The block diagram of the on/off controller is given in Fig. (4.17), where W and $Wref$ are the output width and reference width respectively.

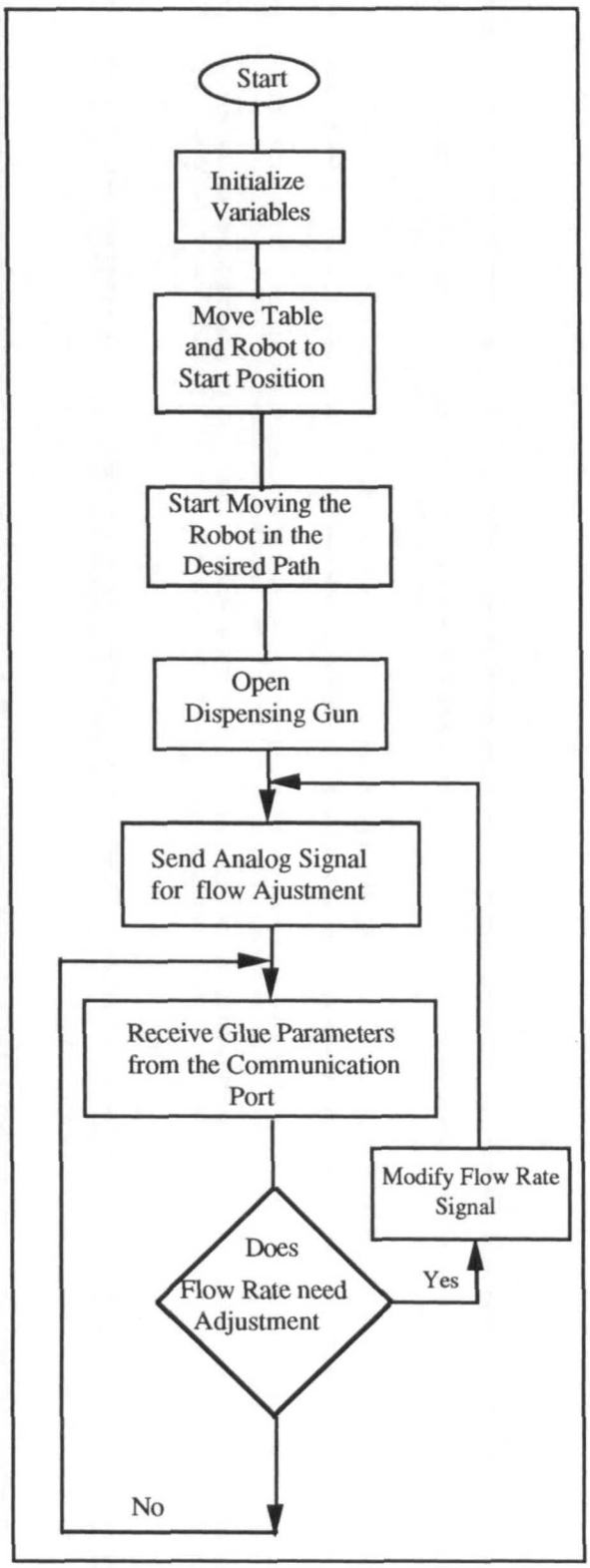

Figure 4.16a: Flow chart for robot trajectory and on-line control.

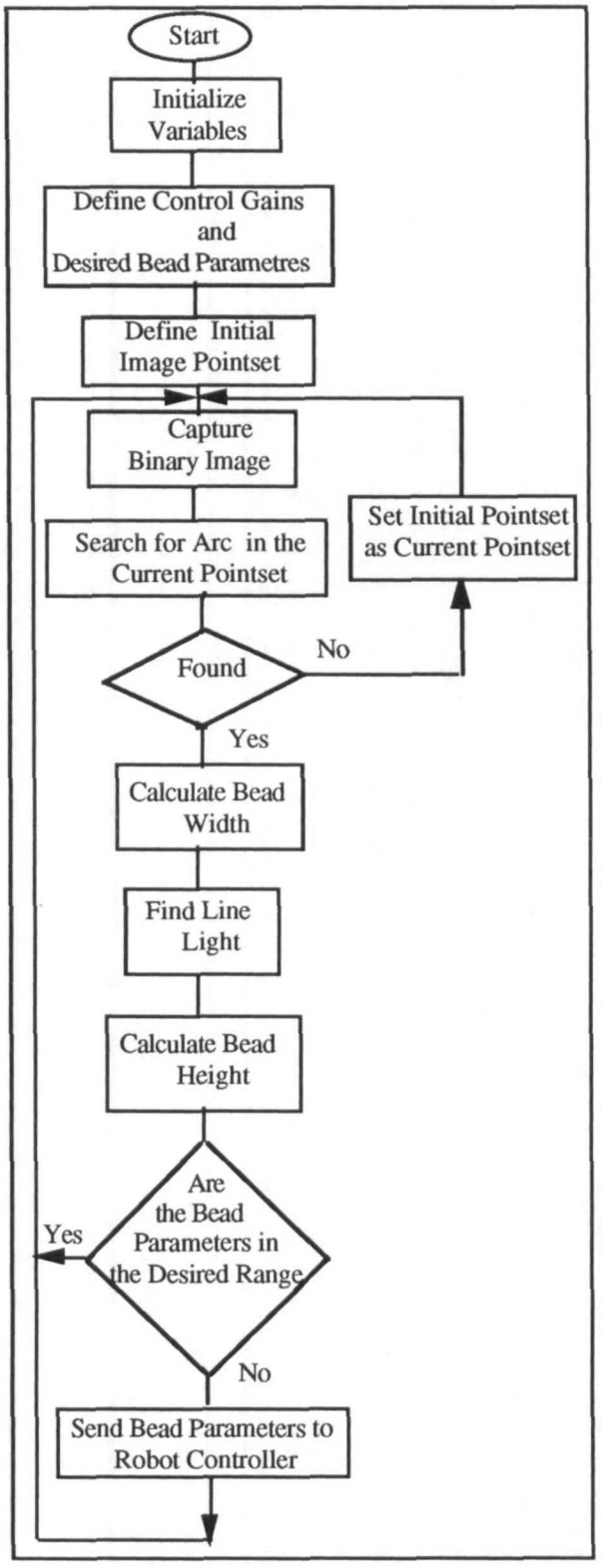

Figure 4.16b: Flow chart for image Calculation.

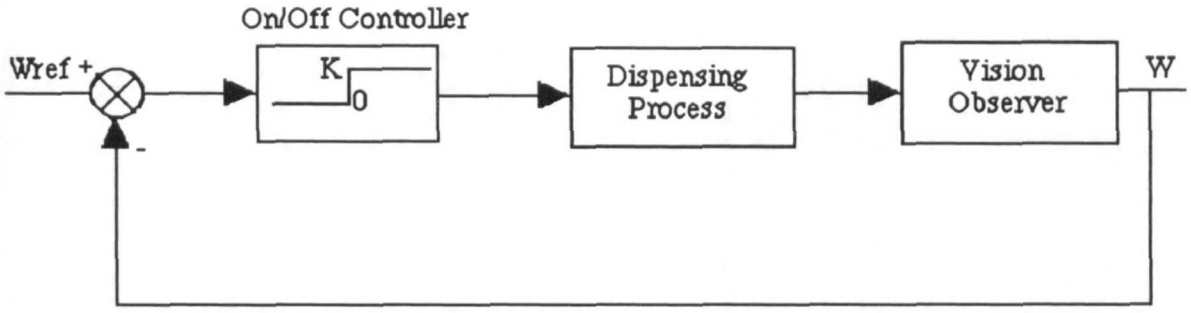

Figure 4.17: Block diagram of the on/off controller.

For communication between the IBM-PC and the Karel system the *Asynch Manager* package is used (some of the features of the package are given in appendix III). Image processing results are sent to the Karel controller using *ASCII* characters via *RS-232C*. On the other end, a procedure written in Karel for receiving the ASCII characters converts them to digital data to be used in the control algorithm.

4.10 Processing Time

The typical processing time in the middle of the bead is given in Tab. (4.1). Most of the processing time is concerned with acquisition of the image and calculating its parameters. This time usually increases when the robot moves faster since the adhesive bead has less time for settling down when the robot is at a higher speed. The dispensing system adjusts the flow rate faster if the analogue signal is in mid-range (2.5-7.5 volts) which is 25% to 75% of the gun opening. Tab. (4.2) shows the time delays which are involved at the beginning of the bead. Capturing the first image takes longer at the beginning of the bead due to the time needed for defining the initial image frame and the distance of the camera from the nozzle (the focusing point of the camera is 45 mm behind the dispensed nozzle). The image processing time is smaller at lower speed, as was expected [Razban 91c].

4.11 On-line Control by-passing Karel Controller

In the Fanuc robot the individual servo motors have a controlled cycle which is updated every 3 milliseconds. However, the on-line control system can only be interrupted in

Speed (mm/sec)	Processing Time (msec)			Dispensed Adjustment Time (msec)	Range of Analogue Signal (V)
	Karel	Vision	Total		
100	128	160 - 220	288 - 348	90.0	1- 5
200	128	160 - 220	288 - 348	88.0	2 - 5
300	128	170 - 220	298 - 348	54.0	4 - 8
400	128	160 - 220	288 - 348	34.0	5 - 8

Table 4.1: Processing time in mid-bead.

Speed (mm/sec)	Delay Time (msec)		Processing Time (msec)	
	Karel Program	Distance of camera from nozzle	First image	Karel program
100	128	696	496	128
200	128	348	596	128
300	128	232	696	128
400	128	174	796	128

Table 4.2: Processing time at the beginning of the bead.

blocks of 32 milliseconds. Thus, the minimum time to take in a signal from the vision system and adapt this to an instruction to be passed to the dispensing system requires a minimum of four 32 msec blocks. This 128 msec (as given in Tab. 4.2) is to be added to the delays of the vision system and the dispensing system.

An alternative strategy for on-line control is to send the signal directly to the dispensing system via a D/A board. The dispensing gun is then controlled by by-passing the robot controller and using an IBM-PC via A/D board (the main feature of the board is presented in appendix IV). This method takes less processing time due to sending the adjusted signal to the dispensing controller directly and by-passing the robot controller. This can be viewed in Fig. 4.12, where the schematics diagram of the cell is presented. The processing time then is shortened by about 128 msec which is the computation time in the robot controller. In the case of control using the IBM-PC, there is also a slight change in software development. The Karel software is then basically for the motion and activation/deactivation of the gun and the control algorithm will be included in the image processing software. This approach has the added benefit that a less sophisticated robot controller than Karel could be used since it does not now need to control the cell.

A switch relay box was also made and implemented between Karel controller, dispensing controller and IBM-PC. The relay has two inputs and one output. The input may be switched on either from the Karel controller or IBM-PC and the output (analogue single value) is sent to the dispensing controller for controlling the amount of gun opening. This allows a flexibility in controlling flow rate either from the Karel controller or the IBM-PC at any time.

4.12 Discussion

The problem of dispensing adhesives can be divided into two areas: those parameters which vary continually, such as temperature, pressure (which has an effect on viscosity and shear rate) and which can be monitored and used as part of real time control strategies to maintain the bead within the required tolerance level, and secondly, those which cause step discontinuities (e.g. air bubbles) for which the control strategy cannot adapt in time to ensure full integrity. In the latter case, some of the parameters can be sensed on-line, others will require rejection or repair of the part after a subsequent inspection stage.

The quality of bead deposition is defined in terms of the consistency of the dispensed bead. This involves both the amount of material and its placement. The consistency of the bead

size and its accurate placement are the most important factors in the performance of the joints. The dispensing process should be designed to produce a consistent and uniform bead regardless of variation in the environment. The quality of the adhesive bead is affected by the parameters which vary continually such as pressure, viscosity, shear rate and temperature. These variations have an affect on the flow rate and subsequently on the adhesive bead parameters.

One implication for on-line control of the length of time taken to adapt the bead parameters is that this technique is better for dealing with gradual changes in parameters, such as those occurring when the temperature of the factory gradually increases and leads to a decrease in viscosity of the adhesive. In such circumstances, the bead can be modified effectively to stay within the prescribed tolerances. The technique is much less suited to step changes in dispensing, such as those occurring when small air bubbles or particles temporarily block the flow. Even if the vision system should happen to detect the event, the chances are that the flow is already back to normal before the dispenser can be adapted. The best technique for these *step-discontinuities* appears to be the use of post-process inspection, using an automated vision system [Sezgin 93]. This is also subject to difficulty as there is a conflict between having a large field of view for rapid processing and the pixel resolution to correctly measure sizes of gaps in the bead, distances from reference edges, etc. An alternative is to traverse the camera over the bead using the robot, but this is a time consuming process which also requires algorithms for visually tracking the bead. Another alternative is to use a number of high resolution cameras, but this is an expensive solution.

The automated dispensing facility was gradually modified to optimise the performance and minimise the time delays between the changes demanded from the robot controller and the implementation of the modified bead on the workpiece. Using booster relays for the Graco system, the dispensing adaptation time was decreased from around 200 msec to 170 msec. This was further lowered by replacing the Graco unit with Nordson Pro-Flo dispensing system. At the robot speed of 200 mm/sec, the adaptation time is 88 msec for Pro-Flo as shown in Tab. 4.1. Further reduction in closed loop adaptation time was achieved using an IBM-PC as the controller and by-passing the Karel controller.

As for the vision system, the total processing time, to measure both width and height, was 160-200 msec. A faster result may be obtained if the height is inferred from a measurement of the width and the flow rate of the bead. However, in general, the time to process the image to give a robust system that will work under all conditions, is quite long. Efforts were made to increase the vision processing speed without adversely affecting robustness. As a result, the vision processing time was reduced to 60 msec.

4.13 Conclusion

A vision system for adhesive bead calculation has been investigated which acts as a feedback for the dispensing control loop. In order to close the control loop, a vision system was used to measure the width and the height of adhesive beads while they are being laid down. An on-line control system has been implemented which can monitor dispensed bead parameters and change the performance of the dispensing system on-line to achieve the desired characteristics. This type of control is adequate for small variations in bead quality. The processing time is the major constraint for real time control. The drawback is, if the quality of the bead is not satisfactory within this interval, the vision system will not be able to inspect it unless a special parallel processor is used. However, the adaptation time can be shortened by the use of an A/D board, to allow command signals to be sent direct from the IBM-PC to the dispensing gun. The processing time can also be altered by using a faster vision system.

An alternative strategy is to change the speed of the robot, rather than the dispensing rate of the gun, as the robot has a quicker response time. However, because the robot must slow down at corners to achieve good position control this is a less preferable option. Also if the robot speed is too high on corners, the camera may not have time to scan the bead at all on the corner. When the robot slows at a corner, the dispensing gun must also cut its flow. This implies either a very fast changing gun, a very slow robot speed, or else the use of prior knowledge of the speed patterns so that the delays in the gun opening can be taken into account by changing the gun opening well ahead of the time where a bead change is required. In practice, a combination of all three aspects is necessary for optimal results. The single axis table and dispensing controller are linked to the robot controller. Thus, the dispensing controller can be addressed directly from the robot controller and the robot controller also controls the table movement. The opening of the dispensed gun is controlled through the robot controller while the adhesive flow rate can either be controlled from an IBM-PC via a D/A board or from the robot controller.

The on-line controller analysed in this chapter is an on/off controller or so called bang-bang controller. However, it is necessary to have a better controller using conventional control such as an integral, or proportional plus integral, controller. This requires a modelling of the bead parameters. Furthermore, for a fully automated cell, a knowledge-based system needs to be used for initial set-up and diagnosis in which modelling of non-linear adhesive flow through the gun is essential. These aspects are covered in the following chapters.

CHAPTER V

ADHESIVE BEAD MODELLING AND CONTROL

5.1 Control of a Dispensed Adhesive Bead

A closed loop feedback scheme for the dispensing process was first implemented using an on/off controller (as described in chapter 4) with the aim of achieving close control of the adhesive bead parameters. The main drawback of an on/off controller is that there are only two possible input levels, fully on and fully off. An improved alternative to the on/off control algorithm is the use of a conventional controller (such as a PID controller) or a predictive controller. This scheme makes use of a vision system as an observer. The bead parameters obtained by image processing are used by the controller to ensure that the bead stays in the desired bandwidth.

Thus, the process variables and the delays in the process have to be identified in order to obtain a mathematical model of the process. The controller can then be designed based on this mathematical model. This chapter describes variables in the dispensing process, delay in the process dynamic modelling of the dispensing process, simulation and the performance of the controller.

5.2 Dispensing Process Variables

The dispensing process consists of four sets of variables: adhesive variables, geometric variables, environmental variables and operating variables.

i) Adhesive variables: these are the physical properties of the adhesive. The main factor is the change in viscosity. The viscosity of the adhesive varies with environmental changes or local temperature fluctuations. However, the viscosity remains constant if the temperature variation is small (see § 2.6.2 for further detail).

The existence of air bubbles in the nozzle is another important factor in the adhesive variable. This may cause fluctuations in the flow rate of the adhesive material, thus affecting the size of the dispensed bead. This may be minimised by de-pressurising the drum and making sure it is free of air before starting a process. However, this is not an easy task when the adhesive is very viscous.

ii) Geometric variables: these include the nozzle length, the nozzle diameter and the internal diameter of the gun which are kept constant for a given process.

iii) Environmental variables. These are: ambient temperature, relative humidity and inappropriate surface properties. A contaminated surface may cause adhesive bead deformation when the adhesive is laid on the surface. This can be prevented by cleaning the surface prior to application and the use of pre-process inspection to ensure it is free from contaminants.

iv) Operating variables. These are: opening of the gun, the operating temperature, delivery pressure and robot speed. The opening of the gun controls the flow rate through the nozzle. Changes in the operating temperature affects the material viscosity and subsequently the flow rate. Any delivery pressure variations in the material (due to the problem of sticking in the pump) will result in a change in the flow rate, which will also affect the adhesive viscosity. This variable is uncontrollable and represents a major source of disturbance in the dispensing process. The speed at which a robot travels across a work piece is critical to the accuracy of the volume deposited over a given length. The motion of a robot along a given path will need to be as accurate as possible.

5.3 Process Modelling

Industrial processes are usually characterised by the interaction of many variables. A suitable strategy for controlling such a process requires a good knowledge of the process which is represented by a model. The first requirement in the development of a process control is a dynamic process model. The performance of the process control depends very strongly on the accuracy of the process model [Rauwendall 86]. Such a model describes the relationship between the input and the output of the process. The model is usually fitted to a first or second order system since it is difficult to fit models higher than second order to the process. However, the response is usually dominated by one or two dominant poles [Warwick 86, Gorecki 89].

The adhesives dispensing process like many other industrial processes are characterised by the interaction of many variable quantities. A large number of the parameters influencing the dispensing process makes the process automation rather a complicated task. A suitable strategy to control such a process for generating an appropriate input function as a driving force to get a desired output, requires knowledge of the process characteristics from which an appropriate model will be obtained. Such a process model, describing the relationship between output with regard to the input and the disturbances, is

$$y(s) = G(s) * u(s) + d(s)$$

Where $y(s)$, $G(s)$, $u(s)$ and $d(s)$ represent the output, impulse response, input and disturbances in the Laplace transform domain respectively.

The dispensing process can be described by a set of state variables, representing physical characteristics which are likely to vary. The input variables are the command signal for changing the flow rate by adjusting the opening of the gun, and perturbations which are generally unknown. The bead parameters are functions of the opening of the gun which are controlled via actuator signals, delivery pressure, temperature, viscosity, surface tension, density, robot speed and table speed. The sensitivity analysis has shown that the influence of the surface tension on the bead parameters is small [Marshall 91, Razban 92] and its variation is assumed negligible. For a particular adhesive, viscosity (at constant temperature) and density do not vary in a wide range. They are not measurable on line and are assumed constant. Since temperature varies very slowly, it may also be assumed constant for a single run. The variations in delivery pressure are treated as perturbations. The output variables are the width and the height of the bead. These two variables are linked for a given flow rate and robot speed. The input/output block diagram of the process is given in Fig. (5.1).

The process input variables are:
i) actuator command for the opening of the dispensing valve. This is the primary control variable which acts on the system.
ii) disturbance in delivery pressure, DP, which is usually unknown and unobservable.

The environmental temperature effects are a negligible disturbance since the hose is heated well above ambient temperature.

The output variable is the width of the bead which is measured by the vision system. The

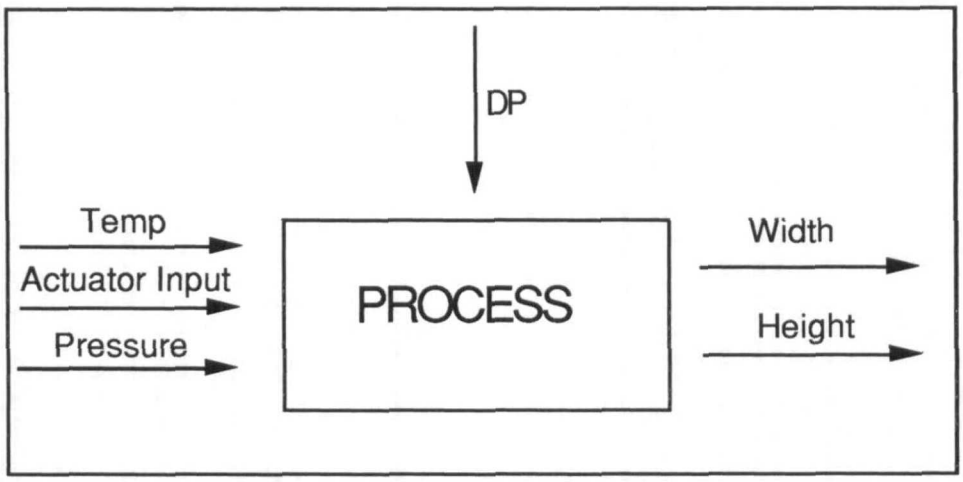

Figure 5.1: Input /output block diagram.

variation of the height of the bead is not used as a feedback variable in this work, since it remains almost unchanged during a run. However, the longer term variation in temperature and hence viscosity can effect the height and so it needs to be checked occasionally.

5.4 Delays in the Process

The delay in the control loop is due to a *transport time* that is the time elapsed between the moment where the bead has been laid down and the moment when it has been seen and processed by camera. Three major delays have been identified in the control loop for which the total delay T_d is:

$$T_d = T_d(A) + T_d(P) + T_d(V)$$

Where;
$T_d(A)$ is the adaptation time of the flow rate from the dispensing system (30-90 msec), which is a function of the robot speed. The viscosity decreases at the higher robot speed which makes the adaptation time shorter.

$T_d(P)$ is a transport lag due to the distance of the camera behind the dispensing nozzle. This ranges from 112.5 msec at robot speed of 400 to 450.0 msec at robot speed of 100 mm/sec. This physical delay always exists. This delay was further reduced to 32.5 msec at 400 mm/sec and 130.0 msec at 100 mm/sec (see § 5.6 for further detail).

$T_d(V)$ is a computational delay due to the adhesive bead acquisition and bead parameters measurement by the vision system, which is 60 msec.

The effects of different delays have been accumulated and it is represented as a single time delay, T_d. The total delay T_d varies with the operating conditions which can be modelled as a function of the robot speed. It decreases as the robot speed increases and this is due to decrease in $T_d(P)$ and $T_d(A)$. The total delay as a function of the robot speed is given in Fig. (5.2). The presence of the delay can complicate the analytical solution of the control design and limit achievement of system performance.

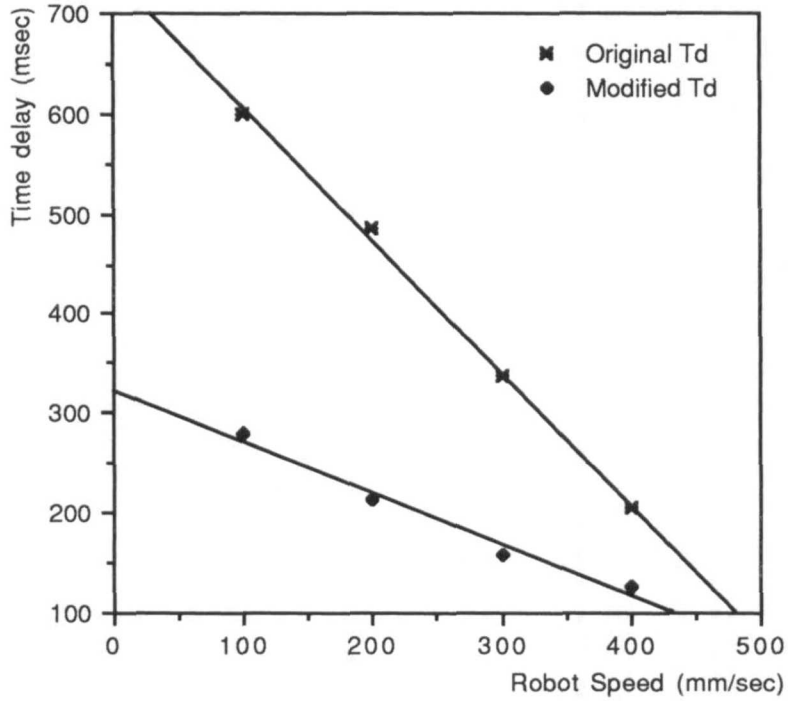

Figure 5.2: Experimental time delays as a function of robot speeds.

5.5 Transfer Function Of the Pure Time Delay

For the process with a time delay, a process response for an input u with a pure time delay T_d, is shifted of the input by the amount of delay. This is given by:

$y(t) = u(t-T_d)$

by using Taylor's expansion:

$y(t)=u(t) - T_d\, d/dt\,(u(t)) + T_d^2/2!\,(d^2/dt^2)u(t) + ...$

using Laplace transform:

$y(s) = u(s) - T_d\, s\, u(s) + T_d^2\, s^2\, u(s)/2 + \cdots$

$y(s) = u(s)\,(1 - T_d\, s + T_d^2\, s^2\, /2 \; - \cdots\cdots)$

$y(s) = u(s)\, e^{-sT_d}$

Where e^{-sT_d} is the transfer function of the pure time delay. It has a gain of unity and a phase of $-\omega T_d$ at the angular frequency ω in the frequency domain. Thus, the time delay introduces an additional phase shift to the process and it is known as having a non-minimum phase element. In the z domain, if the delay is a k multiple of the sampling interval , it would be represented as Z^{-k} .

To approximate a time delay, it is necessary to find a finite approximation of the e^{-sT_d}. Thus, it is necessary to replace exp ($-sT_d$) by the truncated version of its Taylor expansion. Three most common approximations for time delays are [Smith 58, Kuo 75, Donoghue 77, Leigh 82, Schwarzenbach 92]:

$$e^{-sT} = \frac{1}{e^{Ts}} \cong \frac{1}{[1-(Ts/n)]^n}$$

$$e^{-sT} \cong 1 - Ts + \frac{(Ts)^2}{2!} - \frac{(Ts)^3}{3!} + \cdots$$

$$e^{-sT} \cong \frac{(1-\frac{T}{2}s)}{(1+\frac{T}{2}s)}$$

The last approximation technique is called the first order Pade approximation. The Pade approximation is widely used to replace exp ($-sT_d$) as a ratio of two polynomials P(s)/Q(s) (as shown above) of the same order [Marshall 79]. The relation of $P(s) = Q(-s)$ should hold to make the polynomial gain unity. However, in this research, the exact delay has been used for simulation.

5.6 Process Identification

The classical approach to determine process models would be to inject an impulse or step input to the actuator and then to evaluate a transfer function for the resulting transient response. The identification procedure used, was as follows:

i) introduce a step change to the actuator
ii) record the width response for the process
iii) find a model which represents the best representative of the time response.

To find a process model, a series of experiments were performed using a step input for the actuation signal. The bead width was then calculated using the image processing algorithm and time responses for variation in width for speeds in the range 100 mm/sec to 400 mm/sec. The responses show a small overshoot and a short oscillation. Thus, the process can be modelled as a second order system.

Analysing the time responses, it was observed that the response peak time is very short compared to the time delays in the system. It was evident that only a very limited performance would be attainable and with a such large time delays and hence measures to reduce the system time delays were first sought. Of the three major delays in the process described in (§ 5.4), the distance of the camera from the dispensing nozzle has the highest value. Furthermore, it is very difficult to modify the other two sources of delays. The Pro-Flo adaptation time is fixed and the image processing is just 60 msec and it is difficult to make any more improvement. Thus, the vision set-up was modified and the distance of the camera from the nozzle was reduced from 45 mm to 13 mm. This reduces the delay from 32.5 msec at 400 mm/sec and 130.0 msec at 100 mm/sec. Thus, the total delay range is 126.5 msec at 400 mm/sec to 280 msec at 100 mm/sec. The modified time delay as a function of the robot speed is given in Fig. (5.2). The time responses using the modified vision set-up (lower time delays) are given in Fig. (5.3). The camera to nozzle distance could not further to be reduced since it is necessary for the adhesive to impact the workpiece and settle to a reasonably stable condition before the camera can measure its width.

5.7 Control system

The aim of the controller is to maintain the bead parameters within the desired reference values in spite of the disturbances which may affect the process. In general, in order to minimise the undesirable effects of disturbing influences, a closed loop control is necessary (as described in Ch. 4). The block diagram of the closed loop system with an indication of the delays is given in Fig. (5.4). The controller is a numerical controller (based on an IBM-PC) with 60 msec sampling time. It is linked to the flow controller by an A/D board. The closed loop system can be classified as a continuous process, with analogue variables for pressure sensors and the drives, and a computer for processing digital signals. In this case, the process outputs are sent to the computer and they are compared with the reference points, and the control action will then take place.

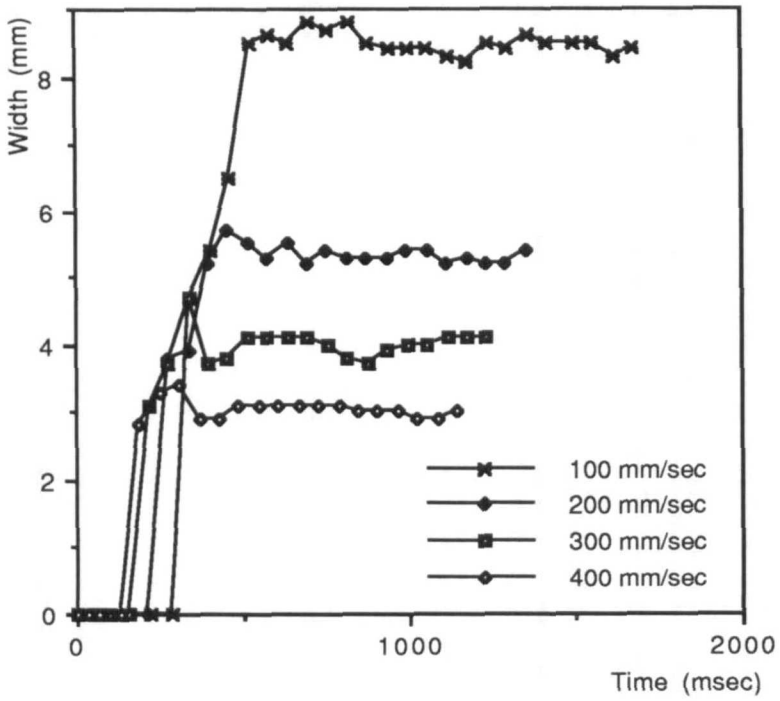

Figure 5.3: Time response of width at different speeds using modified vision set-up.

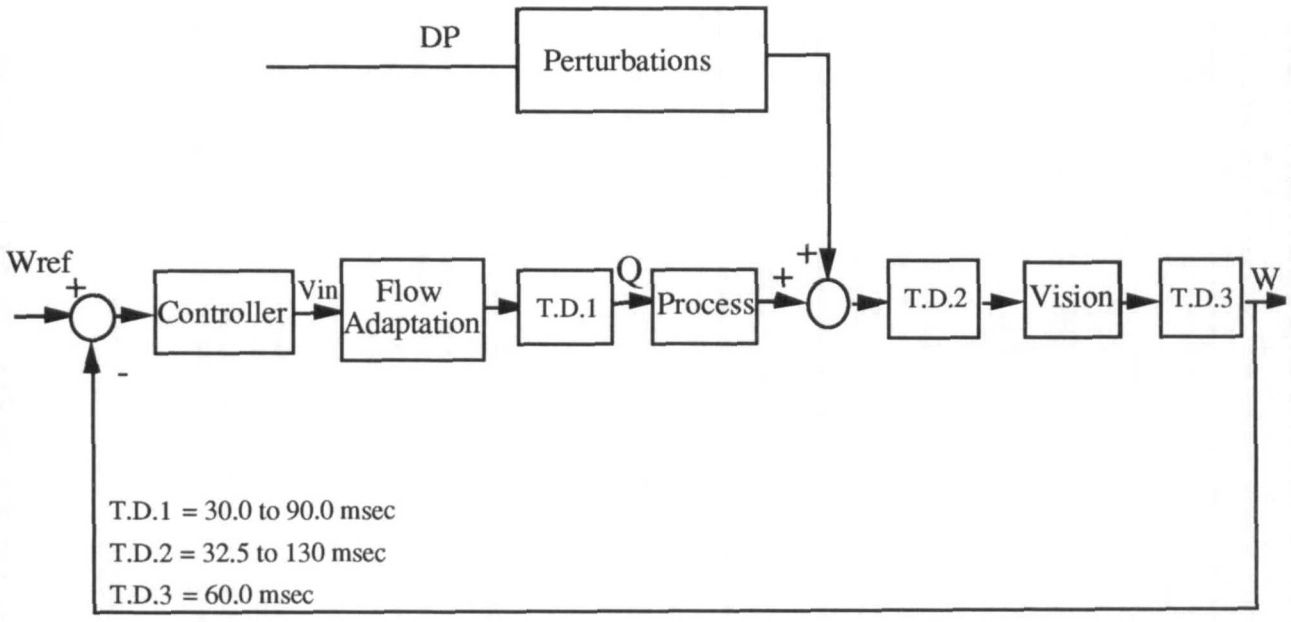

Figure 5.4: Block diagram of the closed loop showing time delays.

Continuous measurements made on the process have to be converted into digital signals. This is achieved by an analogue to digital converter (ADC). This digitised information is then processed by the control algorithm programmed in the computer. Finally the digital command signal is converted to the analogue signal before being sent to the drives. The conversions AD, DA, and the control subroutines are synchronised by a real time clock with a frequency fixed by the sampling period. In the case of vision, the bead measurement is not continuous so the ADC is incorporated in the hardware itself.

The control system operation consists of a sequence of independent steps:
i) The vision system records at the adhesive bead (while the adhesive is being laid by robot) and captures an image.
ii) The image is sent to an IBM-PC via synchronisation signals. The image parameters are analysed and the results are sent to the control algorithm.
iii) The control algorithm checks the results with reference to the set-up and, if it is necessary, updates the actuator signal.
iv) The updated actuator signal is converted using DAC and is sent to the dispense controller for adjustment.

The numerical controller works at a low frequency since the sampling time is 60 msec. The process has a minimum of 32.5 msec delay which is variable as a function of robot speed. The described system belongs to a class of real-time control system in which the feedback signal is sampled at fixed intervals, processed in the computer and returned via a DAC.

5.8 Modelling Simulation

Dispensed adhesive beads need to be modelled as a function of opening of the gun (see § 5.3 for further detail). Transfer function characteristics for the time responses at four different speeds are given in Tab. (5.1). The time response results show that the process can be represented as a second order system with two complex poles which are far from the imaginary axis. The dynamics of the process is quite similar at different robot speeds and the location of the real part of the poles are very close to each other. Thus, the process can be considered as a single lumped parameter dynamic which is independent of the operating condition in series with a time delay whose value varies with operating conditions. Furthermore, the process can be represented as a single transfer function with variable gain for different robot speed.

Robot Speed (mm/sec)	Time Peak (sec)	ζ	ω_n	Maximum Value	Steady State	Transfer Function Poles
100	0.301	0.663	13.95	8.6	8.1	-9.25 ± 10.44j
200	0.241	0.635	16.88	5.7	5.3	-10.72 ± 13.04j
300	0.181	0.522	20.35	4.7	4.1	-10.60 ± 17.36j
400	0.181	0.540	20.62	3.4	3.0	-11.13 ± 17.36j

Table 5.1: Experimental transfer function characteristics at four different speeds.

The process transfer function in the S-domain based on averaging the poles location, is

$$G(S) = \frac{K_a (322.13)}{S^2 + 21.18S + 322.13} e^{-T_d S} \tag{5.1}$$

where K_a (process gain) and T_d (lumped time delay) are the functions of the robot speeds and their values are given in Tab. 5.2. The transfer function simulation graphs and the experimental time responses are given in Figs 5.5 through 5.8 at four different robot speeds.

Robot Speed (mm/sec)	K_a	T_d (msec)
100	2.7	280
200	1.77	213
300	1.37	157
400	1.00	126.5

Table 5.2: Simulated transfer function parameters at four different speeds.

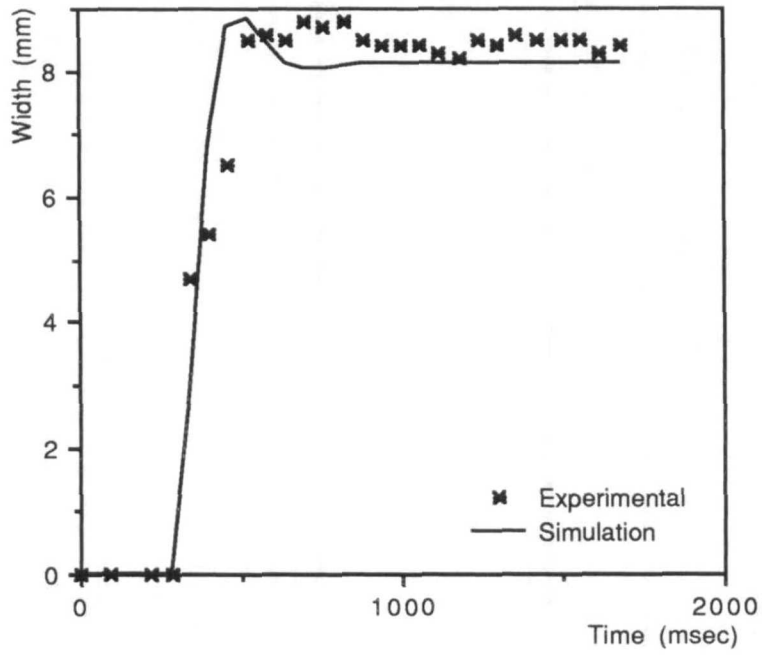

Figure 5.5: Simulated and experimental transfer function at robot speed of 100 mm/sec.

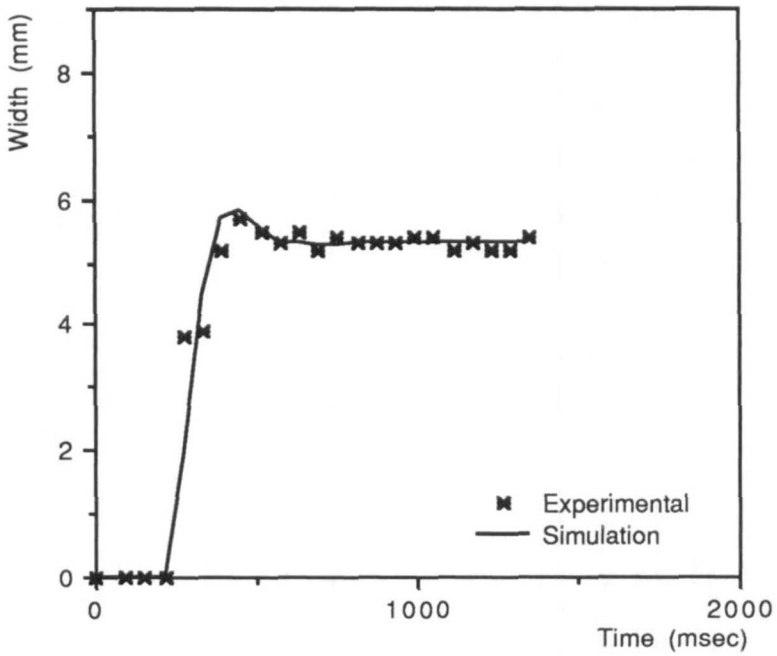

Figure 5.6: Simulated and experimental transfer function at robot speed of 200 mm/sec.

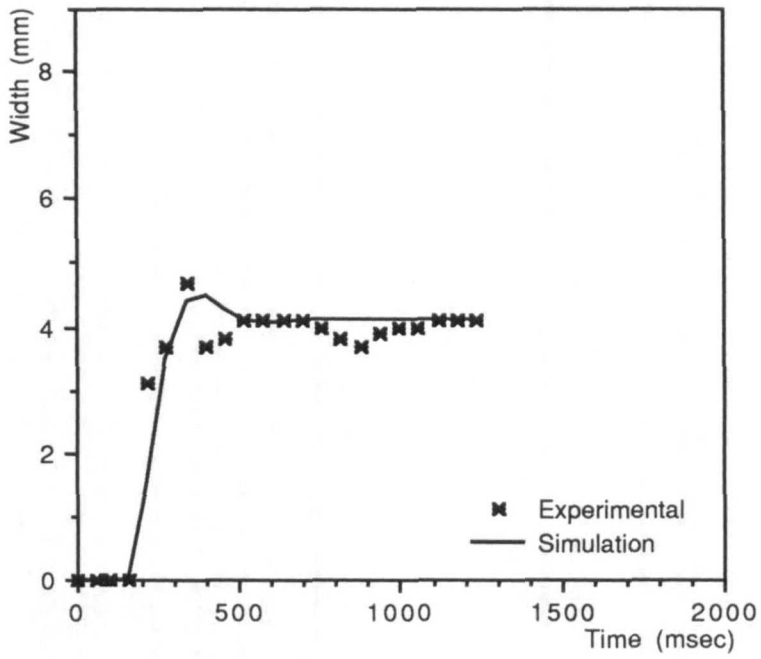

Figure 5.7: Simulated and experimental transfer function at robot speed of 300 mm/sec.

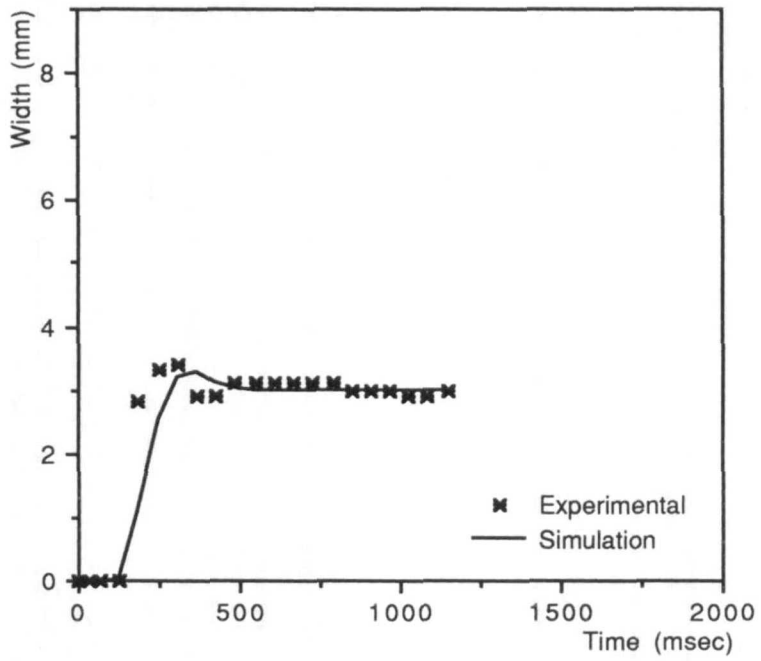

Figure 5.8: Simulated and experimental transfer function at robot speed of 400 mm/sec.

5.9 Control of Processes with Time Delay

Considerable research has been carried out for controlling processes with pure time delay [Marshall 81], and there are a number of schemes to deal with a process with a long time delay. The different controllers in terms of costs, process variations and noise have been discussed by Ross [Ross 77]. Donoghue [Donoghue 77] has looked at designing the multivariable processes with a time delay.

The conventional PID controller and the *Smith's controller* are the two most common controllers for the processes with a long time delay [Bryant 73]. But, Garcia and Morari [Garcia 82] have introduced the concept of *Internal Model control* for processes with a delay. In this scheme the process model is explicitly an internal part of the controller. This is very similar to the Smith's predictor except that the integral and proportional gains are replaced by one parameter called the performance parameter. The Smith's predictor has further been investigated by T. Hagglund [Hagglund 92]. He has introduced a controller called the *PIP controller* where the proportional gain is chosen inversely to the process gain and the integral term is chosen proportional to the process time constant. Self-tuning the controller is another method used by many researchers which is good for small time delay [Clarke75].

5.10 The Conventional Controller

The simplest method of the conventional controller is the proportional controller where the actuating signal is proportional to the error signal. Since the process has a finite steady state gain, the proportional controlled process always exhibits a steady state error. The steady state error decreases as the proportional gain increases but the closed loop response of the process becomes more oscillatory and the settling time increases. If the gain is increased sufficient the process becomes unstable. In order to overcome the above difficulties and to have a zero steady state error, an integral action has to be added to the controller.

The addition of the integrator has a considerable effect on steady state error and it is for this reason that proportional action is combined with the integrator to obtain zero steady state error. Using the PI controller, the process does not perform as well as a process without a delay since the delay introduces an additional phase shift in the closed loop and tends to destabilize the closed loop process. Thus the controller gain has to be reduced which makes the process response slower [Donghue 77].

Adding a derivative action to the PI controller (PID controller) is not appropriate if the process has a long delay and there is a significant amount of noise in the process, although for a small delay, the derivative part can be considered as a prediction mechanism. The aim of the derivative action is to increase the effective damping. The derivative term contributes to an anticipatory type control action. This happens when the output of the controller is modified as the error is rapidly changing, thus anticipating a large overshoot and making some anticipated correction possible. Since the oscillation in the step response of the system is small, adding a derivative term in the controller is not necessary. The major drawback of using the PID controller for a system with time delay is its inability to compensate for the delay [Minter 88], as it waits until there is an error in the process output before taking any corrective action.

5.11 Tuning Control Parameters

There are several ways to adjust the parameters of the conventional controller gains in both the frequency and the time domains. One the simplest and the most common method is based on the rules developed by Ziegler and Nichols [Ziegler 43, Takahashi 69].

The Ziegler-Nichols tuning formula is based on the transient response method, where R_S is the steepest slope, and L is the delay time of the open loop response as given in Tab. (5.3).

	Proportional controller	PI controller
Proportional gain	$1/R_SL$	$0.90/R_SL$
Integral gain	-	$0.27/R_SL^2$

Table 5.3: Ziegler-Nichols tuning formula

Using Ziegler & Nichols heuristic formula, the control gains for the proportional and PI controller were calculated using open loop step responses and the results at four different speeds are given in Tab. 5.4.

Robot speed (mm/sec)	Proportional controller Proportional gain	PI controller	
		Proportional gain	Integral gain
100	0.10	0.09	0.10
200	0.16	0.15	0.21
300	0.25	0.22	0.43
400	0.42	0.38	0.91

Table 5.4: Ziegler-Nichols setting for Proportional and PI controller.

5.12 Digital Control

There are basically three methods to design a discrete time controller for a continuous process as follows:

i) continuous time modelling of the process and continuous controller design followed by discretization of the result

ii) transformation of the continuous modelling of the process to the Z-domain followed by digital control design

iii) the last one is the digital process modelling and the digital control design for the process.

Since the process is continuous, to design a discrete controller (second method), it is necessary to evaluate the pulse transfer of the process using the sample and hold operation (ZOH) of a D/A convertor (Fig. 5.9) as follows :

$$G(Z) = (1 - Z^{-1})\xi(\frac{G(S)}{S})e^{-T_d S} \tag{5.2}$$

The Z-transform of a function f(t) is defined as

$$Z\,(f(t)) = F(Z) = f\,(KT_S)\,Z^{-k}$$

where T_S is the sampling period.

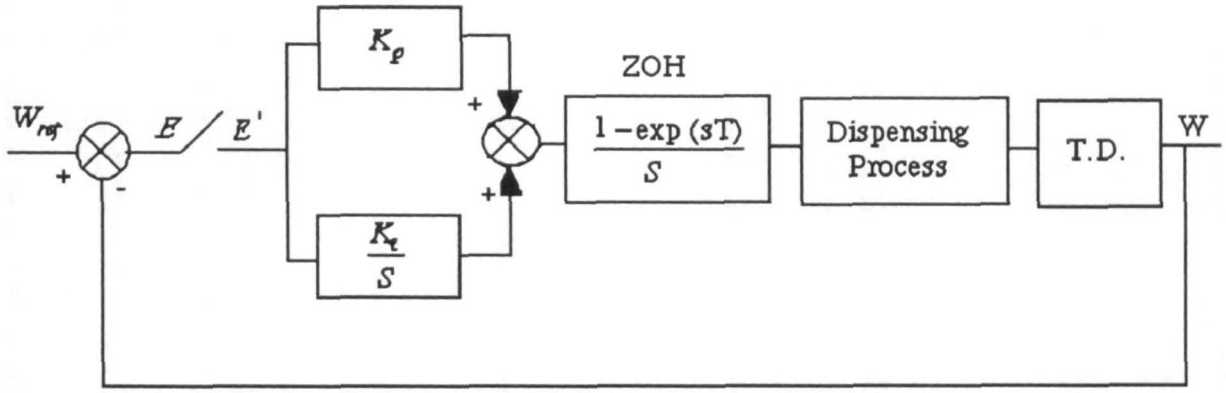

Figure 5.9: Discrete time closed loop block diagram.

The transfer function (Eq. 5.1) was then converted into discrete form using a Z transformation. If $T_d=KT_S$ (K is an integer value, and T_S is a sampling time) then using Eq. 5.2:

$$G(Z) = K_a \frac{b_1 Z + b_2}{Z^2 + a_1 Z + a_2} Z^{-K} \tag{5.3}$$

Where

$$a_1 = -2e^{-aT_s} Cos(bT_s) \qquad b_1 = 1 - e^{-aT_s}[Cos(bT_s) + \frac{a}{b} Sin(bT_s)]$$

$$a_2 = e^{-2aT_s} \qquad b_2 = e^{-2aT_s} + e^{-aT_s}[\frac{a}{b} Sin(bT_s) - Cos(bT_s)]$$

$$a = \zeta\omega_n \qquad b = \omega_n\sqrt{1-\zeta^2} \qquad \zeta \le 1$$

The digital control block diagram of the dispensing process using PI controller is given in Fig. 5.10.

5.13 Control Simulation

The design goal is to obtain a critically damped closed loop system, where the response is as fast as possible. The process model is a second order system with a pure time delay. The dead time compensation reduces the effects of the time delay. For simulation, the process transfer function is Z domain were used.

The proportional controller was first used for the controller simulation. The proportional controller is as follow:

$$U_{i+1} = K_p e_i$$

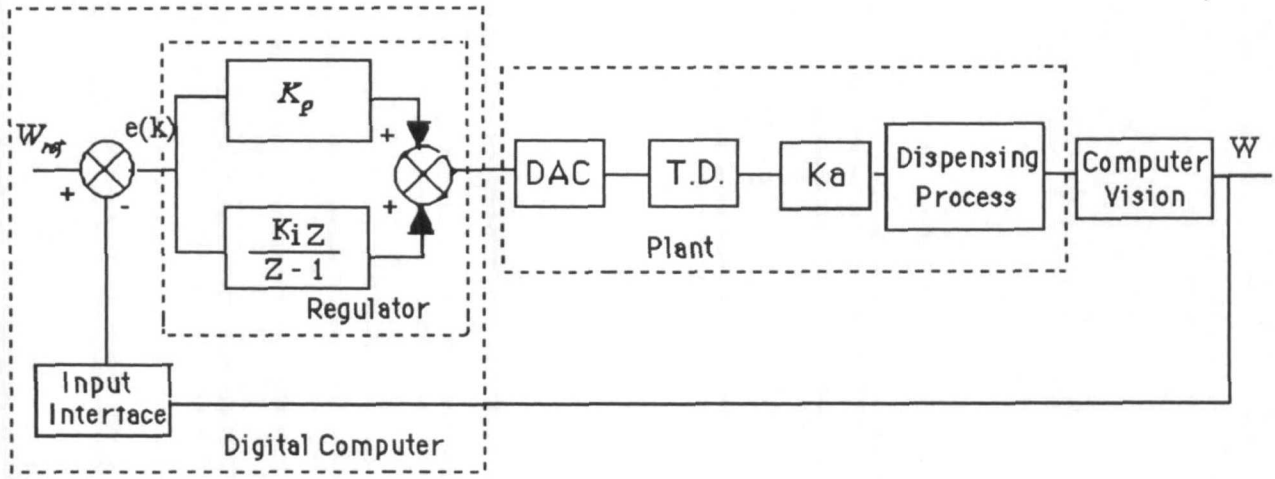

Figure 5.10: Block diagram of the closed loop digital control

Where U_{i+1} is the controller output, K_p is proportional gain and e_i is the error between output and the reference point. Using Tab. 5.4 results (Ziegler & Nichols setting) for the proportional controller of the initial trial, the simulation responses were performed. The *Kp* value was then changed to obtain a better response. The results are given in Figs. 5.11 through 5.14. The closed loop system performance becomes more oscillatory as the proportional gain increases. Eventually, proportional gain reaches the point at which the system never settles. The drawback of this scheme is that a high gain is necessary to limit the steady state error. This does not take into account the saturation of the actuator. This type of controller is unattractive since the steady state error always exists.

To get a zero steady state error, an integral controller needs to be used. The integral controller is:

$$U_{i+1} = \frac{T_s}{K_i} \sum_{j=1}^{i} e_j$$

where T_S is sampling period, K_i is integral gain and the $ej = Wref - Wi$. Time responses were obtained using Ziegler & Nichols setting of the PI controller for initial trial. The gains had to be reduced in order to have less overshoot and better stability performance. The optimum gains were found to be 0.03, 0.06, 0.11 and 0.15 for the robot speeds of 100 through 400 mm/sec as given in Figs 5.15 through 5.18.

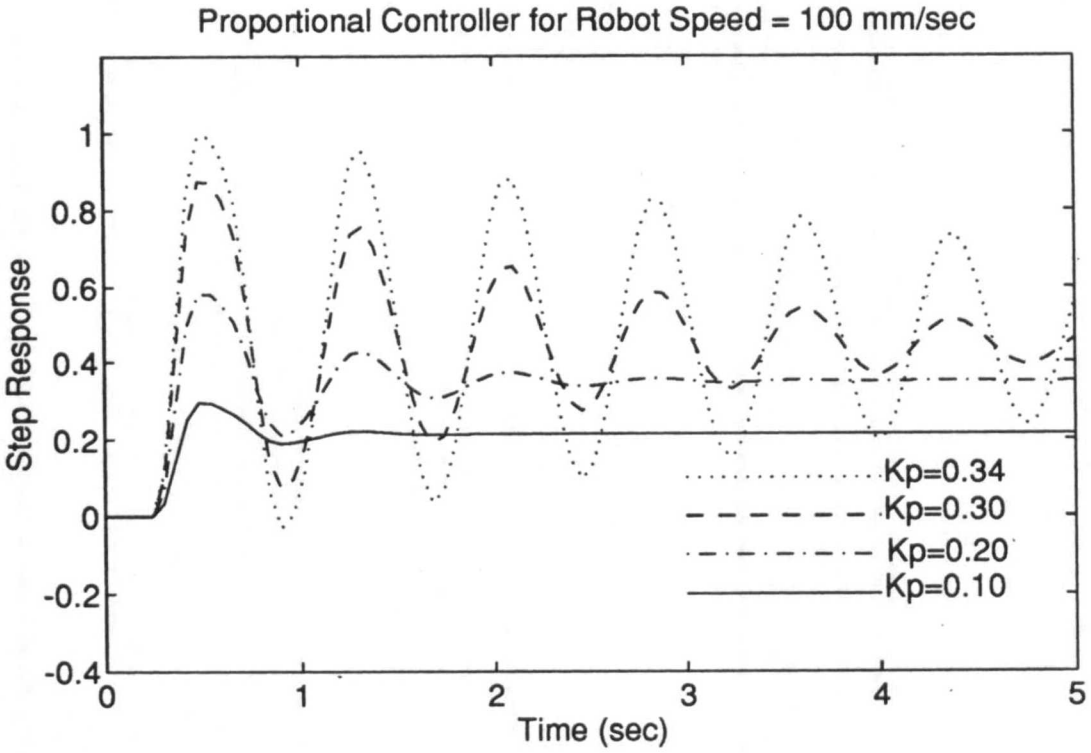

Figure 5.11

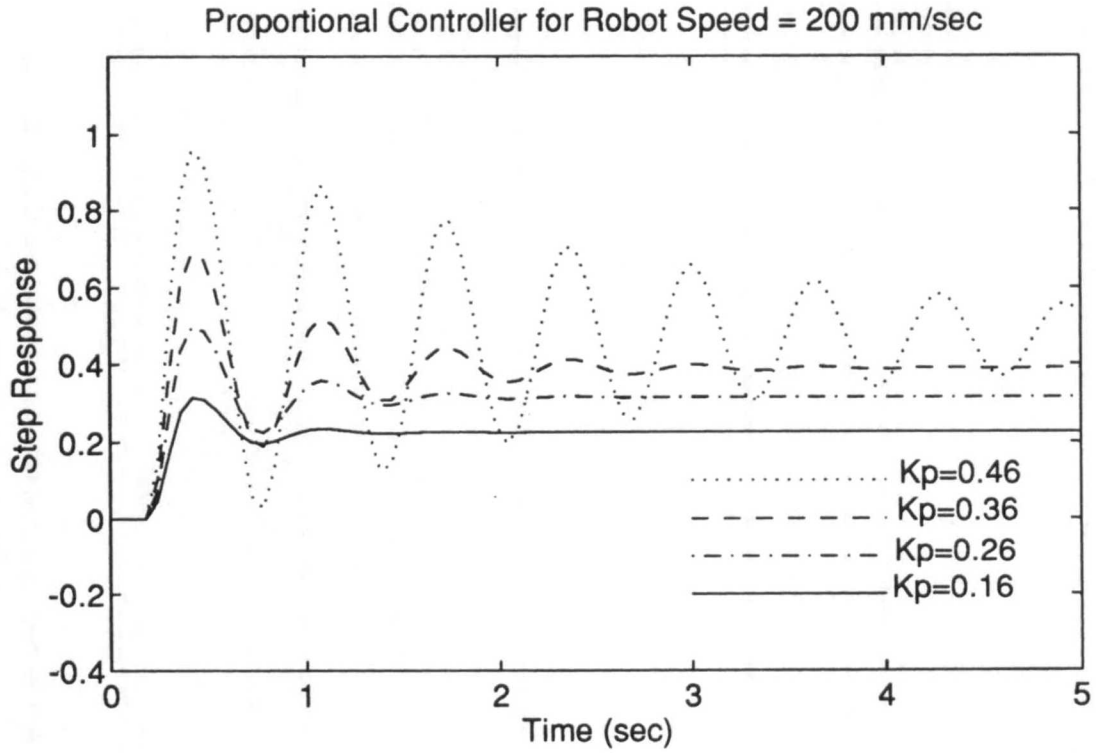

Figure 5.12

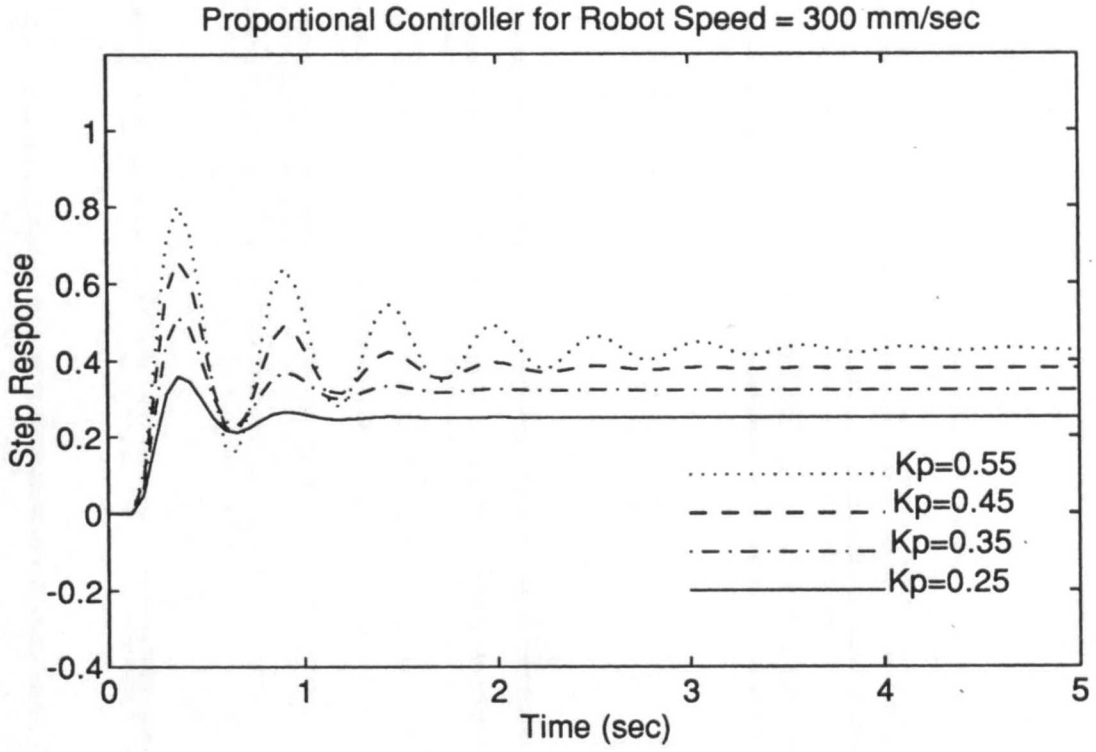

Figure 5.13

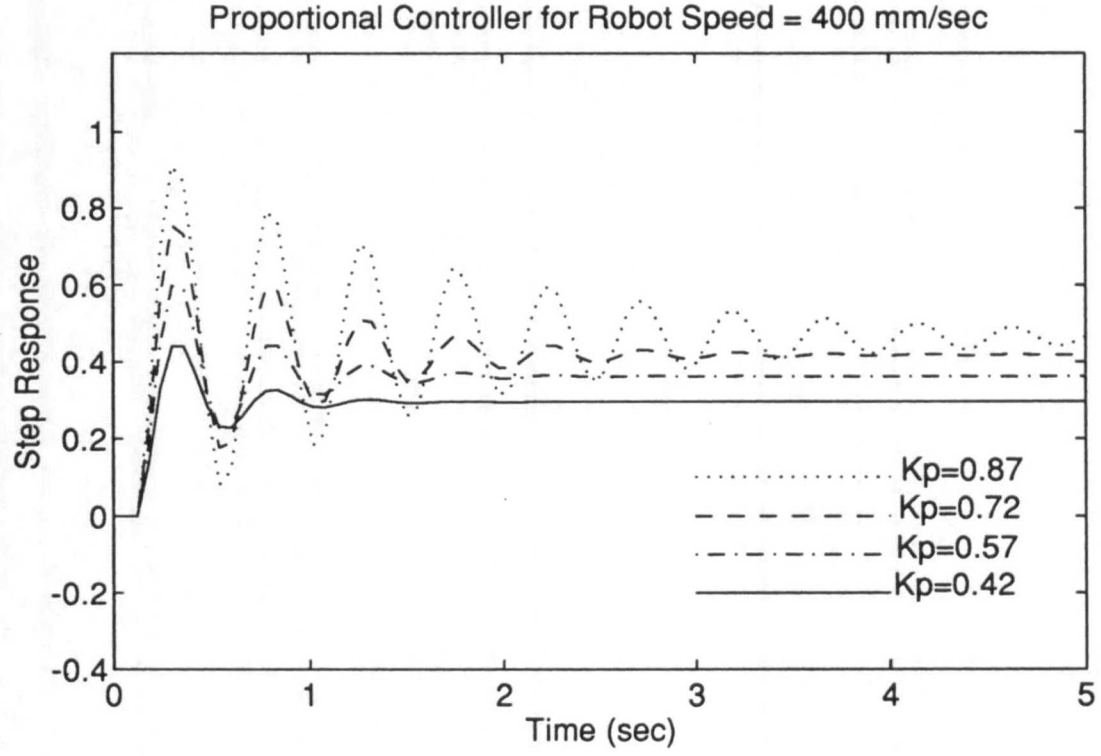

Figure 5.14

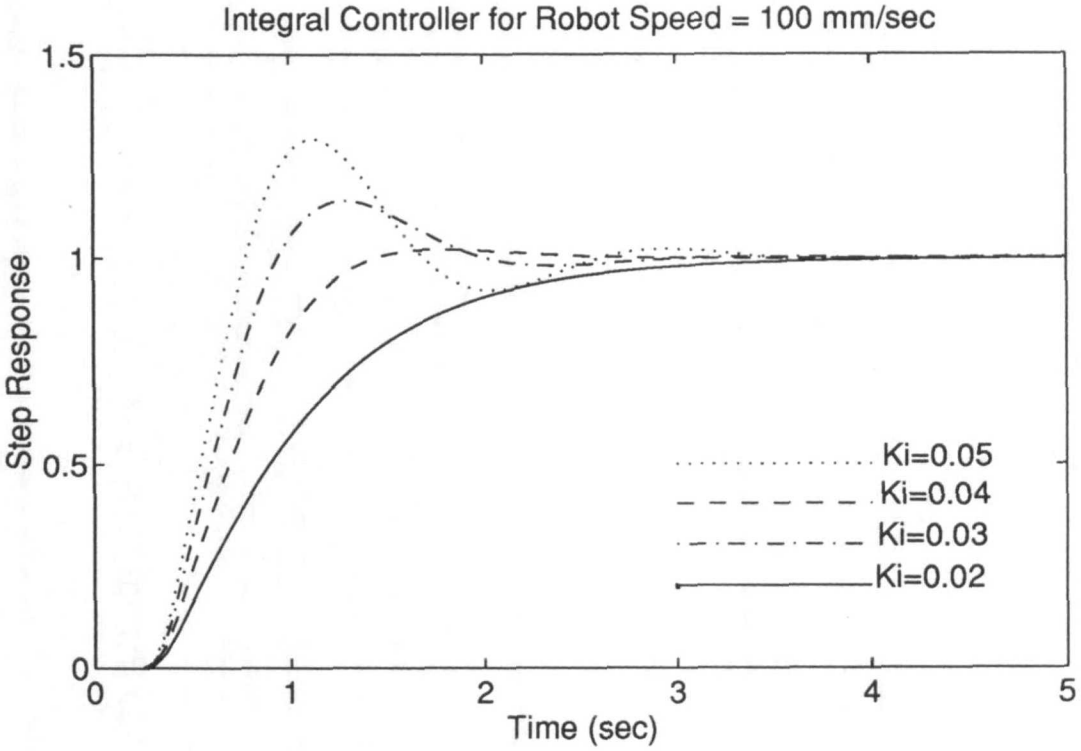

Figure 5.15

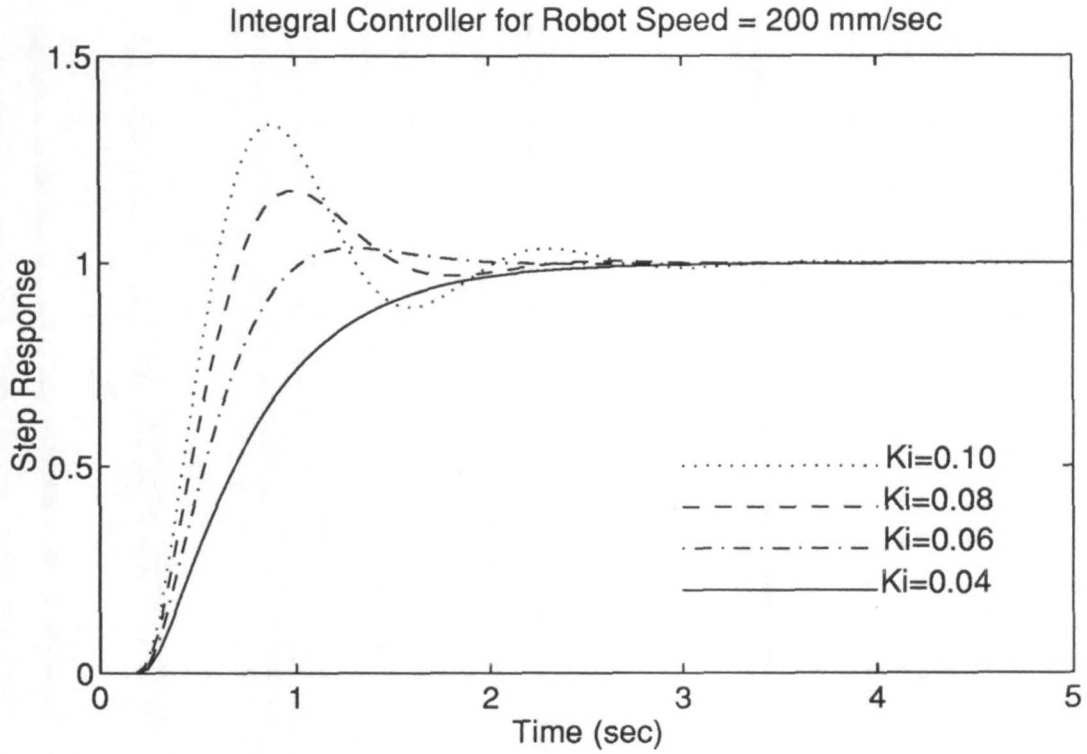

Figure 5.16

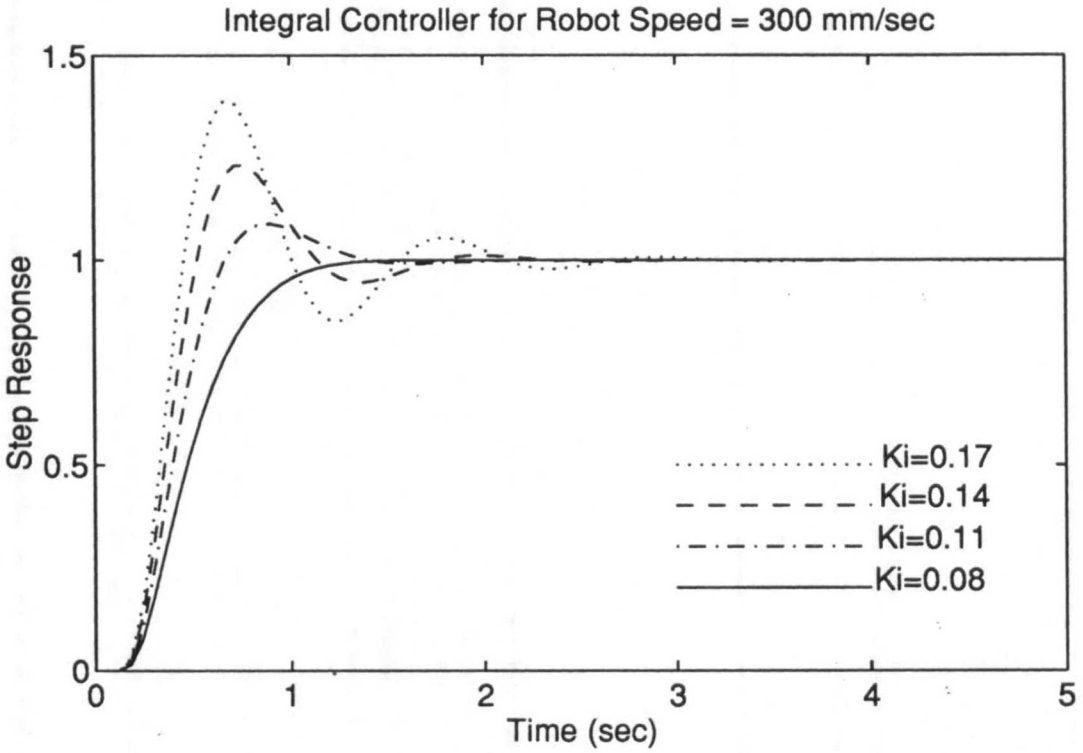

Figure 5.17

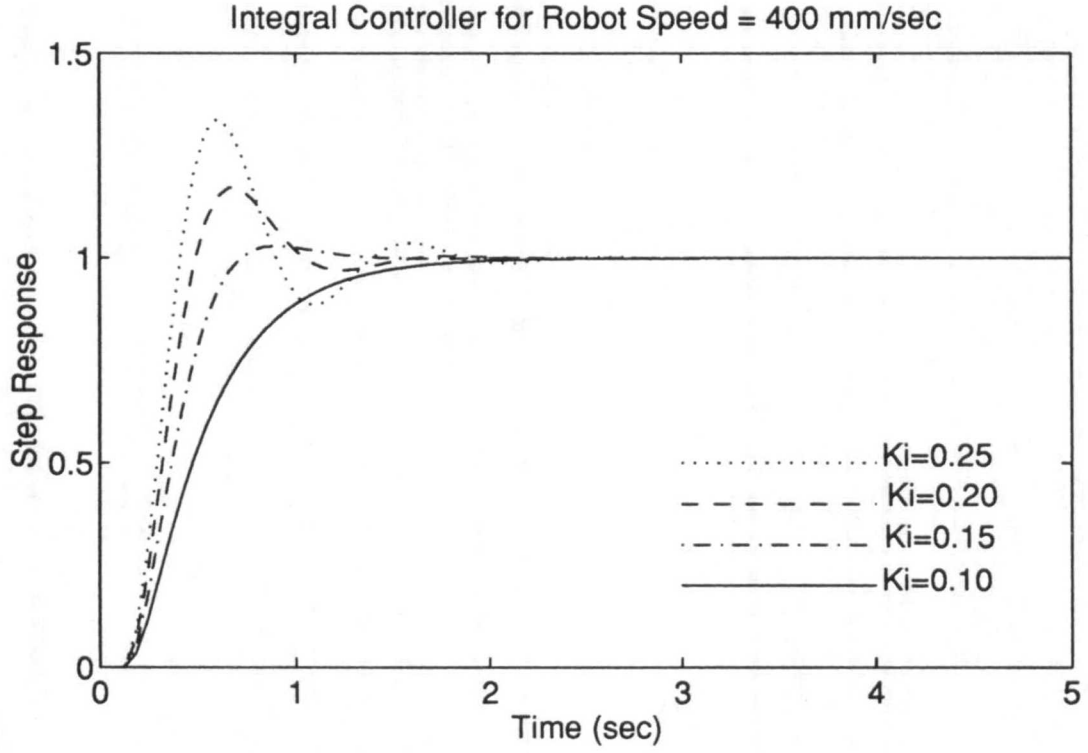

Figure 5.18

To have a faster response, the proportional gain has to be added to the integral term. The PI controller is as follows:

$$U_{i+1} = K_p e_i + \frac{T_s}{K_i} \sum_{j=1}^{i} e_j$$

The selection of the *PI* control parameters is critical to the success of a closed loop control process. If K_p is too high the system will oscillate while the control response is slow if K_p is too low. A correct setting of integral term also improves the control accuracy and performance. However if it is too low it will cause instability in the process.

Using Ziegler & Nichols setting, the tuned PI controller produces sluggish and unstable set point response as shown in Figs. (5.19 - 5.21) for four different robot speeds. thus, it is necessary to modify the Ziegler & Nichols tuning method [Astrom 89, Hang 91]. The purpose of this modification is to speed up the set point response and to improve the damping of the process. Thus, the proportional gain and integral action have to be decreased to overcome this problem. Using the modified setting, keeping the proportional constant as 0.04, 0.07, 0.10 and 0.16 and varying the integral control gain, the time responses were obtained. The graphs at four different robot speeds are given in Figs. 5.22 through 5.25. Comparing step responses using the PI controller (Figs 5.22 through 5.25) with the responses using the integral controller (Figs 5.15 through 5.18), it can be

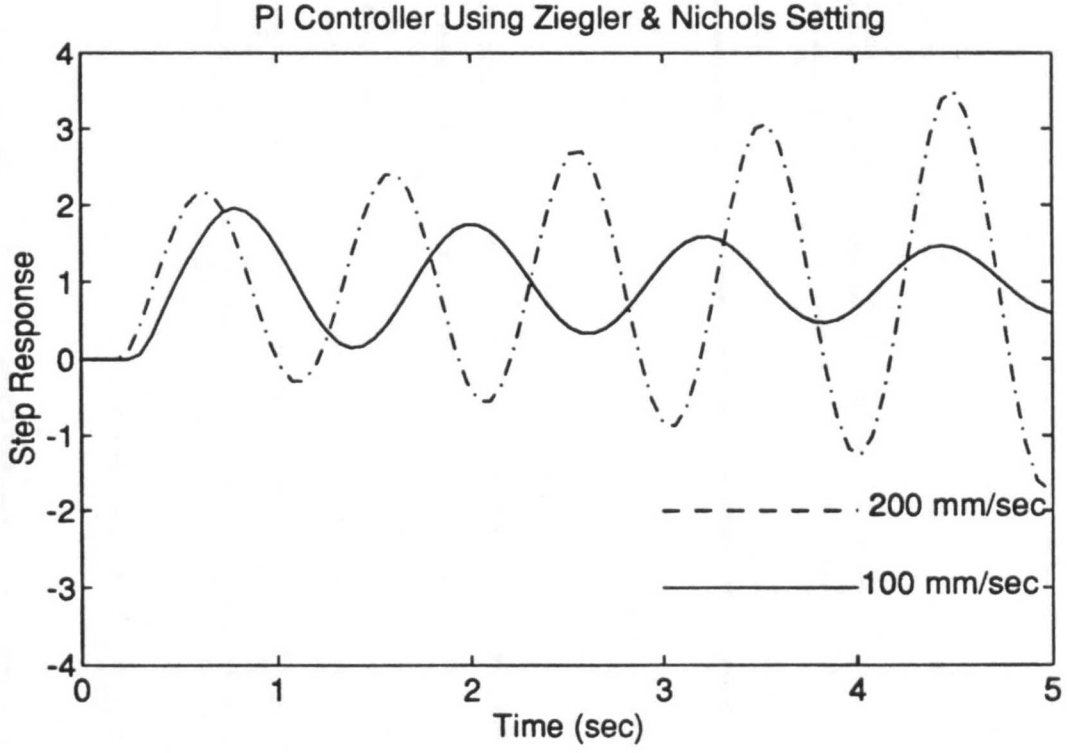

Figure 5.19: PI controller using Ziegler & Nichols setting at robot speed of 100 & 200 mm/sec.

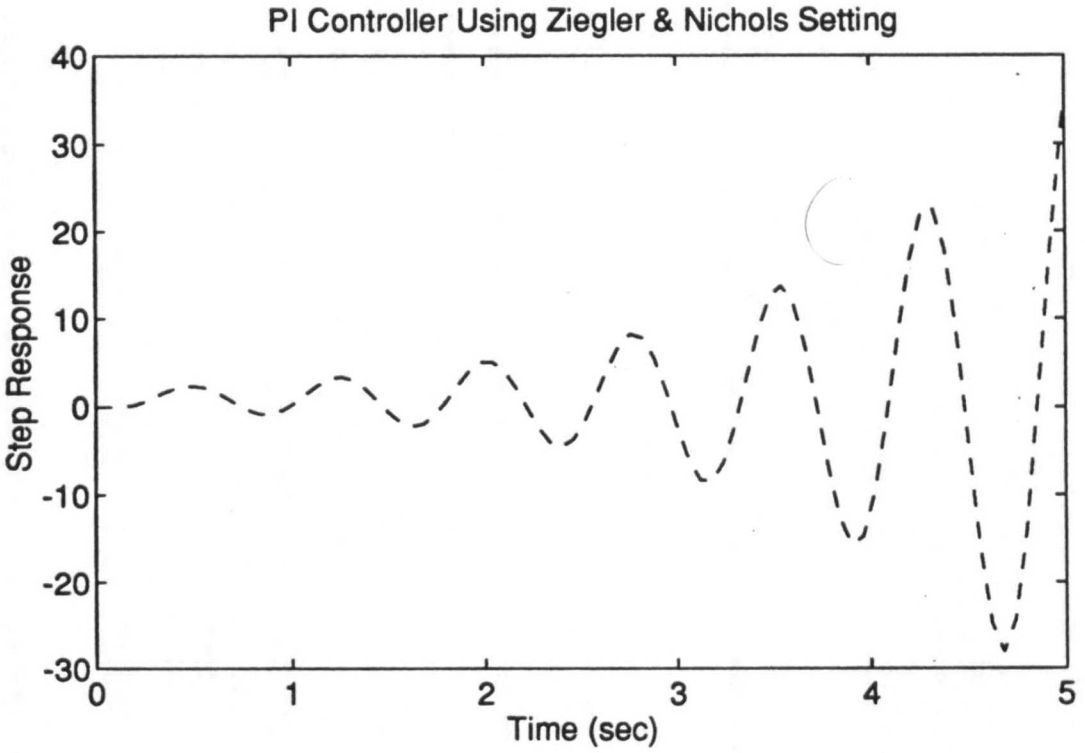

Figure 5.20: PI controller using Ziegler & Nichols setting at robot speed of 300 mm/sec.

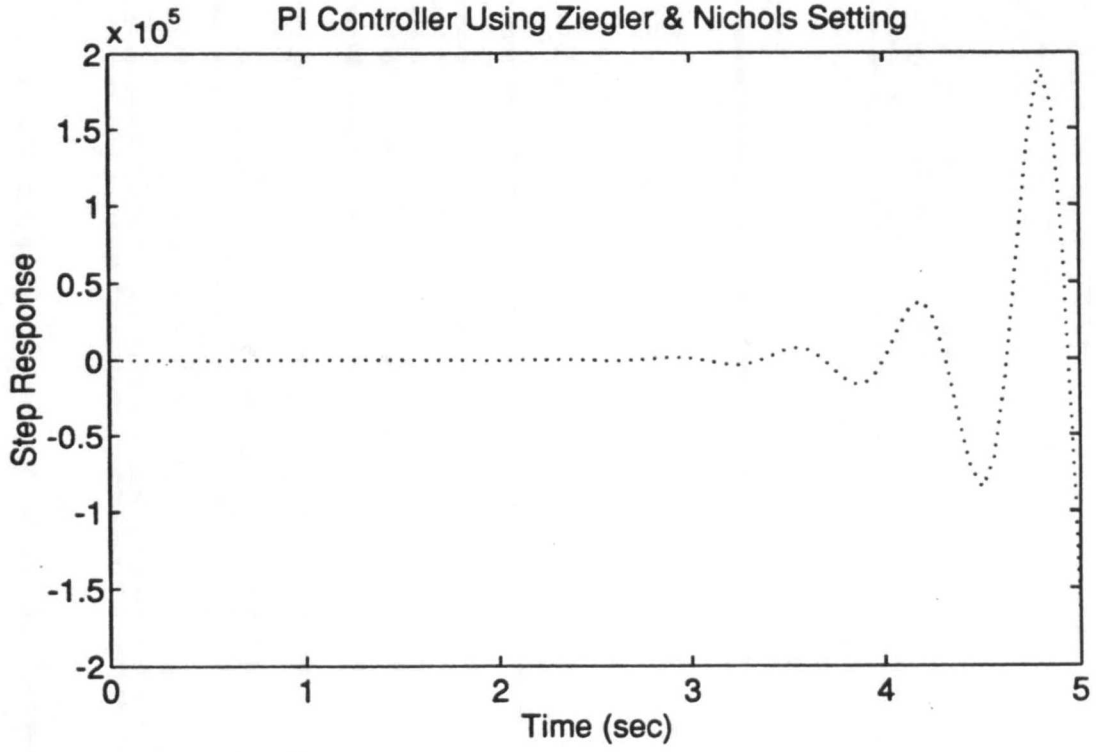

Figure 5.21: PI controller using Ziegler & Nichols setting at robot speed of 400 mm/sec.

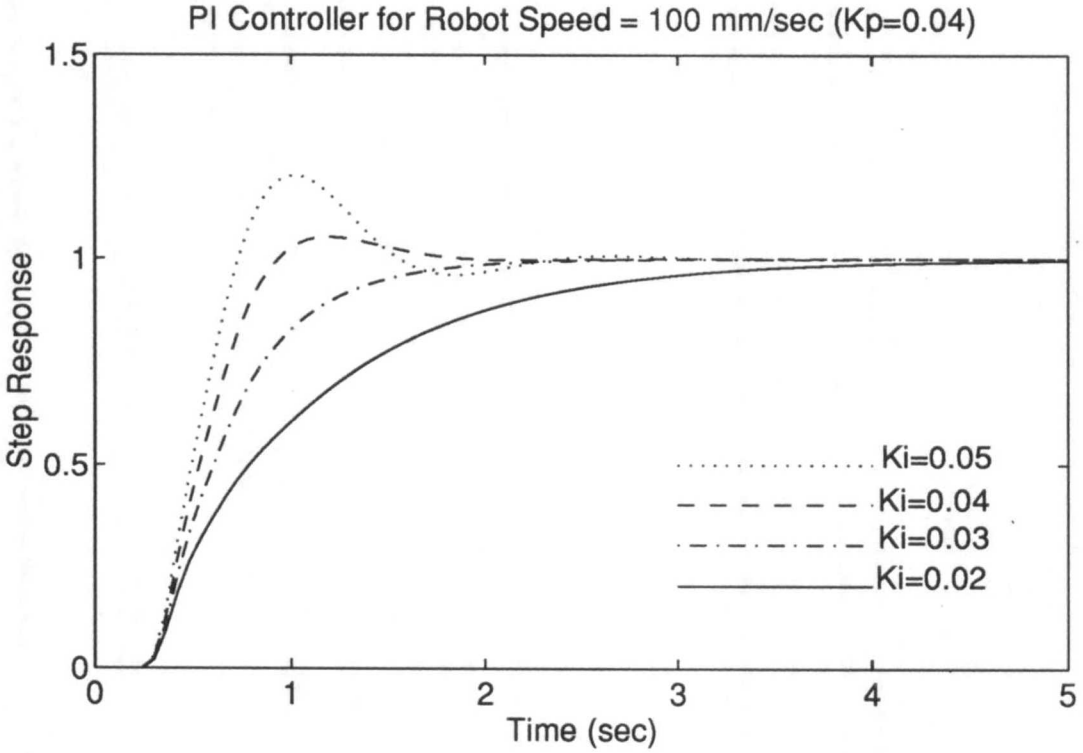

Figure 5.22

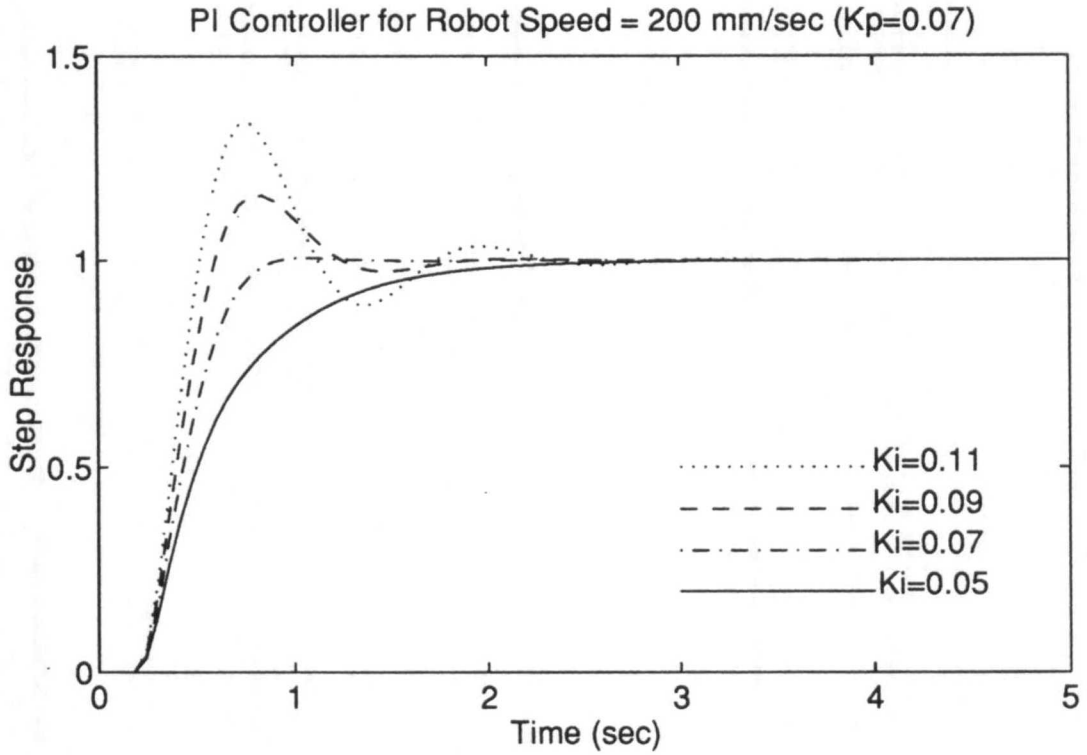

Figure 5.23

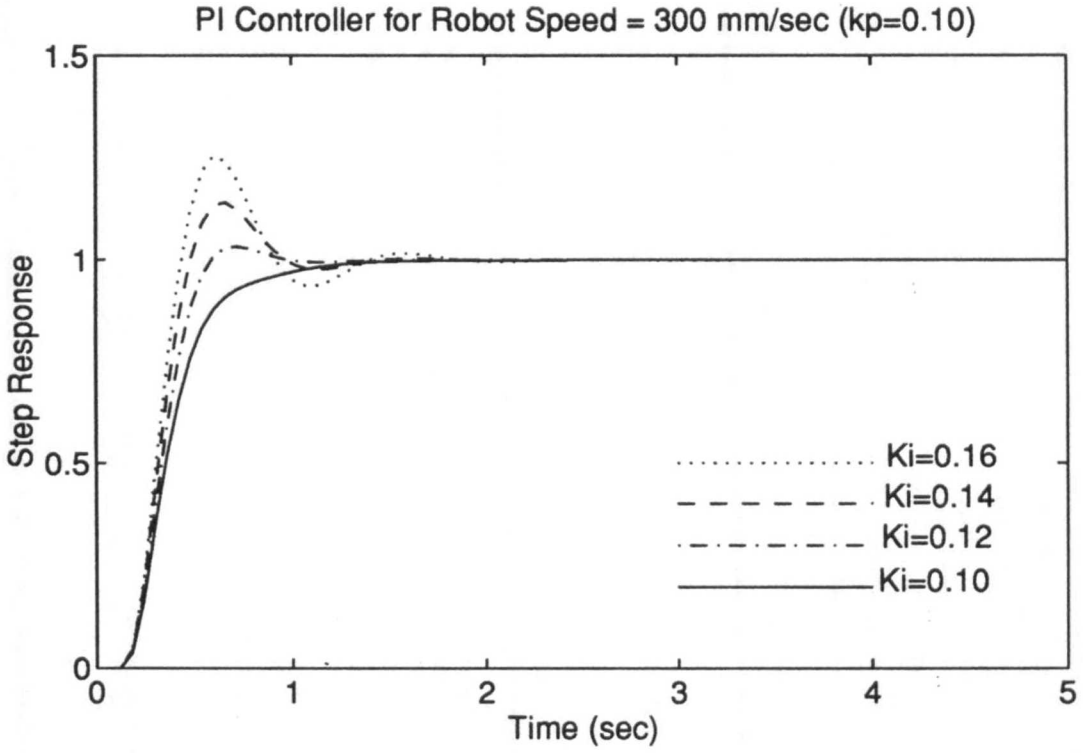

Figure 5.24

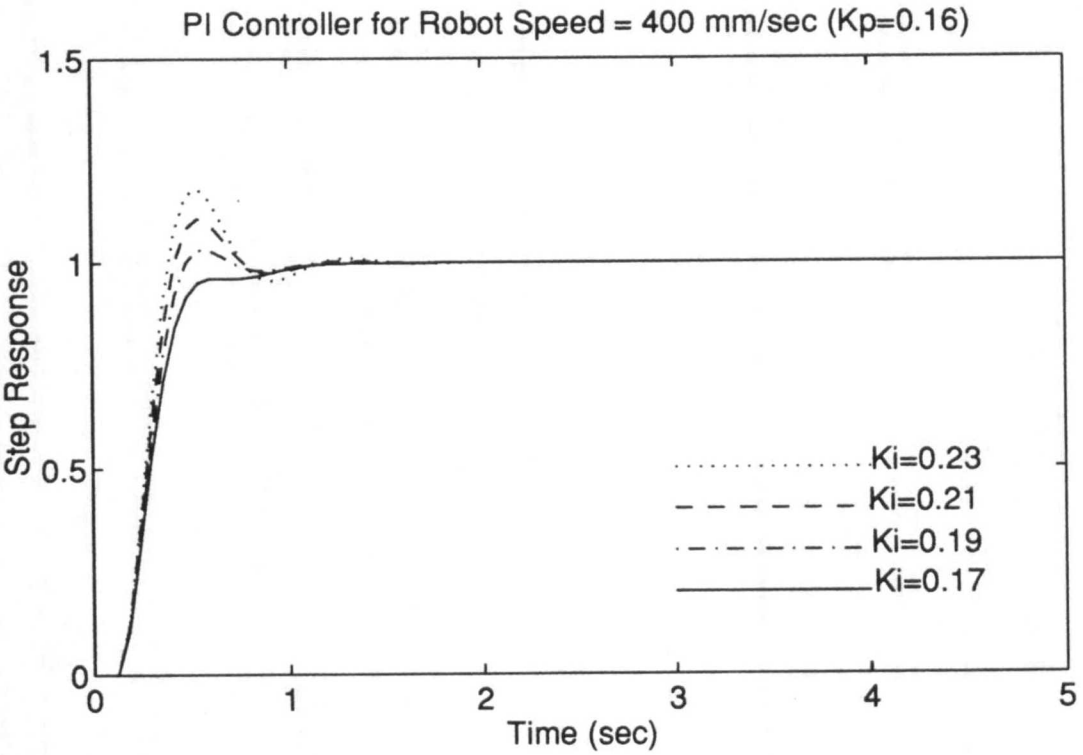

Figure 5.25

observed that the responses using the PI controller are faster. Furthermore, Tab. 5.5 gives the summary of the Ziegler & Nichols setting with the optimum setting which was found in this study. Fig. 5.26 gives the integral gain in PI controller as a function of time delay.

Robot speed (mm/sec)	Ziegler & Nichols setting		Optimum setting	
	Kp	Ki	Kpo	Kio
100	0.09	0.10	0.04	0.03
200	0.15	0.21	0.07	0.07
300	0.22	0.43	0.10	0.11
400	0.38	0.91	0.17	0.17

Table 5.5: Comparison of Ziegler & Nichols with optimum setting.

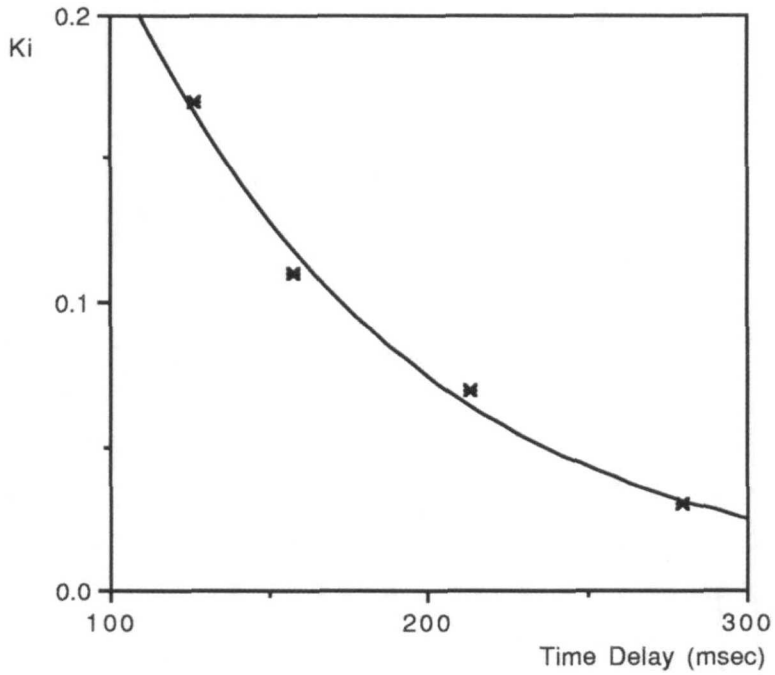

Figure 5.26: Integral gain of the PI controller gains as a function of time delay.

5.14 Smith's Predictor

The Smith's predictor was proposed in 1950's to improve the closed loop performance for systems with time delays. The Smith predictor works well with set point changes but not for disturbances and it is also sensitive to model errors [Morari 89]. A main feature of the Smith's predictor method is its use of a delay-free equivalent controller. The controller design is based on a process without a delay and the main information received by the controller comes from the model of the process so that the output is a delayed version of the corresponding delay-free system output. The delay is essentially removed from the feedback loop, therefore the controller can operate at higher gains making for a faster response. This requires a need for an explicit system model. Smith's principle usually applies to the process when the plant and delay appear in series.

The predictive Smith's controller introduces a phase lead to the process similar to the derivative action which offsets the destabilization of the effects of the time delay. The robustness of this algorithm is of course highly dependent on the model accuracy. If the model is good, the response time could be very small. When the model does not match the process well, the response time may even be longer than in the previous case. The Smith predictor is a non-adaptive predictive controller and is good for a non-adaptive predictive control of a linear process with a known model. An important consideration is what happens if the model mismatches from the actual process. Mismatch between the controller model and the process can cause instability in the process. Thus, the conventional controller has an advantage here due to the fact that its performance is unaffected by a small mismatch between controller and process models [Ross 77].

Assumption used in the Smith's method are:

i) no initial conditions in the system
ii) there is no unknown initial function in the delay
iii) there is no noise in the system.

The Smith's predictor has the following scheme:

i) The model is connected in Parallel with the process. The model has two parts, a process model without any delay which has minimum-phase elements and a pure time delay model.
ii) A suitable driving function is obtained using the process model and the controller which is based on this model.

This scheme is given in Fig. 5.27, where U is the controller output, D is the process disturbance, G_p is the process transfer function, T_d is the process delay, G_{pm} is process model transfer function without a delay, T_{dm} is the delay model and y_m is the process model output without a delay. The transfer function of the closed loop system in the S-domain is:

$$G(S) = \frac{C(S)G_p(S)e^{-ST_d}}{1 + C(S)G_{pm} + C(S)(G(S)e^{-ST_d} - G_{pm}(S)e^{-ST_{dm}})} \tag{5.4}$$

where $C(S)$ is the controller.

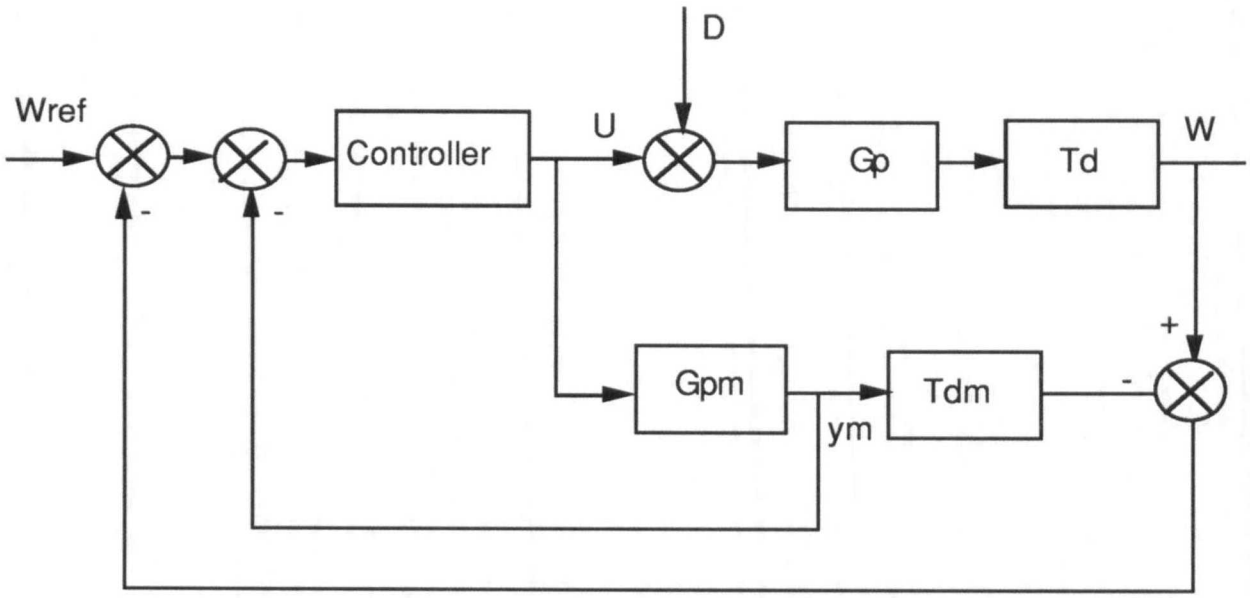

Figure 5.27: Smith's Predictor block diagram.

5.15 Simulation of the Smith's Predictor

To realise the Smith predictor, the following steps need to be taken:

i) design a controller for a delay-free system based on the optimum setting where the values are given in Tab 5.6.

ii) realise the regulator based on the process model output with and without a delay as shown in Fig. 5.28.

Figs. (5.29) through (5.32) give the step responses using Smith predictor and PI controller with optimum setting. Process responses using Smith predictor give a faster response than PI controller since the controller is designed based on the delay free process model.

Robot speed (mm/sec)	Optimum setting	
	Kpo	Kio
100	0.09	0.10
200	0.15	0.21
300	0.22	0.43
400	0.38	0.91

Table 5.6: PI optimum setting for Smith's predictor.

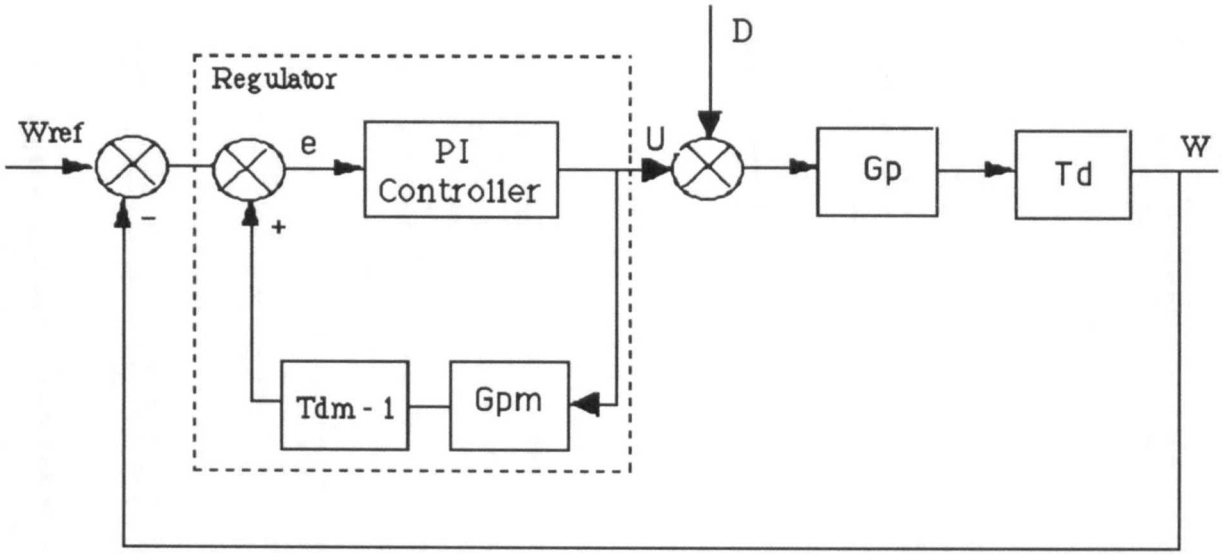

Figure 5.28: Smith's Predictor Implementation

5.16 Robustness & Mismatches

Robustness is the ability of a controller to maintain closed-loop stability in the case of variations in the process parameters. One of the major reasons for the wide of usage of PI controllers is their excellent robustness. The trade-off between performance and robustness

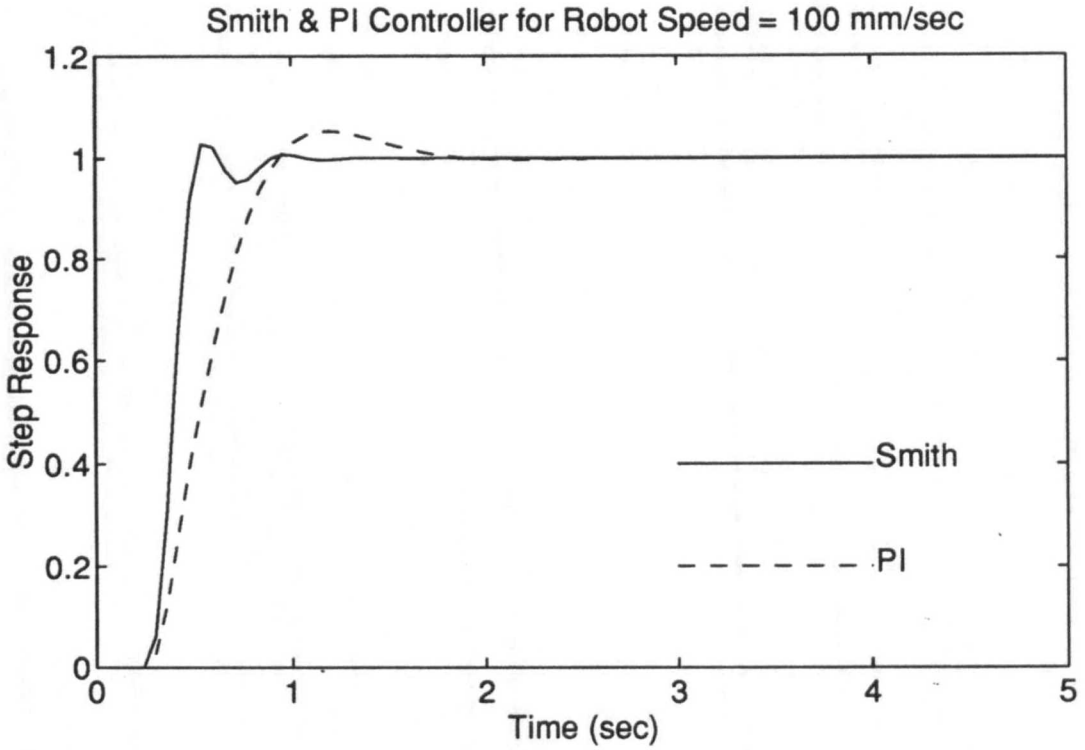

Figure 5.29

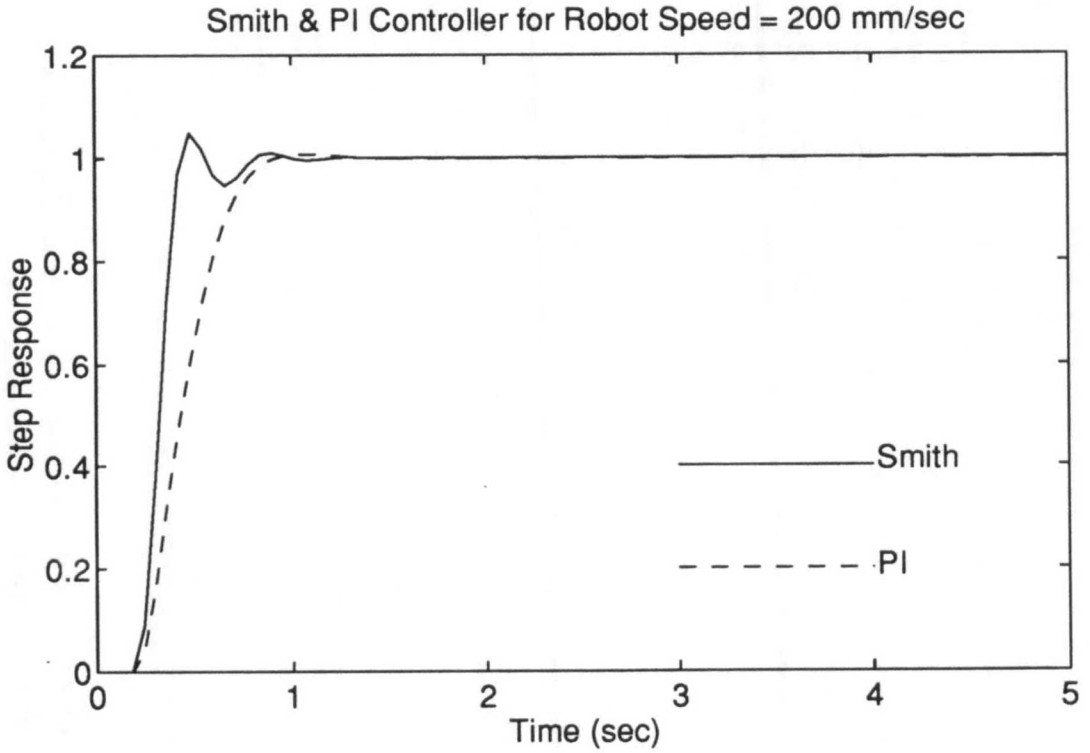

Figure 5.30

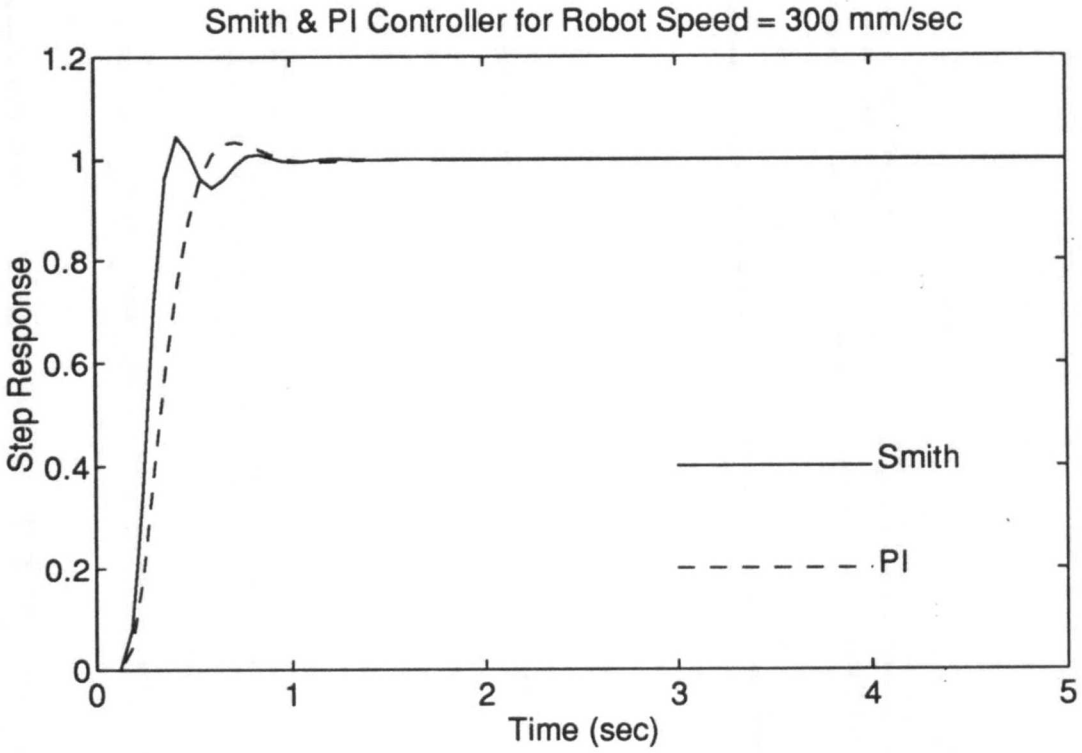

Figure 5.31

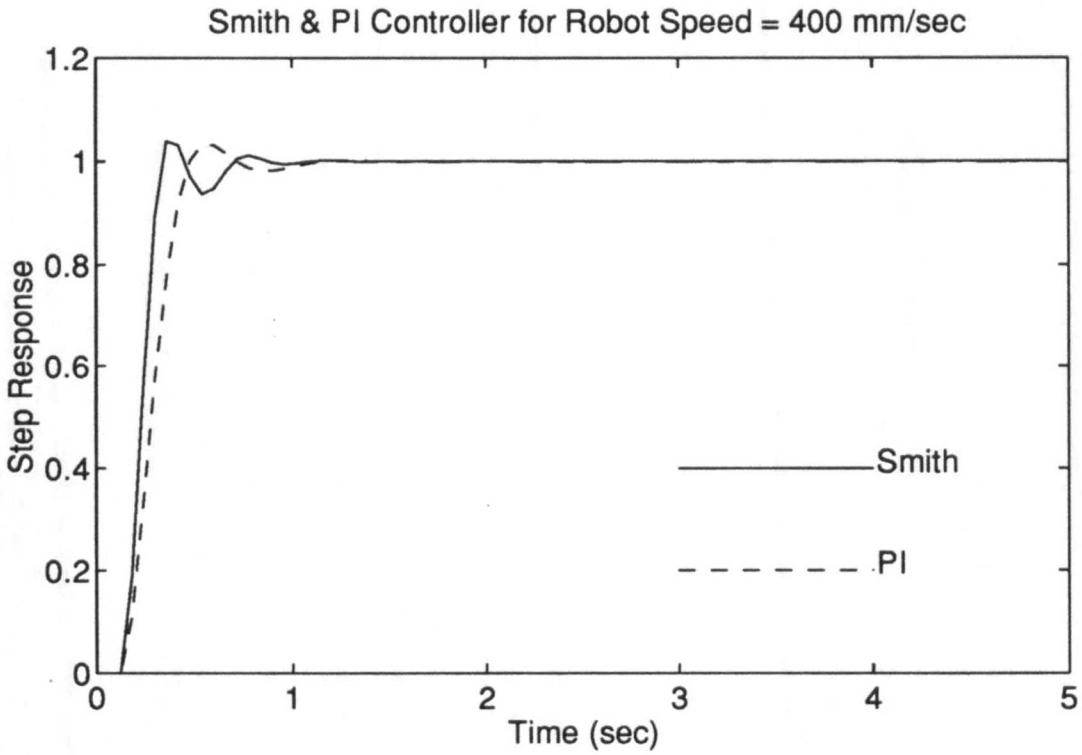

Figure 5.32

is most evident for the process with time delay. For the processes with time delay, any mismatches between the process model and the actual processes can be disastrous and can lead to a series instability problem.

The performance and robustness of a model based controller depends on how well a model is able to capture the dynamics of a process. It is important that the controller performance to be well even when the process behaviour is different than the process model. Thus, the model accuracy has to be investigated. Furthermore, the controller has to be robust enough which can also be held if there is a model uncertainty. The accuracy of the predictions depend on how well the plant and the delay has been modelled. The term $(G_p(S)e^{-ST_d} - G_{pm}e^{-ST_{dm}})$ in Eq. (5.4), which is the differences between the actual plant and the model of the plant is called *mismatch*.. The dynamic of the controlled process depends on the magnitude of this mismatch term. There are two types of the mismatches. *Temporal mismatch* which is the error in delay modelling and *parametric mismatch* which corresponds to the difference between the actual plant and its model.

To investigate temporal mismatches for Smith's predictor design, a series of simulations was performed to find the process performance. The delay in the process for the robot speed of 100 mm/sec is 0.28 sec (see § 5.4 for further detail). The delay model was reduced to 0.20, 0.15, 010 and zero to investigate the effect of imperfect representation of time delay model in the regulator as given in Figs. (5.33) and (5.34). Process performance deteriorate as the delay mismatch gets larger and eventually for the case where the model delay was set to zero (Fig. 5.34), the process is completely unstable. This shows the importance of accuracy in the delay modelling.

For parametric mismatch, the process gain was varied as given in Figs. (5.35) and (5.36). The process becomes unstable when the gain was set to zero. One of the coefficients of the transfer function a1m (which corresponds to $2\zeta\omega_n$) was also varied. It was found that the effect the mismatch for the transfer function coefficient which represents the process time constant is not as large as the mismatch in the time delay as given in Fig. (5.37).

The disturbance in the process is caused by fluctuation in the pressure delivery. Pressure fluctuation is caused by the problem of sticking in the pump. The best way to compensate for the disturbance is the use of feedforward control. Since for the feedforward control, the disturbance model is required which is not obtainable, design of the feedforward controller for the disturbance rejection was not considered.

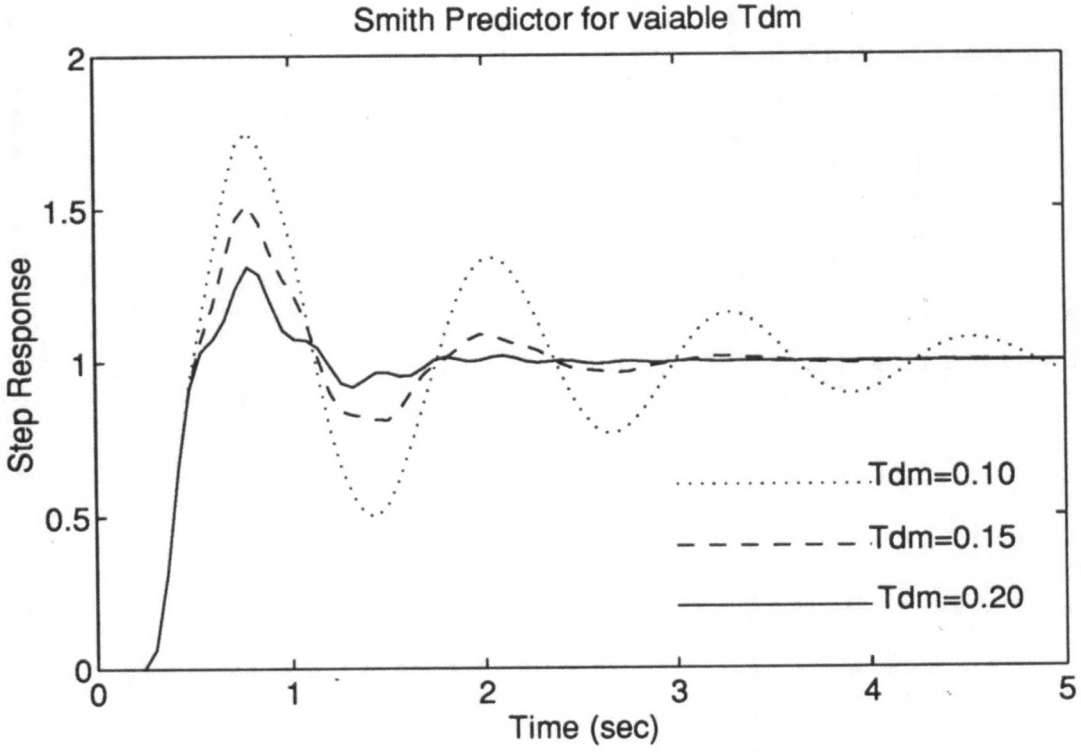

Figure 5.33

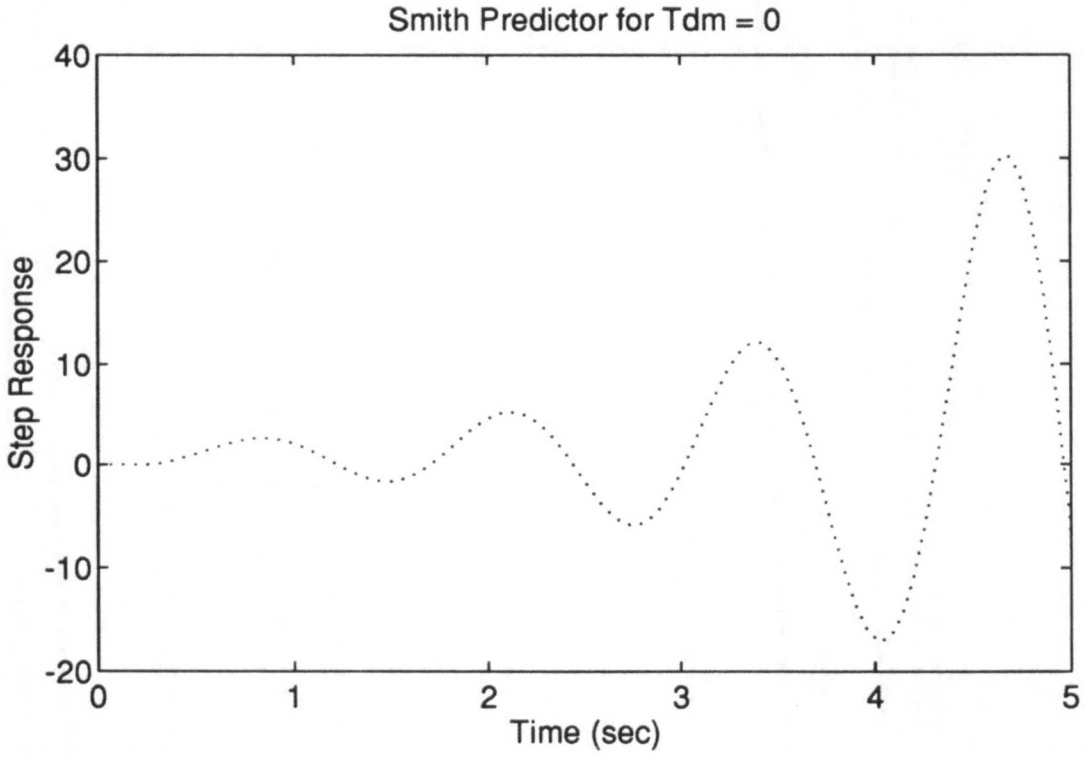

Figure 5.34

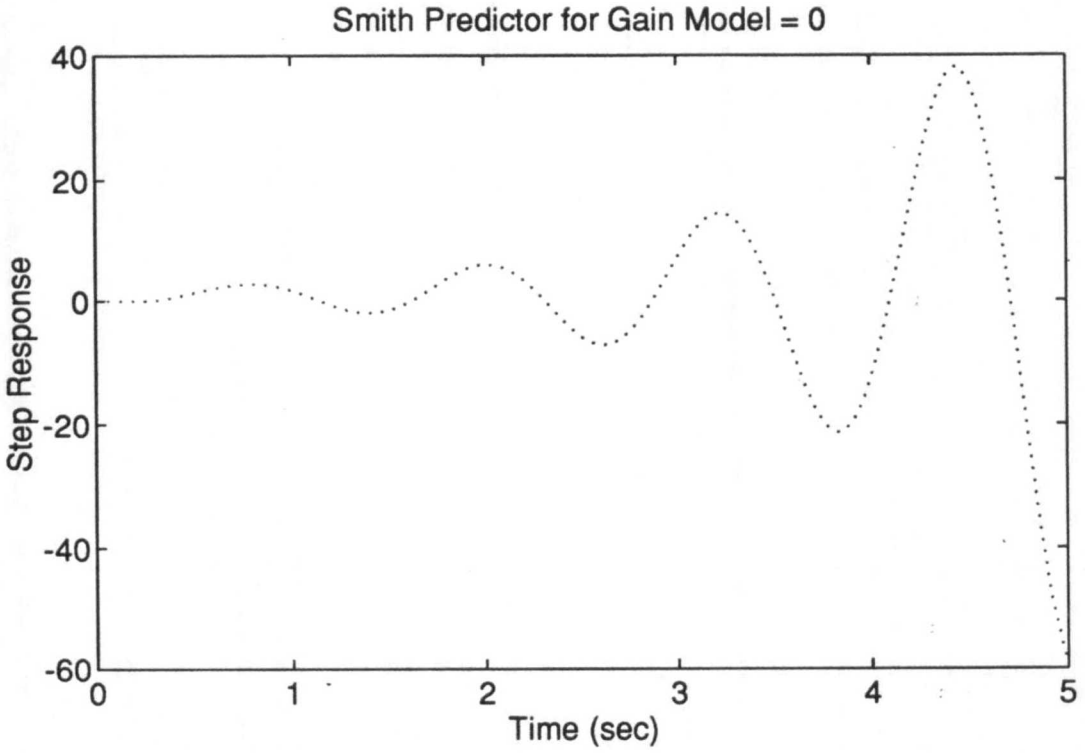

Figure 5.35

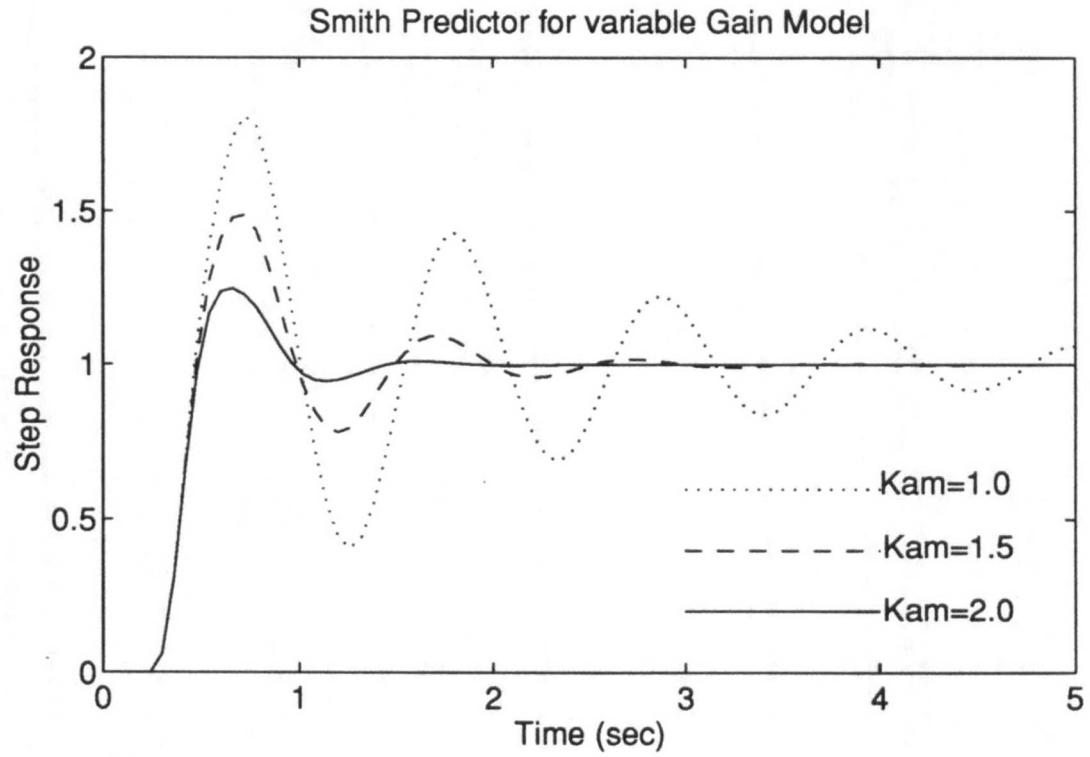

Figure 5.36

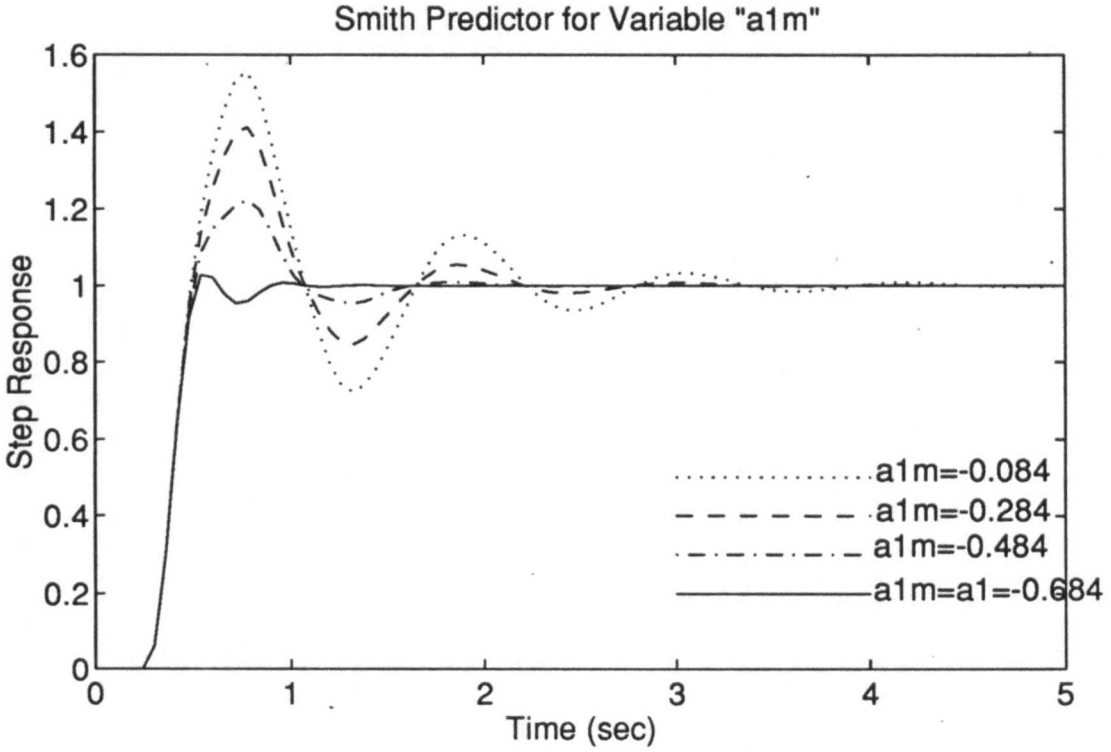

Figure 5.37: Smith predictor for variable transfer function coefficient

5.17 Realisation of the PI controller

Although, in theory, the Smith method gives a significant improvement to the response, the improvement in practice is limited due to the sensitivity of the stability of the process to small changes in the process parameters [Luyban 85]. Thus, the PI controller was realised for the process.

The implementation of a PI controller has a number of problems which need to be overcome [Bennett 82, Leigh 85, Johnson 84, Astrom 90].

i) The actuator might not complete its movement by the end of each sampling period.
ii) The integral term might be driven to the saturation point.
iii) There is a large disturbance when the controller is switched on.

Since the controller is a dynamic system, it is important that the state of the process be correct when the controller is switched on from the manual mode to the automatic mode. Care must be taken to make sure that the value of the integrator has to be correct at the time of switching. Thus, the control software has to monitor the plant and the integral action to be calculated even when the controller is not in full action. This smooth transition between

two stages is called *bumpless transfer* . This initialisation scheme is shown in Fig. (5.38) where M(k) and sum (k) represent the manual control and the sum of the integral action respectively.

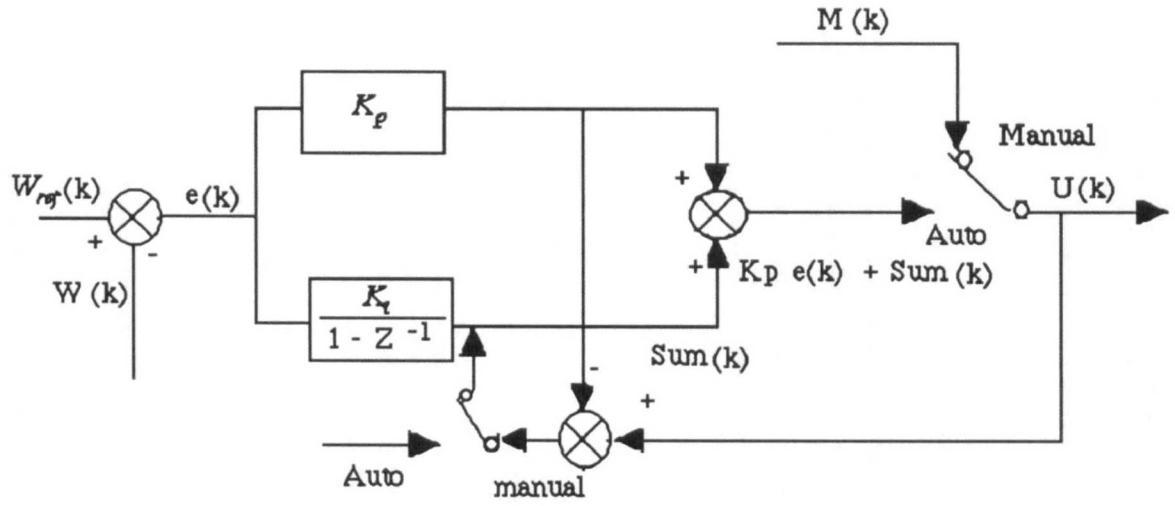

Fig. 5.38: Integrator initialisation in PI controller.

Another problem in the implementation of the PI controller is *integrator wind up* or *integrator saturation* . This problem occurs when the control error is so large that the integrator saturates the actuator. The integrator needs to be re-initialised when the error sign reverses. The upper and lower limits for integral action is also need to be used. Thus, making the controller input-output within a stable region.

Sudden changes in step input gives rise to the error signal which is formed as a difference between the set point and the measured output. Filtering the set point provides some smoothing in the error signal. However, this problem exits when derivative action is present.

The digital control loop has the following procedure:

i) the process output is measured, compared with the desired value and the error is calculated
ii) the initial integral action is calculated using manual setting and the set point error of the output with reference value
iii) the integrator is re-initialised if the error sign is revered

iv) the actuating signal is then obtained by using the error and applying a PI control algorithm
v) the new input is applied to the process
vi) wait for the next sampling time

Using the PI control algorithm, the step responses were obtained at four different robot speeds. The step responses without using a controller and using PI controller at four different robot speeds are given in Figs. 5.39 - 5.42. The responses for robot speeds of 100 to 300 mm/sec have small overshoot but they follow the adhesive bead set point very closely. The response of the robot speed of 400 mm/sec has a small overshoot. One of the main sources of the error at high speed is bouncing of the robot at the beginning of the node due to the heavy load (camera, laser diode dispenser gun) at the end effector. Another source of error is time lag between dispensing adhesive and the time for taking the image. Although a lower time lag is better for a control algorithm but the adhesive has less time to settle which affects the accuracy of the vision system.

5.18 Conclusion

The predominant use of a conventional controller such as PI controller in process control stems from their robustness. Even cases of processes with significant time transport delay, where methods such as Smith's predictor could provide a better response, the PI controller is preferred because of the potential sensitivity to model mismatch of the smith predictor. The major disadvantage of PI control is that the resulting system is relatively slow.

The dispensing process has a long delay due to the distance of the camera from the dispensing nozzle, flow rate adaptation time and the computational time taken for image processing. The dispensing process was analysed as a single lumped parameter dynamics with a pure time delay which is a function of the operating condition. Different types of conventional controller (such as proportional, integral and proportional plus integral) were simulated to find the optimal controller. The proportional controller performance was very poor with a large steady state error. The PI controller response was faster than using the integral controller. It was also shown that the Smith predictor controller has a faster response than PI controller but is very sensitive to the process modelling.

To have a robust controller, the PI controller was realised and was implemented. Using the PI controller, the response (including the error bars) was very close to the set point. The control performance is worst at higher speed although the transportation lag is smaller. This basically is due to the vision system since at the lower speed, the adhesive has more time to

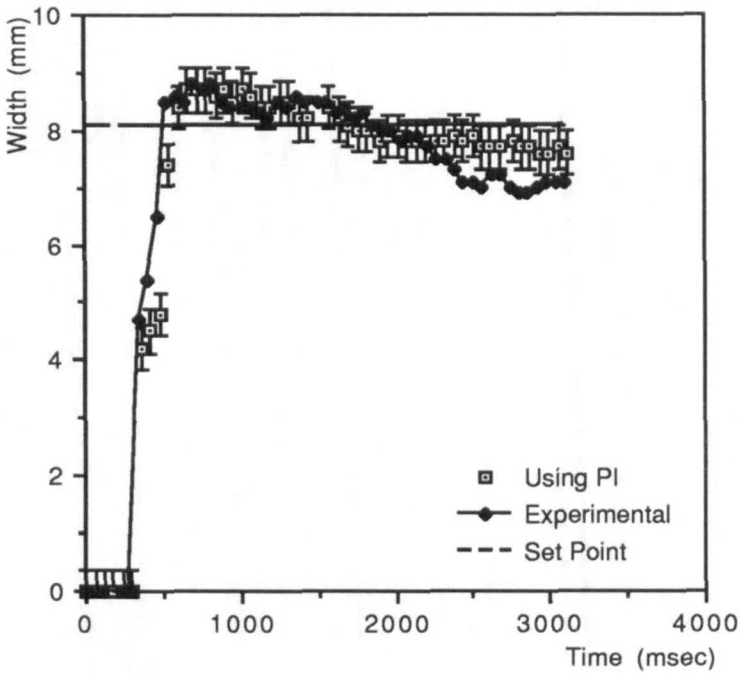

Figure 5.39: PI controller for robot speed =100 mm/sec

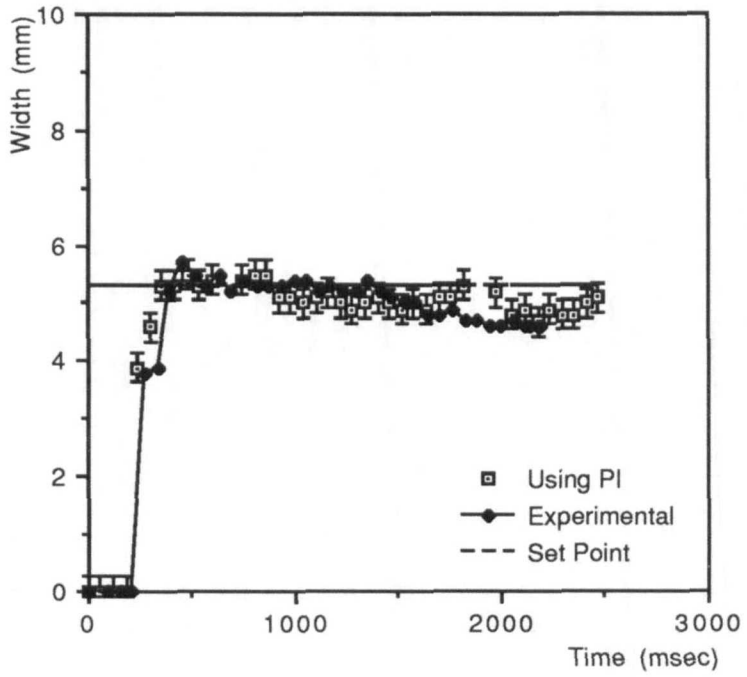

Figure 5.40: PI controller for robot speed =200 mm/sec

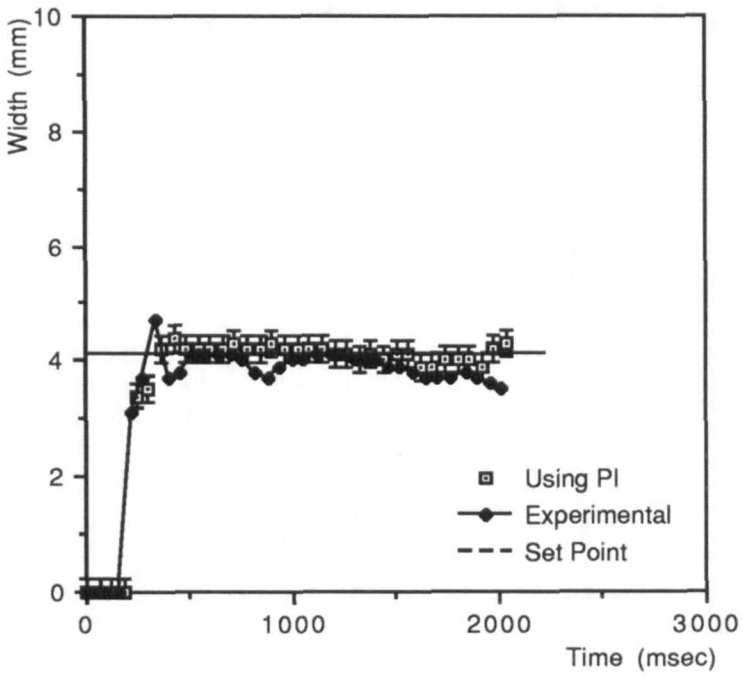

Figure 5.41: PI controller for robot speed = 300 mm/sec

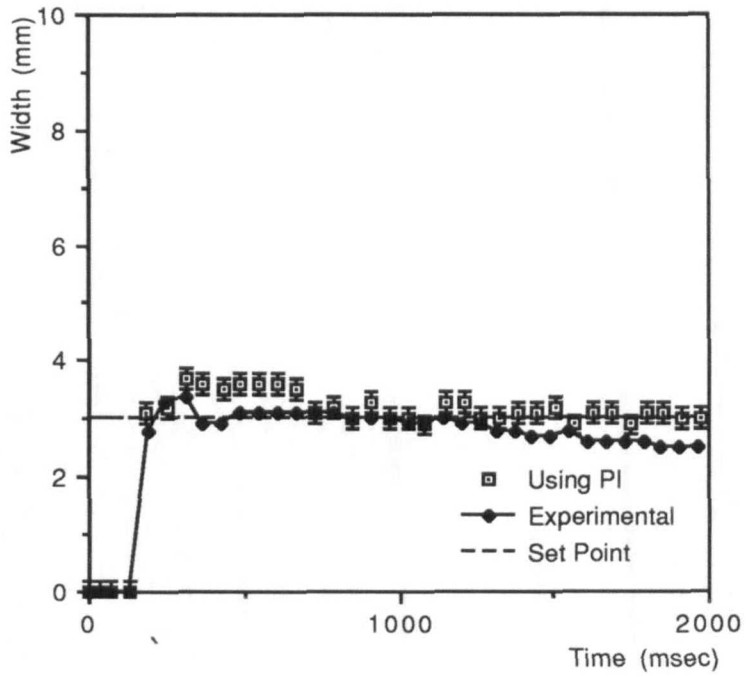

Figure 5.42: PI controller for robot speed = 400 mm/sec

settle down and it is easier to analyse the captured image. Another source of error at higher speed is due to the bouncing of the robot at some nodes. This is due to the robot payload which carries the camera, laser diode and the dispensing nozzle. This effect has been reduced by using a spring suspender to hold the adhesives hose. To have a better response, the adaptive controller needs to be investigated in which the control gains can be modified on-line.

CHAPTER VI

ANALYTICAL MODELLING OF ADHESIVE MATERIAL

6.1 The Necessity of Material Modelling

The rheological behaviour of the adhesives are analysed, to find a constitutive equation for representing an adhesive model. Because, for a given adhesive, it is often necessary to perform many ad hoc adjustments and tests to produce optimal adhesive beads at different operational and environmental conditions. Upon the modelling of material properties which provides an initial approximation for dispensing the flow, the automated dispensing cell can adapt to the operational conditions where the model also provides for its initial set-up and diagnosis. This modelling method can also be applied to similar adhesives with known rheological data and nozzle flow rate.

6.2 Non-Newtonian Fluids

Some basic concepts of non-Newtonian fluid mechanics and rheology are reviewed, since the flow of an adhesive material through the gun and nozzle is closely based on this theory.

Non-Newtonian fluids (such as most polymers) are distinguished from the Newtonian fluids (all gasses and liquids) such that the viscosity μ is no longer only a function of the pressure and the temperature, but it also depends on other factors such as the shear rate $\dot{\gamma}$ [Barnes 89]. The non-Newtonian fluids are either *pseudoplastic* (i.e. shear thinning, such as virtually all polymers) where viscosity decreases as the shear increases, or *dilatant* (i.e. shear thickening) with an inverse property [McKelvey 62]. Virtually all polymer materials such as Elastosol M23 (used in the experimental investigation here) have shear thinning behaviour. The viscosity in a non-Newtonian fluid has a complex behaviour (as discussed below). While ideally, viscosity should be determined experimentally for any small

changes of pressure and/or temperature. This is not feasible without an excess of experimentation and a modelling approach should be employed.

The rheological behaviour of non-Newtonian fluids cannot be represented through a single constitutive equation, because of the dependence of the apparent viscosity on the shear rate and/or time (for time dependent fluids). However, for non-Newtonian fluids with negligible elastic effects, the semi analytical-empirical *generalised Newtonian fluid* method, which is a generic expression and accounts for the shear rate dependent behaviour of the viscosity, can be used as a substitute if the *Deborah* number (the ratio of the relaxation time of the material to a characteristics time scale of deformation) is low [Tadmor 79]. This method is widely used in modelling of the non-Newtonian industrial flows.

The empirical Hershel-Bulkely model which is frequently used, describes the behaviour of generalised Newtonian fluid and its modified version to account for thixotropic effects, and provides an expression for the shear stress as:

$$\tau = (\tau_y + c\dot{\gamma}^{n})(1+t)^{m'} \tag{6.1}$$

where τ_y is yield shear stress, c power law coefficient (or consistency index), n power law exponent (or flow behaviour index, being larger or smaller than unity for pseudoplastic or dilatant fluids respectively), m' time power index, and t characteristic time (from the commencement of shear behaviour or the time to the end of shear for recovery behaviour). Note that the indices m', n, c are usually functions of temperature and vary for different fluids. This expression (Eq. 6.1) reduces to $\tau = \mu\dot{\gamma}$ for Newtonian flow, where n is unity and c is the same as the Newtonian viscosity with m' and τ_y being zero. This power law expression (Eq. 6.1) can be fitted to experimental data to determine the above constants. However, it has some disadvantages [Bird 87] as; the viscosity can not be described for very low and very high shear rates, there is no way to relate c and n to molecular weight and concentration and so τ can not be determined only through c and n alone.

6.3 The Adhesive Characteristics

The Elastosol M23, which has a wide range of applications from joint sealing to structural bonding, is used as the adhesive in the automated cell for experimental procedures here. It has a pseudoplastic behaviour, and is based on sulphur-cured liquid polybutadiene polymers with excellent corrosion resistance and the ability to withstand high temperatures which result from the application (e.g. from an automotive paint stoving oven).

Furthermore its shear strength is compatible with a toughened epoxy designed for automotive application. This polybutadience adhesive (e.g. Elastosol M23) has the advantage over epoxy that its shear strength increases as heating time increases in contrast to the latter material [Ludbrook 84].

The shear stress data was obtained using a bob and cup viscometer by placing the adhesive in between the cylindrical cup and bob, where the bob was rotated at a constant speed and consequently the required torque was measured. Then after approximately five minutes, the steady state shear stress was measured (see § 6.5 for further details). The experimental errors are about 5 percent. The initial and the steady state values of the shear rate for Elastosol M23, is provided for different values of rotational speed of bob and of temperatures (Tab. 6.1 and Figs. 6.1 & 6.2).

Rotational Speed of Bob (rev/min)	Initial Shear Stress (Pa)				Steady State Shear Stress (Pa)			
	15.5 °C	25 °C	38 °C	50 °C	15.5 °C	25 °C	38 °C	50 °C
5	1886.0	1422.4	894.4	745.6	1016.0	822.4	579.2	512.0
10	2782.0	1745.6	1403.2	1016.0	1693.0	1064.0	774.4	676.8
20	3629.0	2555.2	1819.2	1451.2	2371.0	1790.4	1064.0	966.4
40	5443.0	3131.2	2515.2	2225.6	3435.0	2515.2	1790.4	1257.6
70	6194.0	4819.2	3483.2	3096.0	4838.0	3483.2	2540.8	1905.6
100	-	5915.2	4112.0	3774.4	-	4355.2	3145.6	2273.6

Table 6.1: Initial & steady state shear stresses of Elastosol M23.

6.4 Rheological Flow Model

In general, each adhesive has unique properties and characteristics that must be considered in the application planning. However, the Elastosol M23 has a broad pattern of the rheological characteristics typical of non-slumping materials, which means it does not flow spontaneously under its own weight (i.e. a low shear stress). Thus, the method utilised here, can be used for any material with non-slumping characteristics.

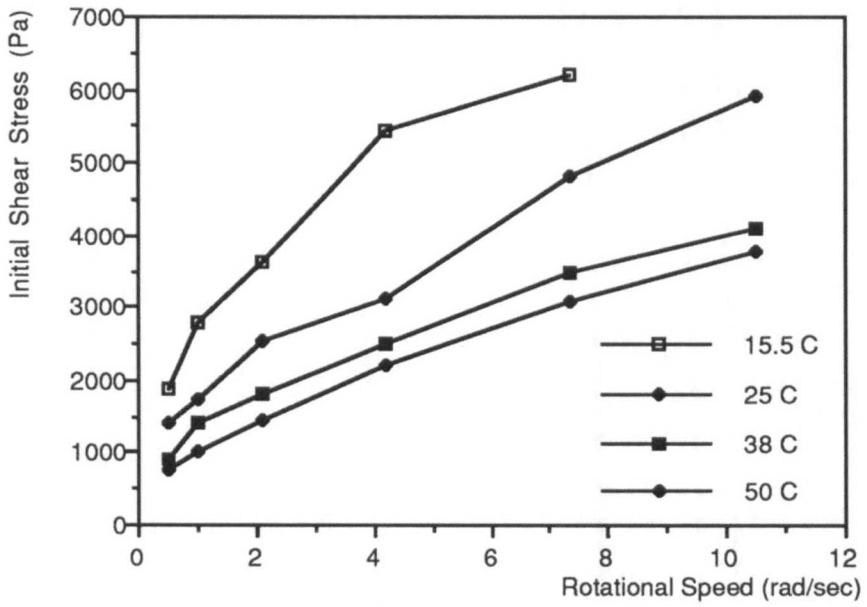

Figure 6.1: Initial shear stress of adhesive as a function of rotational speed at various temperature.

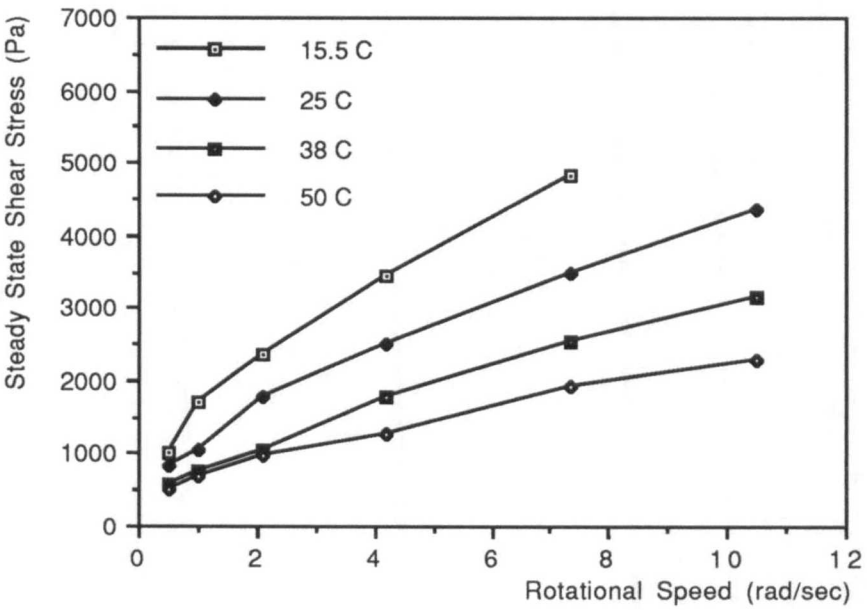

Figure 6.2: Steady state shear stress of adhesive as a function of rotational speed at various temperature.

The regression analysis of the data points from the shear stress versus natural log of rotational speed, shows that at low values of the viscometer's rotational speed, the shear

stress and consequently τ_y approaches to zero (as shown in Figs. 6.3 and 6.4). With further assumption of m being zero, the expression for the shear stress (Eq. 6.1) reduces to:

$$\tau = c\dot{\gamma}^{n} = c(B\Omega)^{n} = C\Omega^{n} \tag{6.2}$$

where Ω is the rotational speed with B its coefficient (see § 6.5 for further details) and $C = c\,B^{n}$.

6.5 Evaluation of Rotational Speed Coefficient

To find the relation between shear rate and rotational speed, the geometrical description of the bob and cup viscometer and shear stress relation in a coaxial cylinder need to be analysed. The coaxial cylinder is the most common type of rotational viscometry. A cylinder of radius r_b (bob) is suspended in a container of adhesive of radius r_c (cup). The adhesive covers the inner cylinder and the bob rotates with an angular velocity Ω as shown in Fig. (6.5).

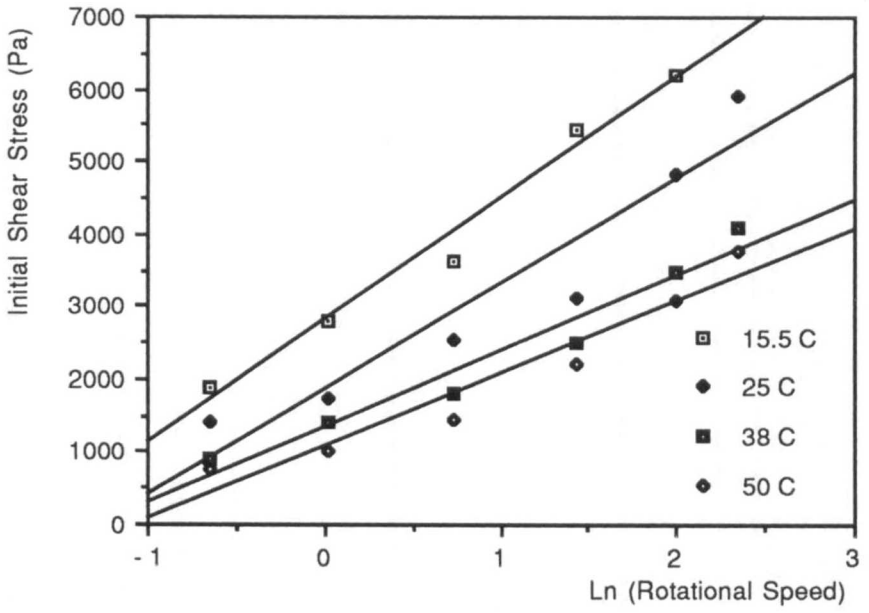

Figure 6.3: Initial shear stress as a function of Ln (rotational speed) at various temperature.

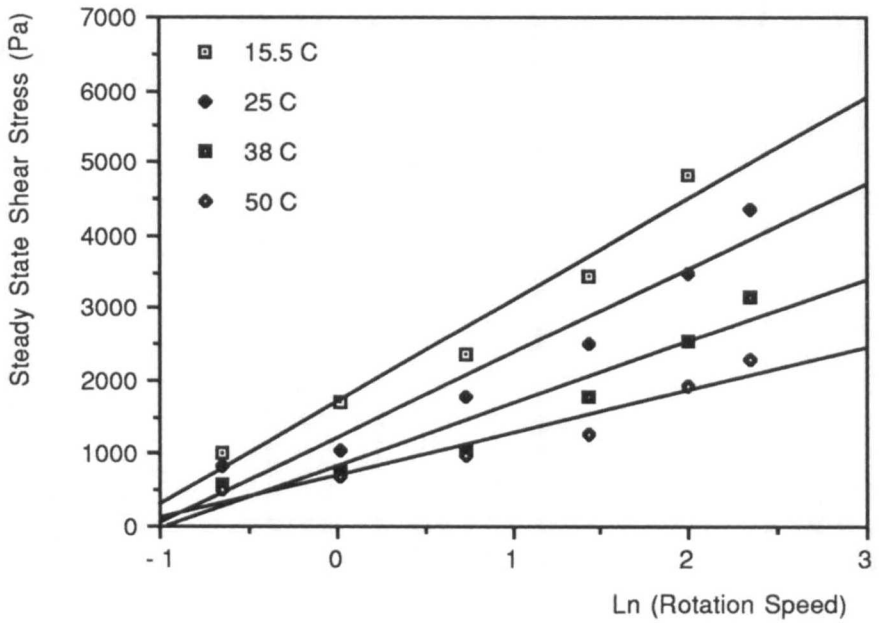

Figure 6.4: Steady state shear stress as a function of Ln (rotational speed)

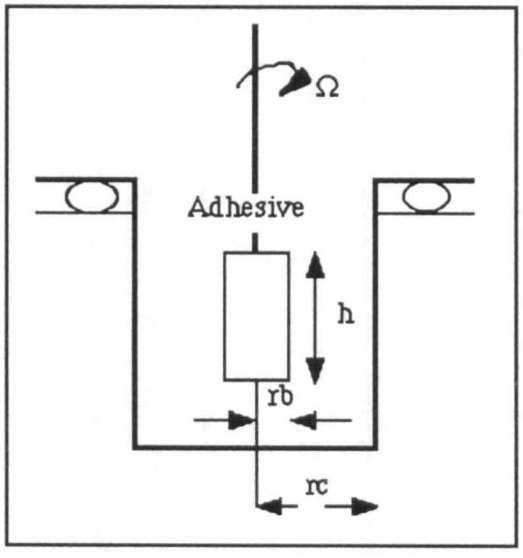

Figure 6.5: Bob and cup viscometer.

It is assumed that the adhesive rotates with the same angular velocity as the bob, while the cup is stationary. The bob's torque $M = F\,r$ (where F is the applied force and r is the effective radius), is then measured at a constant rotational speed. Therefore, the shear stress per unit area (noting that $A_b = 2\,\pi\,h\,r$, with h as bob's height) is:

$$\tau = \frac{F}{A_b} = \frac{M}{2\pi hr^2} \tag{6.3}$$

The shear rate as a function of rotational speed (as shown in Fig. 6.6) for pseudoplastic flow, using equation (6.2), can be written as follows:

$$\dot{\gamma} = -r\frac{d\omega}{dr} = (\frac{\tau}{c})^{1/n} \tag{6.4}$$

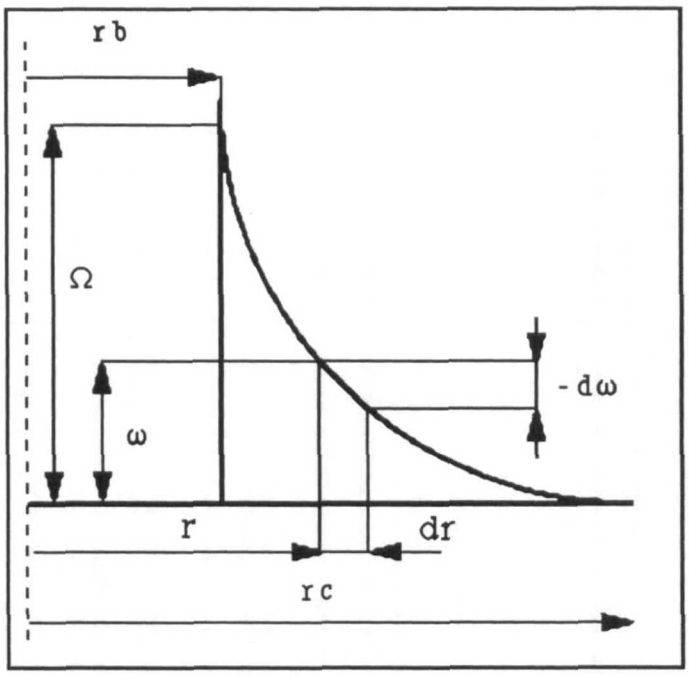

Figure 6.6: Geometrical graph of the rotational speed.

By differentiating the expression for the shear stress (Eq. 6.3) with respect to r, $dr = -(r/2\tau)d\tau$, then with use of Eq. 6.4:

$$d\omega = \frac{1}{2\tau}\left(\frac{\tau}{c}\right)^{1/n} d\tau \qquad \Rightarrow \qquad \omega = \frac{1}{2c^{1/n}} \int \tau^{\left(\frac{1}{n}-1\right)} d\tau$$

Then, by implying the boundary conditions

$$\omega = 0 \quad \text{at} \quad \tau = \tau_b \qquad \& \qquad \omega = \Omega \quad \text{at} \quad \tau = \tau_c$$

Thus, the expression for Ω is:

$$\Omega = \frac{n}{2}\left(\frac{\tau_{rb}}{c}\right)^{1/n}\left[1 - \left(\frac{\tau_{rc}}{\tau_{rb}}\right)^{1/n}\right]$$

Next by using rheological equation (Eq. 6.4) applied at r_b and geometrical condition of $\tau_{rc}/\tau_{rb} = (r_b/r_c)^2$ and further use of Eq. 6.2, the coefficient of rotational speed is:

$$B = \frac{2}{n}\left[1 - \left(\frac{r_b}{r_c}\right)^{2/n}\right]^{-1} \tag{6.5}$$

Where the ratio of bob radius to the cup radius is 0.5.

6.6 Power Law Constants Evaluations

To find power law exponent, n, and power law coefficient, c, the logarithm of the shear stress τ is plotted as a function of the logarithm of the rotational speed Ω (both of which are measured quantities) as given in Figs. (6.7) and (6.8) respectively.

Using linear regression for Figs. (6.7) and (6.8), the slope of the curve represents the power law index (it is constant for steady state and it is a function of temperature for initial case) and the intersection of the curve with y-axis represents the natural logarithm of the power law coefficient at the experimental temperature.

The rotational speed coefficient (B) and the power law exponent (n) are constant for steady state (B_{SS} =3.83, n_{SS} = 0.573) but they are a function of temperature for the initial state. The rotational speed coefficient and power law exponent data using Fig. (6.7) and equation 6.7 are given in Tab. (6.2). The rotational speed coefficient and power law exponent are plotted as a function of temperature as shown in Figs. (6.9) and (6.10) respectively.

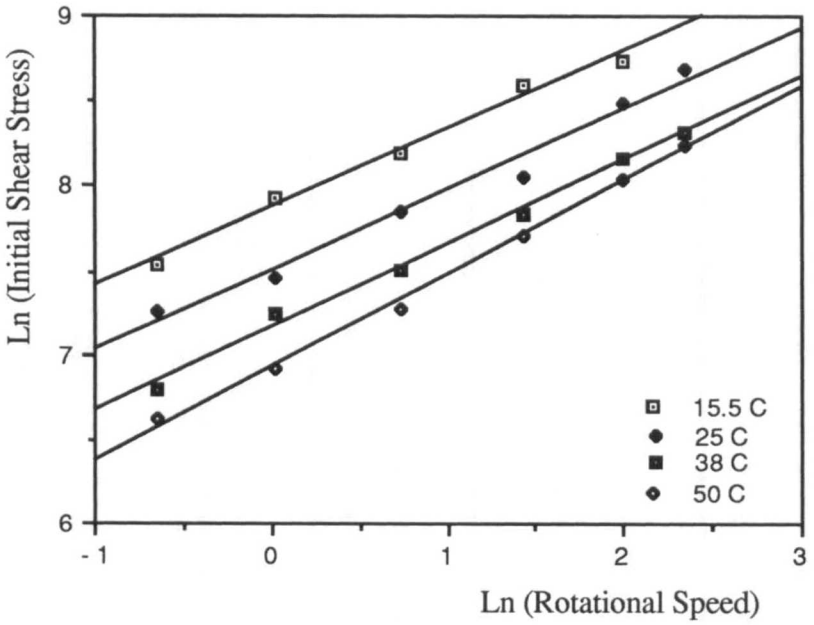

Figure 6.7: Ln (initial shear stress) as a function of Ln (rotational speed) at various temperature.

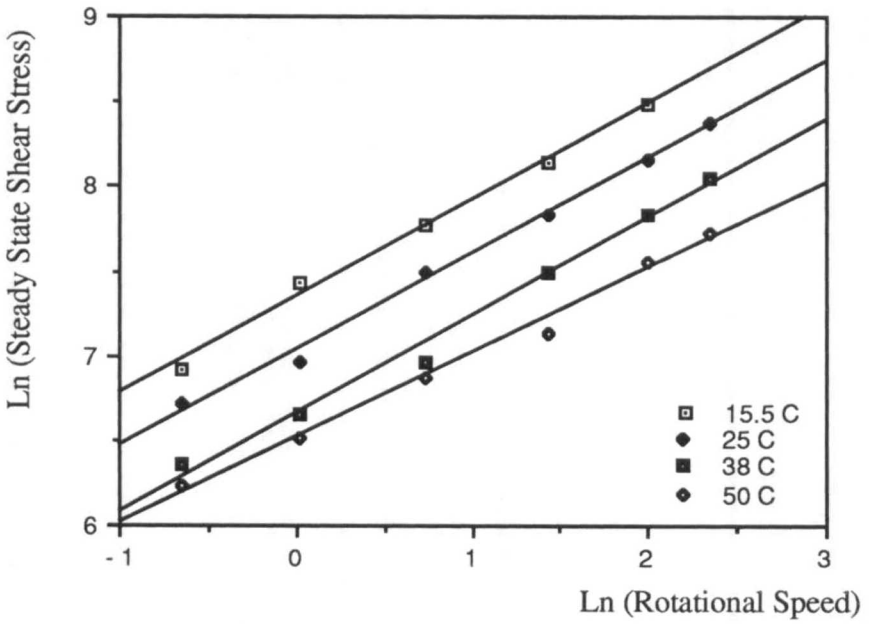

Figure 6.8: Ln (steady state shear stress) as a function of Ln (rotational speed) at various temperature.

Temperature (°C)	Initial State	
	B	n
288.5	4.59	0.458
298.0	4.57	0.461
311.0	4.31	0.494
323.0	3.96	0.549

Table 6.2: Rotational speed coefficient and power law exponent as a function of temperature for initial state.

Thus, the rotational speed coefficient and the power law exponent as a function of temperature can be obtained from the Figs. (6.9) and (6.10) and the result is given in section 6.7.

The consistency index c was then evaluated, which is also a function of temperature. The most common expression for the temperature dependence of the consistency index is as follows [Rauwendaal 86] :

$$c = Ae^{-\alpha(T-T_R)} \tag{6.8}$$

where α and A are the material constants.

To find equation (6.8) constants, Ln(C) data for the initial state and the steady state was obtained at four different temperatures using Figs. (6.7) and (6.8) and are given in Tab. (6.3).

The graphs of the Ln(C) as a function of difference temperature are given in Figs. (6.11) and (6.12) for initial and steady states respectively.

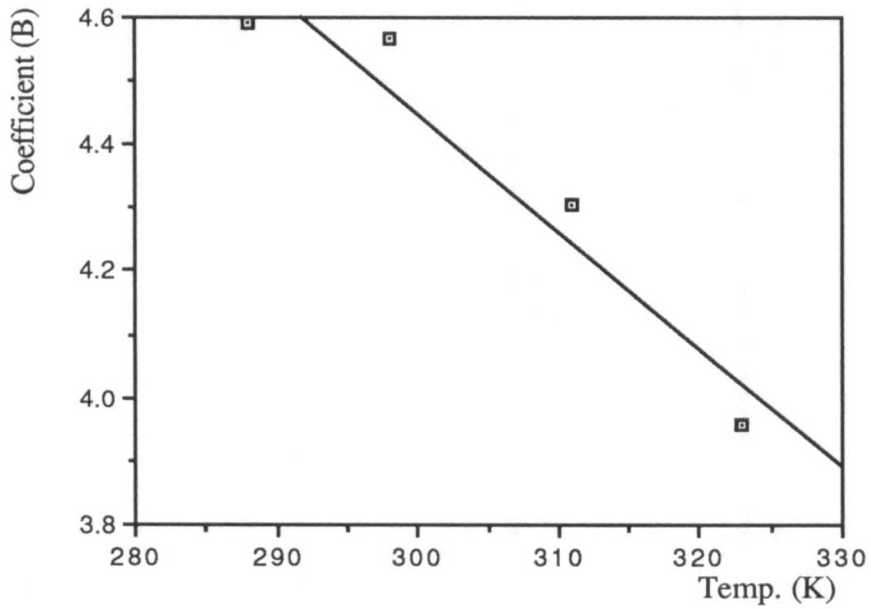

Figure 6.9: Coefficient (B) as a function of temperature for initial state.

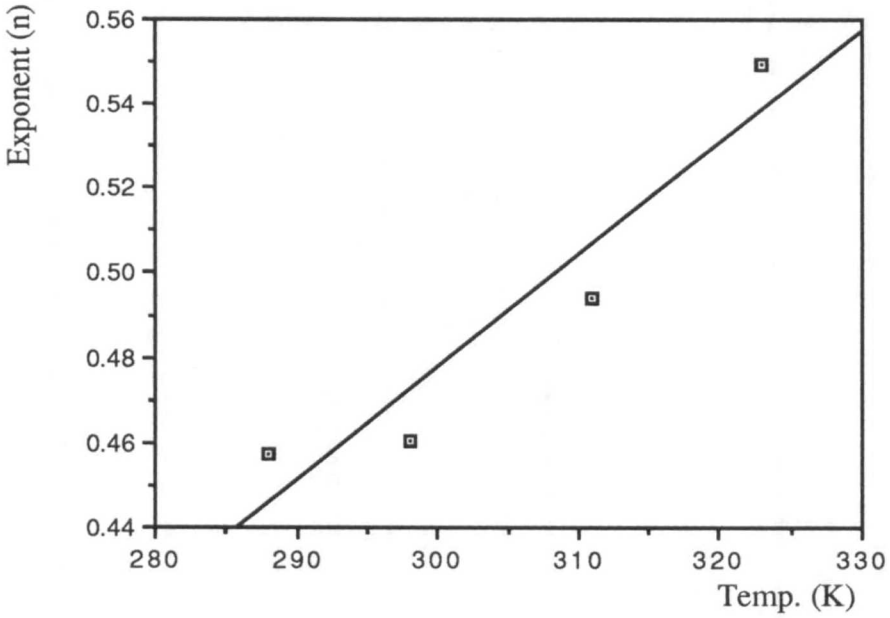

Figure 6.10: Power law exponent "n" as a function of temperature for initial state.

$T - T_R$	Ln (C)	
	Initial State	Steady state
-7.5	7.88	7.35
2.0	7.50	7.03
15.0	7.16	6.66
27.0	6.93	6.52

Table 6.3: Ln (C) as a function of inverse temperature data.

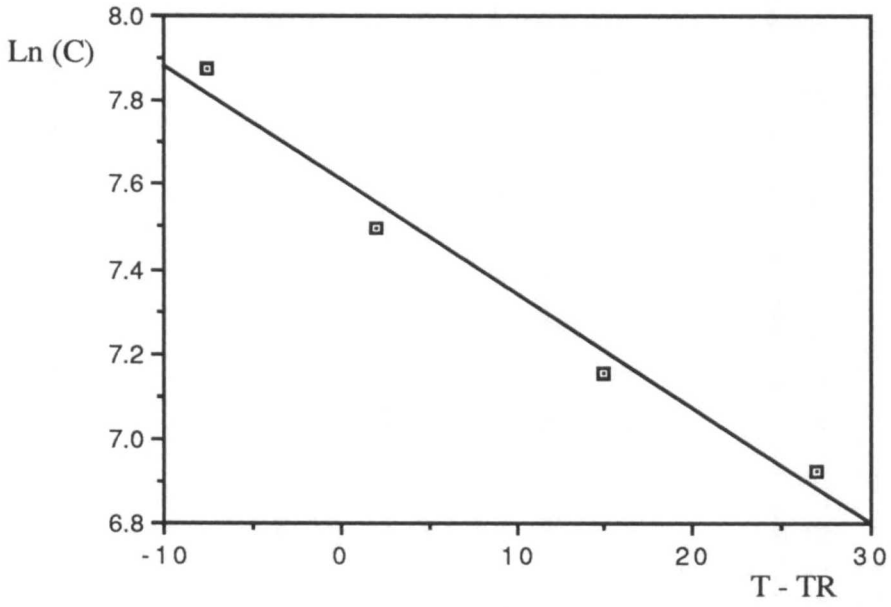

Figure 6.11: Ln (C) Power law coefficient as a function of temperature difference for initial state.

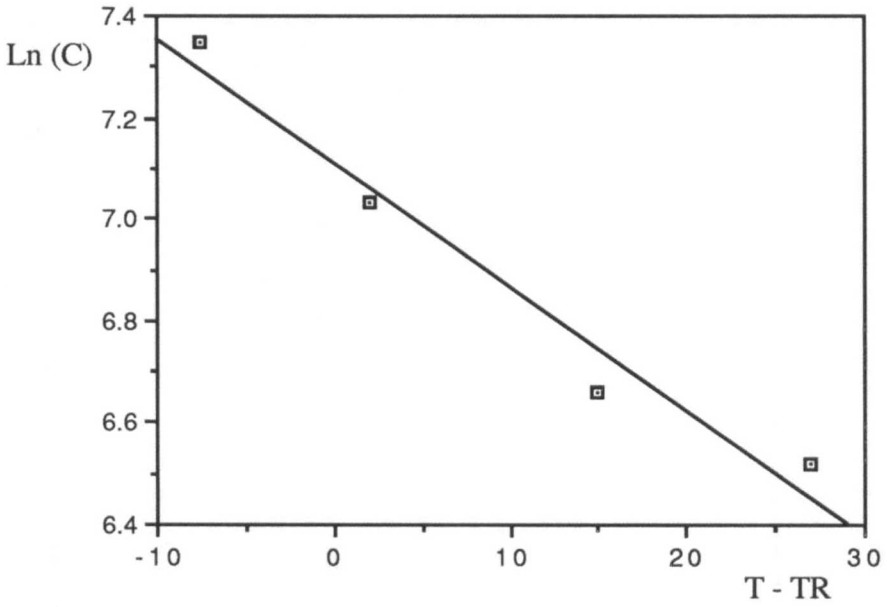

Figure 6.12: Ln (C) as a function of temperature difference for steady state.

Thus, α and A were obtained using Figs. (6.11) and (6.12). The modified power law coefficient, C and the power law coefficient, c were then determined. The results are given in the following section (§ 6.7).

6.7 Rheological Equation of M23

The modified power law coefficient, C , power law coefficient , c , power law exponent, n, and rotational speed coefficient, C , for initial and steady state with their correlation coefficients are found to be:

$$C_{init.} = 2022.9e^{2.7*10^{-2}(T-T_R)} \qquad R = 0.988$$

$$c_{init.} = \frac{2022.9}{B_{init.}^{n_{init.}}} e^{2.7*10^{-2}(T-T_R)}$$

$$n_{init.} = -0.331 + 2.692 \times 10^{-3} T \qquad R = 0.952$$

$$B_{init.} = 10.109 - 1.885 \times 10^{-2} T \qquad R = 0.963$$

$$C_{S.S.} = 1225.9e^{2.4*10^{-2}(T-T_R)} \qquad R = 0.982$$

$$c_{S.S.} = \frac{1225.9}{B_{init.}^{n_{init.}}} e^{2.4*10^{-2}(T-T_R)}$$

$$n_{ss} = 0.573 \pm 0.006$$
$$B_{ss} = 3.831 \pm 0.056$$

The shear stresses as a function of rotational speed and shear rate are:

$$\tau_{init.} = 2022.9\Omega^{n_{init.}} e^{2.7*10^{-2}(T-T_R)} \qquad \tau_{S.S.} = 1225.9\Omega^{n_{S.S.}} e^{2.4*10^{-2}(T-T_R)} \qquad (6.9)$$

$$\tau_{init.} = 2022.9(\frac{\dot{\gamma}}{B_{init.}}) e^{2.7*10^{-2}(T-T_R)} \qquad \tau_{S.S.} = 567.9(\dot{\gamma})^{0.573} e^{2.4*10^{-2}(T-T_R)} \qquad (6.10)$$

The temperature is in degrees Kelvin.

The initial and steady state viscosity profile are evaluated using analytical shear rate and analytical shear stress at four different temperatures. The results are given in Figs. (6.13) and (6.14) respectively.

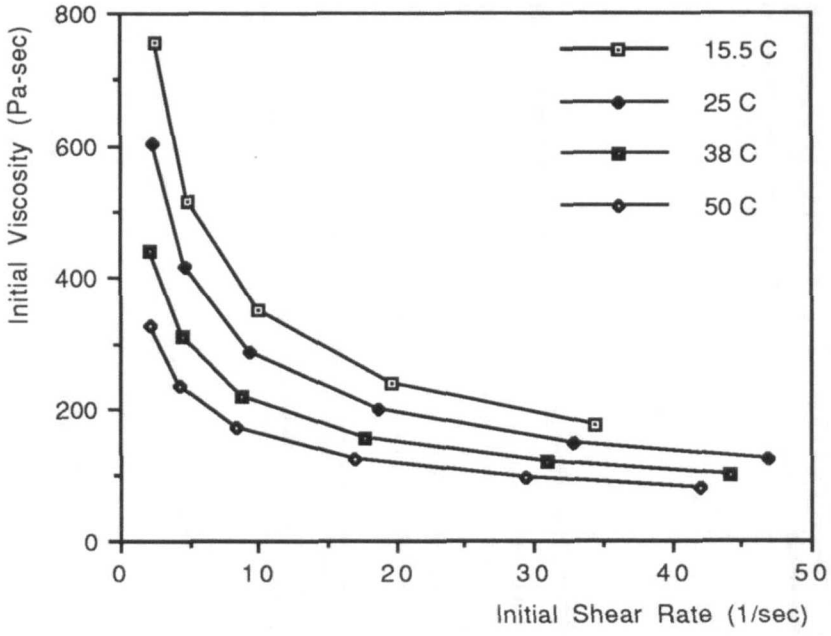

Figure 6.13: Initial viscosity profile of adhesive at four different temperatures.

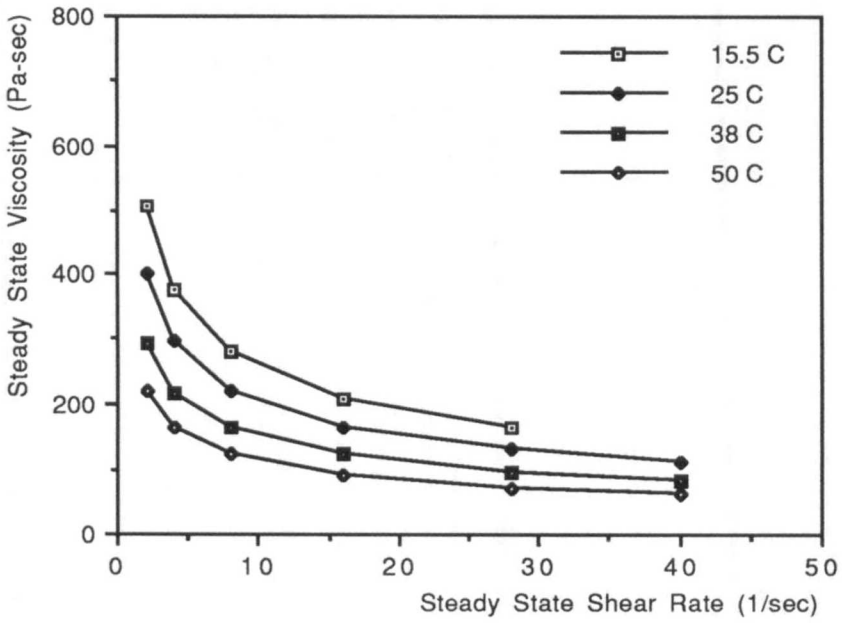

Figure 6.14: Steady state viscosity profile of adhesive at four different temperatures.

6.8 Comparison of Theoretical and Experimental Data

The analytical results using equations (6.9) is given in Tab. (5.4) and the result along with experimental data for initial state and steady state are plotted in Figs. (6.15) and (6.16). The theoretical equations are empirical, and it is assumed that they are valid for the flow through the pipe. Viscosity in the pipe may also be a function of pressure in which at high pressure, the rheological behaviour may be affected. The effect of pressure on viscosity becomes usually significant at pressures higher than 35000 kPa [Rauwendaal 86].

The error between the analytical and experimental data is given in Tab. (6.5), and the plots of the error for initial state and steady state are given in Figs. (6.17) and (6.18) respectively. The majority of the errors are less than 10 percent. Considering the 5 percents error in the experimental data and ignoring the effect of time in the analytical analysis, the results are reasonable. The errors in the steady state are also lower than in the initial state due to the fact that obtaining the experimental data for the initial state is more difficult and is less accurate than the steady state.

Rotational Speed of Bob (rev/min)	Initial Shear Stress (Pa)				Steady State Shear Stress (Pa)			
	15.5 °C	25 °C	38 °C	50 °C	15.5 °C	25 °C	38 °C	50 °C
5	1858.0	1412.0	970.3	686.1	1016.0	805.9	587.2	438.4
10	2531.0	1958.0	1378.0	996.6	1511.0	1199.0	873.5	652.2
20	3447.0	2715.0	1958.0	1448.0	2248.0	1783.0	1299.0	970.2
40	4695.0	3763.0	2780.0	2103.0	3344.0	2653.0	1933.0	1443.0
70	6025.0	4899.0	3691.0	2842.0	4608.0	3656.0	2664.0	1989.0
100	-	5796.0	4422.0	3444.0	-	4485.0	3268.0	2440.0

Table 6.4: Analytical data for Elastosol M23, using power law expression.

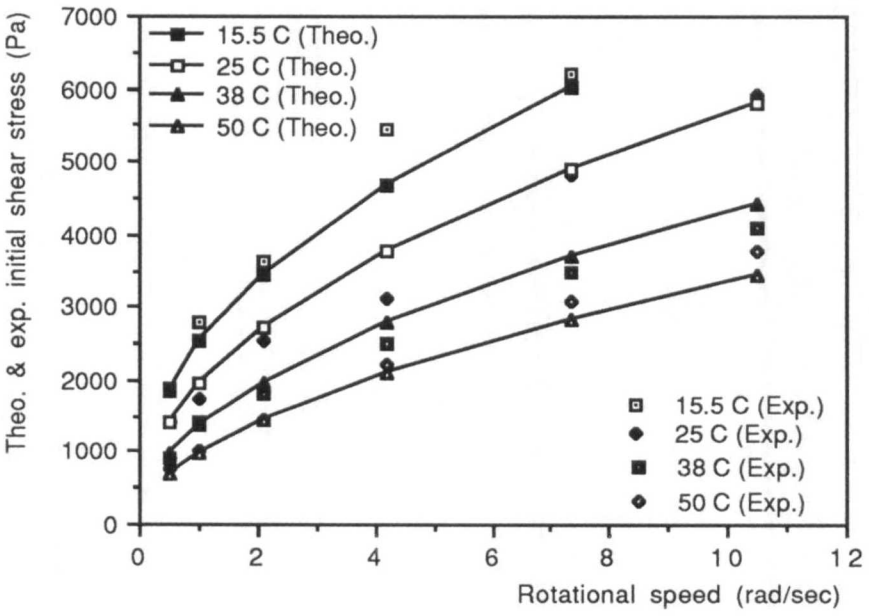

Figure 6.15: Theoretical best-fit and experimental data for initial state shear stress as a function of rotational speed.

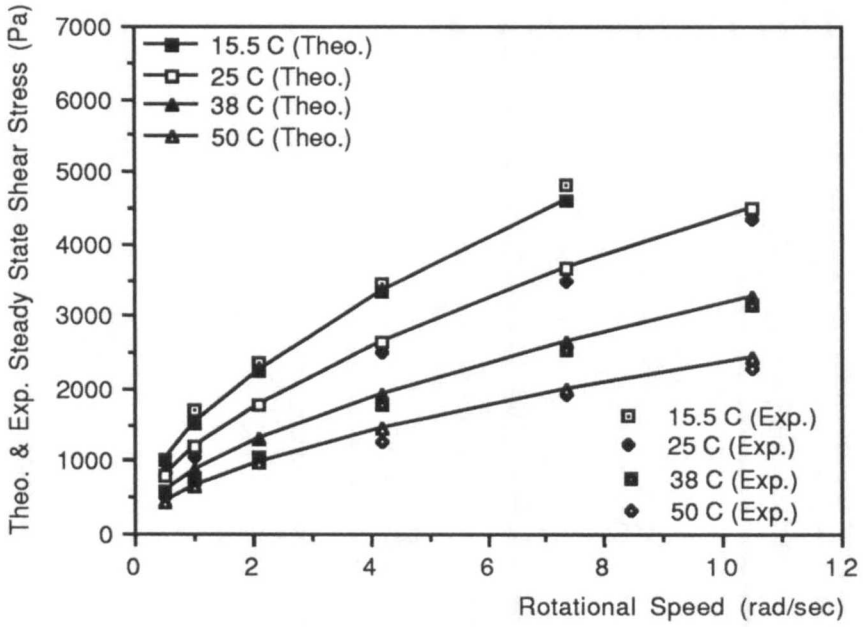

Figure 6.16: Theoretical best -fit and experimental data for steady state shear stress as a function of rotational speed.

Rotational Speed of Bob (rev/min)	Initial Shear Stress Errors				Steady State Shear Stress Errors			
	15.5 °C	25 °C	38 °C	50 °C	15.5 °C	25 °C	38 °C	50 °C
5	1.48	0.73	-8.49	7.98	0	2.01	-1.38	14.38
10	9.02	-12.17	1.80	1.91	10.75	-12.69	-12.80	3.63
20	5.02	-6.25	-7.63	0.22	5.19	0.41	-22.09	-0.39
40	13.74	-20.18	-10.53	5.51	2.65	-5.48	-7.96	-14.74
70	2.73	-1.66	-5.97	8.20	4.75	-4.96	-4.85	-4.38
100	-	2.02	-7.54	8.75	-	-2.98	-3.89	-7.32

Table 6.5: % Error between analytical data and experimental values.

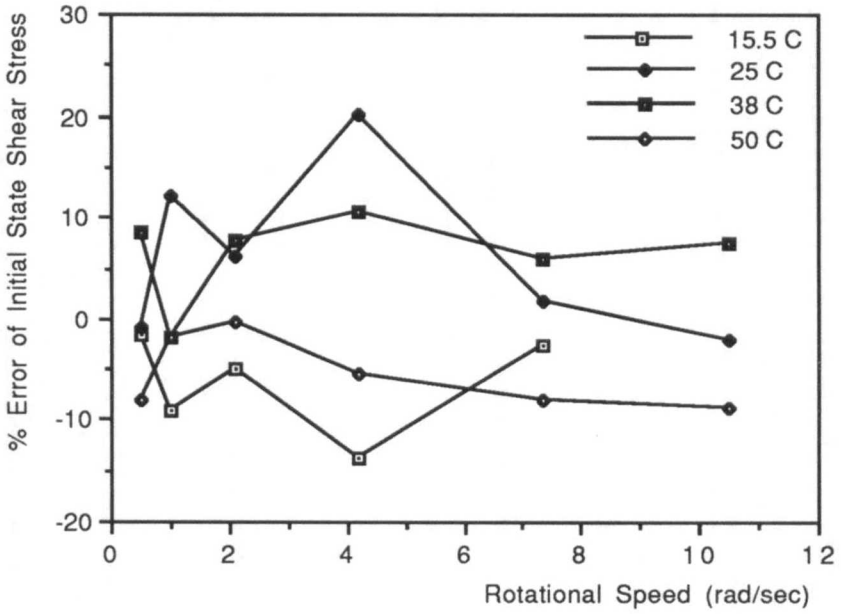

Figure 6.17: % Error of initial state shear stress.

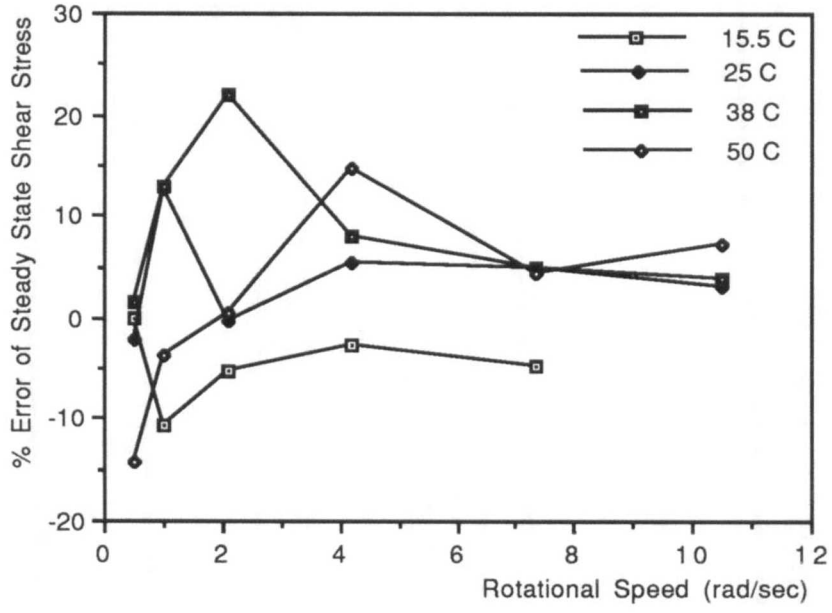

Figure 6.18: % Error of steady state shear stress.

6.9 Conclusion

The rheological model of the adhesive was obtained using a power law expression. This model is generic and is based on the experimental data. It can be used for different types of adhesives with similar rheological characteristics providing the information regarding shear stress as a function of rotational speed at different temperatures has been obtained. By having the power law expression, the flow rate through the gun and the nozzle can be calculated by using the power law exponent and power law coefficient.

To simplify the analysis, the time factor was not considered in the theoretical analysis, which is one of the sources of the errors between the analytical and experimental values. The errors in the steady state however are lower due to the fact that the data were taken after 5 minutes. The analytical values are also closer to the experimental values at the lower temperature which can be caused by homogeneity of the temperature at the low values. There is a possibility that temperature to be less homogeneous at the higher values and the viscosity dependence on temperature is also stronger which causes the higher error between the analytical and experimental values.

This analysis gives the characteristics of the adhesive material which can be used for analytical modelling of the flow through the gun and the nozzle as described in the next chapter (Ch. 7).

CHAPTER VII

THEORETICAL MODELLING OF THE DISPENSED FLOW

7.1 The Flow Modelling

Having obtained the rheological model of the adhesive material using the power law expression in chapter 6, the next step is to use the rheological model to find the flow through the nozzle. Subsequently, the resulting adhesive bead thickness can be obtained using the mass balance equation. These data can be used for initial set-up of the knowledge-based system.

Here, the flow through the gun and the nozzle need to be obtained. Thus, the theoretical and experimental flow rate of the dispensed adhesives are analysed. The nozzle entrance and end effects are also discussed.

7.2 Flow Through The Pipe

A model of the dispensed flow through the gun requires familiarity with fluid flow through a pipe. The procedure for finding the flow rate through a pipe for a generalised non-Newtonian fluid is very similar to the Newtonian fluid, except for the additional complexity introduced by the variable viscosity.

The motion of fluid in pipes with a uniform cross section using a cylindrical coordinate system, can be described by the equations of conservation of mass, energy and momentum as follows [Tadmor 79, Wilkinson 60]:

$$\frac{D\rho}{Dt} = -\rho \nabla . V \tag{7.1}$$

$$\rho\frac{DE}{Dt} = -(\nabla q) - P(\nabla.V) - (\tau:\nabla V) + \dot{S} \tag{7.2}$$

$$\rho\frac{DV}{Dt} = -\nabla P - (\nabla.\tau) + \rho g \tag{7.3}$$

Where ρ is density, t is time, V is velocity, E is specific internal energy per unit mass, q is heat flux, τ is shear stress, p is pressure $\dot{S}$ is a thermal energy source term and g is the gravity. Using cylindrical coordinates (r, θ, z) and assuming steady, isothermal fully developed incompressible flow, the continuity equation will be as follows:

$$\frac{1}{r}\frac{\partial}{\partial r}(r\,v_r) + \frac{1}{r}\frac{\partial v_\theta}{\partial \theta} + \frac{\partial v_z}{\partial z} = 0$$

Due to the symmetry, the velocity is independent of "θ", so, $V_\theta = 0$, and because of fully developed flow $(\partial v_Z/\partial z) = 0$. Thus, the continuity equation reduces to:

$$\frac{\partial}{\partial r}(r\,v_r) = 0$$

After integration, $r\,v_r = C$. Using the boundary condition of $v_r = 0$ at $r = R$, radius of the tube, then $C = 0$, therefore $v_r = 0$. Hence the only velocity component is v_z which is a function of, r. Therefore, neglecting entrance and exit effects $v_Z = v_Z(r)$, $v_\theta = 0$, $v_r = 0$, $p = p_O$ @ $z = 0$ and $p = p_L$ @ $z = L$.

7.3 Viscous Heating Effect

The energy equation describes the temperature distribution in a non-isothermal fluid. The adhesive flow can be considered isothermal since the hose is insulated. However, in the viscous fluid, significant viscous heating is generated at the high shear rate [Middleman 77]. An easy way to estimate the increase in temperature due to viscous dissipation is to consider the dynamic dissipation (work done due to the pressure drop) which is transformed into thermal energy. Assuming an adiabatic flow, the first law of thermodynamics leads to the following expression for the change in temperature:

$$\dot{m}\rho c_p dT = \dot{m}\,dp \qquad \Rightarrow \qquad dT = \frac{dp}{\rho c_p}$$

where ρ is density of the adhesive ($\rho = 1.50 \pm 0.05$ gr./cc) and c_p is the specific heat ($c_p = 1.15 \pm 0.08$ J/gr.).

The increase in temperature is about 1.3 °C for the maximum pressure drop of 2200 kPa. The actual value of the temperature increase is even smaller since some heat is lost at the boundaries. Thus, the viscous heating effect can be neglected.

7.4 Analytical Flow Rate Using the Power Law Model

Since the viscous heating is negligible, only the equations of motion, continuity and the rheology are required to describe the flow.

Using the assumption mentioned in sections 7.2 and 7.3, the momentum equation (Eq. 7.3), the pressure change in r and θ directions are zero [(dp/dr) = 0, (dp/dθ) = 0], and the pressure change in the z direction is:

$$\frac{dp}{dz} = \frac{1}{r}\frac{d}{r}(r\,\tau_{rz}) + \rho\, g$$

Replacing P = p - ρ g z, the above equations can be written as follows:

$$\frac{1}{r}\frac{d}{dr}(r\,\tau_{rz}) = \frac{P_o - P_L}{L}$$

After integration

$$\tau_{rz} = \frac{(P_o - P_L)\,r}{2\,L} + \frac{C_1}{r}$$

using the boundary condition, C_1 has to be zero, otherwise shear stress is infinite at the centre. The shear stress at the wall (r = R) is:

$$\tau_R = \frac{P_0 - P_L}{2L}R \tag{7.4}$$

The τ_{rz} in terms of τ_R is

$$\tau_{rz} = \tau_R \frac{r}{R} \tag{7.5}$$

Using the power law equation for the shear stress from chapter 6 (Eq. 6.2):

$$\tau_{rz} = k\dot{\gamma}^n = k\left(-\frac{dv_z}{dr}\right)^n \tag{7.6}$$

where $\dot{\gamma}$ is a positive quantity and is, $\dot{\gamma} = -\frac{dV_z}{dr}$

Using equations (7.5), (7.6) and (7.4), the velocity profile is

$$V_z = \left(\frac{(P_0 - P_L)R}{2Lc}\right)^{\frac{1}{n}} \frac{R}{\frac{1}{n}+1}\left[1-\left(\frac{r}{R}\right)^{\left(\frac{1}{n}+1\right)}\right] \tag{7.7}$$

Then, the volumetric flow rate is:

$$Q = \int_0^{2\pi}\int_0^R V_z r dr d\theta$$

After normalisation of r:

$$Q = 2\pi R^2 \int_0^1 V_z \frac{r}{R} d\left(\frac{r}{R}\right)$$

Using equation (7.4), the flow rate as a function of pressure drop is:

$$Q = \frac{\pi R^3}{\frac{1}{n}+3}\left[\frac{(P_0 - P_L)R}{2cL}\right]^{\frac{1}{n}} \tag{7.8}$$

7.5 Experimental Flow Rate Through The Nozzle

The flow rate is a function of gun opening cross-sectional area (which is controlled through the movement of the carbinade needle in the gun) and pressure in the gun. However the gun opening is controlled via an analogue input voltage. The gun diagram is given in Fig. (7.1). The needle position in the gun for the cases of completely closed (input voltage = 0) and completely open (input voltage =10 V) are given in Figs. (7.2a) and (7.2b) respectively. After passing through the gun, adhesive flows through a nozzle for dispensing. The nozzle has a constant diameter as shown in Fig. (7.3).

The gun opening cross-sectional area and gun pressure as a function of the input analogue voltage are given in Figs. (7.4) and (7.5) respectively for the steady state values. The Gun pressure was measured by a "Piezoelectric" pressure transducer located after the gun opening and 23.5 mm above the nozzle inlet as shown in Fig. (7.1).

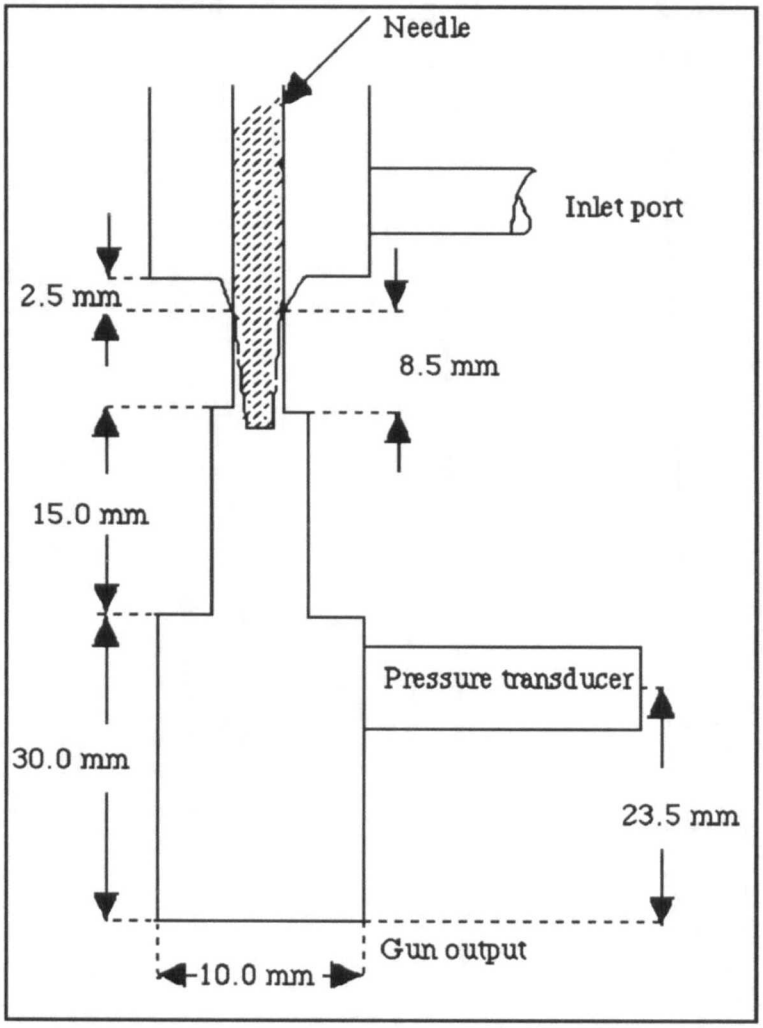

Figure 7.1: The gun diagram and needle.

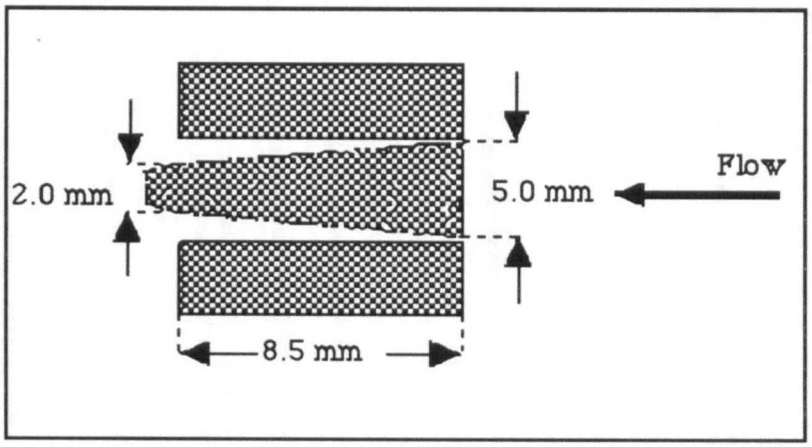

Figure 7.2a: Needle position for a closed gun.

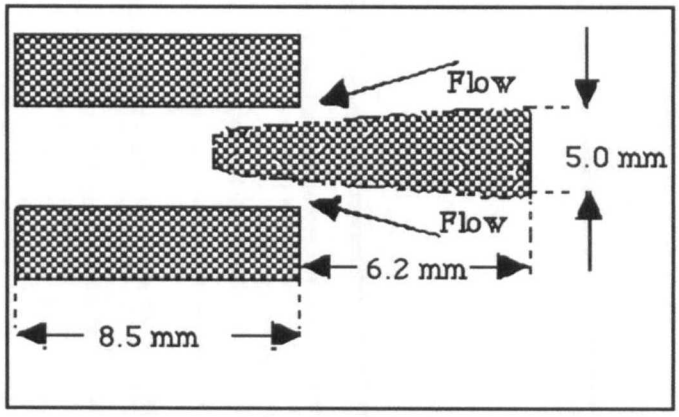

Figure 7.2b: Needle position for an open gun.

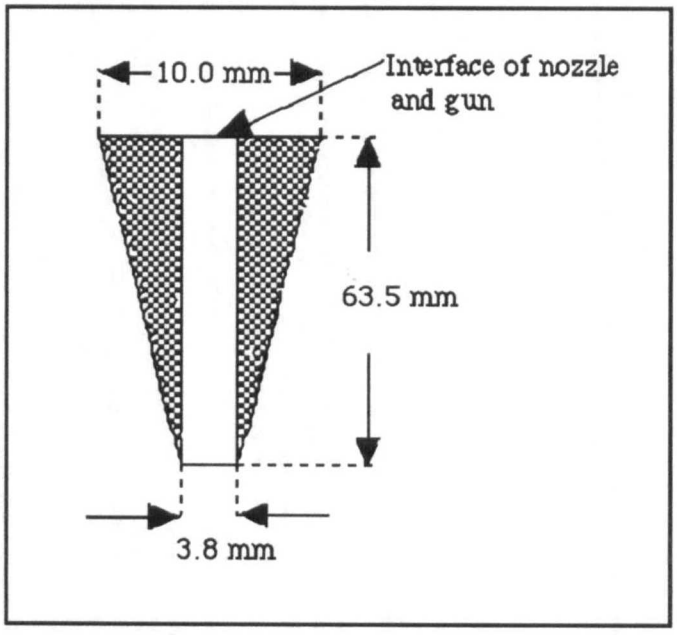

Figure 7.3: Nozzle diagram (Diameter = 3.8 mm).

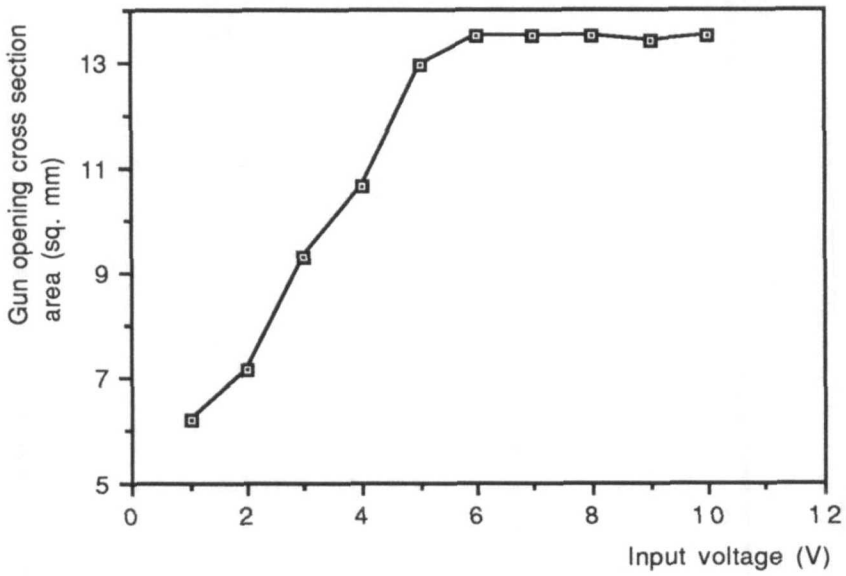

Figure 7.4: Gun opening cross section area as a function of input voltage.

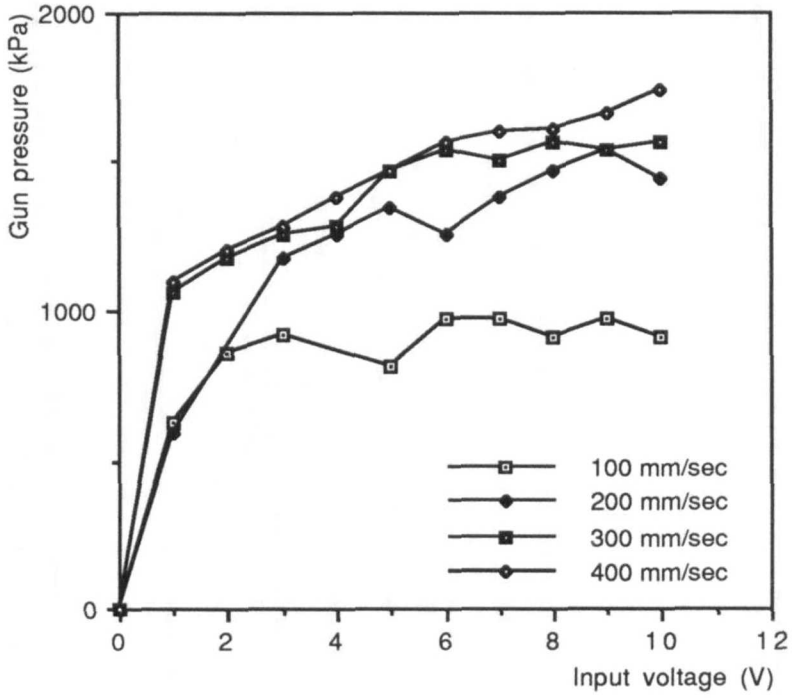

Figure 7.5: Gun pressure as a function of input voltage.

Experimental data were then obtained by dispensing adhesive over a desired trajectory at robot speeds relative to the workpiece of 100, 200, 300, and 400 mm/sec. The average velocity in the nozzle was constant for each robot speed. The volume flow rate for each case at different step inputs was obtained by finding the net weight of each sample, the dispensing time and using the adhesive density which is 1.5 gr./cc. The graph of experimental flow rate data with error bars at three different speeds as a function of input voltage and gun pressure are given in Figs. (7.6) and (7.7) respectively.

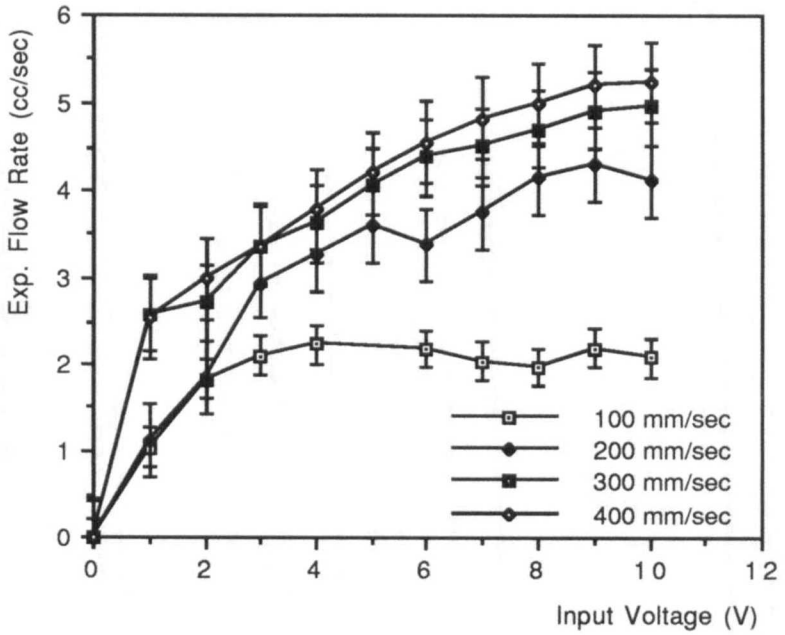

Figure 7.6: Experimental flow Rate with error bars at four different speeds.

7.6 Theoretical Flow Rate Analysis Through The Nozzle

Theoretical data were then obtained by using rheological equations (Eqs. 6.9 and 6.10) and the flow through a pipe (Eq. 7.8) for both initial and steady state cases. The *Piezoelectric* transducer location is 23.5 mm above from the nozzle inlet (Lg = 23.5 mm) and the length of nozzle (LN = 63.5 mm). The schematic diagram of the dispensing gun is given in Fig. (7.8). The diameter of the gun after the pressure transducer is constant (D_g=10.0 mm) and the diameter of the nozzle is also constant (D_N=3.8 mm). The pressure at the interface of nozzle and gun P_2 needs to be calculated due to the difference between gun diameter, D_g and nozzle diameter, D_N.

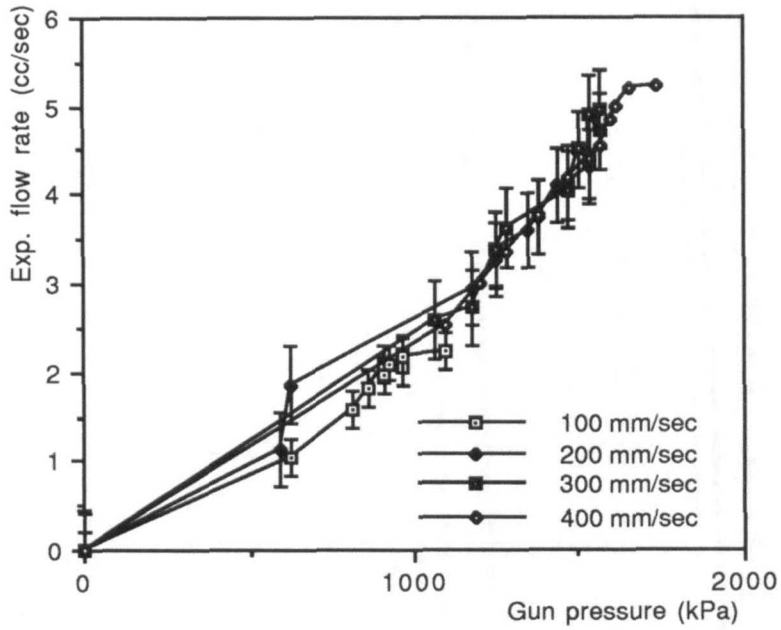

Figure 7.7: Experimental flow rate as a function of gun pressure.

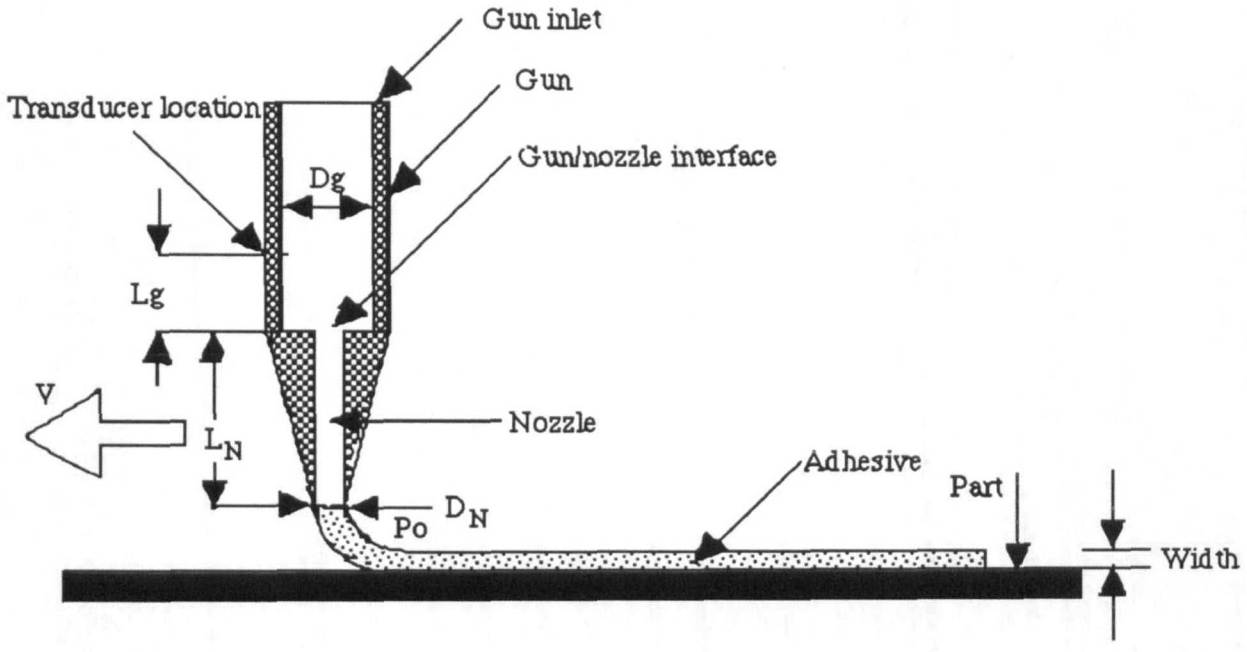

Figure 7.8: Schematic diagram of dispensing gun.

For calculation of interface pressure, assuming continuity at interface region, which is as follows:

$Q_g = Q_n$ (where Q_g and Q_n are the gun and nozzle flow rates) and
$DP_T = DP_g + DP_N + DP_{g/N}$ (where DP_T , DP_g , DP_N and $DP_{g/N}$ are the total pressure drop, gun pressure drop, nozzle and nozzle entrance pressure drop, respectively).

The pressure drop in the gun is very small compared to the pressure drop in the nozzle since the gun is much shorter and wider than the nozzle. The pressure drop due to entrance and exit effects at the nozzle is also negligible (see § 7.7 for further detail). By using the flow through the pipe (Eq. 7.8) for the flow rate at the gun and nozzle interface, the interface pressure can be found to be:

$$P_2 = \frac{P_0 + \left(\frac{R_g}{R_N}\right)^{3n+1}\left(\frac{L_N}{L_g}\right)P_1}{1 + \left(\frac{R_g}{R_N}\right)^{3n+1}\left(\frac{L_N}{L_g}\right)} \qquad (7.9)$$

where

P_0, P_1 and P_2 are the exit pressure, pressure transducer reading, and interface pressure at the nozzle and gun,
R_g and R_N are the gun and nozzle radii, and
L_g and L_N are the gun length after pressure transducer, and the nozzle length respectively.

7.7 Nozzle End Effects

The flow in the nozzle is assumed fully developed since the L/D ratio of the nozzle is 16.7 and the Reynolds number is less than unity [Middleman 77]. Furthermore, *swelling* effects are about 12% and the sagging effect is approximately 10% in the exit region as shown in Figs. (7.9) and (7.10) respectively. The swelling effects can be reduced by using a longer nozzle for dispensing to increase L/D ratio. Thus, the elasticity effects are very small [Lodge 64, Bird 87]. Therefore, the nozzle entrance and exit pressure drops are very small due to the small effects of the elasticity [Mckelvey 62, Middleman 77].

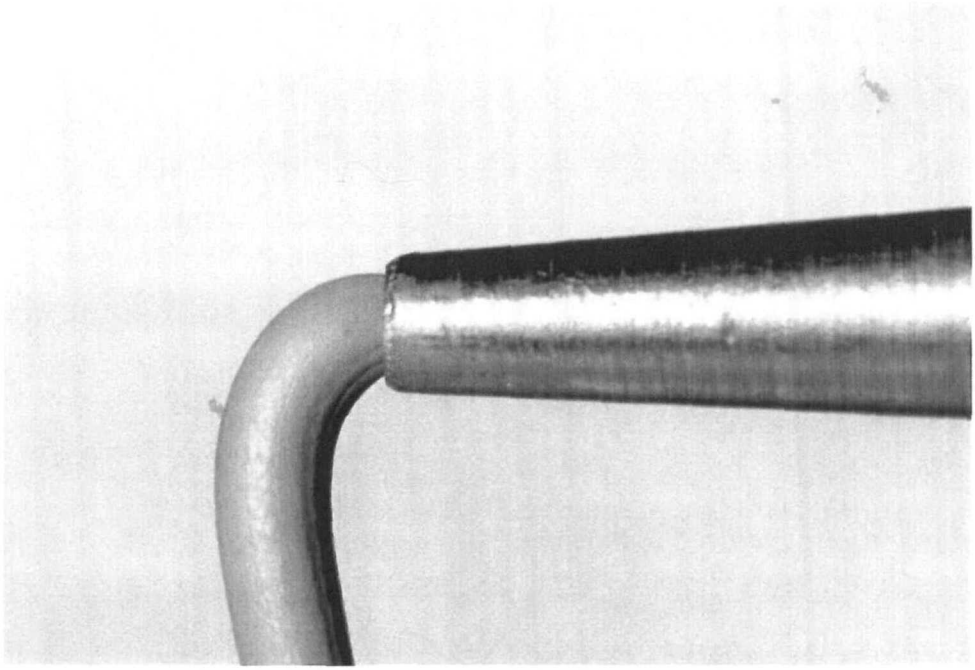

Figure 7.9: Swelling effects of the free stream of adhesive in the nozzle exit region.

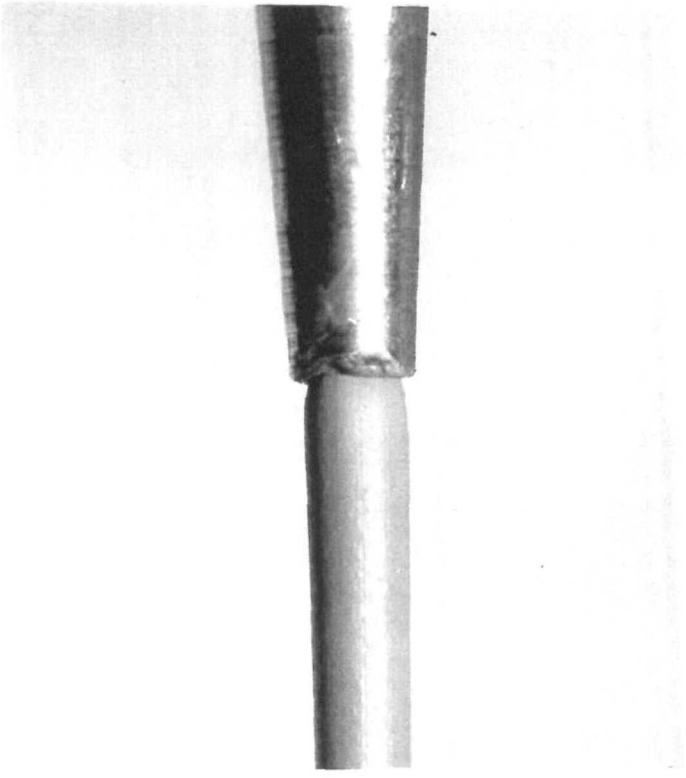

Figure 7.10: Sagging effects of the free stream of adhesive in the nozzle exit region.

7.8 Theoretical Flow Rate Calculation

Having found the interface pressure using (Eq. 7.9) for both initial and steady states, the initial and steady state flow rates can be calculated by using flow equation through the pipe (7.8). The data was taken at 35 °C. These results along with experimental flow rate at four different speed are given in Tables. (7.1) through (7.4). The graphs of the experimental flow rate along with both initial and steady state flow rates at different robot speeds are also given in Figs. (7.11) through (7.14).

7.9 Comparison of Experimental & Theoretical Flow Rate

The flow rate plots (Figs. 7.11-7.14) show some fluctuations which are the effects of the high pump pressure and adhesive shear thinning. This happens more often at lower speeds. The effect is smaller at higher speeds, which makes the pressure and the flow rate graphs very smooth at 400 mm/sec. The adhesive resistance is almost constant at higher speed so

Input Voltage (V)	Flow rate (cc/sec) Theoretical (initial state)	Flow rate (cc/sec) Theoretical (steady state)	Flow rate (cc/sec) Experimental case
1.0	0.513	0.718	1.044
2.0	1.077	1.369	1.822
3.0	1.263	1.571	2.094
4.0	1.849	2.190	2.238
5.0	0.948	1.224	1.565
6.0	1.411	1.731	2.182
7.0	1.411	1.731	2.043
8.0	1.215	1.520	1.969
9.0	1.411	1.731	2.193
10.0	1.215	1.520	2.079

Table 7.1: Flow rate data for the speed of 100 mm/sec.

Input Voltage (V)	Flow rate (cc/sec) Theoretical (initial state)	Flow rate (cc/sec) Theoretical (steady state)	Flow rate (cc/sec) Experimental case
1.0	0.453	0.645	1.128
2.0	0.513	0.718	1.856
3.0	2.153	2.499	2.951
4.0	2.480	2.826	3.265
5.0	2.903	3.241	3.604
6.0	2.480	2.826	3.384
7.0	3.051	3.384	3.743
8.0	3.518	3.831	4.138
9.0	3.849	4.141	4.301
10.0	3.359	3.679	4.111

Table 7.2: Flow rate data for the speed of 200 mm/sec.

Input Voltage (V)	Flow rate (cc/sec) Theoretical (initial state)	Flow rate (cc/sec) Theoretical (steady state)	Flow rate (cc/sec) Experimental case
1.0	1.734	2.071	2.577
2.0	2.153	2.499	2.723
3.0	2.480	2.826	3.372
4.0	2.617	2.961	3.622
5.0	3.518	3.831	4.052
6.0	3.849	4.141	4.391
7.0	3.682	3.985	4.502
8.0	4.019	4.300	4.709
9.0	3.849	4.141	4.915
10.0	4.019	4.300	4.968

Table 7.3: Flow rate data for the speed of 300 mm/sec.

Input Voltage (V)	Flow rate (cc/sec) Theoretical (initial state)	Flow rate (cc/sec) Theoretical (steady state)	Flow rate (cc/sec) Experimental case
1.0	1.849	2.190	2.533
2.0	2.281	2.628	2.995
3.0	2.617	2.961	3.368
4.0	3.051	3.384	3.787
5.0	3.518	3.831	4.202
6.0	4.019	4.300	4.549
7.0	4.194e	4.462	4.831
8.0	4.282	4.544	4.985
9.0	4.553	4.793	5.199
10.0	5.024	5.221	5.242

Table 7.4: Flow rate data for the speed of 400 mm/sec.

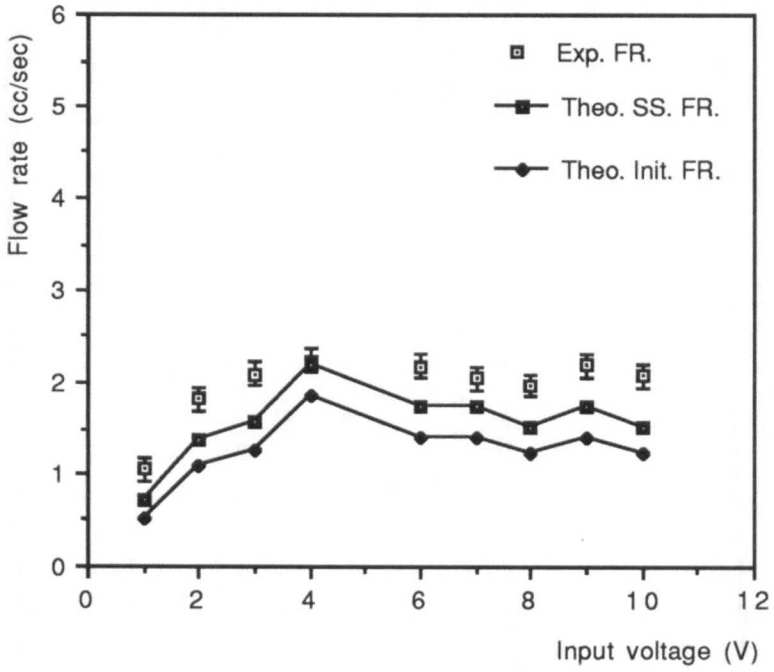

Figure 7.11: Experimental and Theoretical flow rate at 100 mm/sec.

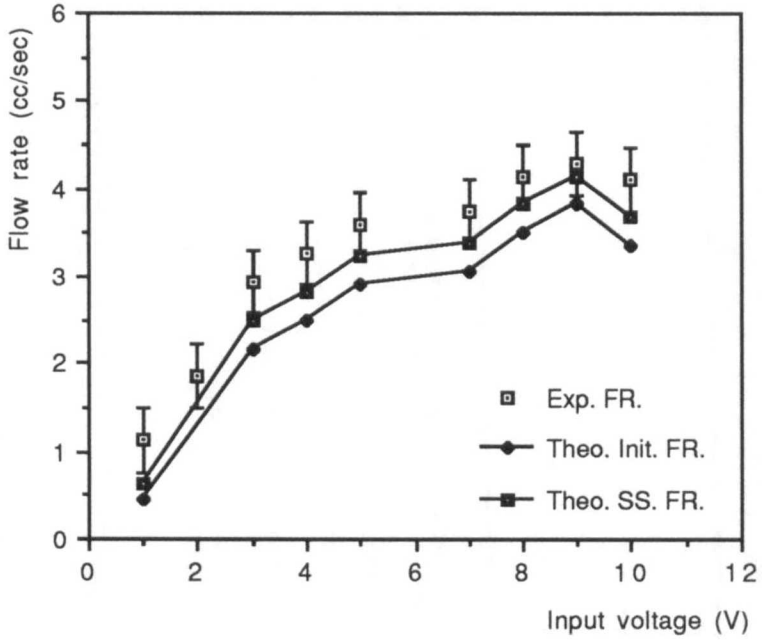

Figure 7.12: Experimental and Theoretical flow rate at 200 mm/sec.

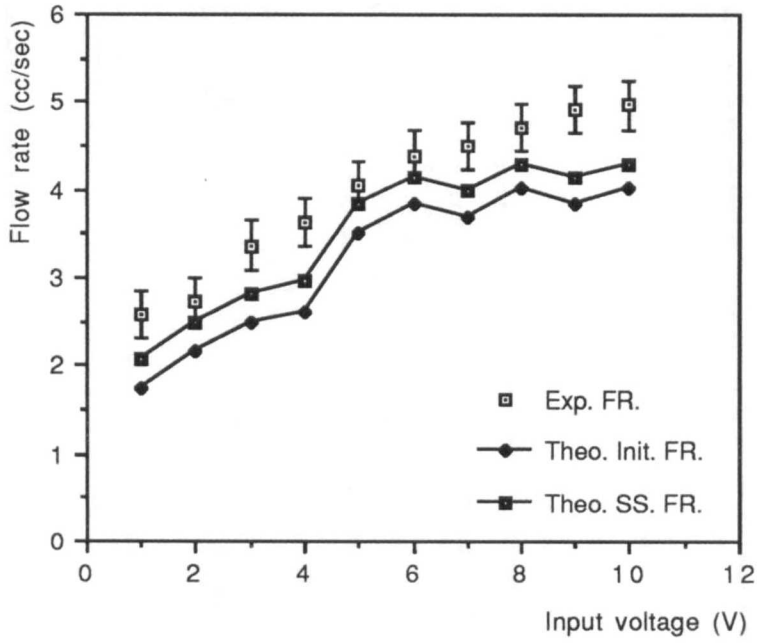

Figure 7.13: Experimental and Theoretical flow rate at 300 mm/sec.

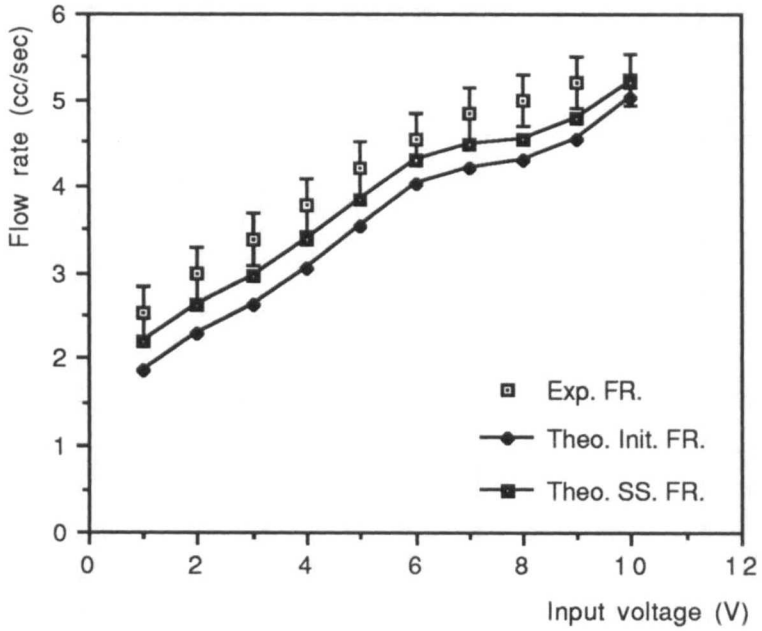

Figure 7.14: Experimental and Theoretical flow rate at 400 mm/sec.

the problem of sticking in the pump does not exist. An easy way to avoid this problem is to dispense the adhesive at lower pump pressure, but this may cause too thin a bead for a very viscous adhesive at higher speed. Another possibility is to vary pump pressure at different speeds which introduces another variable to the model.

After analysing the flow rate data, both initial and steady state results follow the same pattern as the experimental results. This shows a strong effect of the pressure on the flow rate. Both data obtained using initial and steady state adhesive models can be related very closely to the experimental flow rate. However, since gun cross sectional area is very small and the L/D ratio of the nozzle is very large, the flow rate can be described by steady state viscosity data rather than initial values. The end effect was considered negligible since the swelling phenomenon was not observed. Furthermore, there is a more complicated solution that is to consider slip boundary conditions [Mooney 31, Wilkinson 60, Cohen 85, Yilmazer 89]. An analytical solution was considered for no-slip boundary conditions since the purpose of this research was modelling of the flow and the extensive study of the molecules migration effects was not necessary.

7.10 Comparison of experimental and theoretical bead thickness

Having found the theoretical flow rate, the next step is to find the diameter of the dispensed adhesive bead by assuming a cylindrical shape bead and using the mass balance equation as follows:

$$D_b = \sqrt{\frac{4Q}{\pi V_R}} \tag{7.9}$$

Where D_b is the bead dispensed diameter, Q is the volumetric flow rate and V_R is the speed of the robot.

These results are compared with the experimental width which was obtained by the vision system while the adhesive was being laid. Comparisons of predicted deposited bead thickness with experimental data are given in Figs. (7.15 - 7.18). The major source of error comes from the fact that there is a transport lag between laying down the adhesive and taking an image by the vision system (as explained in detail in § 5.4). The adhesives settle down during this period, making the deposited bead wider. Furthermore, the theoretical results are closer to the experimental values since the delay is shorter at higher robot speeds.

7.11 Conclusion

The aim of this chapter was to analyse the adhesive flow rate through the dispensing nozzle. Flow rate through the nozzle can be calculated by using a power law exponent and coefficient (§. 6.7). Furthermore, the deposited bead thickness was calculated theoretically and was compared with the experimental results which was obtained using the vision system while the bead was being laid. These result can be used for the initial set-up of the system and as an aspect of diagnosis when using a knowledge-based expert system. Using this approach it is possible to achieve an "almost right first time" setting for viscous adhesive and sealant dispensing, thus avoiding the long and costly series of ad-hoc adjustments that would otherwise be required.

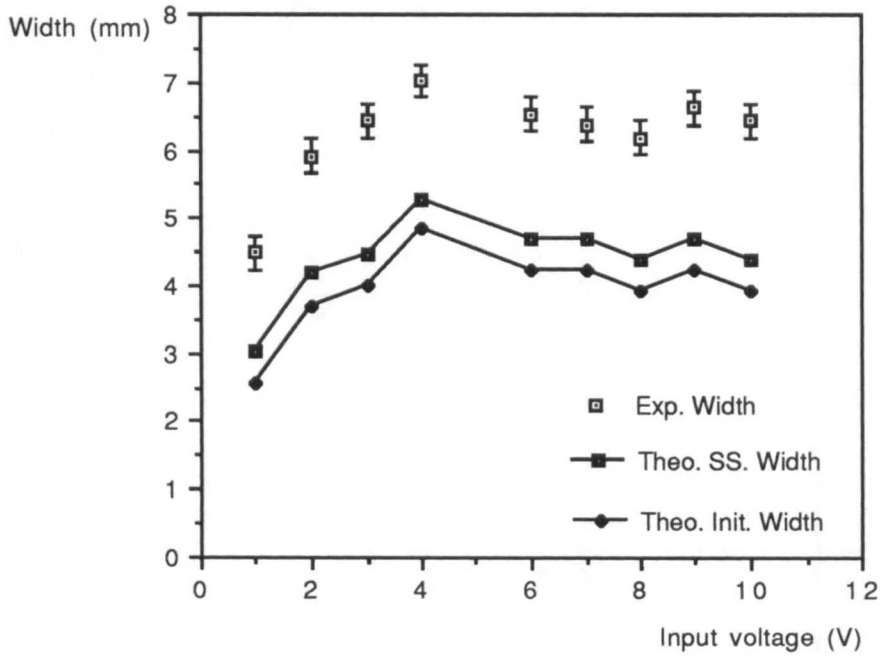

Figure 7.15: Theoretical and experimental width as a function of input voltage at 100 mm/sec robot speed.

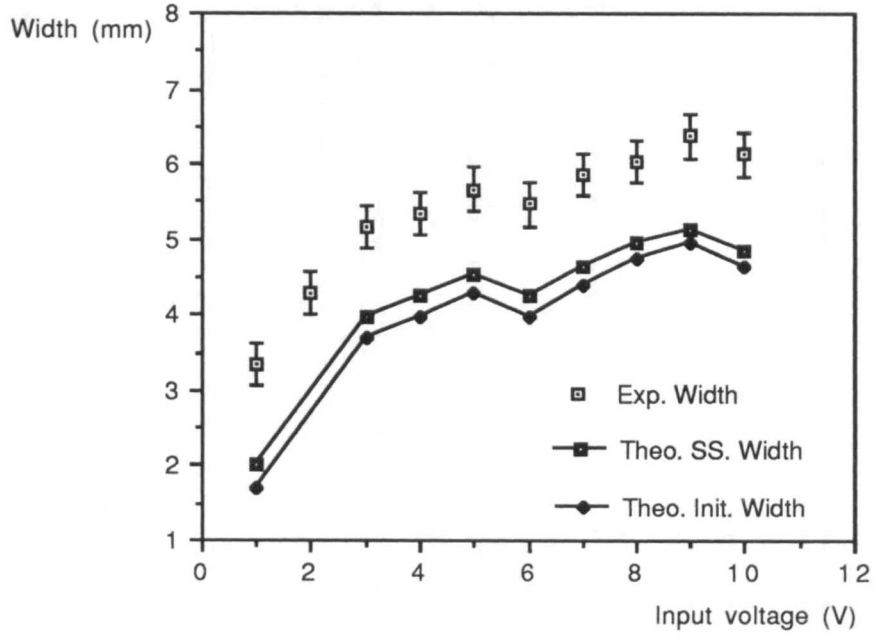

Figure 7.16: Theoretical and experimental width as a function of input voltage at 200 mm/sec robot speed.

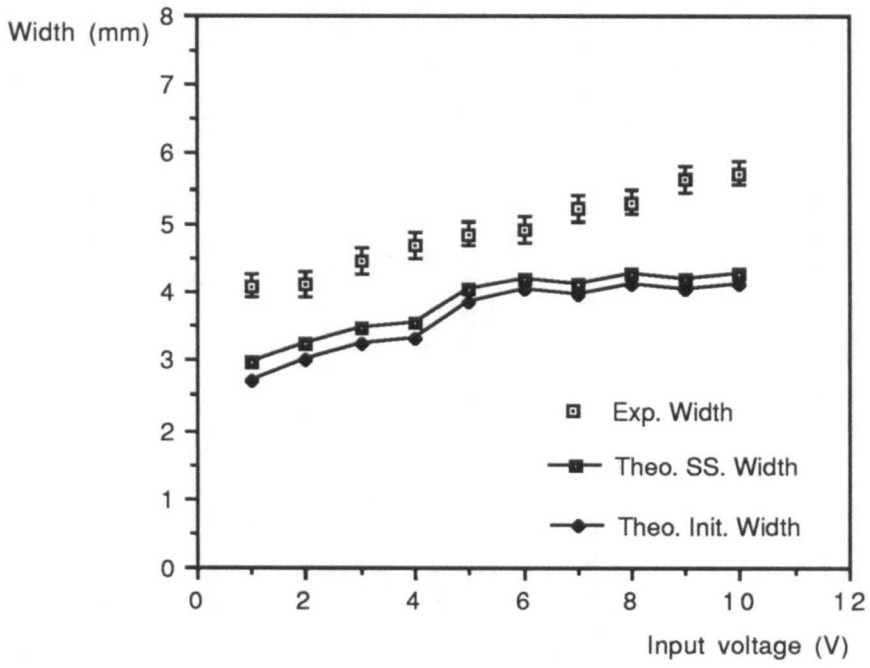

Figure 7.17: Theoretical and experimental width as a function of input voltage at 300 mm/sec robot speed.

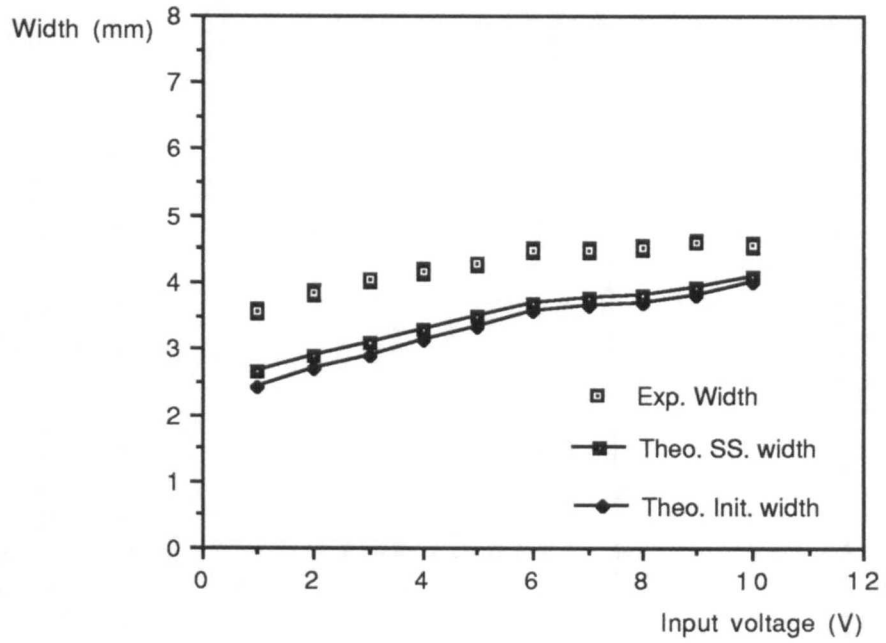

Figure 7.18: Theoretical and experimental width as a function of input voltage at 400 mm/sec robot speed.

CHAPTER VIII

HIERARCHICAL CONTROL

8.1 Overall Process Control

The supervision of industrial processes has been a subject of significant development due to increasing demands on reliability and automation. Most supervisory controllers are based on heuristic knowledge. A typical industrial cell such as for automated adhesives and sealants dispensing is made up of a number of processes linked by material, energy and information flows. The automated cell has an overall set of control aims that are to some extent dependent on external factors.

To have a realistic and robust total control scheme, the overall control cell has to be decomposed into subsystems. Each subsystem control is performed according to different criteria such as between the system, location, relative time scale or combination of those criteria. Since the automated dispensing process is a real-time system, the automated cell is decomposed into activities based on the time scale criteria and the information flow between the component parts of the cell.

8.2 Muti-Level Control

The process knowledge is the major factor of the process automation. Sensors are key elements of the process control system to provide the information about the state of the process. The automated adhesives & sealants dispensing processes are provided with sensors for the important process variables such as opening of the gun, pressure in the gun and pressure in the hose. The measured signals are converted to electrical signals using transducers. Desired control actions are determined by information processing of the measured signals, and control actions are communicated, converted and sent to actuators.

The variables effecting the dispensing process were discussed in detail in (§ 5.2). These variables can be categorised as sets of controllable and uncontrollable variables. The controllable variables are: robot speed, table speed, nozzle size, opening of the gun, on-line temperature, pump pressure, nozzle pressure gain and PI controller gains. These

variables can be controlled during a run or from run to run. The uncontrollable variables are: adhesive age, surface tension, ambient temperature and relative humidity. The adhesive age can be monitored by the operator checking the expiry date. The effect of surface tension is small. Drifts in the ambient temperature can be compensated by heating the component to always ensure it is at a consistent temperature above ambient. There are other factors such as adhesive viscosity and adhesive shear rate which cannot be measured on-line, but they are functions of temperature and can be kept constant during a run.

The control scheme is given in Fig. (8.1). The overall control can be decomposed into different levels as follow:

i) Control during the run: this is a low level controller and is achieved by using a conventional controller such as a PI controller with a time scale in the range of msec. The low level controller is successful for gradual changes. A well designed path trajectory is required during the run. In this level the amount of the initial gun opening is obtained based on the desired dispensed bead using the calibration curve of bead width as a function of the gun opening. The controller gains are then determined according to the process model, time delay and the robot speed. The exact model of the process is not required since a PI controller is not very sensitive to the process model (see Ch. 5 for further detail).

The robot path trajectory is generally defined by a range of taught positions along a desired path, called nodes. The robot speed and the bead dimension are usually variable for a given component such as a car door. Thus, the low level controller has to be initialised if, for a given location, the desired bead size or the robot speed is changed. For some applications such as applying adhesive around a car door or applying sealant along the edge of a windscreen, the bead width needs to be decreased considerably in the corner. Furthermore, the robot speed has to be lowered to achieve good trajectory path tracking of the vision system. This can be achieved by using rule-based system along with a PI controller as follows:

i-a) define the desired bead width and the robot speed at each node along a path trajectory for a given workpiece
i-b) input the control gains at different robot speeds
i-c) input the equation of the bead width as a function of the opening of the gun
i-d) calculate the amount of opening of the gun and the proper control gains based on condition (i-a).
i-e) take into account the transport delay in the dispensing process for a given robot speed.

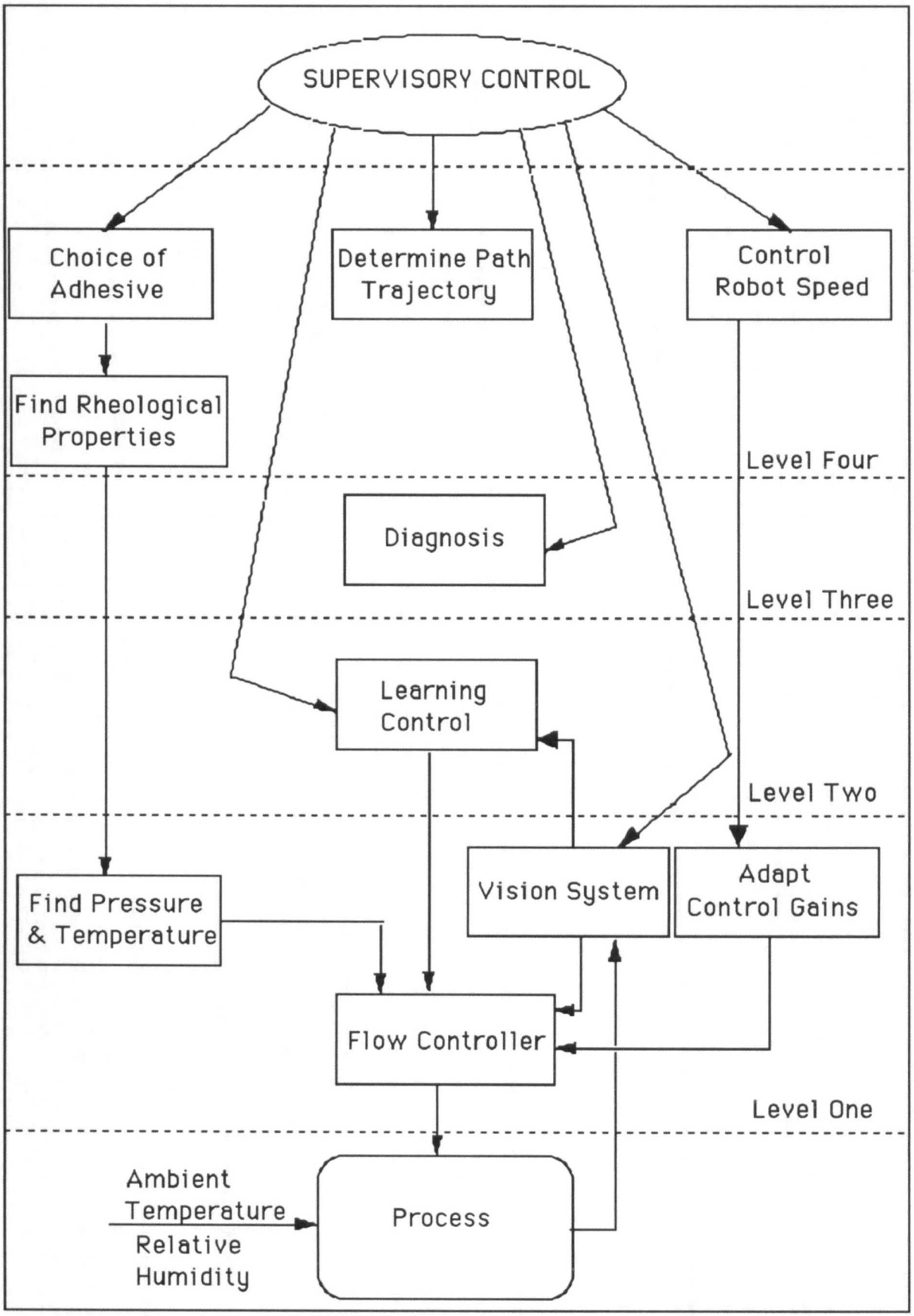

Figure 8.1: Muti-level control scheme.

i-f) initialise the controller algorithm if the size of the desired bead width or the robot speed has been changed at a new node

i-g) apply control algorithm

i-h) calculate the new input

i-i) convert the new input based on the robot speed

i-j) modify the flow rate

i-k) repeat from step (i-d) if the robot speed or the bead width is changed.

ii) Control within the runs: this is the second level of control and is a learning control. The time scale of this section is in minutes. This is basically position adjustment of the step changes of bead if it is not placed in a proper position. This is achieved by running the robot around the desired trajectory so the system estimates the time at which the opening of the gun should be adjusted and when the changes actually occur. Information about the desired time is acquired from the robot, and information about the time when this really happened, is obtained by vision system while laying a bead. Since the camera is trailing the nozzle tip, the vision system will see a delayed image of the dispensed bead. The robot time is calculated based on the distance of the camera from the dispensing nozzle tip and the robot speed. These results are compared with the timing made by the vision and any discrepancy in the times is corrected by updating the node timing in the controller. Thus, the subsequent beads are laid with step changes at the right location. This is shown in Figs (8.2) and (8.3) with a series of parallel adhesive bead, where the step change position has been corrected by using learning control in four runs. The first strip represents the initial dispensed bead and the subsequent strips are using learning control and previous strip information. The second strip shows an over-compensation. The third strip pulls it back a little whilst the fourth pulls it back further and gives the desired result.

iii) Diagnosis: this is the third level of the controller and ensures that the dispensing process runs adequately. If a fault occurs and the fault cannot be solved using on-line control, the diagnosis module is activated. The diagnosis part checks for unexpected faults that might happen in the systems. Some of the possible faults are:

iii-a) discontinuity in bead due to a nozzle blockage.

iii-b) air bubble in the adhesive due to the air in the adhesive container

iii-c) no image was captured due to bad connection or not having a proper lighting

iii-d) no output from the nozzle due to low air pressure in the pump or nozzle size is too small for a given adhesive

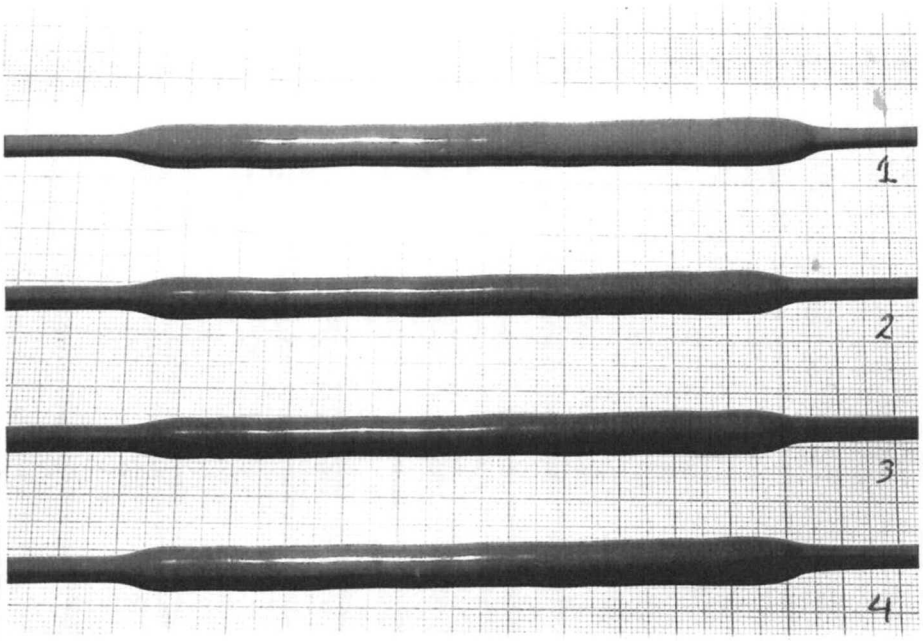

Figure 8.2: The effect of learning control for a step change.

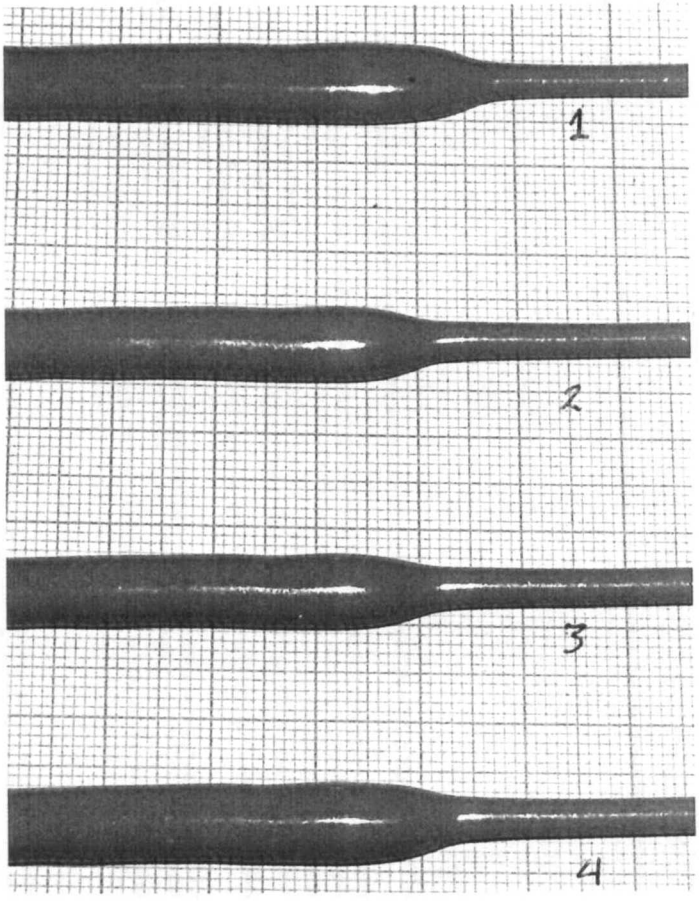

Figure 8.3: The effect of learning control at the beginning of a step change.

iii-e) gun stitching due to high servo gain or the high distance of the nozzle tip from the component surface

iii-f) low flow rat due to the low pump pressure or low temperature

iii-g) slumping in the bead due to low distance of the nozzle tip from the component surface

iii-h) robot does not response due to signalling problem in I/O board or fault in serial communication.

These are some of the faults which might occurs in the dispensing cell. Knowledge from the automated cell operation can be translated into sets of rules in a simple or compound form of *if* and *then* statements such as:

if
the bead width is too narrow and the on-line controller can not function properly
then
check the pump air pressure line
if
it is at maximum, turn up the temperature controller
if
the temperature is at the upper limit for a given adhesive
then
the existing nozzle needs to be replaced with a lager size nozzle.

iv) Set-up phase: this is the fourth level of the controller. The initial system set-up is determined based on the environmental conditions, adhesive characteristics and the desired output. This can be achieved using rheological properties of the dispensing adhesive flow (see Chs. 6 & 7 for further detail). The system set-up consists of two parts: the short term set-up and the long term set-up.

iv-a) In the short term set-up, the path trajectory, desired bead dimension and robot speed are required. The adhesive or sealant materials are unchanged in this part. Path trajectory can be designed either by teaching the points along the path using the teach pendant of the robot or using a standard CAD package to specify the coordinates. The coordinate information is then sent to the robot controller using the RS-332 serial port. Based on the robot speed and the desired bead width at each point along the path trajectory, the initial

set-up for pressure and temperature of the dispensing adhesive can be obtained using rheological information of the given adhesive from a data-base (see chapters 6 & 7 for further detail).

iv-b) The long term set-up involves the change of adhesive or sealant which does not happen very often. The rheological properties of the new adhesive has then to be obtained and included in the data-base if it does not already exist. The step (iv-a) is then repeated. In some cases when the switch has made from an adhesive or sealant with low viscosity to a very viscous adhesive, the nozzle and gun orifice might need to be replaced as well with a larger one.

8.3 Process Parameters

The adaptation of the parameters influencing the dispensing process occurs in a wide range of time scales. The effects of the system variables on the bead parameters with their time scales are given in Figs. (8.4a) & (8.4b). The knowledge from this figure can be translated into rules and can be used to recover the faults in the automated cell.

Pressure delivery and temperature act in the same way. An increase in pressure or temperature results in an increase in the adhesive flow rate. When changing the pressure the transient duration is relatively short. On the other hand, changes in temperature are not so quick. The case of lowering the temperature is particularly difficult and the system needs to be purged to empty the hot adhesive in the hose. Thus, for relatively short term changes of the maximum desired flow rate, pressure should be modified and the temperature be kept constant. Temperature changes can be used as a long term parameter to obtain the maximum flow rate.

The nozzle size and the gun orifice size have also a major effects on the material delivery. Since for changing these parts, the system need to be shut down, it is not feasible for short term adaptation. Furthermore, if the nozzle has to be replaced for a given material, the initial material set-up then has to be modified. However, the nozzle size is usually kept constant for a given adhesive or sealant.

The rule-based system representation was considered for different levels of intelligent control. The rule-based controllers are usually useful for the control of complex process. Rules are a simple way to represent knowledge of the adhesive dispensing process. The rules used at levels one and two are in the form of *forward chaining* and is the most appropriate since:

i) ample data from the sensors may be assumed,
ii) there is a small number of possible actions the need to be taken,
iii) it is very simple to implement.

In the rule-based system, the rules are represented in the form of *if* (the antecedent) and *then* (the consequent) statement.

In the higher levels of the supervisory controller such as diagnosis, the *backward chaining* regimes might be needed in order to ensure that the data was used efficiently to reason about the required goals.

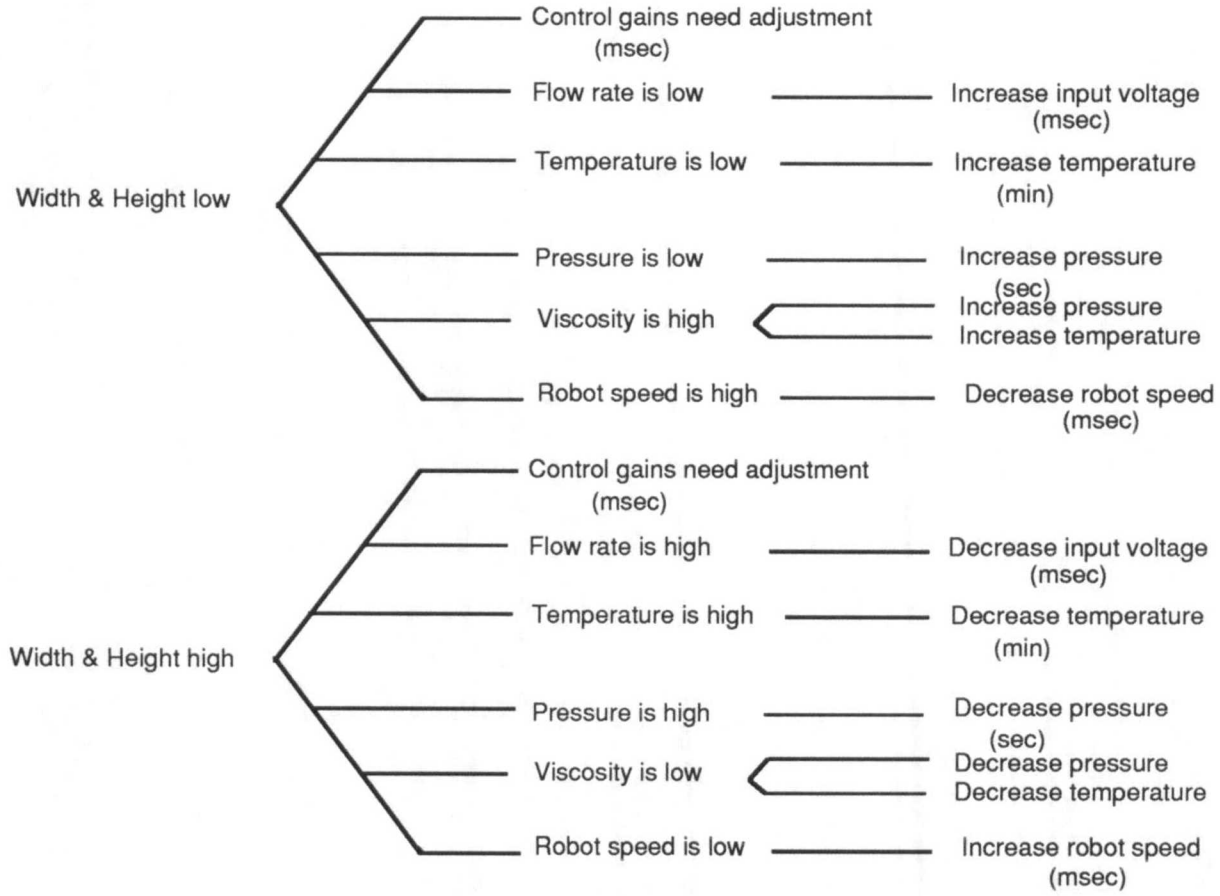

Figure (8.4a): Variation of the bead parameters as a function of system variables.

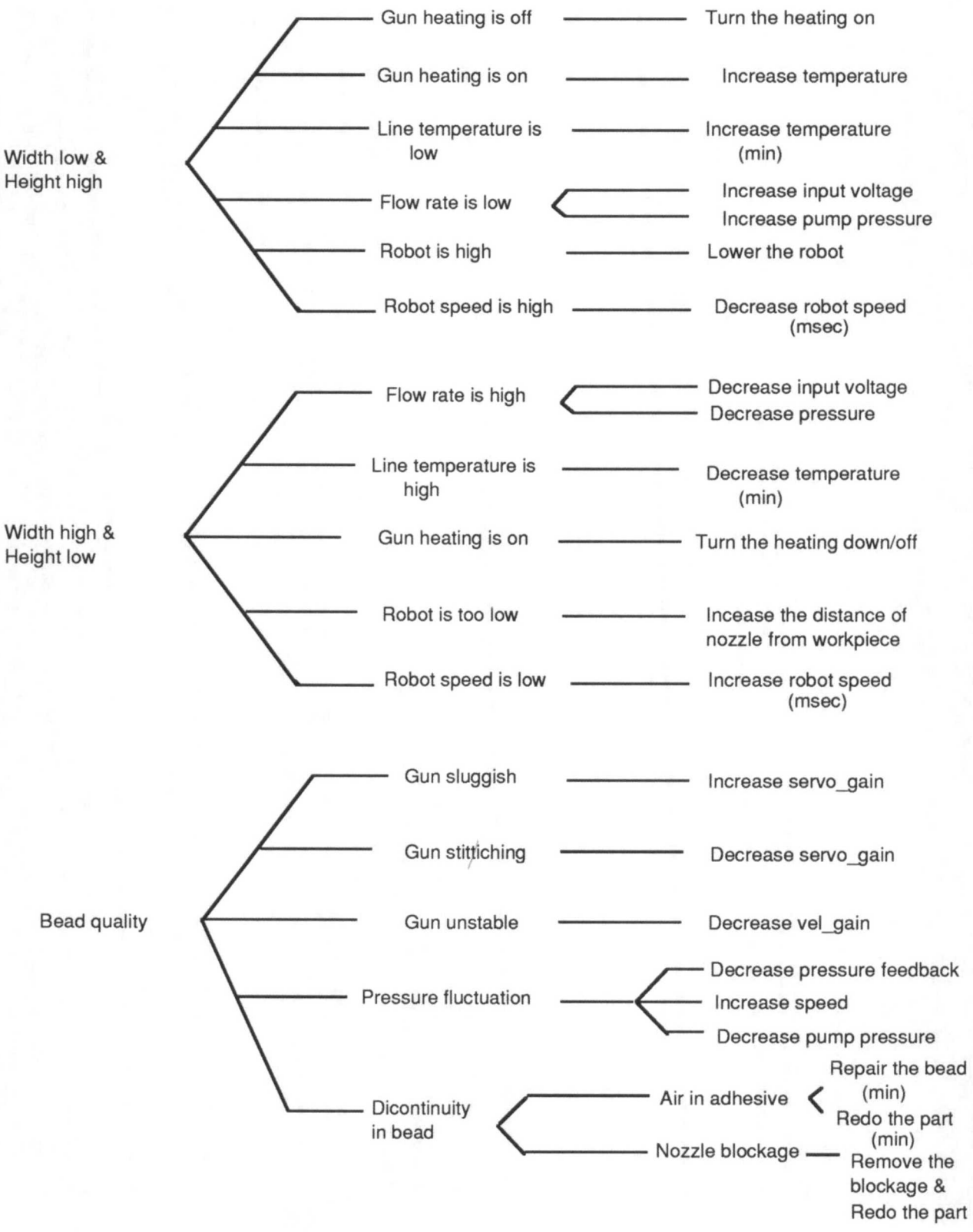

Note: The nozzle size is considered to be constant
& the environmental effects are not considered.

Figure (8.4b): Variation of the bead parameters as a function of system variables.

8.4 Knowledge Elicitation

Knowledge acquisition is required to provide logical, control and interface specifications. There are several levels of knowledge elicitation which need to be considered.

i) The knowledge required for diagnostic and environmental factors is:

i-a) the performance of the robot and the single axis table to achieve a desired trajectory.

i-b) fault detection which may be caused by a nozzle blockage.

i-c) temperature and pressure setting for the adhesive dispenser, hose and high pressure pump.

i-d) temperature and relative humidity of the environment.

i-e) determination of the vision coordinates.

ii) The knowledge required on a day to day basis or in between shifts, which will be part of the diagnosis, is:

ii-a) the change of the adhesive characteristics (based on environmental factors).

ii-b) the effect of temperature on the adhesive.

ii-c) the age of the adhesive.

iii) The knowledge required on a run to run basis is:

iii-a) information about the bead size which is obtained by the vision system.

iii-b) the necessary time correction of node position (i.e. where changes in the bead width takes place) for the subsequent run.

iii-c) discontinuity in the adhesive bead.

iii-d) modification to the adhesive path.

iv) The required knowledge during the run is:

iv-a) how to change the flow rate based on desired parameters and using a PI controller.

iv-b) initial flow rate set-up based on the desired bead parameters and robot speed.

8.5 Conclusion

The adaptation of the dispensing process occurs over a wide range of time scales. Thus, the hierarchy supervisory controller has been decomposed into subsystems. The effects of the system variables on the bead parameters with their time scales have been determined. To have a fully automated adhesive dispensing cell, the use of a knowledge based system for different levels of control is appropriate. The KBS can be used along with a conventional controller to achieve a better deposited bead quality which is essential for structural bonding. The KBS is used on a run to run basis during the dispensing process to modify the node position. The KBS can also be used at a supervisory level for system set-up and for cell diagnosis.

CHAPTER IX

CONCLUSION AND FUTURE WORK

9.1 Summary of the Thesis

The aim of this research, as stated in Ch. 1, was the automation of the adhesive and sealant dispensing system. This includes general hardware design and construction, software design and realisation, material modelling, and the development of sensing and control techniques.

An overview has been presented of the existing state of dispensing processes for adhesives and sealants in the current industry. The advantages and disadvantages of using automation systems for adhesives and sealants have also been covered. The use of a vision system for on-line quality inspection has been argued.

An automated manufacturing cell has been developed for dispensing beads of adhesive and sealants using on-line control. Although on-line quality inspection has previously been used for the slower process such as arc welding, this is the first time that the concept of a closed loop system has been introduced for adhesives and sealants dispensing. A structured vision system was developed for on-line inspection of the adhesive and sealant dispensing process. The robot controller, vision system and the dispensing flow controller have been integrated together. Information is sent between different components in the cell using RS232C serial port, input/output digital and analogue signals. The on-line inspection of the process requires continuous measurement of the adhesive and sealant parameters (i.e. width and height). This information was then fed to an on-line control facility to ensure that the bead is maintained within the desired tolerance range.

The automated adhesive dispensing process was modelled using a lumped parameter dynamic system with a long time delay which depends on the operating conditions. The variation of the time delay was modelled as a function of the robot speed. Different types of conventional controllers (e.g. proportional, integral and PI) and Smith's predictor were used for simulation of the process, and the optimum gains were obtained.

The robustness of the on-line controller system is an important criterion which must be taken into account. Robustness can be for either stability or performance of the process. The process should be controlled if the process model is not exact or changes in the environmental conditions occur. The main reason for the wide usage of PI controllers is their excellent robustness. The trade-off between performance and robustness is most evident for the process with time delay. For the processes with time delay, any mismatches between the process model and the actual processes can be disastrous and can lead to a serious instability problem. Although the Smith's predictor response is faster than a PI controller, it is very sensitive to the process modelling. Thus, the PI controller was realised and implemented for the process.

The rheological model of the adhesive was obtained using a power law expression. This model is generic and is based on the experimental data. It can be used for different types of adhesive where the elastic effects are small, by using the experimental data of shear stress as a function of rotational speed at different temperatures. By having the power law expression, the flow rate through the nozzle can be calculated by using the power law exponent and coefficient.

The nozzle flow rate and deposited bead thickness was obtained theoretically by using the geometrical data and adhesive power law expression. These results can be used for the initial set-up of the system and as an aspect of diagnosis when using a knowledge-based expert system. Using this approach it is possible to achieve an "almost right first time" setting for viscous adhesive and sealant dispensing thus avoiding the long and costly series of ad-hoc adjustments that would otherwise be required.

The first and second level of the supervisory controller have been implemented. These are a series of rule-based control algorithms for control gain correction for a PI controller and node position adjustment using a learning algorithm.

9.2 General Conclusion

The quality of bead deposition is defined in terms of the consistency of the dispensed bead. This involves both the amount of material and its placement. The consistency of the bead size and its accurate placement are the most important factors in the performance of structural joints. The dispensing process should be designed to produce a consistent and uniform bead regardless of variation in the environment. The quality of the adhesive bead is affected by those parameters which vary continually such as pressure, viscosity, shear rate

and temperature. These variations have an affect on the flow rate and subsequently on the adhesive bead parameters.

The dispensing of adhesives and sealants encompasses many dynamic factors that are changing constantly. To design an automated system for the dispensing of adhesives and sealants two major factors need to be considered for different levels of the cell control and bead inspection: robustness and the real time constraint. The automated dispensing facility was gradually modified to optimise the performance and minimise the time delays between the changes demanded from the robot controller and the implementation of the modified bead on the workpiece.

Vision robustness and performance are vital for the on-line controller since the vision has been used as an observer. The sampling time in the process is fixed and is based on the vision processing. Efforts have been made to increase the vision processing speed without adversely affecting its robustness. As a result, the vision processing time was reduced to 60 msec. Further reduction in image processing time is beneficial for on-line control as long as robustness stays intact.

To have a constant flow of information between the cell components, a full integration of the cell was necessary. This can be achieved using input/output, analogue signals, A/D board and serial communication between the cell components. This also has the advantage of lowering the time delay in the control loop (see Ch. 4 for further detail). The cell integration is also required for overall cell supervisory control .

The process time delays were identified and were shortened by modification of the vision set-up and by lowering the vision software processing time. This is an important factor in control design. The processes with lower transport lags are usually easier to control. However, in the dispensing of adhesives and sealants, there is a trade-off between a lower transport lag and accuracy of the captured image. The transport lag between the camera and the nozzle tip is needed to allow the dispensed material to settle. This is the main reason the vision bracket was designed in such a way as to have a minimum transport lag between vision and the dispensed nozzle tip with a robust image processing.

For PI controller design, process modelling is necessary. The dispensing process was analysed as a single, lumped-parameter dynamic with a pure time delay which is a function of the operating condition. Using a PI controller, the process with time delay does not perform as well as a process without a time delay, since the delay introduces an additional phase shift in the closed loop and tends to destabilize the closed-loop process. Thus the controller gain has to be reduced which makes the process response slower. The Smith's

predictor has a faster response than the PI controller but is very sensitive to the process modelling.

The predominant use of a conventional controller such as a PI controller in process control stems from its robustness. Even cases of processes with significant time transport delay, where methods such as Smith's predictor could provide a better response, the PI controller is preferred because of the potential sensitivity to model mismatch of the Smith predictor. The major disadvantage of PI control is that the resulting system is relatively slow.

One implication for on-line control of the length of time taken to adapt the bead parameters is that this technique is better for dealing with gradual changes in parameters, such as those occurring when the temperature of the factory gradually increases and leads to a decrease in viscosity of the adhesive. In such circumstances, the bead can be modified effectively to stay within the prescribed tolerances. The technique is much less suited to step changes in dispensing, such as those occurring when small air bubbles or particles temporarily block the flow. Even if the vision system should happen to detect the event, the chances are that the flow is already back to normal before the dispenser can be adapted. The best technique for these *step-discontinuities* appears to be the use of post-process inspection, using an automated vision system.

An alternative strategy is to change the speed of the robot, rather than the dispensing rate of the gun, as the robot has a quicker response time. However, because the robot must slow down at corners to achieve good position control this is a less preferable option. Also if the robot speed is too high on corners, the camera may not have time to scan the bead at all on the corner. When the robot slows at a corner, the dispensing gun must also cut its flow. This implies either a very fast changing gun, a very slow robot speed, or else the use of prior knowledge of the speed patterns so that the delays in the gun opening can be taken into account by changing the gun opening well ahead of the time where a bead change is required. In practice, a combination of all three aspects is necessary for optimal results.

The rheological model of the adhesive obtained in this work can be used for different types of adhesives with similar rheological characteristics where the elastic effects are small. The flow rate through the gun and the nozzle can subsequently be calculated by using the power-law exponent and power-law coefficient. Furthermore, the deposited bead thickness can be obtained theoretically using analytical flow rate. The elastic effects for this type of adhesive were observed to be small due to low swelling effects. Thus, the pressure drop in the nozzle was assumed to be negligible. This is not the case for all types of adhesives. For highly visco-elastic materials, elastic effects need to be considered. Furthermore, the slip boundary condition was neglected since the study of the detailed migration of material

molecules was not the purpose of this work. These result can be used for the initial set-up of the system and as an aspect of diagnosis when using a knowledge-based expert system.

The overall control levels were decomposed in different subsystems for a better control of the whole cell. For a fully automated cell, a rule-based system needs to be used during the run, within the runs, for initial set-up and for diagnosis. The rule-based method is considered to be a simple way to represent knowledge of complex processes such as adhesives and sealants dispensing.

9.3 Recommendation for Future Work

The following work is suggested here in different parts of the project for further development:

i) Material modelling

i-a) Investigate the material modelling further by taking into account elasticity effects.
i-b) Use different modelling method such as a Sisko model [Bird 87] for the adhesive for comparison with power-law expression..
i-c) Try different types of adhesives or sealants for the automated cell and use the analysis obtained in chapters 6 and 7.

ii) On-line inspection & control

ii-a) Investigate ways to improve the vision-algorithm processing time using alternative vision hardware.
ii-b) Redesign the vision bracket using a lighter material such as carbon fibre, and put the camera and the laser diode in the compact compartment.
ii-c) Investigate the use of on-line vision inspection for three dimensional surfaces.
ii-d) Improve the control-algorithm performance using different types of controller such as an adaptive controller.
ii-e) Investigate the use of a rule-based controller instead of the PI controller.
ii-f) Investigate ways to reduce the transport lags in the process.
ii-g) Investigate dispensing control strategy for three dimensional components, particularly where corners are used that make access difficult for the dispensing gun and the vision system.

iii) Supervisory control

iii-a) Investigate different AI methods, such as fuzzy logic and neural networks for the supervisory controller.

iii-b) Investigate the possibility of applying these methods to other processes with similar characteristics.

REFERENCES

[Anon 84b] Anon, A., "Industry could demonstrate boost adhesive bonding", auto Industry, April 1985, pp. 10.

[Astrom 89] Astrom, K.J., Hang, C.C. and Persson, P., "Towards intelligent PID control", Proc. of the IFAC Workshop of Artificial Intelligence in Real-time Control, 1989, pp. 53-58.

[Astrom 90] Astrom, K.J. and Wittenmark, B., Computer controlled systems, 2nd ed., Prentice-Hall Intr., Inc., Englewood Cliffs, N.J., U.S.A., 1990.

[B.P. Chemicals 87] Speciality coatings adhesives & sealants, material safety data sheet, B.P. Chemicals Ltd., Sully, South Glamorgan CF6 2YU, U.K., 1987.

[Barnes 89] Barnes, H.A., Hutton, J.F. and Walters, K., An introduction to rheology, Elsovier press, Oxford, 1989.

[Batchelor 85] Batchelor, B.G., "Principles of the digital image processing", Automated visual inspection, Ed. B.G. Batchelor, D.A. Hill and D.C. Hodgson, 1985, IFS, U.K.

[Bennett 82] Bennett, S. and Linkens, D.A., Computer control of industrial processes, Peter Peregrinus Ltd., 1982.

[Bird 87] Bird, R.B., Armstrong, R.C., Hassager, O., Dynamics of polymeric liquids, John Wiley & sons Inc., New York, 1987.

[Bolhouse 86] Bolhouse, R.A., Stone, S. M., "Automated seam sealing using machine vision", Proc. of Vision 86 Conf., Detroit, MI, U.S.A., pp. 7.21- 33.

[Anon 84a] Anon, A., "Gantry machine in package deal on gluing', Auto Industry, Nov. 1984, pp. 9.

[Bowles 85] Bowles, P.J. & Garrett, L.W., "Robots for sealing and adhesive applications", Handbook of Industrial Robotics, 1985, pp. 1264-1270.

[BRA 83] British Robotic Association, "Robot Facts 1982", BRA 1983.

[Braggins 86] Braggins, D.W., "Systems integration in commercially available robotic vision systems", Proc. of 6th Intr. Conf. on Robot Vision and Sensory Control, Paris, France, Ed. by M Briot, June 1986, pp. 1-10.

[Bryant 73] Bryant, G.F., Iskenderoglu, E.F., and McClure, C.H., "Design of controllers for time-delay systems", Automation of tandem mills, ed. G.F. Bryant, The Iron and Steel Institute Pub., 1973, pp. 81-106.

[Chandraker 90] Chandraker R., West, A.A., Williams, D.J., "Intelligent control of adhesive dispensing", Intr. J. Computer Integrated Manufacturing, Vol. 3, No. 1, 1990, pp. 24-34.

[Clarke75] Clarke, D.W., Gawthrop, P.J., "Self tuning controllers", Proc. IEE Control & Science, Vol. 122, No., 9, Sept. 1975.

[Clocksin 85] Clocksin, W.F., Bromley, J.S.E. Davey, P.G., Vidler, A.R. and Morgan, C.G., "An implementation of model-based visual feedback for robot arc welding of thin sheet metal", Intr. J. of Robotics Research, Vol. 4, No.1, Spring 1985, pp. 13-26.

[Cohen 85] Cohen, Y. and Metzner, A.B., "Apparent slip flow of polymer solutions", Journal of Rheology, Vol. 29, No. 1, 1985, pp. 67-102.

[Considine 86] Considine, D.M., "Robot technology fundamentals", in the Handbook of industrial automation ed. by D.M. Considine and G.D. considine, Chapman Hall Pub., New York, N.Y., 1986, pp. 262-319.

[Corby 83] Corby, N. R., "Machine vision for robotics", IEEE Trans. on Industrial Electronics, Vol. IE-30, No. 3, Aug. 1983, pp. 282-290.

[Corby 84] Corby, N.R., "Machine vision algorithms for vision guided robotic welding", Proc. 4th Intr. Conf. on Robot Vision and Sensory Technology, London, U.K., 1984, pp. 137-147.

[Critchlow 85] Critchlow, A.J., Introduction to robotics, Macmillan Publishing Company, New York, New York., 1985.

[Davies 90a] Davies, B.L., Razban, A. and Forrest, A.K. "The use of automated system in dispensing adhesive", Proc. of 28th Int. MATADOR Conf. on CIM, FMS and Robotics , Manchester, UK., April 1990.

[Davies 90b] Davies, B.L., Razban, A. and Forrest, "The use of robots and adaptive control in the automated dispensing of adhesives", Plastics and Rubber Institute, 1990, 24/1-4, Proc. of 4th Int. Conf. "Adhesives 90", Cambridge, UK. , Sept. 1990.

[Donoghue 77] Donghue, J.F., "Review of control design approaches for transport delay processes", ISA Transactions, Vol. 16, No.2, 1977, pp. 27-34.

[Dueweke 83] Dueweke, N., "Robotics and adhesive, an overview", Adhesive age, Vol. 26, No. 4, Apr. 1983, pp 11-16.

[Dufour 83] Dufour, M. and Begin, G., "Adaptive robotic welding using a rapid image pre-processor', Proc. of 5th Intr. Conf. on Robot Vision and Sensory Technology, Cambridge, MA., U.S.A., ed. by B. Rooks, 1983, pp. 641-647.

[Efstathiou 93] Efstathiou, J., Davies, B.L., Razban, A. and Harris, S., "Expert systems for an adhesive dispensing robot", Prc. of 6th Int. Conf. on Industrial and Engineering Applications of Artificial Intelligence and Expert Systems, June 1993, Edinburgh, UK.

[Engelberger 80] Engelberger, J.F., Robotics in Practice: Management and application of industrial robots, Kogan Page Ltd. Pub. Company, London, U.K., 1980.

[European Adhesive & Sealants 90] Adhesives and sealants: a business transition, European Adhesive and Sealants, June 1990.

[Fanuc 87] Fanuc Robot S-series, Fanuc Ltd., Japan, 1987.

[Fenner 79] Fenner, R.T., Principles of polymer processing, Macmillan Press Ltd., London, 1979.

[Garcia 82] Garcia, C.E., and Morari, M., "Internal model control - part I. a unifying review and some results", Ind. Chem. Eng. Process Des. Dev., 1982 , pp 308-323.

[Gorecki 89] Gorecki, H., Fuksa, S., Grabowski, P. and Korytowski, Analysis and synthesis of time delay systems, Polish Scientific Pub., John Wiley & Sons, 1989.

[Gonzalez 82] Gonzalez, R.C. and Safabakhsh, R., "Computer vision techniques for industrial applications and robot control", Computer, 1982, Vol. 15, No. 12, pp. 17-32.

[Hagglund 92] Hagglund, T. ," A predictive PI controller for processes with long dead times", IEEE control Systems Magazine, Feb. 1992, pp. 57-60..

[Hang 91] Hang, C.C., Astrom, K.J., Ho, W.K., "Refinements of the Ziegler-Nichols tuning formula", IEE Proceedings-D, Vol. 138, N0.2, 1991, pp. 111-118.

[Hartley 83] Hartley, J., Robots at work, IFS Publications Ltd., U.K., 1983.

[Haung 84] Haung B. and Ruddle, J.L., "Requirements of sealant application robots" Robot 8 Conf. Proceedings, June 84, Detroit, MI, pp 7.1-7.7.

[Hayes 76] Hayes, B.J., Larsen, R., MacDonald, N.C. and Reid, J.E., "The transport industries", Industrial adhesive and sealant, Hutchinson Benham, London, edited by B.S. Jackson, 1976, pp 91-131.

[Hitchen 89] Hitchen, C. and Grieve, R.J., "The automated application of two part epoxy adhesive bead", presented at Structural Adhesives in Engineering II Conf., Bristol, U.K., Sept. 1989.

[Industrial Robot 89a] "The art of bonding", The Industrial Robot, Sept. 89, Vol. 16, No. 3, pp. 135-7.

[Industrial Robot 89b] "Robotic seam sealing into next generation", The Industrial Robot, Sept. 89, Vol. 16, No. 3, pp. 138-42.

[Industrial Robot 92] "Sealing roof panels on escort and orion cars", Industrial Robot, vol. 19, No. 2, 1992, pp. 40.

[Jablonowski 86] Jablonowski, J. and Posely, J.W., "Robotic terminology", Handbook of robotics, pp. 1271.

[Johnson 84] Johnson, R.L., "A robotic solution to liquid sealer application", Robot 8, June 84, pp. 7.8.

[Johnson 84] Johnson, C.D., Microprocessor based process control, Prentice Hall, Inc., Englewood Cliffs, N.J., U.S.A., 84.

[Joyce-Loebl 88] Vision software reference manual, Joyce-Loebl Ltd., Newcastle upon Tyyne, U.K., 1988.

[Kak 85] Kak, A.C., Albus, J.S., "Sensors for intelligent robots", Handbook of industrial robotics, Ed by S.Y. Nof, 1985, pp. 214-230.

[Karel 87a] Karel system reference manual Vol. I, II, Ver. 1.50P. GMF Robotics Corp., Auburn Hills, MI, U.S.A., 1987.

[Karel 87b] Karel language reference manual, Ver 1.50P. GMF Robotics Corp., Auburn Hills, MI, U.S.A., 1987.

[Kelly 85] Kelly, M.P. and Duncan, M.E., "Robots in the automobile industry", Handbook of industrial robotics, edited by Nof, 1985.

[Kuo 1975] Kuo, B., "Automatic control systems, 3rd edition, Prentice Hall, Englewood Cliffs, N.J., 1975.

[Lawley 87] Lawely, E.D., "Adhesives in the automotive Industry", Industrial applications of adhesive bonding, Elesevier Applied Science publishers, London, ed. by M.M. Sadek, 1987, PP 94-95.

[Leeds 89] Leeds, W.A., Adhesives and the engineer, published by Mech. Eng. Pub. Ltd., London 1989.

[Leigh 85] Leigh, j.R., Applied digital control, Prentice Hall International, U.K., Ltd., London, U.K., 1985.

[Ljung 87] 7) Ljung, L., System identification: Theory for the user, Prentice-Hall, Inc. 1987.

[Lodge 64] Lodge, A.S., Elastic liquids, An introductory vector treatment of finite-strain polymer rheology, Academic Press, London, 1964.

[Loughlin 89] Loughlin, C., "Tutorial: line scan cameras", Sensor Review, Vol. 9, No. 4, 1989, pp. 195-202.

[Ludbrook 84] Ludbrook, B.D., "Liquid polybutadience adhesives, Int. J. Adhesion and Adhesives, Vol. 4, No. 4, Oct. 1984.

[Ludbrook 85] Ludbrook, B.D, "The influence of robots on the future use of adhesives in the automotive industry", Proc. of 2nd Int. Conf. of Robots in automotive Industries 15-17 May 1985, Birmingham, UK.

[Luyben 85] Luyben, W.L., Process modelling, simulation, and control for chemical engineers, McGraw-Hill Pub., New York, 1985.

[Malek-Zvarei 87] Malek-Zvarei, M, Jamshidi, M, Time-delay systems, optimizations and applications, North-Holland Pub., Amsterdam, 1987.

[Marechal 91] Marechal, T., Theoretical model of an automated adhesive dispensing system", MSc. Thesis, Imperial college, 1991.

[Marshall 79] Marshall, J.E., Control of time delay systems, peter Peregrinus Ltd., 1979.

[Marshall 81] Marshall, J.E. Cholar, A., Glanhad, B., "Survey of time delay systems control methods", Proc. of Inter. Conf. on Control and its Applications, March 1981.

[McGinnis 91] McGinnis, K. and Beham, G., "Hand-held dispensing equipment reduces waste and saves costs", Adhesives Age, Oct. 91, pp. 18-19.

[Mckelvey 62] McKelvey, J.M, Polymer processing, John Wiley & sons Inc., New York, 1962.

[Middleman 77] Middleman, S., Fundamentals of polymer processing, McGraw Hill Company, New York, 1977.

[Minter 88] Minter, B.J. and DG Fisher, D.G., "A comparison of adaptive controllers: academic vs industrial", Proc. of American control conference, 1988, pp. 1653-58.

[Mooney 31] Mooney, M., "Explicit formulas for slip and fluidity", Journal of Rheology, Vol. 2, No. 2, 1931, pp. 210-222.

[Morari 89] Morari, M. and Zafiriou E., Robust process control, Prentice Hall International, U.K., Ltd., London, U.K., 1989.

[Nayak 89] Nayak, N. and Roy, A., "An integrated system for intelligent seam tracking in robotic welding", Part I & II, Proc. of IEEE Intr. Conf. on Robotics and Automation, May 1989, Cincinnati, Ohio, U.S.A., pp. 1892-7 & 1898-1903.

[Nordson 90] Pro-Flo Microprocessor Controller, Manual no. 42-43, Nordson Corp., U.S.A., Pub. P/N 108 068, April 90.

[Pilarski 84] Pilarski, R.J., "Robotic adhesive Dispensing bonding and Sealing", Journal of Robotics Today, Vol. 6, No. 5, Oct. 1984, pp 35-37.

[Politi 90] Politi, R.E., "Structural adhesives in the aerospace industry", Handbook of Adhesives, Third Edition, edited by I. Skerit, Von Nostrand Reinhold, New York, New York, 1990, pp. 713-728.

[Preedy 85] Preedy, J.E., Burchall S.P. and Ioannou , A., "Robotics - the potential to automate adhesive bonding', Proc. 1985 ASE Conf., London, UK.

[Rauwendaal 86] Rauwendaal, C., Polymer Extrusion, Hanser Pub., 1986.

[Razban 91a] Razban, A. and Davies, B.L., "An automated system for dispensing adhesives", Int. Journal of Adhesion and Adhesives, Vol. 11, No. 3, July 1991.

[Razban 91b] Razban, A., Sezgin, O.S. and Davies, B.L., "Real time control of automated adhesive dispensing", Proc. of IEE, Third Int. Conf. on Software Engineering for Real Time Systems, Cirencester, UK., Sept. 1991.

[Razban 91c] Razban, A. and Davies, B.L, "On-line control of a manufacturing cell using visual inspection", Int. Journal of Computer Integrated Manufacturing, Vol. 4, No. 5, Sept.-Oct. 1991.

[Razban 92] Razban, A., Bryant G.F. and Davies, B.L., " Dynamic modelling and control simulation of automatically dispensed adhesive beads", Proc. of IEEE Int. Conf. on Industrial Electronics, Control, and Instrumentation, Nov., 1992, San Diego, California, U.S.A.

[Razban 93] Razban, A., Davies, B.L. and Bryant, G.F., "Control aspects of adhesive dispensing cell", Proc. of 12th World Congress Intr. Federation of Automatic Control, July 93, Sydney, Australia.

[Razban 94] Razban, A. and Davies, B.L." Analytical modelling of materials for dispensing ", has been accepted for publication in the Intr. Journal of Adhesion Science and Technology.

[Robin 88] Robin, J. Cockett, B., " Aspects of expert systems", Advanced Computing Concepts and Techniques in Control Engineering, 1988, pp 3-30.

[Ross 77] Ross, C.W., "Evaluation of controllers for dead time processes", ISA Transactions, Vol. 16, No.3, 1977, pp. 25-34.

[Sawano 84] Sawano ,S., Ikeda , J., Utsumi, N., Ohtani, Y., Kikuchi ,A., Ito, Y, Kiba, H., "A sealing robot system with visual seam tracking." Robotica, Vol. 2, pp. 41-46,1984.

[Scafe 88] Scafe, A.P, "Robotic sealant and adhesive systems", Proc. of Robot 12 and Vision 88 Conf., Detroit, MI, U.S.A., 5-9 June 88, pp. 6.33-39.

[Scheidle 90] Scheidle, B., "Structural adhesives and the car", European Adhesives and Sealants, March 1990, pp. 18, 36.

[Schmitt 86] Schmitt, L.A., Gruver, W.A. and Ansari, A., "A robot vision system based on two dimensional object oriented models", IEEE Trans. Sys. Man., Vol. 16, No. 4, 1986.

[Schrieber 84] Schrieber, R.R., "Applying sealants with robots at Pontiac", Robotics Today, Oct 84, pp. 42.

[Schwarzenbach 92] Schwarzenbach, J. and Gill, K.F., System modelling and control, E. Arnold Pub., London, 92.

[Sezgin 93] Sezgin, O.S., "Automated inspection methods for robotic adhesive and sealant dispensing processes", Ph. D. Thesis, Imperial College, April 1993.

[Skeist 90] Skeist, I and Miron, J, "Introduction to adhesives", Handbook of adhesives, 3rd edition, Edited by I. Sekerist, Van Nostrand publishers, New York, 1990, pp. 3 - 20.

[Smith 58] Smith, O.J.M., Feedback control systems, New York, McGraw-Hill, 1958, pp. 299-347.

[Smyth 87] Smyth, B.E., "Fourier analysis and its application to machine vision", Proc. of Vision 87 Conf., June 1987.

[Tadmor 79] Tadmor, Z. and Gogos, C.G., Principles of polymer processing, Wiley, New York, 1979.

[Takahashi 69] Takahashi, y., Rabins, M.J., Auslander, D.M., Control and dynamic systems, Reading, MA, Addison-Wesley Pub., 1969, pp. 343-350.

[Teagle 85] Teagle, P.R., Recent advances in mechanical impedance analysis instrumentation for the evaluation of adhesive bonded & composite structures", Proc. of ASE 85, pp. 120-157.

[Toda 80] Toda, H. and Masaki, I, "Kawasaki vision system - model 79A", Proc. Intr. symposium on Industrial Robots, 10th Intr. Conf. on Industrial Robots, Italy, 1980, pp. 163 - 174.

[Tucker 89] Tucker III, C.L., Fundamental of computer modeling for polymer processing, Hanser publishers, New York, 1989.

[Turner 90] Turner, H., Robotics Dispensing of sealants and adhesives, Handbook of adhesives, 3rd edition, Edited by I. Sekerist, Van Nostrand publishers, New York, 1990, pp. 743-756.

[Van Wazer 63] Van Wazer, J.K., Lyons, J.W, Kim, K.Y. and Colwell, R.E., Viscosity and flow measurement: A laboratory handbook of rheology, Noter science publishers, New York, 1963.

[Warwick 86] Warwick, K, Industrial digital control systems, ed. K. Warwick and D.Rees, Peter Peregrinus Ltd, Exeter, U.K., 1986.

[Webb 88] Webb, G. and Wehmeyer, K.R., "Real-time robot guidance using visual contour matching techniques", Proc. of Robot 12 & Vision 88, Detroit, MI, U.S.A., June 1988, pp. 14.19 - 30.

[Wilkinson 60] Wilinkson, W.L., Non-Newtonian fluids, fluid Mechanics, mixing and heat transfer, Pergamon Press, 1960.

[Yilmazer 89] Yilmazer, U. and Kalyon, D.M., "Slip effects in capillary and parallel disk torsional flows of highly filled suspensions", Journal of Rheology, 1989, Vol. 33, No. 8, pp. 1197-1212.

[Zaber 90] Zaber, R., The evaluation of material conditioning to a technology, SAE technical paper series no. 90075, 1990.

[Ziegler 43] Ziegler, J.G. & Nichols, N.B., "Optimum setting for automatic controllers", Trans. ASME 65, 1943, pp. 433-444.

APPENDIX I

JOYCE LOEBL VISION SOFTWARE

I.1 Required Procedures

From the procedures available in IVGENIAL, the main areas of interest for adhesive dispensing bead inspection are image acquisition, thresholding, object detection and object measurements.

In the next sections, the basic principles of the Joyce Loebl software for use in the above tasks are discussed.

I.2 Image Representation

The image can be represented as a grey image (real image), (where every pixel has grey value (0 to 63) and 0=black, 63=white) or binary image (thresholding image), (where every pixel is either 0=black, or 63=white). The binary image occupies one frame while the grey image takes 6 frames space. Thus, each RAM can store one grey image and two binary images. It is therefore, better to use the binary image for real time control since it is faster. The data structure for an image which needs to be defined, is as follows:

```
Image := Record
            Origin      : Point;
            Res         : Integer;
            Lsbit       : Integer; {0..7}
            Nobits      : Integer; {0..8}
            Framenum    :Integer; {0,1,2,3,4}
            Whole       :Pointset;
            End;
```

The image then, will be defined by using the procedure:

DEFIMAGE (image, frame, x-origin, y-origin, resolution, first plane, plane number)

Where

Image is the name of image.

Frame is a number of block of memory which an image resides (0=VRAM, 1,2,3,4=DRAM).

X-origin, Y-origin are the coordinates of the image origin, where point (0,0) is the top left corner of the screen.

Resolution is either "Half" (256x252), "Full" (512x504), or "Double" (1024x1008).

First Plane is the first plane occupied by the image (0-7)

Plane Number is the number of planes occupied by the image
(1=binary image, 6=grey image).

I.3 Image Acquisition

When the image is captured by the camera, the analog signal is fed to an A/D convertor resulting in a 64-grey scale image. The grey image is converted to a binary image by using slicing logic based on threshold values. By setting the threshold values, any input from the convertor being greater than or equal to the lower threshold and less than or equal to the higher threshold will result in an overlay pixel being written into the two overlay planes (6 and 7), thus enabling real time thresholding. Then the digitized image data can either be stored in the "VRAM"and used as a display or produce a live image on the external monitor bypassing the "VRAM" as shown in Fig (I.1).

The required procedures are:

- **Vthresh**, This is used for defining the threshold values, "threshold.min" (low threshold value), and "threshold.max" (high threshold value). These values are between (0-63). The resulting thresholded image occupies planes 6 and 7 of the "VRAM".

- **Photo**, is for capturing an image from the camera by copying its contents to the "VRAM".

- **Live**, This can be used instead of "photo", by bypassing the "VRAM", and sending the image directly to the external monitor.

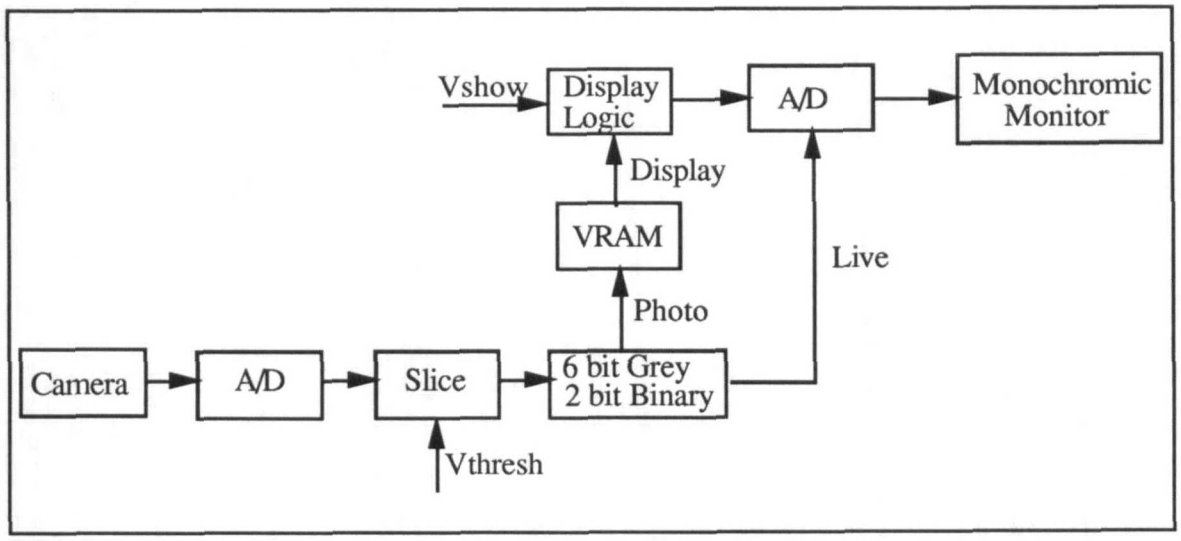

Figure I.1: Image acquisition and display block diagram.

- **Display**, this is used for displaying the contents of the "VRAM" to the external monitor.

- **VSHOW** (greyon, plane6on, plane7on), is for selective display for images stored in "VRAM". The variables are Boolean.

If **Greyon** is true , then the grey image which occupies panes (0-5) of "VRAM" is displayed.

If **Plane6on** or **plane7on** is true, a binary image will be displayed on top of a grey image.

I.4 Thresholding

The two types of thresholding are:

i) Manual, where the low and high values are defined by the user.
ii) Automatic, where the threshold value is obtained from the histogram of the image.

The procedure defining the threshold value is *SLICE*. Manual thresholding is faster which would be more desirable for the real time cases. The values are defined by using threshold.min and threshold.max.

I.5 Pointsets

The pointset is a geometrical description of a part of an image or an object in the image. A pointset can be used for description of either an object in the image or a part of an image. The pointset is good for data reduction and requires less memory than the original image. By assigning a pointset to an object within an image, the operation is focused on the object instead of wasting processing time on the parts of environment which are not desired. Thus, only the relevant parts of the image are processed and the extraction process becomes much faster. The following pointset types (as shown in Fig. I.2) are available in the Joyce Lobel software:

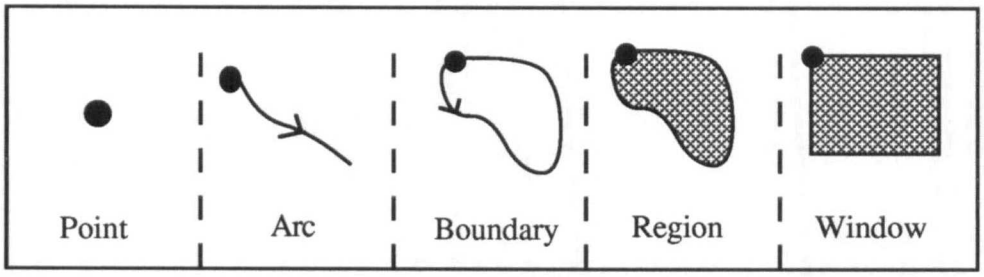

Figure I.2: Types of pointsets in IVGENIAL.

- Point, which has X and Y coordinates of the point and is the simplest pointset.

- Arc, used for curved lines and has X and Y coordinates for each point of the arc.

- Boundary, is for closed curves and has X and Y coordinates for each point of the boundary.

- Region, is for describing the area of closed curves and has X and Y coordinates for each point of the region.

- Window, is for describing the rectangular area of a closed curves. and it has X and Y coordinates of the upper left corner of the window and dimensions of the window (height, width).

The structural form of the pointset is as follow:

```
Pointset := Record
Form            : Psetform;
Origin          : Point;
Wrkpt           : Point;
Xcnt            : Integer;

Case Psetform of
                Pnt:();
                Arc,
                Bndry,
                Rgn : (Npoints      : Integer;
                    Vindex          : Integer;
                    Vorigin         : Integer;
                    Borigin         : Point;
                    Rowmap          : Integer;
                    Wrkvector       : Integer;
                    Vptr            : ads of Vectarray);

                Wndw : (Width       : Windowsize;
                    Height          : Windowsize;
                    Ycnt            : Integer);

End;
```

In the adhesive application, "boundary" (used for object description and is formed by the software through using a procedure) and "window" (defined by the user to limit the portion of the screen for an operation) are used as pointsets. The "window" pointset is defined as follows:

Defwindow (Name, X-origin, Y-origin, Width, Height)
where,

Name is window pointset name
X-origin is X coordinate of the upper left corner of the
Y-origin is Y coordinate of the upper left corner of the
Width is window's width.
Height is Window's height.

I.6 Object Definition

Having defined the pointsets, the object form has to be defined .The Object Definition is the form of the desired objects and are called "Blobs' in "Ivgenial". The definition of the data type is in "Ivtypes" unit which includes the boundary and region description of an object. In boundary Description, the object is represented by 8 vectors (0-7), where zero is pointing to the west and increasing values for vectors going anti-clockwise from there. The region is then formed from the boundary and is stored in "DRAM4".

I.7 Object Detection

After defining an object, the next step is to detect an object on a binary image. The objects can be detected as a blob and with boundary pointset can be represented as a binary image. There are two functions for object detection as follow:

Firstblob (pointset,image, object)

Nextblob (pointset, image, object)

where,

Pointset, is the name of the pointset for search.

Image, is the name of the image defined by the "Defimage" procedure.

Object, is the name of the blob associated with the desired object.

The value of the function is "True", if an object is found within the current setpoint, and is "False", if the end of the setpoint was reached before an object was found. "Firstblob" always starts searching the current pointset from its origin while "Nextblob" resumes searching from the termination point of the previous blob.

After detecting a non isolated white pixel both procedures trace the edge of the blob in an anti-clockwise direction to record the vector list and create a boundary pointset. Having the complete vector list of an object, the image measurements such as width, height, area, perimeter and centre of gravity can be calculated.

APPENDIX II

VISION BRACKET DESIGN

The laser bracket (presented in Fig. II.1) consists of a lightweight aluminium alloy material, bent at an angle of 90 to 180 degrees. Four trapezoids are attached on that angle providing a rigid stand for the laser diode. The surface of the trapezoid that comes in contact with the diode is covered with a thin rubber strip. The laser is held attached to the laser bracket by means of a semi-circular ring attached with two screws to the main bracket.

The dispensing bracket (presented in Fig. II.2) is a single plane that has a longitudinal groove for driving the dispenser vertically on the adhesive surface. The bracket is connected to the front part of the main bracket.

The main bracket (presented in Fig. II.3) is connected to the end-effector of the robot. It has two slots, the first one used for the camera (designed in such a way that only the camera lens can pass through) and the second one used for the laser diode and laser diode bracket.

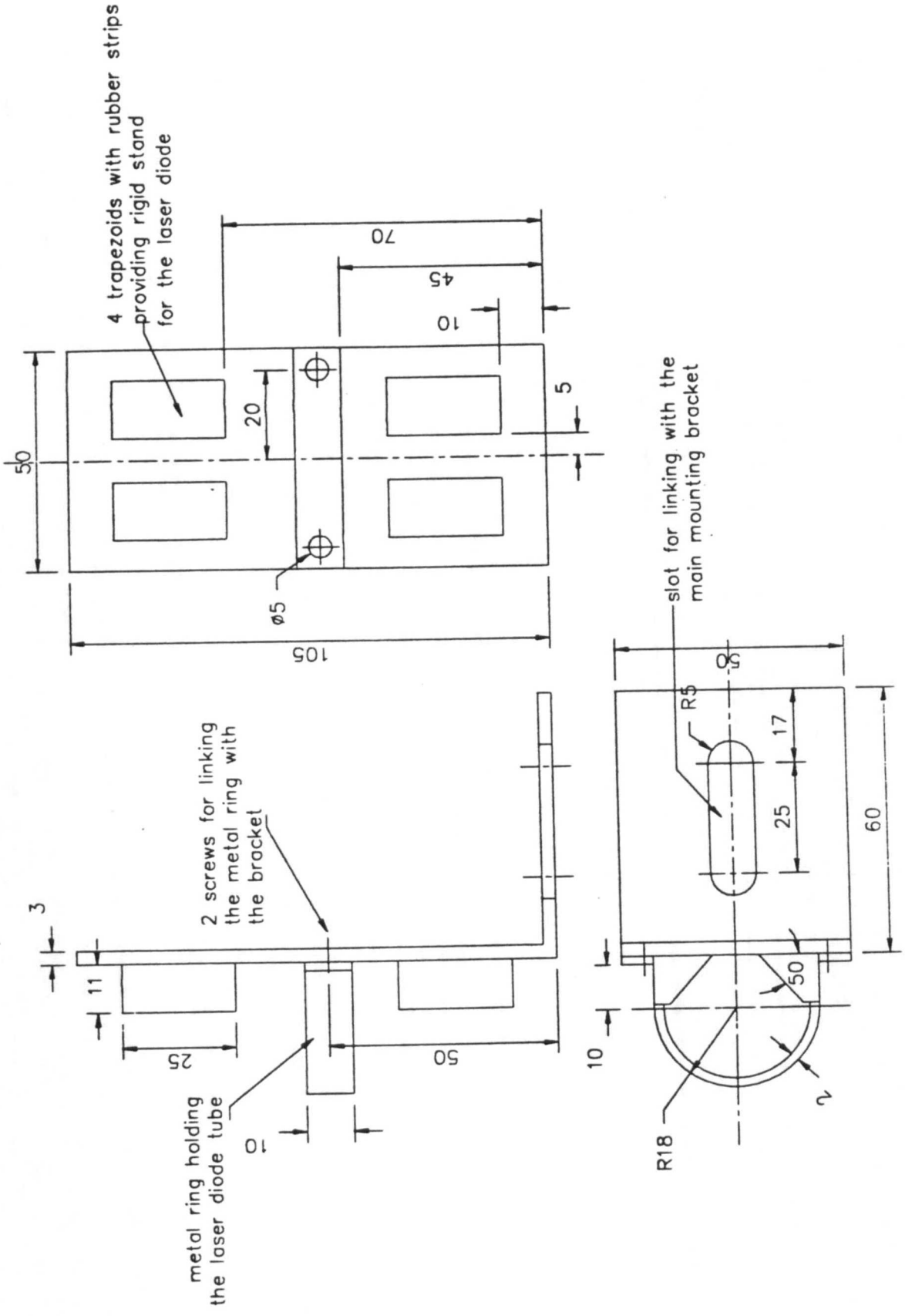

Figure II.1: Mounting bracket for laser diode.

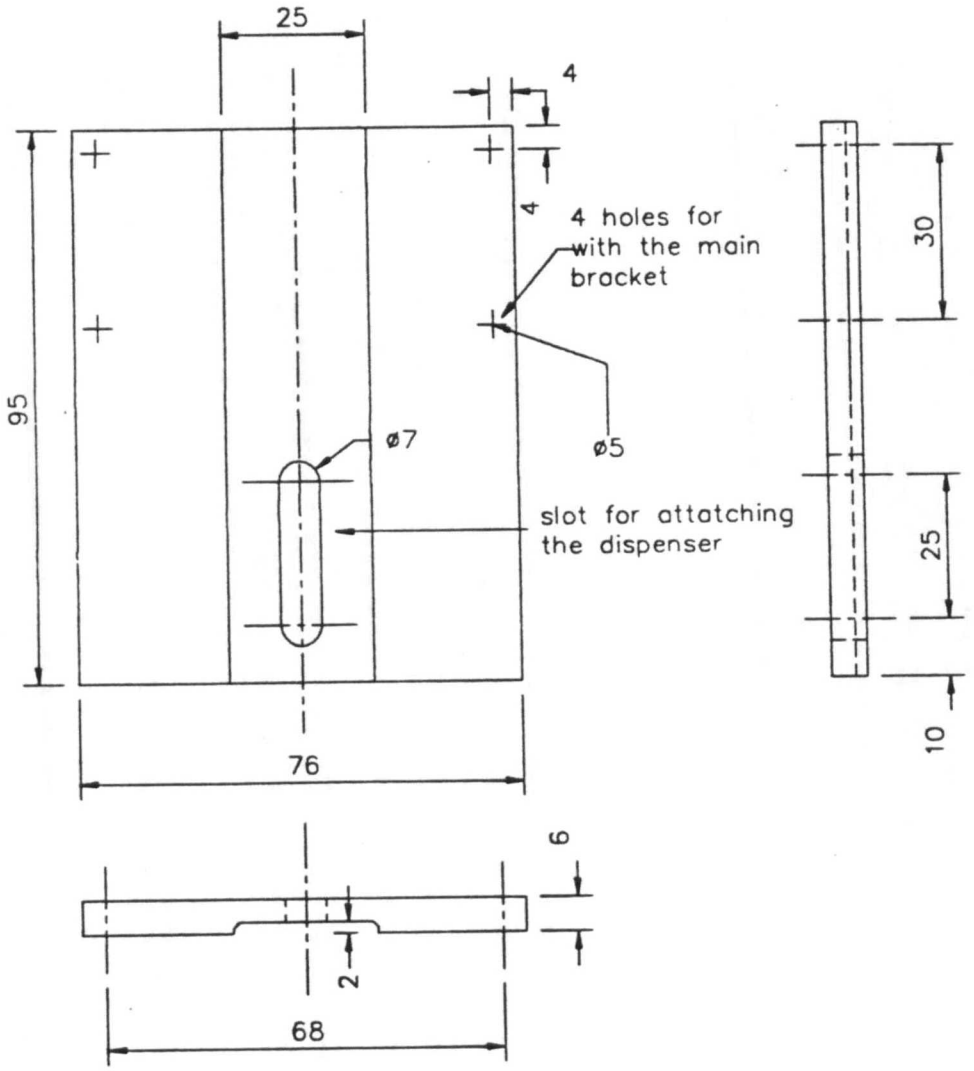

Figure II.2: Mounting bracket for dispensing nozzle.

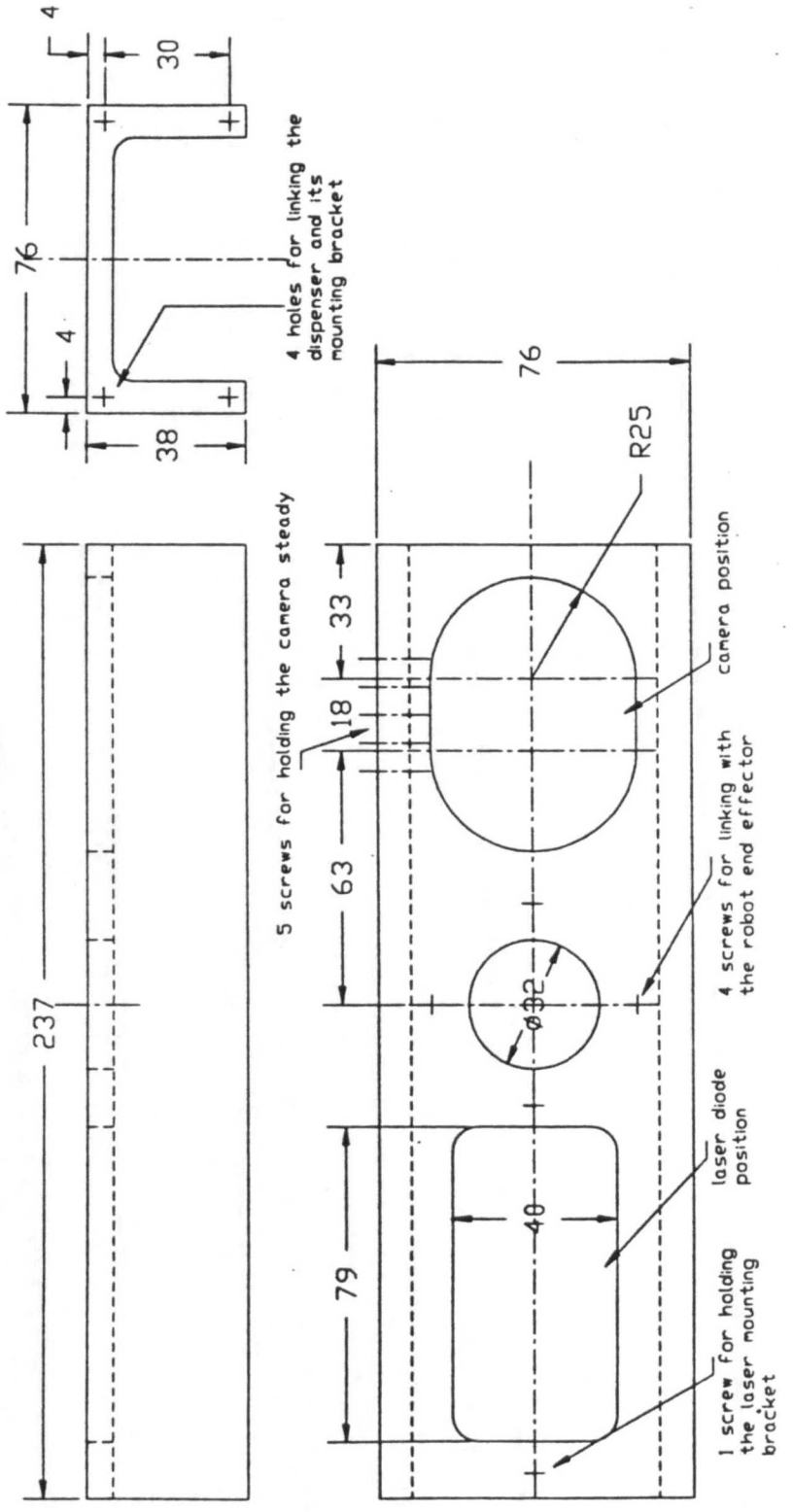

Figure II.3: Main body of the mounting bracket.

APPENDIX III

ASYNCHRONOUS SUPPORT TOOLS FOR CELL COMMUNICATION

The bead parameters can be sent to the Karel controller via a RS-232 serial communication port. This can be done by sending ASCII characters through the serial port to the Karel controller. *Asynchronous Support Tools* software package has been used for sending the data through serial ports.

III.1 Asynch Manager

Asynch manager is a powerful set of functions allowing programmers to develop applications requiring asynchronous communication services. The synch manager has three levels;

- Level Zero, Basic asynchronous support.
- Level One, High level language interface to level zero functions.
- Level Two, Data transfer and modem protocol support.

i) **Level Zero**, the level zero functions provide the most basic asynchronous communication support. All the functions are written in assembly language and drive the INS8250 UART and the Intel 8259A programmable interrupt controller directly.

ii) **Level One**, the level one functions constitute a high level language interface to level zero through a single assembly language gate, "comgate". Comgate provides a clean interface to the level zero functions. By using comgate, relatively low level communication software can easily be written in a high level language.

iii) **Level Two**, the level two functions extend the capabilities of level one, and provides increased robustness and convenience to level one. It has three general categories as follow:

- There are some enhancements of level one.

- Data transfer routines, which implement data transfer protocols. The XMODEM protocol is implemented directly, and others could be supported as well.

- Functions for driving standard modem devices. They support Hayes modem directly, and can be easily modified to support others. All the functions in level two are written in a high level language. This level is most powerful and the easiest one to use.

III.2 Software Development in Level Two

The level two provides three kinds of services:

- Enhancements to level one providing increased robustness and convenience.

- Implementation of data transfer protocols, in particular, the XMODEM file transfer protocol.

- Standard modem control, in particular, for the Hayes modem.

In order to use level two functions, you need to include the level two interface **asynch2.int** and a file **asynch2.use** in your Pascal program.

III.3 Required Functions

The first two required functions for any jobs are;

```
Function    Open_a2 (port_no      : integer;
                     iq_size      : integer;
                     oq_size      : integer;
                     int_level    :integer;
                     port_ads     :integer)
            : integer;
```

Where Port_no; is communication port in use.
iq_size; input queue size, in bytes, and must be greater than 8.
oq_size; Output queue size, in bytes, and must be greater than 8.
The combined input and output should not exceed 65532.
int_level; is the interrupt line value. The default is zero.
port_ads; is the communication address. The default is zero.

The second required function is;

Function **Close_a2** (port_no : integer)
integer;

Where ;

port-no; is the communication port number.

The port can then set-up by using the function;

Function **Setop_a2**(port_no : integer;
const options : option_record)
: integer;

where options; is the record of all port option parameters such as; baud_rate, parity, data_bits, stop_bits, remote_flow_control, local_flow_control, bit_7_trimming, bit_7_forcing, require_cts, and break_time.

The next step is to read or write a string or block of characters to or from communication port. The function is as follow;

Function **Wrtst_a2**(port_no : integer;
consts str : string;
start : integer;
finish : integer;
var last_sent : integer)
integer;

Where;

port_no, is the communication port.

str, string to write.

start, index of the first character to write.

finish, index of last character to write, and this value has to be greater than start.

last-sent, index of last character written. This value is smaller than finish if the output queue fills.

APPENDIX IV

D/A BOARD

The dispensing unit can also be addressed directly from the IBM-PC via a D/A board. The *DT2831G* board is placed in one of the fully bussed expansion slots of the IBM-PC, and is connected to the Pro-Flo dispensing system via a two ways switch by using a DT717 "screw terminal panel". This screw terminal permits all user connections (A/D, D/A, digital I/O, counter/timer) to the DT2831 board to be made on the screw terminals.

IV.1 DT2831G Features

The DT2831G board has the following features:

- A/D subsystem with up to 16 input channels provides 12-bit resolution, and a 512-entry channel-gain list.
- D/A subsystem with 2 independent D/A converters provides 12-bit resolution.
- Eight lines of digital I/O.
- Am9513A system timing controller provides three counter/timer to automatically initiate A/D, D/A, or simultaneous A/D and D/A conversions, and two counter/timers for external uses such as event counting and frequency measurement.
- Interrupts to host processor when conversion is complete or when an error occurs.
- programmed I/O (PIO) or Direct Memory Access (DMA) data transfer modes.
- Sampling rate of 250 kHz.
- Gain of 1, 2, 4, and 8.
- Software-programmable input ranges of (-10V to +10V) for bipolar, and (0 to +10V) for unipolar.

IV.2 Software Support

The DT2831G board supports the following programming languages;

- Microsoft C and Quick C.

- Microsoft FORTRAN.
- Microsoft Quick BASIC.
- Microsoft Quick Pascal.
- Borland Turbo C
- Borland Turbo Pascal.

In the automated adhesive dispensing system, the vision system uses Microsoft Pascal, which makes the processing time faster to use the same language for the D/A board.

IV.3 Software Tools

The software tools provide complete access to the analog and digital I/O tasks performed by DT2831. These tasks are;

- Initialization/termination
- Configuration
- Analog I/O
- Digital I/O
- Buffer Management

Each of these will be discussed in detail in the following sections.

i) Initialization/Termination, the subroutines are:

- **dt_initialize**, opens the DT2831, and it is required before calling any other subroutines.
- **dt_reset**, terminates all operations on a single unit, and returns it to initialized state.
- **dt_terminate**, closes the device when it is no longer required.

ii) Configuration, the subroutines are:

- **dt_get_features**, gives the information about the unit.
- **dt_get_board**, gives the information about the current setting.
- **dt_set_board**, is used to change the current setting.

iii) Analog I/O, the supported subroutines are:

- **dt_get_acq**, gets the current setting of the A/D or D/A operation of the unit.
- **dt_set_acq**, is to change the current setting.
- **dt_start_acq**, starts a buffer cycle, burst, or continuous A/D or D/A operation on a unit.
- **dt_single_acq**, performs a single A/D or D/A operation on a unit.
- **dt_stop_acq**, stops A/D or D/A operations on a unit.

iv) Digital I/O, a single software tool subroutine sets up and controls digital I/O operations;

- **dt_set_dio**, is used both to specify port directions and to perform digital I/O operations.

V) Buffer management, buffers are used to receive data from A/D acquisitions, and to hold data to be written in D/A output operations. The user is responsible for allocating buffer space. For A/D conversions, the size of each buffer is recommended to be some multiple of the CGL size. For D/A conversions, the size of the buffer should be a multiple of the number of the DACs being used. The software tools include the following subroutines :

dt_create_buffer, is used to link a buffer into an internal list of buffers called a buffer transfer list (BLT).

dt_link_xm_buffer, links an extended memory buffer into a BTL.

dt_check_buffer, checks the status of the currently active buffer.

dt_reset_buffer, sets a buffer to "the ready for I/O" state.

dt_wait_buffer, waits for I/O to complete on the currently active buffer.

dt_delete_buffer, removes a buffer from a buffer transfer list.

IV.4 Analog Transfer Types and Methods

The processes used for transferring the data are:

- **Single Value**, a single value is required from the analog to digital conversion or sent to the digital to analog conversion.

- **Buffer Cycle**, processes a single buffer continuously and is used only for D/A conversions. The BTL must contain a single buffer.

- **Burst**, processes all buffers in the BLT once. The conversion stops when all the buffers have been written to the DACs or all the buffers have been filled from the DACs.

- **Continuous**, processes all buffers in the BLT continuously.

The supported transfer types are;

- **Polled**, forces the driver to wait for the conversion to complete, or for an error to occur, before resuming the operation. This is very inefficient and is used for only single value transfer.

- **Interrupt Driven**, causes an interrupt to be generated after each conversion. This is relatively inefficient method, and is used for low performance applications.

- **Auto Initialize DMA**, causes a buffer to be sent to a DAC continuously, without program intervention. This method is used only for buffer cycle transfers, and is used for continuous waveform generation. an interrupt is generated only if an error occurs.

- **Single Channel DMA**, causes a block of data to be sent to the DAC(s) or acquired from the DACs using single DMA channel. An interrupt is generated at the end of each buffer, allowing higher conversion rates to be supported.

- **Dual Channel DMA**, causes a block of data to be sent to the DAC(s) or acquired from the DACs using two DMA channels alternately to acquire or send buffers. An interrupt is generated at the end of each buffer. This method of transfer allows the user to sample and send data at the highest achievable throughput rate of the board, providing gap-free transfers.

IV.5 Required Subroutines

To use D/A board, the library files; **dtst_tls.pas**, **dtst_err.pas**, and **dtst_xmm.pas** need to be included. The procedures **featur**, **put_boar**, **get_boar**, **get_acq**, and **set_acq** are also need to be included. All these procedures are defined in the file called PAS_SUB.PAS. You then need to write your main program for the desired task, which you may use the function which are defined by Data Translation and were described in the previous sections.

IV.6 Software Development in D/A Board

In this section, the description of the main routines will be given. They are as follow;

dt_initialize (device_name, device_handle)

Where;

device_name, is string and specifies the device to be opened. In this case is "DT283x$0".

device_handle, is integer and is used to identify the device in all subsequent subroutine calls.

dt_reset (unit, device_handle)

where;

unit, is integer and specifies the board to be reset. The range is 0 through 3 and in this case is zero.

device_handle, is integer and specifies the device.

dt_get_acq (unit, device_handle, section, acq_struct)

Where,

section is integer and specifies whether A/D or D/A parameters are requested (0=A/D input parameters, 1=D/A output parameters).

acq_struct, this structure is composed of 3 fields in which the subroutine returns setup information for A/D or D/A board.

dt_set_acq (unit, device_handle, section, acq_struct)

Where,

acq_struct, has three fields. The first field of the structure is read only, and is ignored. The second two fields contain set-up information for A/D or D/A operations.